ICS LIB.

VOLUME 38 SECOND SERIES JUL NUMBER 1

5812

THE PHYSICAL REVIEW

A JOURNAL OF EXPERIMENTAL AND THEORETICAL PHYSICS

CONDUCTED BY

THE AMERICAN PHYSICAL SOCIETY

BOARD OF EDITORS

Managing Editor, JOHN T. TATE, University of Minnesota, Minneapolis
Assistant Editor, J. W. BUCHTA, University of Minnesota, Minneapolis
E. U. CONDON, C. J. DAVISSON, F. K. RICHTMYER, K. F. HERZFELD, A. W. HULL,
F. W. LOOMIS, A. J. DEMPSTER, DAVID M. DENNISON, J. C. SLATER

JULY 1, 1931

Scattering of X-Rays by Gases and Crystals — G. E. M. JAUNCEY 1
Temperature and Diffuse Scattering of X-Rays from Crystals — Y. H. WOO 6
Experimental Electron Distributions in Atoms of Monatomic Gases — E. O. WOLLAN 15
Anomalous Scattering of Alpha-Rays — MORRIS MUSKAT 23
Reflecting Power and Grating Efficiency in the Extreme Ultraviolet — H. M. O'BRYAN 32
Atomic Scattering Power of Copper and Oxygen in Cuprous Oxide — G. A. MORTON 41
Analysis of Photoelectric Sensitivity Curves for Clean Metals at Various Temperatures — R. H. FOWLER 45
Relativistic Theory of the Photoelectric Effect — HARVEY HALL AND J. R. OPPENHEIMER 57
Transmission of Electrons through Potential Barriers — N. H. FRANK AND L. A. YOUNG 80
A-Type Doubling and Electron Configurations in Diatomic Molecules — ROBERT S. MULLIKEN AND ANDREW CHRISTY 87
Inverse-Cube Central Force Field in Quantum Mechanics — GEORGE H. SHORTLEY 120
Spectrum of Doubly Ionized Carbon, CIII — I. S. BOWEN 123
Electro-optical Kerr Effect in Gases — E. C. STEVENSON AND J. W. BEAMS 133
Raman Spectra of Certain Organic Liquids — CHARLES S. MORRIS 141
New Absorption Bands of Ammonia, Methyl Bromide, Methyl Iodide and Carbon Dioxide in the Infrared Spectrum — W. W. SLEATOR 147
Transmission of Visible Light through Fog — H. G. HOUGHTON 152
Theoretical Investigation of the Transmission of Light through Fog — J. A. STRATTON AND H. G. HOUGHTON 159
Interference in Thin Metallic Films — HIRAM W. EDWARDS 166
Magnetic Moment of the Diatomic Sulfur Molecule — E. J. SHAW AND T. E. PHIPPS 170
Thermocouples whose Elements are Longitudinally and Transversely Magnetized Wires of Nickel and Iron — WILLIAM H. ROSS 179
P-V-T Relations of NH_4Cl and NH_4Br, and in Particular the Effect of Pressure on the Volume Anomalies — P. W. BRIDGMAN 182
Letters to the Editor — 193
Transverse Barkhausen Effect in Iron, *R. M. Bozorth and J. F. Dillinger*—193; On the Elastic Scattering of Electrons by Spherically Symmetrical Atoms, *F. W. Dotzmann and Otto Halpern*—193; Excitation of High Optical Energy Levels, *J. E. Mack*—193; The Scattering of X-Rays from Polyatomic Gases, *G. E. M. Jauncey*—194; The Effect of Internal Stress on Magnetic Susceptibility, *C. W. Heaps and H. E. Benta*—195; The Entropies of Methane and Ammonia, *W. F. Giauque, R. W. Blue and Ray Overstreet*—195; Electronic Velocities in the Positive Column of High Frequency Discharges, *Egon Hiedemann*—196.
Book Reviews — 199

PUBLISHED BY THE AMERICAN PHYSICAL SOCIETY
EDITORIAL OFFICE: MINNEAPOLIS, MINN.

THE AMERICAN PHYSICAL SOCIETY

OFFICERS OF THE SOCIETY

President:	W. F. G. Swann	Bartol Research Foundation, Philadelphia, Pa.
Vice-President:	Paul D. Foote	The Gulf Companies, Pittsburgh, Pa.
Secretary:	W. L. Severinghaus	Columbia University, New York City
Treasurer:	G. B. Pegram	Columbia University, New York City
Editor:	John T. Tate	University of Minnesota, Minneapolis, Minn.
Local Secretary for the Pacific Coast:	L. B. Loeb	University of California, Berkeley, Calif.

THE PHYSICAL REVIEW

Published by the American Physical Society. Executive office: University of Minnesota, Minneapolis, Minn. Two volumes annually, twelve issues per volume.

First series. From July 1, 1893, to January 1, 1913, the Review was conducted by Edward L. Nicholas, Ernest Merritt and Frederick Bedell, with the financial support of Cornell University. The first four volumes were issued annually; subsequent volumes, semi-annually; thirty-five volumes in all.

Second series. On January 1, 1913, the Review was transferred to the American Physical Society as announced on the first page of the new series which was then begun. Since then it has been conducted by a Board of Editors elected by the Society. Semi-annual volumes begin in January and July. Since July 1, 1929, the Review has been issued twice a month.

Contributors are referred to page 2 of the advertisements for further information.

Annual subscription, throughout the Postal Union, $12.00 in advance.

General index, 1893-1920, $4.00, in advance.

Back Volumes, $9.00 per volume; Back Numbers, $1.50 per copy for issues prior to July 1, 1929 (Vols. 1-33), $.75 per copy for issues subsequent thereto. Postage is free if remittance accompanies order; otherwise postage is extra. No bound volumes can be supplied. The Review offers to purchase a limited number of First Series, Vol. 1, No. 1 (at $2.00 each); Second Series, Vol. 7, No. 1, January 1916; Vol. 7, No. 2, February 1916; Vol. 7, No. 4, April 1916; and Vol. 7, No. 5, May 1916 (at $2.00 each).

Advertisements. Rates will be supplied by the Editor on request. Copy for each number must be received at Minneapolis two weeks prior to the dates of issue; old copy is used until new copy is received. Send electrotypes direct to the printers, George Banta Publishing Co., Menasha, Wis.

Discount of ten per cent is allowed to members of the American Physical Society on purchase of back numbers.

Changes of Address and Complaints of failure to receive the Review, in the case of members of the Physical Society, should be addressed to the Treasurer; in the case of other subscribers, to the Editor. New copies can be sent free in response to complaint of non-delivery only if notice of non-delivery is received within three months of date of issue.

Editorial Correspondence should be addressed to the Physical Review, University of Minnesota, Minneapolis, Minn.

Entered at the post office at Menasha, Wis., as second class matter.
Acceptance for mailing at special rate of postage provided for in section 1103, Act of October 3, 1917, authorized September 6, 1926.

PHYSICAL REVIEW

PREPARATION OF PRELIMINARY ABSTRACTS

An article will not be accepted for publication in THE PHYSICAL REVIEW unless the manuscript is accompanied by an adequate abstract for publication at the beginning of the article. This abstract is intended to aid the reader by furnshing an index and a brief summary of the contents of the article. Besides serving these purposes it should also be suitable for reproduction in abstract journals so as to make it unnecessary for the editors of these journals to have another abstract prepared.

As *an index* it should be complete; all the subjects, major and minor, concerning which new information is presented, should each be given, with sufficient precision so that any reader can tell from the abstract whether the article contains anything of interest to him. The subject indexes of abstract journals are fundamental in reference work. These indexes are prepared exclusively from the abstracts and whatever is omitted from the abstracts cannot be included in the index and may thus be lost. The writer of an abstract should therefore feel himself under an important obligation to his scientific colleagues to make sure that the abstract is accurate and complete, at least as an index.

As *a summary* the abstract should give briefly the conclusions of the article, important advances in experimental technique and theory, and all numerical results of general interest that may be conveniently given including all that might belong in a handbook and table of contents. It should give all the information that readers who are not specialists in the particular field involved might desire to know about the article thus saving them the time and trouble in referring to the article itself. Experience has shown that in general the length of the abstract should be from four to eight percent of the length of the article.

THE PHYSICAL REVIEW, 1923-1925, contains many examples of adequate abstracts. Most of these contain paragraph titles and subtitles which indicate the subjects concerning which new information is given and it is required that authors include such subtitles when all the information contained in the article does not refer to the subject indicated by the title of the article. Such subtitles may be frequently avoided by rewording the title so as to make it more precise.

We have already mailed some of the new sample books of cross section papers

You are entitled to one for the asking. Anyone using cross section papers should be interested. We have added two new kinds to the list. Better write while you have it in mind.

CORNELL CO-OP. SOCIETY

BARNES HALL **ITHACA, N. Y.**

Back Numbers Urgently Wanted of the PHYSICAL REVIEW

We will pay $2.00 each for copies of the January, February, April and May issues of Volume 7, 1916; the January and February issues of Volume 9, 1917; also $1.00 for copies of the January, 1927, issue.

Send to the Physical Review, University of Minnesota, Minneapolis, Minnesota.

8" Rheostat

16" Rheostat

10" Rheostat

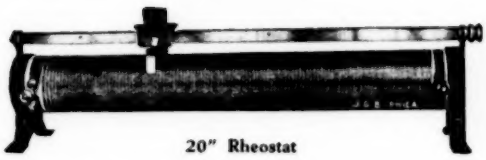
20" Rheostat

Four Popular Sizes of

"JAGABI" RHEOSTATS

TO HELP YOU secure just the right Rheostat when you need it, we carry in stock these four popular sizes of "Jagabi" Rheostats in nearly all of *seventy-six different ratings.*

These range from as low as .34 ohm, 25 amperes, up to 30,000 ohms, .1 ampere. They are wound on porcelain tubes and therefore have low inductance and almost perfect insulation.

Usually we can ship these standardized Rheostats within 24 hours after receipt of order.

Please write for our latest Rheostat Bulletin 1265-P.

JAMES G. BIDDLE CO.

ELECTRICAL AND SCIENTIFIC INSTRUMENTS

1211-13 ARCH STREET, PHILADELPHIA, PA.

At Philadelphia headquarters we maintain a working exhibit of our leading specialties and welcome visitors during office hours.

Taylor Process Fine Wires

PATENT NUMBER 1,793,529

THE TAYLOR PROCESS for making wires from substances which lack ductility, consists in melting the material in a glass or quartz and drawing down to the required size. The process has been so developed that a great many non-ductile substances can now be drawn into wire by it. The elements or alloys, because the drawing is done in glass or quartz, are in a very pure state, although lengths of more than a few feet cannot be obtained. The wires may be had with or without the glass insulation.

We make Taylor Process wire of Pt, Pd, Rh, Au, Ag, Cu, Fe, Co, Zn, Cd, Pb, Sb, Bi, Sn, Se, Te, Tl, Ga, and In, Constantan, Bi-Sn, Cd-Sb (used where large E.M.F. is desired) and many other alloys. Our wires are packed in containers holding one foot and with few exceptions, the sizes are from one mm to one micron. We manufacture too, fine wire by the Wollaston Method, by extrusion and by bare drawing.

Whenever you need wire from unusual materials or in unusual sizes, write us. Very probably we can supply you.

BAKER & CO., INC.
54 Austin St., Newark, N.J.

New York **San Francisco** **Chicago**

L & N SEMI-PRECISION THERMOMETER BRIDGE

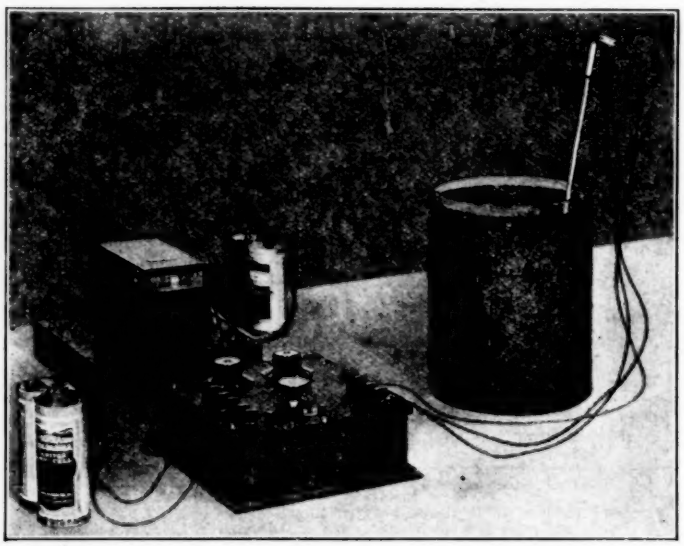

No. 8063 Semi-Precision Thermometer Bridge, No. 2420-b Galvanometer and No. 8125 Nickel Resistance Thermometer, set up for measuring the temperature of a bath.

THE L & N Semi-Precision Thermometer Bridge is principally used for measuring temperature with three or four-lead resistance thermometers. The range is 0-200.1 ohms. The limit of error up to 10 ohms is 0.005 ohm and above 10 ohms is 0.05 per cent. The 2420-b galvanometer is recommended for use with this bridge. Resistance Thermometers for use with this equipment are listed in Catalog No. P-80.

8063 SEMI-PRECISION THERMOMETER BRIDGE **$135.00**

2420-b GALVANOMETER, with inclosed lamp and scale **40.00**
Sensitivity, 25 microvolts per mm.

LEEDS & NORTHRUP COMPANY
4901 STENTON AVENUE PHILADELPHIA, PA.

LEEDS & NORTHRUP

Electrical Measuring Instruments
Potentiometer Pyrometers

Hump and Homo Heat Treating Furnaces
Automatic Combustion Control

G-239

Second Series *July 1, 1931* *Vol. 38, No. 1*

THE
PHYSICAL REVIEW

THE SCATTERING OF X-RAYS BY GASES AND CRYSTALS

By G. E. M. Jauncey
Washington University, St. Louis, Missouri

(Received May 22, 1931)

Abstract

Recently A. H. Compton and Jauncey and Harvey have obtained theoretical formulas for the scattering of x-rays by gases and crystals respectively. By means of these formulas f' values can be calculated. From measurements on the diffuse scattering by rocksalt, Jauncey and Harvey have calculated f' values for the average atom, or $(Na^+ + Cl^-)/2$, in rocksalt. Wollan has also recently obtained f' values for neon and argon. The f' values for the average of neon and argon, or $(Ne+A)/2$ are compared with those for $(Na^+ + Cl^-)/2$ and an excellent agreement is found. Also these two sets of experimental f' values are shown to be in excellent agreement with the quantum mechanics model of Waller and James. It is shown that the difference between f' and f, the true atomic structure factor, is not negligible and that the error in assuming f to be given by f' may be as large as 20 or 30 percent at large values of $(\sin \phi/2)/\lambda$. Also it is pointed out that only f, but not f', values may be used in the Fourier analysis method of unravelling crystal structure.

I. Scattering by Neon, Argon and Rocksalt

In 1930 A. H. Compton[1] developed the theory of the scattering of x-rays by monatomic gases and obtained the formula

$$S = 1 + (Z - 1)f'^2/Z^2 \tag{1}$$

where S is the scattered intensity in a direction ϕ with the primary beam per electron relative to the scattered intensity from a single isolated electron in the same direction ϕ, Z is the number of electrons in an atom of the gas scatterer, and f' is a quantity to be defined later. More recently Jauncey and Harvey [2,3] have developed the theory of the diffuse scattering of x-rays by simple cubic crystals consisting of atoms of one kind and have obtained the formula

$$S = 1 + (Z - 1)f'^2/Z^2 - F^2/Z \tag{2}$$

where F is the atomic structure factor of the atoms in the crystal. The quantity f' in Eqs. (1) and (2) is related to f, the true atomic structure factor, according to[2]

[1] A. H. Compton, Phys. Rev. **35,** 925 (1930).
[2] G. E. M. Jauncey, Phys. Rev. **37,** 1193 (1931).
[3] G. E. M. Jauncey and G. G. Harvey, Phys. Rev. **37,** 1203 (1931).

$$f'^2 = f^2 - \left(Z \sum_{r=1}^{Z} E_r^2 - f^2\right)/(Z-1) \tag{3}$$

where E_r is the average amplitude of the waves scattered by the rth electron in the atom and where the true atomic structure factor f is given by

$$f = \sum_{r=1}^{Z} E_r \tag{4}$$

the difference between F and f is that F contains the effect of the thermal motions of the atoms, while f does not. In virtue of Eq. (4), the quantity

$$Z \sum_{r=1}^{Z} E_r^2 - f^2 = Z^2\left\{\left(\sum_{r=1}^{Z} E_r^2\right)/Z - \left(\sum_{r=1} E_r/Z\right)^2\right\}. \tag{5}$$

The quantity in the braces is essentially positive because the mean of the squares of a set of numbers is greater than the square of the mean of the same set of numbers. Hence in Eq. (3) $f' < f$, unless all the E's are equal. Since it is not likely that the E for a K electron is the same as the E for an L or M electron, it seems that $f' < f$.

Eq. (2) strictly only applies to crystals consisting of atoms of one kind. However, since no diffuse scattering measurements have been made on crystals like sylvine which may be considered as consisting of atoms of one kind, Harvey and the writer[3] were forced to make use of the results obtained by Jauncey and May[4] for rocksalt at room temperature. We treated rocksalt as a crystal consisting of atoms of one kind, the atomic number being $(11+17)/2$ or 14. Also, using the average of the F values for Na^+ and Cl^- obtained by James and Firth[5] at room temperature, we applied Eq. (2) and calculated f' values for an atom which is the average of Na^+ and Cl^-. Just a month before the publication of our papers[2,3] a paper by Wollan[6] on the scattering of x-rays by gases appeared. In particular, Wollan has determined the experimental values of S for neon and argon and from these S values he has by the use of Eq. (1) calculated the f' values for these gases. It is interesting to compare the average of the f' values found for neon and argon by Wollan with the average of the f' values for Na^+ and Cl^- which we have calculated[3] from Jauncey and May's and James and Firth's results. The comparison is shown in Fig. 1, where f' is plotted against $(\sin\phi/2)/\lambda$. The f' values for $(Ne+A)/2$ and for $(Na^+ + Cl^-)/2$ are shown as black circles and crosses, respectively. The two sets of points fall very closely on the same curve for values of $(\sin\phi/2)/\lambda$ less than 0.65 and the agreement is remarkable. For values of $(\sin\phi/2)/\lambda$ larger than 0.65 the f' values seem to separate. However, it is in this region that the Compton effect[7] becomes operative, and this effect was not properly taken account of in the experiments of Jauncey and May, which were done in 1923. Also in this region the experimental error in F be-

[4] G. E. M. Jauncey and H. L. May, Phys. Rev. **23,** 128 (1924).
[5] R. W. James and E. M. Firth, Proc. Roy. Soc. **A117,** 62 (1928).
[6] E. O. Wollan, Phys. Rev. **37,** 862 (1931).
[7] A. H. Compton, Phys. Rev. **21,** 483 (1923).

comes large and also the f' values for the gases become very sensitive to small changes in S. It therefore seems reasonable to suppose that the discrepancy between the (Ne+A)/2 and the $(Na^+ + Cl^-)/2$ f' values at large values of $(\sin \phi/2)/\lambda (\sin \phi/2)/\lambda$ is due to experimental error and to neglect of the Compton effect in the f' values for $(Na^+ + Cl^-)/2$.

In Fig. 1 the broken curve is the F curve for $(Na^+ + Cl^-)/2$ for a temperature of 290°K. The F values shown by this curve were used by Jauncey and Harvey in calculating f' from S for $(Na^+ + Cl^-)/2$. Waller and James,[7a] using the new quantum mechanics, have devised model Na^+ and Cl^- ions and the f values for the model atom of $(Na^+ + Cl^-)/2$ are given by the full curve in Fig. 1. It will be seen that the black circles showing Wollan's f' values for (Ne+A)/2 lie very closely to the Waller-James curve, even out to values of

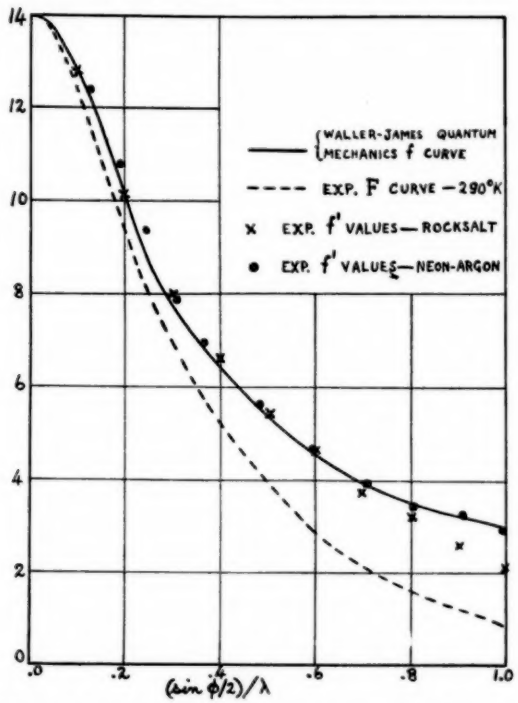

Fig. 1. Comparison of f' values for neon-argon with those for rocksalt.

$(\sin \phi/2)/\lambda$ as large as 1.0. At first sight this seems to show excellent agreement between the Waller and James' model atom and Wollan's experimental results. However, Wollan's values are f' values, whereas Waller and James' values are f values. At the beginning of this paper it was pointed out that $f' < f$ and the question arises as to whether the difference $f - f'$ is or is not negligible.

II. Evaluation of $f - f'$

In order to answer the question just raised, we shall consider model ions of Na^+ and Cl^-. Pauling[8] has shown how model atoms based on the new quan-

[7a] I. Waller and R. W. James, Proc. Roy. Soc. A117, 214 (1927).

[8] L. Pauling, Proc. Roy. Soc. **A114,** 181 (1927).

tum mechanics may be devised. As the calculations are tedious and as it is only desired to obtain the order of magnitude of $f-f'$, we shall assume that the Na^+ ion consists of 2 K electrons and 8 L electrons and the Cl^- ion of 2 K, 8 L, and 8 M electrons, and that no correction need be made for interpenetrating orbits. Let the probability of a given K electron being between the spheres of radii r and $r+dr$ measured from the nucleus of the atom be $u_K dr$, where

$$u_K = (1/2a_K{}^3)r^2 \exp(-r/a_K). \tag{6}$$

In Eq. (6), a_K is a parameter. Similarly there are probability functions u_L and u_M for the L and M electrons respectively given by

$$u_L = (1/a_L{}^5 4!)r^4 \exp(-r/a_L) \tag{7}$$

and

$$u_M = (1/a_M{}^7 6!)r^6 \exp(-r/a_M) \tag{8}$$

If r_m is the radius at which a probability function $u(r)$ becomes a maximum, then, for the respective u's,

$$a_K = r_m/2;\ a_L = r_m/4 \text{ and } a_M = r_m/6. \tag{9}$$

From Pauling's curves,[8] we have taken r_m to be 0.05A and 0.33A, respectively, for the K and L electrons of Na^+ and 0.04A, 0.18A and 1.02A, respectively, for the K, L and M electrons of Cl^-.

Let us take two parallel planes at distances z and $z+dz$ respectively from the nucleus of an atom, and let the probability of a given electron being between the planes be $p(z)dz$. The relation between $p(z)$ and $u(r)$ is, as is obvious from Compton's paper[1]

$$p(z) = (\tfrac{1}{2}) \int_{r=z}^{r=\infty} u(r)dr/r\,. \tag{10}$$

We can therefore immediately obtain the p-functions for the K and L electrons of Na^+ and for the K, L and M electrons of Cl^-. The quantity E_r of Eqs. (3), (4) and (5) is then given by

$$E_r = \int_{-\infty}^{+\infty} p_r \cos kz dz \tag{11}$$

where $k=(4\pi \sin \phi/2)/\lambda$ and the subscript r may represent either a K, L or M electron. Performing the integration of Eq. (11), we obtain

$$\begin{aligned} &E_K = 1/(1+x^2)^2;\ E_L = (1-x^2)/(1+x^2)^4; \\ &E_M = (1-x^2/3)(1-3x^2)/(1+x^2)^6 \end{aligned} \tag{12}$$

where $x=ka_K$, ka_L or ka_M, respectively. In virtue of Eq. (4), values of f, and in virtue of Eq. (3), values of f' can be found. In Fig. 2, the difference $f-f'$ is plotted against $(\sin \phi/2)/\lambda$, curves being shown for Na^+ and Cl^-. It is seen that the maximum values of $f-f'$ for Na^+ and Cl^- are 0.45 and 0.39 respectively, which are not negligible numbers. At $(\sin \phi/2)/\lambda = 0.995$, the values

of $f-f'$ for Na^+ (or neon) and Cl^- (or argon) are 0.44 and 0.19 respectively. At this value of $(\sin \phi/2)/\lambda$, Wollan obtained f' values of 1.37 and 4.49 for neon and argon respectively, so that the true atomic structure factors for neon and argon might be as large as 1.81 and 4.68 if the models we have chosen are reasonably correct. The error in assuming that the true atomic structure factor is given by f' may thus be of the order of 20 to 30 percent in the case of neon and 4 percent in the case of argon. Fig. 9 of Wollan's paper shows the curve for the experimental f' values for neon falling below the curve for the f values for the theoretical Na^+ model. This is as it should be, although it appears that the differences $f-f'$ are somewhat larger than we have calculated for our model Na^+ ion in this paper. However, the curve for $f-f'$ depends on the model chosen. It is at large values of $(\sin \phi/2)\lambda$ that the difference $f-f'$ becomes important, and it is also in this region that the experi-

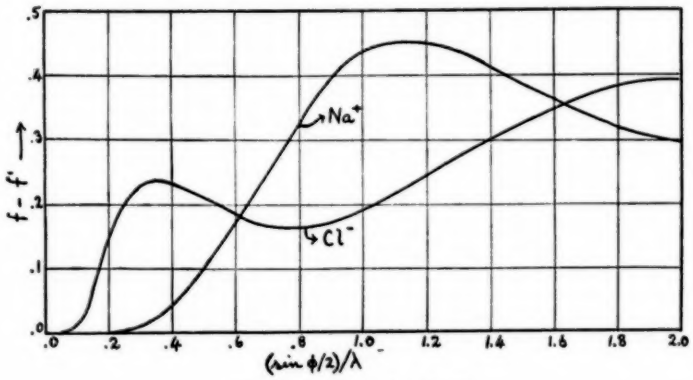

Fig. 2. Curves for $f-f'$.

mental error becomes fairly large. So altogether the values of the true atomic structure factor reported in this region must be subject to considerable error. It should be noted that the Fourier analysis methods of unravelling atomic structure as developed by Duane[9] and Compton[10] are applicable only to f and not to f' values.

The hump which occurs at $(\sin \phi/2)/\lambda = 0.34$ in the $(f-f')$ curve for Cl^- in Fig. 2 is caused by the M electrons. We might average the Na^+ and Cl^- curves of Fig. 2 and obtain a curve for $(Na^+ + Cl^-)/2$ and so obtain some idea of the corrections to be made to the f' values for $(Na^+ + Cl^-)/2$. The f values so obtained in the region of $(\sin \phi/2)/\lambda > 0.65$ fall more closely to the Waller-James curve of Fig. 1 than do the f' values, the agreement being good out to $(\sin \phi/2)/\lambda = 0.80$. When Wollan's f' values are corrected for $f-f'$, his points at large angles fall above the Waller-James curve.

Taking everything into account, it must be said that Wollan's results for neon and argon, our results for rocksalt, and the Waller-James theoretical f values agree very well with one another.

[9] W. Duane, Proc. Nat. Acad. Sci. **11**, 489 (1925).
[10] A. H. Compton, "X-Rays and Electrons," Chapter V.

TEMPERATURE AND DIFFUSE SCATTERING OF X-RAYS FROM CRYSTALS

By Y. H. Woo
Department of Physics
National Tsing Hua University, Peiping, China

(Received May 16, 1931)

Abstract

Since the discovery of the Compton effect it has been evident that the old calculation by Debye of the diffuse scattering of x-rays by a crystal should be amended to take account of the modified radiation, which is generally presumed to be incoherent. Extending the idea suggested by the writer in his theory of x-ray scattering by gases, it is postulated that, in considering the scattering of x-rays by a crystal, only the coherent radiation from the different lattice units will interfere with each other, whereas the incoherent radiation will be simply added up. An expression for the intensity of the diffuse scattering is thence developed which consists of two parts, one taking care of the coherent scattering as originally worked out by Debye and the other accounting for the incoherent scattering. The mathematical formulation is based on the theoretical investigation by Raman and A. H. Compton on the scattering of x-rays by a dynamic atom. The theory is compared with the absolute measurements of the scattering from rocksalt reported by Jauncey and May and the agreement seems to be very close if the temperature factor is taken to be e^{-2M} as calculated by Debye and Waller. The comparison also seems to suggest the presence of the zero-point energy. These are in accord with the conclusions recently drawn by James, Waller and others from a study of the temperature effect on the intensity of the x-rays regularly reflected. The theory therefore seems to account for the so-called excess scattering, for the small scattering in the region of 0° scattering angle, for the position of the maximum scattering as well as the shift of this position with the wave-length of the primary x-rays, for the occurrence of the minimum scattering at about 100° instead of at 90° and finally for the general departure of the scattering curve from that predicted by Thomson's theory. A comparison is also made with Jauncey's experiment on the variation of the scattering by rocksalt with temperature and the result indicates that, owing to the presence of the incoherent term, measurements of this type will not test the present theory. It is pointed out that, being developed for a single crystal in which the atoms are supposed to be arranged with perfect regularity, the theory will not hold for the scattering of x-rays by the so-called amorphous substances. In these substances, the arrangement of atoms evidently introduces a type of irregularity which results in diffusely scattered rays in addition to those due to the thermal agitation. Thus, under certain conditions, only a negligible portion of the coherent intensity of the x-rays diffusely scattered by an amorphous substance is influenced by the temperature. This explains the experimental fact recently reported by Jauncey and Bauer that there is no effect of temperature on the ratio of modified to unmodified rays in the Compton effect. Theoretical predictions for the crystal sylvine are given and absolute measurements performed with homogeneous x-rays should easily test these results.

I. Introduction

THE influence of temperature on the intensity of scattering of x-rays by a crystal was first investigated theoretically by Debye,[1] who based his

[1] P. Debye, Ann. d. Physik **14**, 65 (1914).

work on the dynamical theory of crystal lattices due to Born and Kármán by considering the heat-motions as a series of elastic waves in the crystal. The theory as worked out by Debye requires (1) that the intensity of the interference maximum, i.e. x-rays regularly reflected, should be multiplied by a factor e^{-M}, and (2) that the regular reflection should be accompanied in all directions by diffuse scattering, whose intensity is proportional to $(1-e^{-M})$, where

$$M = \frac{3h^2}{\mu k\Theta}, \frac{\phi(x)}{x} \cdot \frac{1-\cos\theta}{\lambda^2}. \tag{1}$$

In this expression, which refers only to a simple cubic lattice composed of atoms of one kind, λ is the wave-length of the incident x-rays, θ is the scattering angle, μ is the mass of an atom, h is Planck's constant, Θ is the characteristic temperature of the crystal, which occurs in the theory of specific heats, $x=\Theta/T$, where T is the absolute temperature, $\phi(x)$ is a certain function of x, which Debye evaluates in his paper. The formula for M given here supposes that there is no zero-point energy. If such energy be assumed, $\phi(x)/x$ should be replaced by $(\phi(x)/x)+\frac{1}{4}$.

The calculation of Debye has been later examined by Faxén[2] and Waller,[3] each of whom finds for the intensity of diffuse scattering a different expression, which is much more complicated than that obtained by Debye. This, of course, just represents the result of another possible method of attacking the problem and has nothing to do with the validity of Debye's theory.[4] The work of Waller also indicates that for a simple lattice the temperature should be e^{-2M} instead of e^{-M}. This comes out from the fact that the treatment of Waller differs from that of Debye in the method of obtaining the "normal coordinates" in terms of which the energy of the lattice is expressed. As we shall see later, this modification really forms a correction which should be applied to Debye's work.

In the case of regular reflection the theory of Debye as amended by Waller seems to be supported quantitatively for temperatures from that of liquid air up to about 500°K by the recent experiments of James and Firth[5] and others.[6] The diffuse scattering of x-rays by crystals has been studied by Jauncey,[7] who concludes, on the basis of his experiments, that the intensity determined experimentally is considerably greater than the value demanded by Debye's formula and that the intensity varies much more slowly with the temperature than theoretically predicted.

Now since the discovery of the Compton effect it has been evident that a certain fraction of the diffusely scattered x-rays is the modified radiation, which is generally presumed to be incoherent. Owing to the existence of this

[2] H. Faxen, Ann. d. Physik **54,** 615 (1918); Zeits. f. Physik **17,** 266, (1923).

[3] I. Waller, Zeits. f. Physik **17,** 389 (1923); "Upsala Dissertation," 1925.

[4] Cf. P. Debye, Ann. d. Physik **14,** 69, footnote (1914).

[5] James and Firth, Proc. Roy. Soc. **A117,** 62 (1927).

[6] James, Brindley and Wood, Proc. Roy. Soc. **A125,** 401 (1929); James and Brindley, Proc. Roy. Soc. **A121,** 155 (1928).

[7] G. E. M. Jauncey, Phys. Rev. **20,** 405 and 421 (1922).

incoherent radiation it appears that the old calculation of Debye should be modified. The present investigation was therefore undertaken.

II. Intensity of X-rays Diffusely Scattered by Crystals

In two recent papers[8] the writer has developed a general theory of the intensity of total scattering of x-rays by gases on the assumption that, in considering the scattering of x-rays by a polyatomic molecule, only the coherent radiation from the different atoms will produce interference effect, while the incoherent radiation will be simply added up. The theory has been compared with Barrett's experiments[9] on the scattering of x-rays by different gases and the agreement seems to be satisfactory. It appears that the idea just stated is of quite general character and can be applied to the scattering of x-rays by a crystal as well. We shall accordingly postulate that, in considering the scattering of x-rays by a crystal, only the coherent radiation scattered from the different lattice units will interfere with each other according to the classical wave theory, whereas the incoherent radiation will be simply added up. On this view, the intensity of the incoherent radiation scattered from a crystal should be independent of the temperature and therefore Jauncey's conclusion is to be theoretically expected.

In the writer's theory of scattering of x-rays by gases, the mathematical formulation is based on the fundamental investigation according to classical electrodynamics by Raman[10] and A. H. Compton[11] on the scattering of x-rays by an atom in which the electrons are regarded to be arranged with random orientation and with arbitrary radial distribution. The intensity of the x-rays of wave-length λ scattered at an angle θ to a distance R is found to be

$$I_\theta = I_1 + I_2[1 + \gamma(1 - \cos\theta)]^{-3}. \tag{2}$$

In this equation, $\gamma = h/mc\lambda$,

$$I_1 = \frac{Ie^4(1 + \cos^2\theta)}{2R^2m^2c^4}F^2 \text{ and } I_2 = \frac{Ie^4(1 + \cos^2\theta)}{2R^2m^2c^4}\left(Z - \frac{F^2}{Z}\right) \tag{3}$$

where I is the intensity of the primary beam, Z is the atomic number, h is Planck's constant, e and m are the charge and mass of the electron, and c is the velocity of light. The factor F is the atomic structure factor for the scattering atom and for the purpose of the present paper may be defined by the integral

$$F = \int_0^\infty U(r)\frac{\sin kr}{kr}\,dr,$$

where $k = (4\pi/\lambda)\sin\frac{1}{2}\theta$ and $U(r)dr$ is the amount of charge in electrons lying between r and $r+dr$ from the center of the atom. F is a function of $(\sin\frac{1}{2}\theta)/\lambda$ and approaches a value equal to the total number of electrons in the scatter-

[8] Y. H. Woo, Proc. Nat. Acad. Sci. **17,** (1931).
[9] C. S. Barrett, Proc. Nat. Acad. Sci. **14,** 20 (1928); Phys. Rev. **32,** 22 (1928).
[10] C. V. Raman, Indian J. Physics **3,** 357 (1928).
[11] A. H. Compton, Phys. Rev. **35,** 925 (1930).

ing atom for small values of θ. The factor $[1+\gamma(1-\cos\theta)]^{-3}$ in Eq. (2) is introduced by Compton[11] to correct for the change of wave-length in the Compton effect in accordance with the theoretical investigation by Breit[12], Dirac[13] and others. From classical considerations Raman[10] has called attention to the incoherent or "fluctuating" character of the part represented by I_2 and emphasized the fundamental difference in physical nature between I_2 and I_1 which is a perfectly determinate and invariable part representing the diffraction pattern of the atom. Compton has come to the same conclusion by comparing Eq. (2) with Wentzel's quantum theory of x-ray scattering.[14]

Since Debye's calculation for the diffuse scattering is supposed to take account only of the coherent radiation, we have therefore, according to the point of view put forward here, for the scattered intensity from a crystal

$$I_\theta = \frac{NIe^4(1+\cos^2\theta)}{2m^2R^2c^4}\left\{(1-e^{-B})F^2+\frac{Z-F^2/Z}{[1+\gamma(1-\cos\theta)]^3}\right\} \tag{4}$$

where N is the number of atoms per unit volume of the crystal, B is equal to M according to Debye's theory and is equal to $2M$ if the modification suggested by Waller is introduced, and the other notations have the same meaning as those employed in Eq. (2) It will be noticed that the first term on the right-hand side of Eq. (4) is the original expression derived by Debye multiplied by the factor F^2 as suggested by Eq. (2), while the second term takes care of the incoherent part of the diffusely scattered intensity, which was of course entirely neglected in Debye's work.

Eq. (4) may be subjected to experimental test. In sylvine crystal, KCl, the two kinds of atom have very nearly the same size and mass, so that the lattice can be treated as if it were a simple cubic one, to which the expression (1) for M properly applies. Unfortunately no experimental data in this case are available for this test. In the next section a comparison of Eq. (4) with experiments described by Jauncey[15] and Jauncey and May[16] on the scattering of x-rays by rocksalt crystal will be made.

III. Comparison with Experiments

Jauncey and May[16] have recently reported experiments on the absolute measurements of the intensity of the x-rays diffusely scattered from a single rocksalt crystal. Owing to experimental difficulties, filtered x-rays of wave-lengths ranging from 0.3A to 0.9A were employed. According to these authors the spectrum of the x-rays scattered from the crystal shows two very distinct maxima at 0.40A and 0.71A and therefore the average wave-length of the primary x-rays can be roughly taken as 0.545A. The units adopted in this absolute measurement are as follows. According to Thomson's theory, the linear scattering coefficient s per unit solid angle in the direction of the scattering angle θ should be given by

[12] Breit, Phys. Rev. **27,** 242 (1926).
[13] P. A. M. Dirac, Proc. Roy. Soc. **A111,** 405 (1926).
[14] G. Wentzel, Zeits. f. Physik **43,** 1 and 779 (1927).
[15] G. E. M. Jauncey, Phys. Rev. **20,** 421 (1922).
[16] Jauncey and May, Phys. Rev. **23,** 128 (1924); Also Jauncey, Phys. Rev. **20,** 405 (1922).

$$s = \frac{NZe^4}{2m^2c^4}(1 + \cos^2\theta). \tag{5}$$

The value of s obtained from (5) when $\theta = 90°$ is taken as the unit of scattered intensity. The experimental results for s in these units determined by Jauncey and May are plotted against θ as curve I in Fig. 1. It is seen that the experimental curve has two maxima, one at 30° and the other at 15°. These are ascribed by Jauncey and May to be corresponding to the two maxima in the scattered spectrum just mentioned.

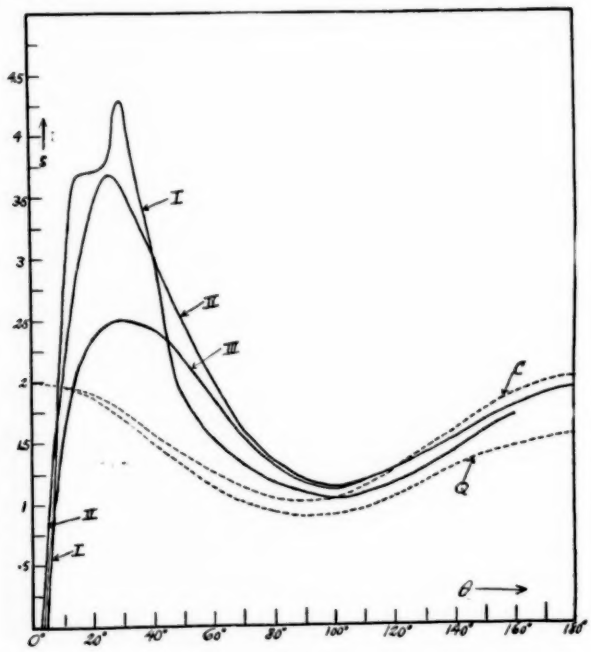

Fig 1.

Strictly speaking, Eq. (4) is not applicable to the case of rocksalt crystal, for the expression of M is calculated for a simple cubic lattice composed of atoms of one kind, whereas the rocksalt contains atoms of Na and Cl. Each kind of atom should have its own values of F as well as its own value of B. To a first approximation, however, we may treat the crystal rock-salt as simple cubic, composed of atoms whose mass is the mean of those of sodium and chlorine and whose atomic number is equal to 14. Keeping this in view, a calculation is made of the intensity of the scattering of x-rays by a rock-salt crystal according to Eq. (4) for a wave-length equal to 0.545A. Taking the characteristic temperature of rock-salt as 281°, we get from Debye's formula

$$B = M = 0.69\frac{\phi(x)}{x}\frac{1 - \cos\theta}{\lambda^2},$$

so that according to Waller the exponent should be

$$B = 2M = 1.38 \frac{\phi(x)}{x} \frac{1 - \cos\theta}{\lambda^2},$$

where the wave-length is in angstrom units. The value of T for the experiments of Jauncey and May is assumed to be 290°K. The values of F^2 are taken as $(F_1^2+F_2^2)/2$ and those of F^2/Z as $(F_1^2/Z_1+F_2^2/Z_2)/2$ where the indices 1 and 2 refer to Na and Cl respectively. In each case the F curve was estimated from the atomic field of Thomas and Fermi. The results of this calculation in the units adopted by Jauncey and May are plotted as curves II and III in Fig. 1. While the curve II shows the results calculated for $B=2M$, the curve III represents those for $B=M$. In both cases, zero-point energy is assumed to exist. If such energy is not assumed, the peak corresponding to the maximum scattering will be slightly depressed. Considering the approximate nature of the calculation as well as the uncertainties regarding the wave-length and the intensity distribution of the primary rays, the agreement between the theoretical curve II and the experimental curve I should be regarded satisfactory. Better agreement could be obtained if the average or effective wave-length be assumed to be shorter than 0.545A. This is certainly not inconsistent with the conditions of Jauncey and May's experiments, but it seems unnecessary to do it here. Thus we may conclude that, on the whole, the experiments of Jauncey and May support Eq. (4) for the case $B=2M$ as calculated by Debye and Waller. This is in accord with the experimental results recently reported by James and Firth[5] and others.[6] Since the peak in curve II will be depressed by assuming no zero-point energy, this comparison seems to suggest the existence of such energy. This is in agreement with the conclusion recently drawn by Waller, James and Hartree.[17] This, however, can not be considered certain, as the comparison made here is of an approximate nature. In order that definite conclusion could be obtained, it is desirable that data be secured on the scattering of homogeneous x-rays.

It is interesting to note that the theory agrees closely with experiment in predicting the positions of the maximum and the minimum in the intensity curve. It is also satisfactory that the theory and experiment agree about the change of the position of the maximum scattering with the wave-length of the primary beam.

In an early paper by Jauncey,[18] the variation of the scattering of x-rays ($\lambda=0.28$A) by rocksalt with temperature has been studied. The results obtained by Jauncey are summarized in Table I. The theoretical values given in the third and fourth columns were calculated by Jauncey from Debye's formula. The average atomic weight of NaCl was taken as 29 and Θ as 260°K. Taking $\Theta=281°$ a calculation is made of the scattering from rocksalt according to Eq. (4) and the results are compared with Jauncey's experi-

[17] Waller and James, Proc. Roy. Soc. **A117,** 214 (1927). James, Waller and Hartree, Proc. Roy. Soc. **A118,** 334 (1928).

[18] G. E. M. Jauncey, Phys. Rev. **20,** 421 (1922). In the same paper Jauncey has also described experiments for a calcite crystal. As calcite is not even approximately simple cubic, we shall not discuss it here.

mental data in Table II. Though the numerical agreement between theory and experiment seems to be very much improved, this comparison rather indicates that, owing to the presence of the incoherent term, experiments of this type will not give data for a test of the present theory.

TABLE I

Scattered Intensity at 568°K. / Scattered Intensity at 290°K.

Scattering angle θ	Experimental value	Theoretical value	
		No zero-point energy	Zero-point energy
15°	1.33	1.87	1.65
30°	1.18	1.37	1.26

TABLE II

Scattered Intensity at 568°K. / Scattered Intensity at 290°K.

θ	Experimental value	Theoretical value			
		$B=M$		$B=2M$	
		No 0-pt. energy	0-pt. energy	No 0-pt. energy	0-pt. energy
15°	1.33	1.69	1.31	1.36	1.28
30°	1.18	1.15	1.11	1.14	1.06

IV. Diffuse Scattering from Sylvine

The close agreement between theory and experiment in the case of rock-salt is extremely interesting, but, in order to place the quantitative treatment of the x-ray scattering on an entirely satisfactory basis, it appears to be of some importance to see whether a similar agreement can be obtained with other crystals. As pointed out above, the sylvine crystal, KCl, can be regarded as if the lattice were simple cubic with a single value of M and the formula (1) properly applies. It seems therefore not out of place here to give briefly a theoretical prediction for this case. Taking $T=290°\text{K}$, $\lambda=0.71\text{A}$, $\Theta=230°\text{K}$, $\mu=6.15\cdot10^{-23}\text{g}$, a calculation is made of the intensity of diffuse scattering from KCl according to Eq. (4). M is found to be $1.72(1-\cos\theta)$ for the existence of zero-point energy and is $1.39(1-\cos\theta)$ for the absence of zero-point energy. Since KCl is generally regarded as ionic lattice, the F curve is calculated as if the atom had an atomic number equal to 18. The results of this calculation are shown in Fig. 2, where the linear scattering coefficient per unit solid angle in the units adopted in section 3 is plotted against the scattering angle θ. The curves I and I′ represent the results cal-

culated for $B=M$ and the curves II and II′ represent those for $B=2M$. In each case the prime curve refers to the theoretical data calculated without zero-point energy. The broken curves marked C and Q are plotted according to the theories of Thomson and Breit-Dirac respectively. It will be noticed that absolute measurements performed with homogeneous x-rays should easily test these predictions. These measurements may perhaps also offer direct information regarding to the zero-point energy, since the differences between the intensities calculated with and without it are considerable, as is shown in Fig. 2.

In this connection it may be mentioned that experiments performed with a single crystal of a metallic element such as Al should also furnish valuable data for testing the present theory.

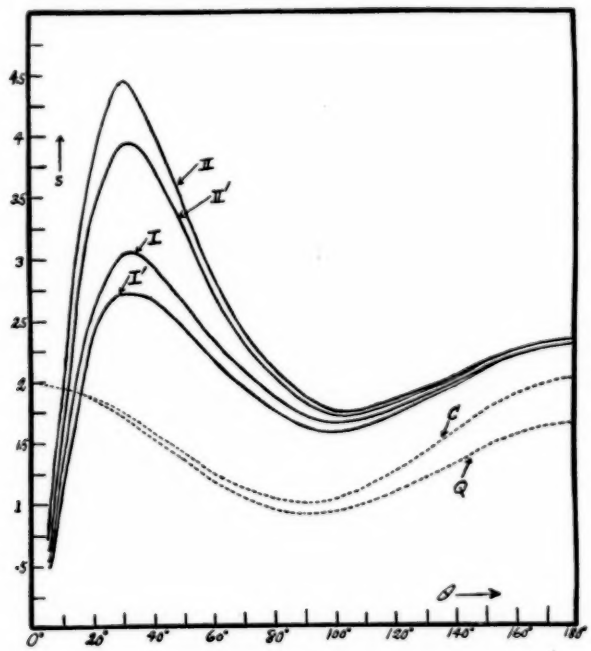

Fig. 2.

V. Discussion

A formula for the intensity of diffuse scattering of x-rays from a crystal has been obtained, which agrees fairly well with the experimental results for rocksalt. That is, the theory seems to account for the so-called excess scattering, for the small scattering in the region of 0° scattering angle, for the position of the maximum scattering as well as the shift of this position with the wave-length of the incident x-rays, for the occurrence of the minimum scattering at about 100° instead of at 90°, and finally for the general departure of the scattering curve from that predicted by Thomson's theory. It should be noted, however, that, according to Eq. (4), the coherent part of the diffuse scattering disappears when the temperature approaches absolute

zero. This means that, the coherent rays at any angle other than that nearly satisfying Bragg's law should be completely extinguished by interference, if the atoms in the crystal have no thermal agitation. This is to be expected, because the present theory is developed for a single crystal in which the atoms are supposed to be arranged with perfect regularity. It is clear that the present theory will not be applicable to the scattering of x-rays by the so-called amorphous substances such as graphite, in which minute crystals are present. In these substances, the arrangement of the atoms evidently introduces a type of irregularity which must make the interference incomplete even though the heat-motions are absent. On this account diffuse scattering will occur which is probably proportional to

$$\left[1 - \frac{\Omega}{V} f(u)\right]$$

as suggested by the recent work of Debye.[19] In this expression Ω is the total volume of the action spheres of all the atoms (or molecules) effective in scattering, V is the volume of the scattering substance and $f(u) = (3/u^3)$ $(\sin u - u \cos u)$, where $u = (8\pi a/\lambda) \sin \theta/2$, a is the radius of the scattering atom (or molecule), λ and θ have their usual significance. The function $f(u)$ has a value 1 when $u = 0$. For solids and liquids Ω/V may be taken as unity. Thus the total coherent intensity of the x-rays diffusely scattered by an amorphous substance should be proportional to

$$[(1 - e^{-\beta}) + (1 - f(u))]F^2. \tag{6}$$

This explains the experimental fact recently reported by Jauncey and Bauer[20] that there is no effect of temperature on the ratio of modified to unmodified rays in the Compton effect. For, under the conditions of Jauncey and Bauer's experiments, only a negligible portion of the coherent intensity will be influenced by temperature as indicated by the expression (6), while the incoherent part is independent of temperature as already remarked. These considerations seem to play a very important role in accounting for the intensity of the x-rays scattered by an amorphous substance as well as for the energy distribution between the modified and the unmodified rays in the Compton effect. A detailed discussion will be reserved for another paper.

As mentioned in the introduction, the effect of temperature on the diffuse scattering has also been investigated by Faxen[2] and Waller.[3] Since, however, the predictions of the theories of these authors seem not to fit with experimental facts which have come to light, we shall not enter into a discussion here.

In conclusion the writer wishes to express his appreciation of the inspiration of his former teacher, Professor A. H. Compton of University of Chicago, U. S. A.

[19] P. Debye, Jour. of Math. and Phys., M.I.T. **4,** 133 (1925) and in German Phys. Zeits. **28,** 135 (1927).

[20] Jauncey and Bauer, Phys. Rev. **34,** 387 (1929).

EXPERIMENTAL ELECTRON DISTRIBUTIONS IN ATOMS OF MONATOMIC GASES

By E. O. Wollan
Ryerson Physical Laboratory, University of Chicago

(Received May 25, 1931)

Abstract

The radial electron distribution in the atoms of helium, neon, and argon is calculated from the writer's recent data for the intensity of x-rays scattered by gases. These curves are found to be in good agreement with similar curves derived from wave mechanics. They represent the electron distribution for the atom in a state of rest and hence show more detail than similar curves calculated with the aid of crystal reflection data. In the case of neon, the experimental data are sufficiently complete to separate the K and L electrons. The smaller radius of these levels in argon make such a resolution impossible for the wave-length of the x-rays used. A comparison of the U curve for argon and with the same curve for the chlorine ion from NaCl at 0°K shows the presence of zero point energy for the ion in the space lattice of the crystal.

Introduction

NOT long after it was shown that measurements of the diffraction of x-rays by crystals gave information regarding the positions of the atoms within the crystal, it was realized that these same data would also give an idea of the distribution of electrons within the atoms of which the crystal was composed. The first calculations of this kind were quite indirect, depending on making various guesses as to the function which would best represent the electron distribution and testing them out by comparing the resulting intensities with the experimental values.

Through the work of Bragg,[1] Compton,[2] Duane,[3] and others the trial and error method was replaced by a more direct calculation of the electron distribution involving the use of Fourier's series.

Although studies of this kind have led to a number of interesting results, there are certain inherent difficulties in the crystal method which can be only partially eliminated. I will briefly mention some of these limitations since they are indirectly connected with this problem.

In making measurements on single crystals difficult corrections for primary and secondary extinction must be made which decrease the precision of the measurement. However, in a large number of crystals the extinction may be reduced to a negligible quantity by grinding the crystal to a very fine powder, and wherever intensity permits, this method is generally employed.

The thermal motion of the atoms has a large effect on the intensity in the higher orders of reflection. If the data are used without correction for this motion the resulting distribution curves give a diffuse picture of the atom

[1] W. H. Bragg, Phil. Trans. Roy. Soc. **215**, 253 (1915).
[2] A. H. Compton, X-rays and Electrons.
[3] W. Duane, Proc. Nat. Acad. Sci. **11**, 489 (1925).

with practically no detail. However, if a given type of thermal motion is assumed, it is possible to get the electron distribution curve corresponding to the atom at rest if measurements of the intensity are made for various temperatures.

Not all crystals permit of a solution for the structure factor corresponding to the individual atoms in the crystal. One difficulty in this connection is that of knowing the association of the valence electron. In analysing the reflection from crystals it has been generally assumed that the atoms exist as ions in the space lattice. It seems that this is not strictly true, but that the valence electron is part of the time associated with the parent atom. Because of this overlapping of the adjacent layers of atoms in the crystal, it does not seem possible by the crystal reflection method to analyse completely the electron distribution in the individual atoms.

In view of the difficulties associated with determining electron distribution from intensity measurements on crystals it is of considerable interest that measurements of the intensity of scattering of x-rays by monatomic gases gives data which are free from these objections. In such gases the interference effect takes place within the individual atoms and not between an atom and its neighbor. This means that thermal agitation and zero point energy play no part in the scattered intensity. One can also make intensity measurements to as small angles as the apparatus will permit and there is no doubt about the number of electrons effective in scattering at zero angle. Although these advantages have been realized for some time an obstacle has stood in the way of utilizing the data thus obtained.* Unlike the regular reflection of x-rays from crystals the intensity of scattering from gases is altered by the presence of the Compton effect. The difficulties which this introduced were only recently overcome by Compton[4] using the solution which Wentzel[5] and Waller[6] had obtained for the scattered intensity on the basis of wave mechanics.

Compton has shown that one can express the density of electrons in the atom by a Fourier integral of the form

$$U(r) = Zr \int_0^\infty B \sin(\pi r x) dx$$

where $U(r)$ represents the number of electrons per angstrom at a distance r from the center of the atom, Z is the atomic number, B depends on the intensity of scattering and is given by

$$B = 2\pi x \left\{ \frac{S-1}{Z-1} \right\}^{1/2}$$

* Rough estimates of electron distribution from data on diffuse scattering by "amorphous" substances have been made by A. H. Compton (Washington University Studies **8,** 98 (1921), X-rays and Electrons p. 79), which agree qualitatively with the results here obtained. A correction similar to that for the Compton effect was made by assuming that the size of the electron was comparable with the wave-length.

[4] A. H. Compton, Phys. Rev. **35,** 925 (1930).

[5] G. Wentzel, Zeits. f. Physik **43,** 1 and 779 (1927).

[6] I. Waller, Phil. Mag. **4,** 1228 (1927).

where S is the scattering per electron** at $x = 4/\lambda \sin(\phi/2)$.

Having measured the values of S the integral can be solved for $U(r)$. It is usually necessary to make part of the solution graphically, and for large values of x some algebraic curve can be fitted to B which will admit of direct integration to infinity. An example of this type of calculation has been given by Compton.

The intensity measurements on which this paper is based were recently made by the writer [7] and here only the electron distribution curves will be discussed.

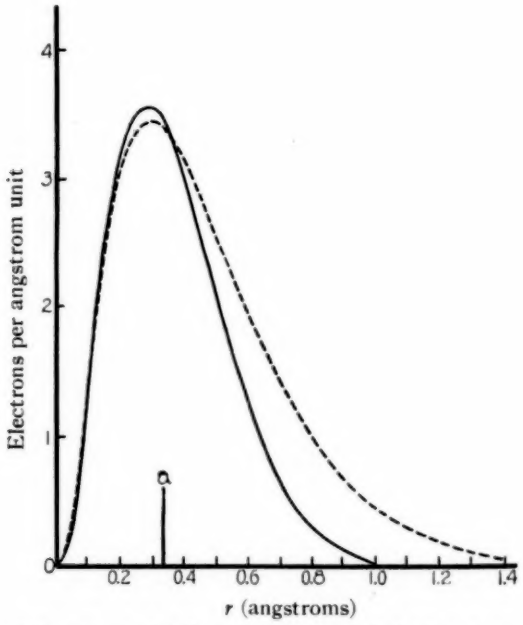

Fig. 1. Radial electron distribution in helium. Solid line from experiment, broken line from wave mechanics.

HELIUM

Calculations of electron distribution from measurements of the intensity of x-rays scattered by gases have been made by Compton using the experimental data of Barrett[8] for helium. He gets a distribution which is in good agreement with a corresponding curve worked out on the basis of wave mechanics. He has also shown[9] that the resulting distribution curves cannot be reconciled with Schrödinger's idea of a continuous distribution of electricity but are in excellent agreement with Heisenberg's interpretation of $\lambda\lambda^*$ as the probability of a discrete electron being present at a given point.

** S_x represents the classical value of the scattering per electron. Its relation to the experimental value can be found in refs. 7 and 5.

[7] E. O. Wollan, Phys. Rev. **37,** 862 (1931).

[8] C. S. Barrett, Phys. Rev. **32,** 22, (1928).

[9] A. H. Compton, Technology Review **33,** 19, (1930), Jour. Opt. Soc. **21,** 81, Fig. 6, (1931).

The solid line of Fig. 1 represents the electron distribution for helium as calculated from the writer's data. The maximum lies at a slightly smaller value of r than the above mentioned curve from the data of Barrett. Here the broken line represents the same function derived by Hartree[10] from wave mechanics. There is seen to be good agreement at least regarding the maximum and the inner part of the atom. At larger values of r the experimental curve indicates a less diffuse atom. The difference is perhaps within the experimental errors of the determination which rapidly become greater for larger values of r. The first Bohr orbit as calculated by Pauling[11] comes at 0.33A, slightly farther out than the maximum of either of these curves.

Although the data for helium here used are in fairly good agreement with those of Barrett they are slightly lower for all values of the scattering angle ϕ. This may be due to slight impurities which Barrett suspected in his helium. One advantage of the data used here is the fact that measurements were carried to smaller values of ϕ so that the B curve is more completely determined.

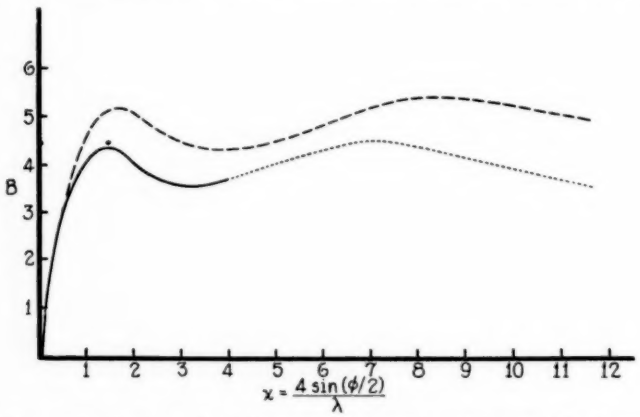

Fig. 2. Broken line B curve for Na^+ from wave mechanics, solid line experimental part of B curve for neon, dotted line shows how this curve was extrapolated to get electron distribution in neon.

Neon

In calculating the electron distribution for the neon atom the extrapolation of the B curve becomes more difficult. Although B must approach zero for large values of x, it is still increasing at the largest values of x used in the experiments. As is evident from Fig. 2, the B curve must accordingly reach a maximum for some value of x greater than 4. To get as logical an extrapolation of this curve as possible, the F values corresponding to the electron distribution for the Na^+ ion calculated by James and Waller and Hartree[12] from wave mechanics were determined for large values of x. This curve is shown by the broken line in Fig. 2. The solid line represents the B curve from the experimental data and the dotted line shows how this curve was extrapolated to get the electron distribution in neon. Almost any reasonable extrapolation would

[10] D. R. Hartree, Proc. Am. Phil. Soc. **24,** 89 (1928).
[11] L. Pauling, Proc. Roy. Soc. **A114,** 181 (1927).

give a distribution curve not far different from the one shown in Fig. 3 and in any case the K and L shells would be resolved. The electron distribution curve for neon is in good agreement with that for the Na^+ ion calculated from wave mechanics. The Na electrons are concentrated closer to the center of the atom as one would expect due to the larger nuclear charge.

In this case the x-ray instrument has an optical resolving power sufficient to show most of the details of the atom. The resolving power could be increased by measuring the intensity at larger angles or decreasing the wave-length of the radiation. These are the same factors which affect the resolving power of a microscope.

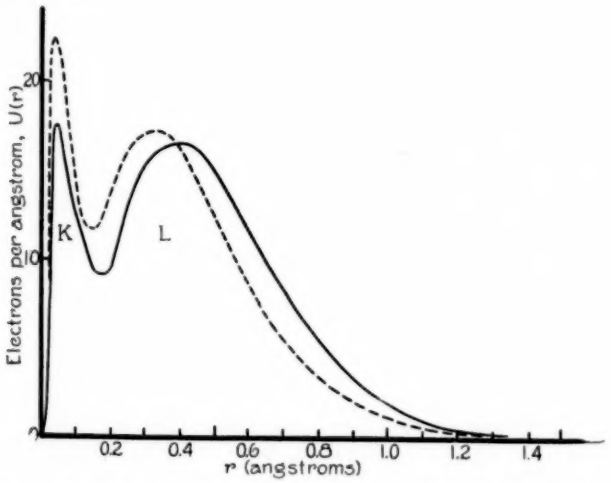

Fig. 3. Radial electron distribution curves. Solid line neon from experiment, broken line Na^+ from wave mechanics.

Argon

An inspection of the F curve for argon and the corresponding curve from wave mechanics for $\frac{1}{2}(K^+ + Cl^-)$, Fig. 4, will show that the agreement is very satisfactory. One would therefore expect to get an electron distribution curve which would also agree with the corresponding wave mechanics curve.

If one extrapolates the experimental B curve as shown by the dotted line of Fig. 5 the U curve for argon shown in Fig. 6 is obtained. The points on the curve for values of r greater than 0.5A fluctuated somewhat and the dotted curve represents the mean values. This electron distribution curve does not show the detailed structure in the K and L shells that is present in the theoretical curve.[13] The difference must be due to a detailed structure in the B curve for larger values of x than those reached in these experiments.

Here is a case where the x-ray microscope did not have sufficient resolving power to bring out the finer structure of the atom. If the wave-length were decreased it is possible that a distinct resolution of the K and L electrons could be affected.

[12] R. W. James, I. Waller and D. R. Hartree, Proc. Roy. Soc. **A118,** 334, (1928).
[13] R. W. James and G. W. Brindley, Proc. Roy. Soc. **A121,** 155 (1928).

Fig. 7 shows a comparison of the electron distribution curve for argon with the similar curve derived from crystal reflection data for Cl^- at 0°K and

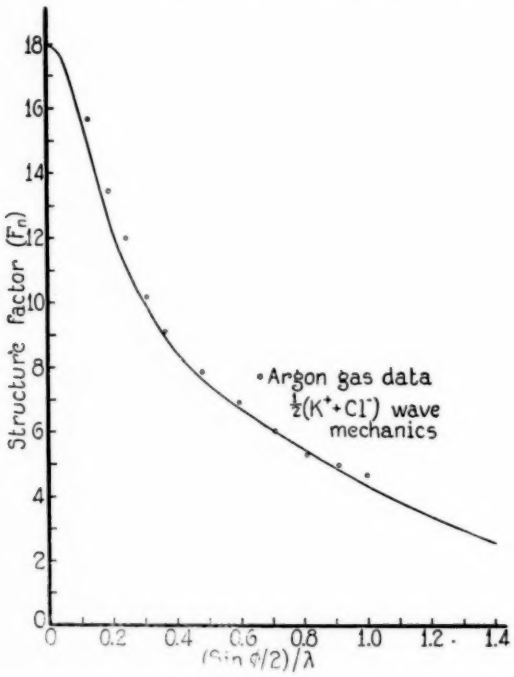

Fig. 4.

900°K. The electron distribution curves for the Cl^- ion were calculated from the data of James and Firth[14] for NaCl and the value at 0°K was gotten with

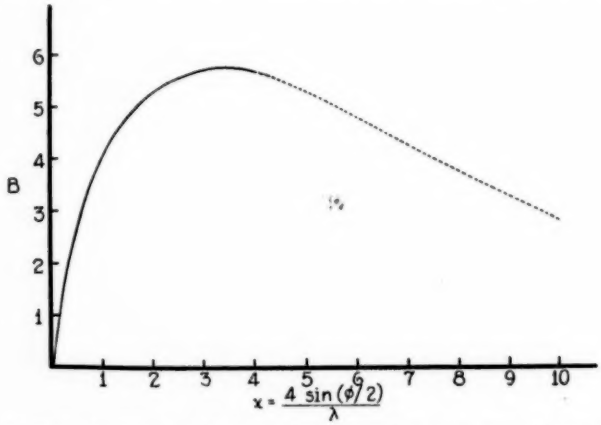

Fig. 5. Experimental and extropolated portion of *B* curve from which electron distribution in argon was determined.

the aid of the Debye-Waller temperature factor. The effect of thermal motion in the chlorine ion is quite apparent in the increased distance of the peaks of

[14] R. W. James and Elsie M. Firth, Proc. Roy. Soc. **A117,** 62 (1927).

electron density from the center of the atom as the temperature increases from 0° to 900°K. Similarly, the fact that the chlorine peak for 0°K is at a considerably greater distance than the argon peak, is strong evidence for zero point

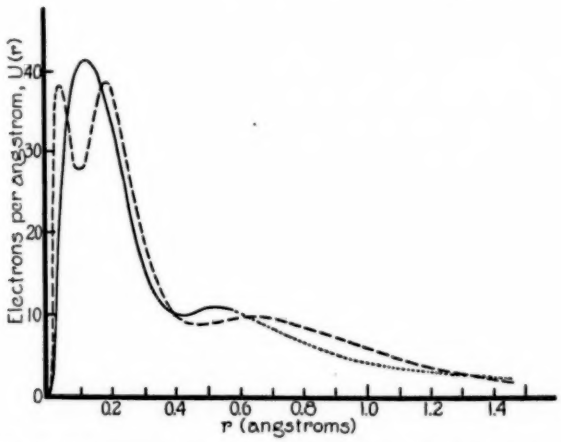

Fig. 6. Radial electron distribution curves. Solid line argon, broken line average of K^+ and Cl^- ions from wave mechanics.

motion of the chlorine ions.* James and Firth have reached the same conclusion by comparing their observed crystal reflection data with that calculated

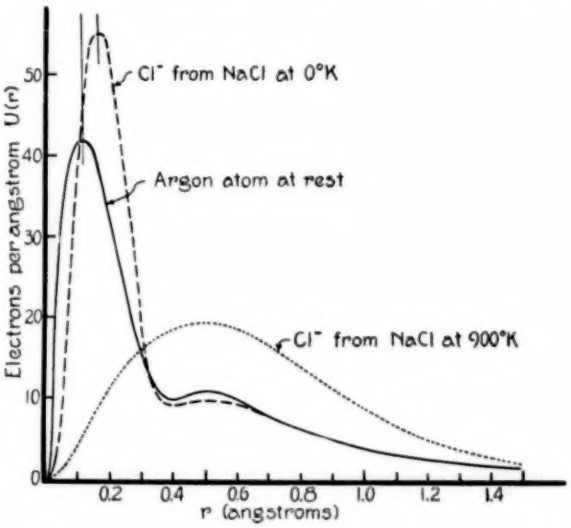

Fig. 7. Electron distribution curves showing effect of thermal agitation and zero point energy.

from wave mechanics. The present evidence however avoids the assumption of any theory of atomic structure.

* A suggestion of zero point energy was made on the basis of preliminary scattering data from argon by A. H. Compton, Technology Review **33,** 19 (1930).

Conclusion

The application of intensity measurements of x-rays scattered by gases to the determination of electron distribution curves gives results which are in agreement with those derived from wave mechanics. The curves represent the electron distribution for the atom in a state of rest and hence show greater detail than similar curves derived from crystal reflection data.

The difference between the electron distribution in argon and Cl^- at 0°K is good evidence for the existence of zero point energy.

The B curves and the electron distribution curves of neon and argon show a relation of optical resolving power to the wave-length and aperture analogous to that of a microscope. The information regarding the structure of the atom which one gets in this way is probably as reliable as would be gotten if an optical system could be devised to handle x-rays as can be done for visible light.

The writer takes pleasure in acknowledging the assistance and helpful suggestions which he has received from Professor A. H. Compton.

THE ANOMALOUS SCATTERING OF ALPHA-RAYS

By Morris Muskat
Gulf Research Laboratory

(Received May 23, 1931)

Abstract

The well-known wave mechanical expression giving the scattering function, to a first approximation, as an integral over the potential field of the scattering system, is inverted so as to give the potential field as an integral over the observed intensity of scattering. This is applied to the problem of determining the potential field causing the anomaly in the α-ray scattering by Mg as observed by Rutherford and Chadwick and Bieler. This anomaly, defined as the difference between the observed scattered intensity and that predicted theoretically on the basis of a Coulomb potential field, is represented by an empirical analytic expression in two different ways. It is shown that the potential fields for both representations as derived by the above-mentioned inversion are essentially the same, and their form depends almost entirely on the single fact that the curve for the anomaly shows a marked minimum. In magnitude, this potential field never exceeds 10 percent that of the Coloumb potential. It oscillates in sign, and falls off very rapidly as one recedes from the scattering atom. It is pointed out that the small numerical value and oscillatory character of this potential field is in marked contrast to the assumptions that have been made hitherto, most of which have been that the potential is of the form of $1/\rho^n$, $n \geqq 2$, ρ being the distance from the center of the nucleus. It is finally noted that if the derived potential field is given an electrostatic origin it is equivalent to a series of shells of alternating sign of charge with a spacing of the order of 1.5×10^{-13} cm. This is just the inference drawn by Rutherford and Chadwick as to a possible cause for the anomaly.

A NUMBER of attempts have been made recently to explain the anomalous scattering of alpha-rays by the wave mechanics.[1] Just as in the case of the classical investigations of this problem,[2] the method used has been that of assuming a certain potential field to represent the scattering atom and computing from this the intensity of scattering to be expected. To the extent that this calculated intensity agreed with that observed experimentally, the assumed potential field has been considered as a correct representation of the atomic system.

In the present paper the potential field will be computed directly from the observed intensity of scattering according to a formula given in a recent "Letter to the Editor."[3] It will be shown that the anomalous part of the intensity observed by Rutherford and Chadwick and by Bieler[4] may be ex-

[1] A. C. Banerji, Phil. Mag. **9,** 273 (1930); G. Beck, Zeits. f. Physik **62,** 331 (1930); H. S.W. Massey, Roy. Soc. Proc. **A127,** 671 (1930); C. Moller, Zeits. f. Physik **62,** 54 (1930); **66,** 513 (1930); Nature **125,** 459 (1930). T. Sexl, Naturwiss. **18,** 247 (1930); Zeits. f. Physik **67,** 766 (1931).

[2] E. S. Bieler, Proc. Camb. Phil. Soc. **21,** 686 (1923); P. Debye and W. Hardmeier, Phys. Zeits. **27,** 196; 574 (1926).

[3] M. Muskat, Phys. Rev. **35,** 1583 (1930).

[4] E. Rutherford and J. Chadwick, Phil. Mag. **50,** 889 (1925); E. S. Bieler, Roy. Soc. Proc. **A105,** 434 (1924).

plained by a potential field whose magnitude never exceeds 10 percent that of the Coulomb field, which oscillates in sign, and falls off very rapidly as one recedes from the scattering system.

Following the previous investigations on electron and alpha-ray diffraction problems, Born's perturbation theory will be taken as the basis for the computations, and it will be assumed that the potential fields in question are static and spherically symmetrical. On these assumptions the diffracted wave, at a distance r from the center of the scattering system, is given, to a first approximation, by

$$\psi_1 = -\frac{8\pi^2 m e^{ikr}}{h^2 ur}\int_0^\infty \rho V(\rho)\sin\rho\, u d\rho, \tag{1}$$

where m is the mass of the scattered particle, of velocity v, $V(\rho)$ is the potential energy of the particle at a distance ρ from the center of the diffracting system, and $u=(4\pi mv/h)\sin\theta/2=2k\sin\theta/2$, θ being the angle of scattering. Eq. (1) shows that to this approximation the amplitude of the scattered wave depends linearly on the potential field of the scattering atom.

Although the Coulomb value for $V(\rho)$ would make the integral in Eq. (1) diverge, the exact solution[5] of the problem for a Coulomb field shows that the classical Rutherford-Darwin value for $|\psi_1|^2$ is obtained. If then, it be supposed that the anomaly in the observed scattering is caused by a deviation, $V_1(\rho)$, from the Coulomb potential, Eq. (1) may be written as

$$\psi_1 = \psi_R - \frac{8\pi^2 m e^{ikr}}{h^2 r\, u}\int_0^\infty \rho V_1(\rho)\sin\rho\, u d\rho \tag{2}$$

where ψ_R is the Rutherford-Darwin value of ψ_1, namely

$$\psi_R = -\frac{16\pi^2 mZe^2}{h^2 r\, u^2}e^{ikr} \tag{2a}$$

Z being the atomic number of the element upon which the α-rays are falling.

The separation of ψ_R from the integral in Eq. (2) can be justified with somewhat more rigor if one uses Wentzel's device and represents the Coulomb potential by a term e^{-br}/r and then proceeds to the limit of $b\to 0$. However the use of Born's first approximation seems to have been seriously questioned in the last papers by Möller and Sexl. Still Möller shows in detail that the strict Coulomb potential is anomalous in that the first approximation gives the accurate solution although the second approximation is infinite. As it does not seem reasonable that on adding to the Coulomb potential a small perturbation, such as we shall find our V_1 to be, this anomalous validity of Born's first approximation should be vitiated, it has been explicitly assumed as the basis of our analysis.

The observed scattered intensity is given by $\psi_1\psi_1^*$. If this, considered as a function of u, does not fall to 0 as long as u is finite, one can take for ψ_1 simply the quantity e^{ikr} times the positive or negative square root of the numerical

[5] W. Gordon, Zeits. f. Physik **48,** 180 (1928).

value of the observed scattering. Removing this factor through the substitution

$$\psi = Se^{ikr} \tag{2b}$$

Eq. (2) becomes

$$S_1 - S_R = -\frac{8\pi^2 m}{h^2 ru}\int_0^\infty \rho V_1(\rho)\sin \rho u d\rho \tag{2c}$$

where now, since S_R is numerically negative, the negative value of $\sqrt{\psi_1\psi_1^*}$ will be taken in determining S_1. The left hand side is then to be interpreted as the anomaly in the observed scattering, expressed as a function of u.

Considering now S_1-S_R as experimentally determined, Eq. (2c) is an integral equation determining the potential $V_1(\rho)$ causing the anomaly in question. Supposing that both $\rho V_1(\rho)$ and $u(S_1-S_R)$ satisfy the Dirichlet conditions and vanish at ρ and $u=0$ Eq. (2c) is a Fourier integral equation, the solution of which is obtained by inversion, as

$$\rho V_1(\rho) = -\frac{h^2 r}{4\pi^3 m}\int_0^\infty u(S_1 - S_R)\sin \rho u du. \tag{3}$$

This is equivalent to (2) of our previous note, except that there the scattering was considered as a whole. As is there pointed out, the functional form of S_1-S_R is to be used in (3), since $\psi_1\psi_1^*$ cannot be experimentally determined for values of u greater than $2k=4\pi mv/h$.

This equation will now be applied to the anomalous scattering of alpha-rays as observed by Rutherford and Chadwick, and Bieler.[4] The experimental data of Bieler were plotted as $(S_1/S_R)^2$ against θ and those of Rutherford and Chadwick were plotted as $(S_1/S_R)^2$ against the reciprocal of the energy of the alpha-rays. Massey[1] has combined both sets of data and plotted them as $(S_1/S_R)^2$ against $v\sin\theta/2$. The curve given by Massey for Mg has been recomputed so as to be in a form suitable for our purposes. The result is the continuous curve in Fig. 1, the circles being the experimental points indicated in Massey's graph.

It may seem that the continuous curve in Fig. 1 is hardly sufficient to determine a *functional form* for S_1/S_R. Nevertheless, it is certainly the case that it indicates the fundamental feature of S_1/S_R, which is namely, the pronounced minimum in the curve. And as this minimum has been the difficult feature to explain by the theories thus far developed, we shall content ourselves with stressing just this characteristic of the phenomena. Further, it should be emphasized that this minimum is after all the most significant part of the curve as far as indicating the nature of the potential field of the scattering system, whereas the details of the rise and fall in the curve are relatively quite unimportant. To prove this the data in Fig. 1, will be extrapolated and represented in two quite different functional forms, and it will then be shown that the final value of $V_1(\rho)$, as given by Eq. (3), is essentially the same for both types of representation.

Thus, first, it will be assumed that, contrary to the trend of the data already available, S_1/S_R is symmetrical about the minimal value of u, and is in fact given by an inverted error curve, asymptotic to the value, $S_1/S_R=1$. That is,

$$\frac{S_1}{S_R} - 1 = -Ae^{-q^2(u-u_0)^2} \tag{4}$$

the constants having the values: $A=0.45$; $q=2.42\times10^{-13}$; $u_0=2.1\times10^{13}$.

Secondly, as a less violent extrapolation from the experimental data S_1/S_R will be assumed to be unsymmetrical about the minimal point, the

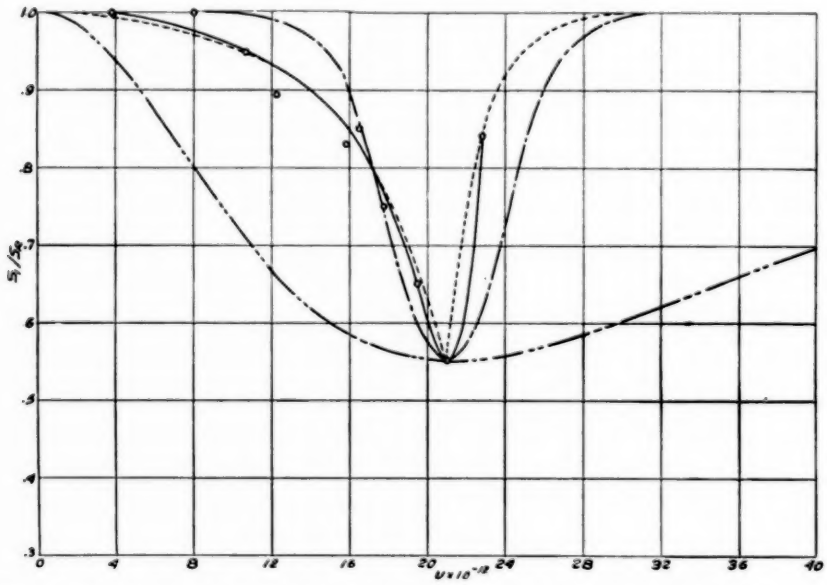

Fig. 1. Experimental and theoretical scattering ratios plotted as a function of $u=2k\sin\theta/2$.
o: Experimental points;—Massey's curve, recomputed; — — — assumed ratios according to Eq. (4); - - - - assumed ratios according to Eq. (5) — — — — Scattering ratios if $V_1=-ce^{-\alpha\rho}$.

assymmetry being such that the curve for S_1/S_R will follow closely the empirical data as far as it goes. For this case, then

$$\left.\begin{aligned} \frac{S_1}{S_R} - 1 &= -Ae^{a_1(u-u_0)} \qquad u \le u_0 = 2.1\times10^{13} \\ \frac{S_1}{S_R} - 1 &= -Ae^{a_2(u_0-u)} \qquad u \ge u_0 = 2.1\times10^{13} \end{aligned}\right\} \tag{5}$$

$$A = 0.45;\ a_1 = 21\times10^{-14};\ a_2 = 5.76\times10^{-13}.$$

The graphs corresponding to these functional forms for S_1/S_R are given in Fig. 1 as the dotted curves. In spite of the difference between these curves, the functions $V_1(\rho)$ determined from them will be seen to differ only inappreciably.

To determine $V_1(\rho)$ one has now to insert Eqs. (4) and (5) into Eq. (3) and evaluate the integrals. For both cases the integrals are of the form

$$\rho V_1(\rho) \sim \int_0^\infty \frac{f(u) \sin \rho u}{u} du$$

taking into account the value of ψ_R given in Eq. (2a). As in neither case a direct evaluation has been possible, the above integral has been rewritten as

$$\int_0^\infty \frac{f(u) \sin \rho u}{u} du = \int_0^\rho d\rho \int_0^\infty f(u) \cos \rho u du.$$

This is permissible since for such functions $f(u)$ as correspond to Eq. (4) and (5) the integral $\int_0^\infty f(u) \cos \rho\, u du$ is uniformly convergent in ρ. After evaluating the inner integral, the integration with respect to ρ was carried out graphically.

Thus, in the case of Eq. (4) the integral to be evaluated first is

$$I = \int_0^\infty \cos \lambda z e^{-(z-p)^2} dz$$

where $\lambda = \rho/q$ and $p = qu_0$. As even this has not been found in the standard texts the method used to evaluate it approximately will be indicated.

It may be readily verified that I, as a function of λ, satisfies the differential equation

$$\frac{d^2I}{d\lambda^2} + \lambda \frac{dI}{d\lambda} + \left(p^2 + \frac{1}{2} + \frac{\lambda^2}{4}\right) I = -\frac{p}{2} e^{-p^2}.$$

It follows that I may be written in the form:

$$\left.\begin{aligned} I &= \left(\frac{\pi^{1/2}}{2} + \int_0^p e^{-z^2} dz\right) e^{-\lambda^2/4} \cos p\lambda - \frac{e^{-p^2-\lambda^2/4}}{2} \int_0^\lambda e^{z^2/4} \sin p(\lambda - z) dz \\ &\leqq \left(\frac{\pi^{1/2}}{2} + \int_0^p e^{-z^2} dz\right) e^{-\lambda^2/4} \cos p\lambda : \lambda < 2p \\ &\leqq \pi^{1/2} e^{-\lambda^2/4} \cos p\lambda : p > 3. \end{aligned}\right\} \quad (6)$$

For large values of λ the asymptotic expansion for I may be used. This is easily found to be

$$I = e^{-p^2} \sum_1^\infty \frac{(-1)^n H_{2n-1}(p)}{\lambda^{2n}} \quad (6a)$$

where H_{2n-1} is the Hermite polynomial of order $2n-1$.

As in the present case $p = qu_0 = 5.08$, the last expression in Eq. (6) suffices for all the present purposes and even when $p\lambda \sim [(2n+1)/2]\pi$ since the correction term is always less than e^{-p^2}/p. Hence

$$\rho V_1(\rho) \leqq \frac{4Ze^2A}{q(\pi)^{1/2}} \int_0^\rho e^{-\rho^2/4q^2} \cos \rho u_0 d\rho \quad (7)$$

where A is defined in Eq. (4). For the case of Eq. (5), the first integration may be carried out directly, with the result that

$$\left.\begin{aligned}\rho V_1(\rho) = -\frac{4Ze^2A}{\pi}\int_0^{\rho} d\rho\Bigg(&\frac{a_1\cos\rho u_0 + \rho\sin\rho u_0 - a_1 e^{-a_1 u_0}}{a_1^2+\rho^2}\\ &-\frac{\rho\sin\rho u_0 - a_2\cos\rho u_0}{a_2^2+\rho^2}\Bigg)\end{aligned}\right\} \tag{8}$$

Eqs. (7) and (8) were evaluated graphically, and the results are plotted in Fig. 2. For comparison the Coulomb potential V_c is included in the figure. It will be seen that the potential $V_1(\rho)$ is for all values of ρ less than even 10 per-

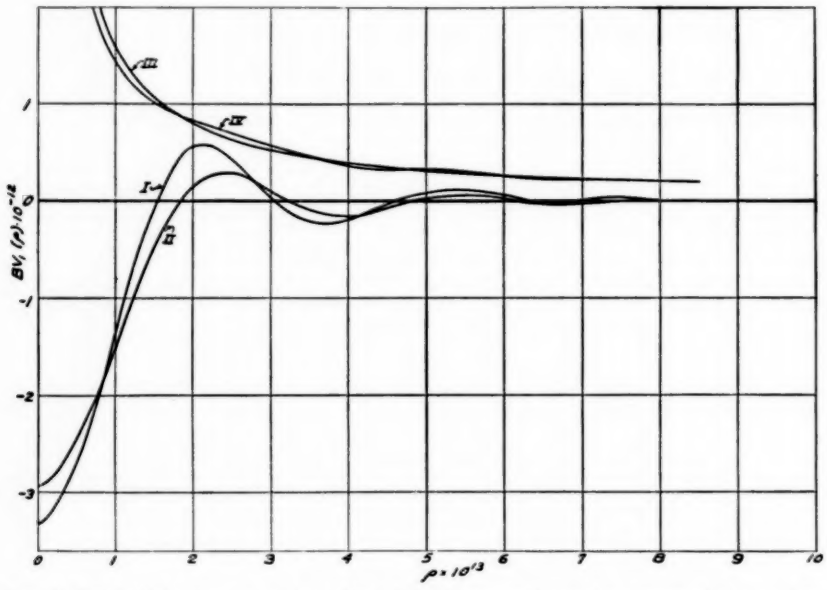

Fig. 2. Potential curves as a function of the distance from the center of the nucleus.
I. $BV_1(\rho)\cdot 10^{-12}$ as computed from Eq. (4); II. $BV_1(\rho)\cdot 10^{-12}$ as computed from Eq. (5); III. $BV_c(\rho)\cdot 10^{-12}$—Coulomb potential; $BV_c=\pi/2\rho$; $B=\pi/4\,Ze^2$; IV. $B(V_c+V_1)\cdot 10^{-12}$—resultant nuclear potential field.

cent of the Coulomb value, and falls off in an essentially exponential manner with increasing ρ. The resultant potential V_c+V_1 is plotted as curve IV in the same figure. This curve shows still more clearly the relative magnitudes of V_1 and V_c in that this resultant curve differs almost inappreciably from the unperturbed Coulomb curve.

The following point must be mentioned. Although for all practical purposes $V_1(\rho)$ as derived from both of the above expressions for S_1/S_R is vanishingly small for $\rho>10^{-12}$cm it is seen from equation (6a) that $\rho V_1(\rho)\sim 1/\rho$ and from Eq. (8) that $\rho V_1(\rho)\sim$const. for very large values of ρ. Thus it appears that the $\rho V_1(\rho)$ that has been derived is not expressible as a Fourier integral although to justify the inversion of the integral in Eq. (2c) one must assume that both the integrability and the Dirichlet conditions are satisfied by

$\rho V_1(\rho)$ as well as equivalent ones by $u(S_1-S_R)$. The reason for this apparent contradiction is obviously that the functional forms of S_1/S_R as given in Eqs. (4) and (5) are such that $u(S_1-S_R)$ also fails to satisfy the conditions assumed for them. To satisfy the latter it is necessary that S_1/S_R-1 and $\partial/\partial u(S_1/S_R-1)$ vanish at $u=0$, and these conditions the expressions in Eqs. (4) and (5) do not fulfill. Fortunately this can be corr cted without altering the above solution in any essential way. Thus, multiplying the right sides of Eqs. (4) and (5) by some factor such as $(1-e^{-\beta^2u^2})$, β being any arbitrary large number, will correct everything; this can be readily verified by carrying through the integration which will show that the non-integrable terms of $\rho V_1(\rho)$ as given in Eqs. (7) and (8) are just cancelled out so as to leave $\rho V_1(\rho)\sim 1/\rho^3$, for $\rho\to\infty$. Furthermore, with sufficiently large values of β the added factor will cause only an inappreciable change in the form of the assumed scattering curve. This at the same time will mean that $\rho V_1(\rho)$ will suffer no essential change for small values of ρ, since the added factor will involve a correction to $\rho V_1(\rho)$ of the order of ρ/β for small values of ρ. One can therefore feel satisfied that under the assumptions already stated the $V_1(\rho)$ presented in the curves of Fig. 2 is the necessary consequence of the scattering curves given in Fig. 1.

That the potential curves computed from Eqs. (4) and (5) are essentially the same is obvious. Certainly the exact value of $V_1(0)$ or the roots of $V_1(\rho)=0$ can have no great significance in view of the uncertainty of S_1/S_R even in the region where experimental data are available. However, the main features of the curves for $V_1(\rho)$ are without question largely determined by the mere existence of the pronounced minimum in the empirical values for ψ_1/ψ_R.

As observed above, the potential function $V_1(\rho)$ never even approaches the value of the Coulomb potential. Although it does oppose the Coulomb potential for the smallest values of ρ it actually aids it for other values. It is of interest to note that both the fact that the above $V_1(\rho)$ is always small as compared to the Coulomb potential and that it oscillates in sign is in marked contrast to the types of potential that have been previously assumed for $V_1(\rho)$. Heretofore, $V_1(\rho)$ has been assumed to be a potential always opposing that due to the Coulomb forces and far exceeding the latter for sufficiently small values of ρ. Thus Banerji, Massey, and Sexl suppose $V_1(\rho)$ to be of the form A/ρ^n where $n\geqq 2$. Moller, in effect, assumes that $V_1(\rho)$ just numerically counterbalances the Coulomb potential, except for a constant, up to a certain value of ρ, after which it vanishes entirely. Involved in such assumptions, for cases where $n>2$, is the difficulty that Eq. (1) diverges, thus necessitating the introduction of an arbitrary distance at which the integration in Eq. (1) is stopped. In the present treatment of the problem, all that has been necessary is the assumption that $\rho V_1(\rho)$ and $u(S_1-S_R)$ are representable as Fourier integrals, an assumption which certainly does not contradict any known empirical data and which involves no arbitrary physical restriction upon the atomic system in question.

It may seem that this assumption with regard to $\rho V_1(\rho)$ and $u(S_1-S_R)$ largely predetermines the oscillatory character of $V_1(\rho)$ and the fact that it is

always small as compared to the Coulomb potential. It is true that it has been explicitly assumed that $\rho V_1(\rho)$ vanishes at $\rho = 0$. However, in the present case even $V_1(0)$ has been found to be finite even though these conditions were not strictly satisfied. Furthermore, the above discussion shows that the strict adherence of $u(S_1 - S_R)$ to the requirement of integrability is of no importance in determining the numerical value of $V_1(\rho)$ except for very large values of ρ in which there is no particular physical interest anyway. Finally, to see that the oscillatory character of our $V_1(\rho)$ is not a necessary consequence of the fact that $u(S_1 - S_R)$ is integrable over the infinite range of u, one need only suppose that $u(S_1 - S_R)$ has a form such as $ue^{-\beta u}$ or $ue^{-\beta u^2}$ and put it into Eq. (3). It will be readily verified that such scattering functions give perfectly monotonic functions for $V_1(\rho)$. On the other hand, to see that the oscillatory character is a necessary feature of our potential curves one may neglect the oscillations and suppose that $V_1 = -ce^{-\alpha\rho}$. From Eq. (2c) it will be found that this V_1 corresponds to

$$\frac{S_1}{S_R} - 1 = -\frac{\alpha c u^2}{Ze^2(u^2 + \alpha^2)^2}. \tag{9}$$

A plot of this result, as given in Fig. 1, shows at once that although the curve has a minimum this minimum does not have even approximately the sharpness of the empirical scattering curve of Fig. 1. It should therefore be clear that in so far as Born's first approximation is a valid representation of the solution of the scattering problem, the potential function $V_1(\rho)$ that has been derived is the necessary implication of the features characteristic of the observed scattering data.

The physical interpretation of our $V_1(\rho)$ is not obvious. In our former note it was pointed out that if one should wish to consider the nucleus as well as the exterior electrons as radially distributed charges, one could get the net classical charge density by taking the Laplacian of the potential functions determined from the scattering experiments. As the Coulomb potential is a harmonic function one would get only the electrostatic equivalent of the $V_1(\rho)$ which might well be due to the exterior electronic charge distribution. This would apply especially to electron scattering ratios where it is known that the anomalous scattering, excluding the Ramsauer effect, is probably due to the effect of the extranuclear electrons. However, although as far as the present analysis is concerned, $V_1(\rho)$ need have no relation to electrostatic forces, it is, nevertheless, of interest to see what kind of charge density would be implied by the above $V_1(\rho)$ in case it be assumed that it is of an electrostatic origin. As the charge between ρ and $\rho + d\rho$ is proportional to $\rho\partial^2/\partial\rho^2(\rho V_1(\rho))$ it is readily seen from Eqs. (7) and (8) that this charge vanishes at $\rho = 0$, and oscillates in sign for $\rho > 0$. In particular, this charge distribution corresponds to a series of shells of alternating sign of charge with a spacing of the order of 1.5×10^{-13} cm.

Strangely enough, this oscillatory character of the electrostatic charge equivalent of $V_1(\rho)$ is just the type of explanation suggested by Rutherford

and Chadwick for the anomalous results they had found. However, as far as the wave mechanical treatment of the problem is concerned, this is only a *possible* interpretation of $V_1(\rho)$ and a definite statement cannot be made until we have further information about the structure of the nonradioactive nuclei.

In any case it is clear that since $V_1(\rho)$ is vanishingly small for $\rho > 5 \times 10^{-13}$ cm it refers to an effect of the nucleus of the Mg atom. This result is also in accord with the classical analysis of the problem according to which large angle scattering or scattering with high speed particles imply a close approach to the nucleus. Here, the anomaly is most pronounced for values of u of the order of 2×10^{13} which corresponds to large angle scattering or high velocity α-rays. Hence one would classically expect that the potential very near the nucleus would be the cause of the anomaly.

Finally, it should be pointed out again that our $V_1(\rho)$ has no more reality than has the equivalence of the Mg nucleus to a static potential field. Certainly for collisions that result in nuclear disintegration or α-particle capture such an assumption will not be valid. However for such collisions in which the atom is only temporarily disturbed the representation of the atom by a potential field may well be a sufficiently close approximation for describing the general features of the collision process.

In conclusion, it should be added that although the above numerical data applied only to Mg, the same general results apply to Al in so far as its observed scattering gives a systematic variation with u and possesses a definite minimum.

The writer wishes to thank Dr. A. E. Ruark for reading and constructively criticising the manuscript of this paper.

REFLECTING POWER AND GRATING EFFICIENCY IN THE EXTREME ULTRAVIOLET

By H. M. O'Bryan
Rowland Hall, The Johns Hopkins University

(Received May 9, 1931)

Abstract

A concave glass grating of one meter radius of curvature with 30,000 lines to the inch has been selected to make quantitative measurements of grating efficiencies and reflecting powers between 200A and 1,000A. A water-cooled vacuum spark between tungsten electrodes made an extremely intense and sufficiently constant source. Small plane gratings were crossed with the concave grating so that the efficiency of the small grating could be determined for several wave-lengths and all angles of incidence. The results show that gratings which are efficient at normal incidence are not at all suitable near grazing incidence. The reflecting powers of glass and gold mirrors at 388A and 770A have been measured for all angles of incidence. The values of the reflecting power of glass for several angles of incidence and wave-lengths from 50A to 4800A are given. The influence of reflecting power, groove form, and surface smoothness on the efficiency of a grating are discussed.

Introduction

THE ruled diffraction grating is at present the only means of obtaining the spectrum of wave-lengths between soft x-rays and the limit of transparency of fluorite. The most important factors affecting the efficiency of a grating are the form of the diffracting groove and the reflecting power of the grating surface. This reflecting power is determined by the smoothness of the surface as well as the optical properties of the substance. The ideal grating is one which will concentrate all of the incident energy into a single spectral order and is approximated by the echelette grating[1] for infrared wave-lengths. In the ultraviolet region reflecting powers are much lower than in the visible region, except near grazing incidence. This fact has been recognized by Thibaud,[2] Hoag,[3] Osgood[4] and others who have used gratings with the light incident near grazing incidence. Edlén and Ericson[5] in Siegbahn's laboratory have been very successful in obtaining spectra around 100A.

The use of gratings with the light incident near the normal to the surface has some advantages. Spectrographs for this arrangement are easier to construct and focus. These two arrangements are greatly different in dispersion, astigmatism, aberrations and the solid angle subtended by the grating. These factors which also govern the intensity of spectra are not discussed in this paper.

[1] R. W. Wood, Physical Optics, p. 227.
[2] J. Thibaud, Comptes Rendus **182,** 55 (1926).
[3] J. B. Hoag, Astrophys. J. **66,** 227 (1927).
[4] T. H. Osgood, Phys. Rev. Supp. **1,** 228 (1929).
[5] Edlén and Ericson, Zeits. f. Physik **59,** 656 (1930).

Apparatus

The vacuum spectrograph shown in Fig. 1a was similar to that described by McLennan[6] with the grating mounted at almost normal incidence. A Holweck molecular pump with an oil fore-pump made it possible to evacuate the spectrograph from atmospheric pressure to about 10^{-5} mm of mercury in an hour. This pressure was well below that required to prevent a parasitic discharge from extending into the body of the spectrograph and fogging the photographic plate. The pressures were observed by means of an ionization gauge connected to the center of the spectrograph. The molecular pump was connected to the end of the spectrograph and electrode chamber as shown in Fig. 1a, by an all metal tube system and a short flexible copper bellows of 2 cm bore and a total length of 20 cm. No mercury was present in the vacuum system and no liquid air traps were used.

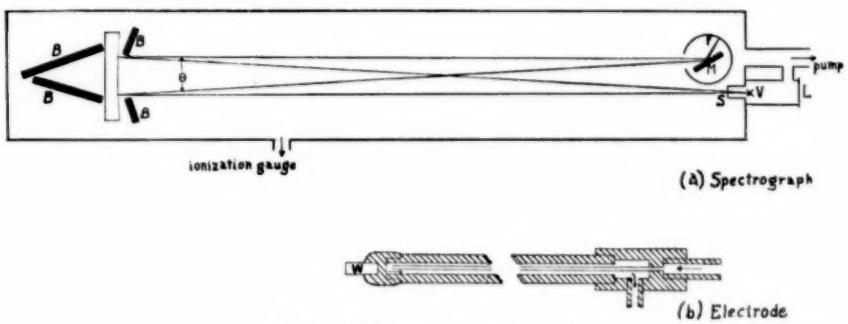

Fig. 1. Diagram of apparatus.

A 50,000 volt transformer drawing about 30 amperes at 115 volts was used to excite the vacuum spark. Across the secondary of the transformer was a 0.01 microfarad condenser consisting of aluminum plates separated by 2 cm of transformer oil in a glass battery jar. The external spark gap which was in series with the vacuum gap was cooled by a current of compressed air. The vacuum spark gap V (Fig. 1a) was about 4 cm from the slit S. The electrodes were about 3 mm in diameter and less than 0.5 mm apart. For the studies of the concave gratings copper electrodes were used, as the groups of copper lines in the region below 1000A are easily recognized. The water-cooled tungsten electrodes shown in Fig. 1b were more satisfactory for the quantitative measurements because the tungsten was less rapidly eaten away by the discharge. Tungsten rods about 6 mm long were welded into copper holders, the various parts of which were held together with silver solder. Water was circulated to within 2 mm of the base of the tungsten electrodes. With this cooling and the Holweck pump, it was possible to run the discharge continuously and not destroy the high vacuum. A few seconds of continuous operation without cooling would raise the electrodes to a red heat. For most of the experiments the spark was operated intermittently by a relay in the primary of the transformer at the rate of 15 times a minute with the discharge

[6] J. C. McLennan, Proc. Roy. Soc. London **98**, 114 (1920).

continuing about one-twentieth of the total time. Under these conditions the spark could be operated for periods as long as two or three hours before it was necessary to adjust the position of the electrodes. After about five minutes of continuous operation, enough tungsten was eaten away so that the spark gap was too large for the discharge to pass.

It is of particular importance in photometric measurements to reduce as much as possible the amount of scattered light which reaches the photographic plate. In order to study the sources of scattered light, the slit was illuminated by a carbon arc through the window *L* and a small mirror inserted in the position of the photographic plate so that the grating end of the spectrograph was visible. This intense illumination immediately showed that even the blackened metal surfaces, at the extreme end of the spectrograph, scattered an appreciable amount of light. Pieces of polished black glass *B* (Fig. 1a) were more effective than any blackened metal surfaces available, as there was no diffuse reflection and the regularly reflected light could be deflected from the photographic plate. With glass gratings the light transmitted by the grating was caught by a wedge of two pieces of black glass. The angle was made small enough so that any light returned through the grating had been reflected a great many times.

Schumann plates, from Adam Hilger and Company, which proved more sensitive than the oil coated plates, were used to study the short wave-length limit of the spectra and light scattered by each grating. Ordinary commercial films coated with one part Cenco pump oil in ten parts of amyl acetate were used for the photometric measurements. This particular concentration seemed to give the optimum sensitivity for Eastman Commercial safety films. Before developing, the films were washed in acetone.

Concave Gratings Examined

The spectra given at normal incidence by several gratings of one meter radius of curvature with 30,000 lines to the inch are shown in Fig. 2. The first four are of the copper spark on Schumann plates and the last of the tungsten spark on an oil sensitized film. The spectrum (a) is that given by a very light ruling on a soft glass whose refractive index in the visible is 1.617. On the original plate the group of lines extending to 200A was distinctly visible and there was very little scattered light present in the spectrum. The grating was then etched with hydrofluoric acid to produce maximum intensity of the visible spectrum by the method described by R. W. Wood.[7] The spectrum (b) given by the grating after etching shows the effect of the etching. No lines of wave-length less than 400A now appeared and only a very few of the group near 500A. The region on the plate between the central image and 200A showed a large amount of scattered light. The presence of the streaks across the spectrum caused by dirt on the slit showed that the grooves themselves were the scattering elements. This type of scattered light is very undesirable for it is focused along with the spectrum. The use of filters of glass quartz and

[7] R. W. Wood, Phil. Mag. **2**, 310 (1926).

fluorite showed that this light was mostly of wave-lengths between 2000A and 1300A.

Five rulings on this same kind of glass of refractive index 1.617 were tested and the original rulings gave spectra extending to 200A and were comparatively free from scattered light. Etching with hydrofluoric acid in every instance was detrimental to the efficiency for wave-lengths less than 600A. The effect of a slight amount of etching was not as great as if the etching was continued for a longer time. The etching evidently enlarges the groove so that it is better able to diffract visible light but is roughened so that it scatters more light and fails to diffract the shortest wave-lengths.

A lightly ruled speculum grating gave the spectrum shown in Fig. 2c. With a prolonged exposure it was possible to detect the group at 150A, but so much scattered light was present that the photograph is not shown here. A heavily ruled grating on speculum showed very few lines below 500A. This is in agreement with the experience of others[8] with gratings of about 15,000 lines

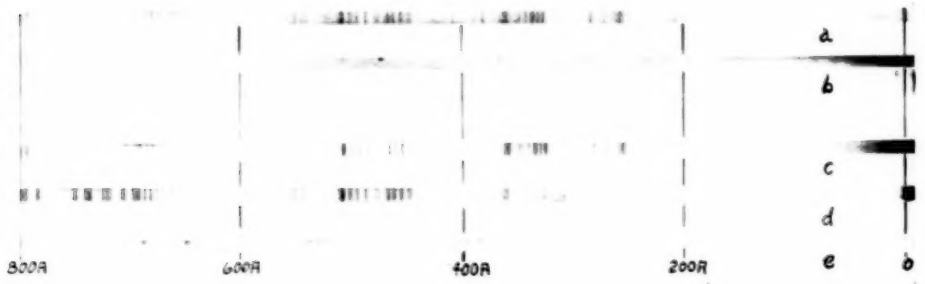

Fig. 2. Spectra from concave gratings.

per inch. The spectrum of a ruling on a "hard" glass of refractive index of 1.52 shown in Fig. 2d is like that in (a) but extends only to 250A instead of 200A with the other glass. As only one ruling was made on this "hard" glass, it is impossible to say whether this short wave-length limit of 250A was determined by the reflecting power of the glass or the type of ruling. On the soft glass, five rulings were tried and it appears that the short wave-length limit of 200A is determined by the reflecting power of this glass at normal incidence.

It is not possible to compare closely the efficiencies of glass and speculum gratings by this method. For normal incidence both lightly ruled glass and lightly ruled speculum are definitely superior to the etched glass or heavily ruled speculum for wave-lengths less than 600A. The durability and greater freedom from scattered light make the glass gratings more desirable for some kinds of work.

Crossed Gratings

Small trial plane gratings were inserted at *M*, Fig. 1a, so that the plane of the ruled surface coincided with the axis of the cylindrical film with the rulings parallel to this axis and perpendicular to the rulings of the concave grat-

[8] Millikan, Bowen and Sawyer, Astrophys. J. **53,** 150 (1921).

ing. The spectrum (Fig. 2e) used was that of the tungsten spark with the slit approximately 0.7 mm². These small gratings could be rotated through a ground joint from outside the spectrograph so that the spectrum of the concave grating was incident at any desired angle between grazing incidence and 10° from normal incidence. The spectra of these crossed gratings were photographed on a concentric oil sensitized film inside the cylinder at *F*. In order to interpret the intensities of the spectra a number of step exposures were made with the spectrum of the concave grating reflected from the second grating at 2° from grazing incidence. At this small angle no orders of the second grating were detectable and practically all light went into the central image. A recording Moll photometer was used to obtain the relative intensities of the spectra compared to the step exposures at grazing incidence.

In Fig. 3 are shown the spectra of the crossed gratings together with sketches of the possible groove forms of the small gratings. The wave-lengths are those of the spectrum formed by the concave grating and the numbers re-

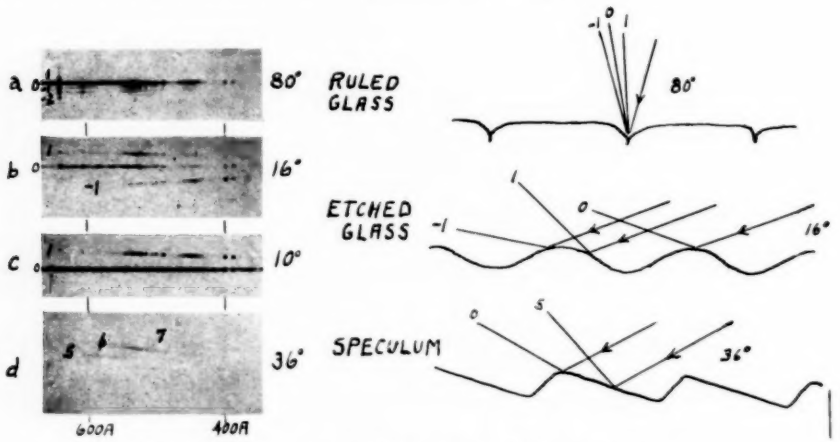

Fig. 3. Spectra of crossed gratings and shape of grooves.

fer to the spectral orders produced by the second grating. Inside orders, i.e., those between the central image and the tangent to grating are marked with a negative sign and the central image zero. The angles are those between the direction of the incident light and plane of the grating.

The spectra (a) were from a lightly ruled glass grating near normal incidence. At 650A, the central image contained about 4 percent of the total energy of this wave-length incident on the grating and the brighter first order about 1 percent. The intensities at 400A were too small to be measured. The orders on one side of the central image were much brighter than on the other, and this must be due to asymmetry in the groove form. At angles of incidence less than 30°, almost no spectra were obtained from the lightly ruled glass gratings. A possible form of the grooves of this type of grating is shown. The groove is apparently rather small, compared to the spacing for near grazing incidence the grating is more like a mirror, giving no spectra at any angle less than 20° from grazing incidence. Four gratings of this type gave spectra of

about the same intensities. Sputtering these gratings with an almost opaque film of gold did not change the distribution of energy in the various orders which was characteristic of the ruled groove. The efficiency of the gratings was not changed by the gold film and later measurements of the reflecting powers of glass and gold showed the two were about equal near normal incidence. If the measurements of the reflecting powers of various substances are made at normal incidence it may be possible to find one which will increase considerably the efficiencies of gratings for the region between 400A and 2000A.

The spectra of an etched glass grating are shown in Fig. 3b and c. At 16° from grazing incidence and 400A the first inside order contained 6 percent of the total energy of this wave-length incident on the grating, the central image 5 percent and the first outside order 3 percent. At 10° the same grating gave an outside order of 10 percent. Several other etched gratings gave spectra of about the same intensities at these angles. The groove form for this type which is sketched is that suggested by Professor Wood as one produced from the ruled glass by the eating away of the surface at a constant rate in all directions by the hydrofluoric acid. The parts of the groove which may act as small mirrors concentrating the energy into the different spectral orders are indicated. The effective reflecting power for the inside orders is larger as these are reflected nearer grazing incidence and this factor will tend to increase the intensities of these orders. These etched gratings gave only extremely faint spectra at normal incidence as was found in the examination of the concave gratings. It is very probable that the hydrofluoric acid leaves a surface which is very rough to the shorter wave-lengths at normal incidence.

A small fragment of a speculum grating with 15,000 lines to the inch which gave a very bright first order and faint central image in the visible region, gave the spectra shown in Fig. 3d at 36° from grazing incidence. This bright visible first order indicates that the groove has one broad and rather flat side which makes an angle of about 10° with the grating surface as shown in the sketch. The fifth, sixth and seventh outside orders between 400A and 700A which are shown in the photograph coincide almost exactly with the direction of regular reflection from a plane mirror placed at an angle of 10° with the grating surface. In this instance the grating of 15,000 lines to the inch concentrates the ultraviolet wave-lengths in a few orders as the echelette concentrates visible light. This effect was found at other angles of incidence but not clearly enough to reproduce. The grating did not show spectra at normal incidence probably on account of the small reflecting power and the roughness of the groove surfaces at this angle.

Experiments with twelve gratings, of which three have been described in detail here, show that efficiency for normal and for grazing incidence requires gratings of quite different type. Near grazing incidence (less than 15°) the reflecting power of most substances will be 50 percent or more, and the choice of a material for a grating will be determined by physical properties which facilitate ruling. The ruled metal grating of the echelette type, modified to take advantage of the increase in reflecting power at small angles may become

surprisingly efficient in the extreme ultraviolet and soft x-ray regions. Such gratings will be extremely difficult to rule, as it will be necessary to examine the trial rulings with ultraviolet light instead of visible light to obtain information regarding the shape of the groove formed by the ruling point. Although the examination of a ruling with short wave-lengths gives more information about the groove form than with longer wave-lengths, it is possible to predict partially the behavior of the ruling at 200A by examining it with 500A. The etched glass grating is particularly easy to rule as only a very light ruling is needed with the hydrofluoric acid forming the groove. This means less time spent in selecting the diamond point and less wear on the diamond.

It is probable that the results of these studies on the groove form and grating efficiency at 400A will be useful in ruling gratings for the soft x-ray region.

Reflecting Power

Preliminary determinations of the reflecting powers of glass and gold mirrors at various angles of incidence between 200A and 1000A were made with the hope of improving the efficiency of gratings in this region. The reflecting powers of these two substances proved to be of the same order of magnitude and not sufficiently different to make either greatly superior for a grating surface.

Selected pieces of plate glass 4 cm by 14 cm were inserted at M, Fig. 1a on the axis of the cylindrical film. The angle θ subtended by the beam from the grating surface was made about one degree to increase the "angular" resolving power of the reflection measurements. The dispersion on the photographic film was 8.6A per mm in one dimension and 0.78° per mm in the other. The intensities of the reflected spectra were compared with exposures reflected at $1\frac{1}{2}°$ from grazing incidence by a recording Moll photometer, and the fraction reflected calculated by use of the photographic reciprocity law. In order to obtain the comparison exposures, the mirror was set at $1\frac{1}{2}°$ and the photographic film rotated about its axis. To reduce any drift in intensity of the source, half of the reflected spectra were taken before the comparison exposures were made and the remainder afterwards.

Fig. 4a shows the experimental values of the reflecting power of gold at 388A between 0° and 40° compared to the reflecting power at $1\frac{1}{2}°$. These values were taken from four films using two sputtered gold mirrors. The variations in these experimental values are probably due to unsteadiness of the spark and variations of sensitivity of the photographic film. The extension of the curve to grazing incidence from $1\frac{1}{2}°$ indicates that only a small error would have been introduced by assuming 100% reflection at $1\frac{1}{2}°$. For the other curves the value at 0° has been obtained by extending the curve from $1\frac{1}{2}°$ and the entire curve expressed as fractions of this value. The reflecting powers of gold at 388A and 770A are shown in Fig. 4c and similar curves for glass in Fig. 4b.

At normal incidence both substances reflect 5 percent of 770A and give positive evidence of regular reflection at 388A. The effect of surface roughness

is greater at this angle and wave-length than in any of the other values and may decrease the reflecting power considerably. It is known that gratings partially polarize the diffracted light to an extent which varies with the wave-length. The use of crossed gratings in the earlier part of this work showed that the ratio of intensities of the polarized components at 650A was less than five. The photographic laws whose validity have been assumed in computing the reflected intensities may introduce an error in the values reported. Harrison[9] has shown that the oil sensitized photographic plate is a well behaved combination and it is expected that the errors introduced by photographic laws are relatively small.

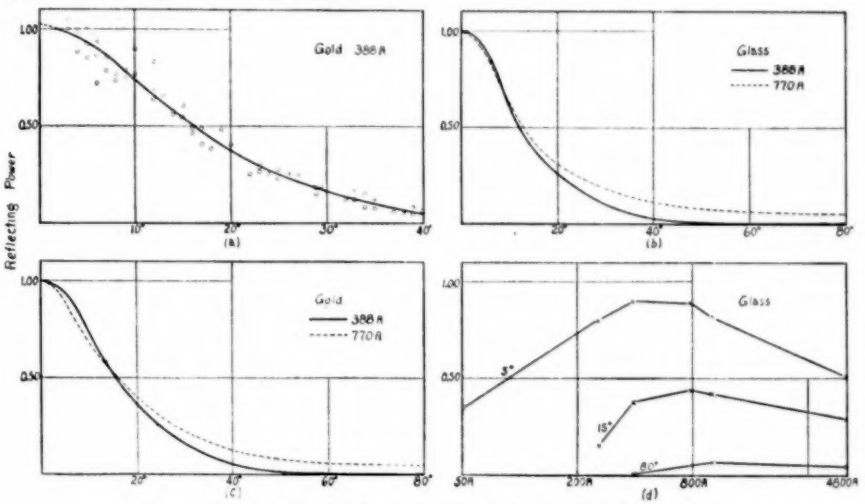

Fig. 4. Reflecting powers of glass and gold.

It is estimated that the probable experimental error is about 5 percent near grazing incidence, and 2 percent near normal incidence. At the present time, however, some of the sources of error mentioned above cannot be evaluated.

The reflecting powers of glass at 80°, 15°, and 5° for wave-lengths from the visible region to the $K\alpha$ line of carbon are shown in Fig. 4d. The values at 4800A are those for unpolarized light as computed by Fresnel's equations. The value at 50A is that given by Dershem[10] and the intermediate values as determined by the method described in this paper. The curve given by Gleason[11] for 45° incidence is in general agreement with those presented here. The shift of the maximum of reflecting power toward shorter wave-lengths as grazing incidence is approached cannot be entirely due to the decreasing influence of surface roughness.

Summary

Gratings of 15,000 and 30,000 lines per inch behave in the region below 1000A much like echelette gratings in the visible region. The intensity of the

[9] G. R. Harrison, Jour. Op. Soc. Am. **19**, 267 (1929).
[10] E. Dershem, Phys. Rev. **34**, 1015 (1929).
[11] P. R. Gleason, Proc. Nat. Acad. of Sci. **15**, 551 (1929).

spectra are largely determined by the reflecting power, shape of the groove and smoothness of the surface. In order to obtain a large reflecting power and smooth appearing groove surface for wave-lengths below 500A it is necessary to have the light incident at angles of less than 20° from grazing incidence. The reflecting power which is effective in determining the efficiency of a grating is that for half the angle by which the spectral order under consideration is deviated from the direction of the incidence light.

At present, for use near grazing incidence the etched glass grating is more suitable for it has an efficiency of the order of 8 percent at any angle near grazing incidence, and is readily ruled. The ruled metal grating will be more efficient but will be extremely difficult to rule and can only be used to great advantage at one definite angle of incidence. Near normal incidence either a lightly ruled glass or speculum grating will be satisfactory. Sputtering a glass grating with any substance with greater reflecting power should increase the efficiency.

These studies were suggested by Professor R. W. Wood and the gratings which were ruled on the Rowland engines were made available by him.

ATOMIC SCATTERING POWER OF COPPER AND OXYGEN IN CUPROUS OXIDE

By G. A. Morton
Rockefeller Institute for Medical Research,
Massachusetts Institute of Technology

(Received May 8, 1931)

Abstract

Atomic F-curves for the copper and oxygen in Cu_2O, have been obtained for $K\alpha$ radiation of copper from a measurement of the principal powder reflexions. The F-curves are compared with the F-curves for metallic copper and for oxygen in NiO and found to be identical.

MEASUREMENTS of the reflecting power of cuprous oxide for the $K\alpha$ radiation of copper were made, in order to compare the atomic F_{Cu}-curve of the combined copper with that of metallic copper[1] and also that of oxygen with the F_O-curve of oxygen in NiO.[2]

The ionization spectrometer and high potential source used in this work have been described in previous publications.[3] A Siemens-Phoenix copper target tube operating at a potential of 30 KV served as the source of x-rays. The radiation was filtered with 0.001 inches of nickel foil in order to cut down the background scattering from the Cu_2O. The ionization current was measured with a Cambridge Compton electrometer having a sensitivity of 11 meters per volt (scale distance = 2 meters).

Samples were prepared by pressing into a suitable briquet, cuprous oxide which had been powdered until it would pass through a 325 mesh sieve. The surface of each briquet was filed to remove preferred orientation which might occur due to crystal grains coming in contact with the smooth metal of the press.

Two specimens of Cu_2O were used. Analyses for the copper content of the specimens showed for No. 1, 87.4 percent and No. 2, 86.0 percent of copper as compared with 88.8 percent for pure Cu_2O. The results given below are computed from measurements on specimen No. 1. A comparison of the reflexions from No. 1 and No. 2 showed no difference in intensity within the accuracy of the measurement, except for the (200) reflexion. The (200) reflexion for No. 2 is greater than that for No. 1, on the other hand the results indicate that No. 1 is greater than the correct value, and by approximately the same amount. These discrepancies are due to a small amount of CuO present, a strong reflexion of which occurs at about the same angle of reflexion as the (200) of Cu_2O. The amount of CuO present is not sufficient to reduce the intensity of the other reflexions by an amount that could be detected.

[1] A. H. Armstrong, Phys. Rev. **34**, 931 (1929).
[2] R. W. G. Wyckoff, Phys. Rev. **35**, 583 (1930).
[3] R. W. G. Wyckoff and A. H. Armstrong, Zeits. f. Krist. **72**, 319 (1929).

Measurements of the radiation reflected from a set of planes were made by taking intensity readings, at intervals of five minutes of ionization chamber angle, over the width of the line. (The slits limiting the beam entering the ionization chamber, subtended an angle of 9′.) These intensities were plotted against ionization chamber angle. Thus plotted the area under the resulting curve is proportional to the power of the reflected beam. The area under the curve for the (200) plane was taken equal to 100 units, the other reflexions being measured in these units. To place the measurements on a standard scale the (220) reflexion for NaCl was also measured in terms of the same units.

Since the power $P_{[hkl]}$ of the reflection from a plane $[hkl]$ is given by[4]

$$P_{[hkl]} = \frac{1}{32\pi}\lambda^3 \frac{e^4}{m^2c^4} \frac{1}{r} \frac{\rho'}{\rho\mu} N^2F^2jP_0 \frac{1+\cos^2 2\theta}{\sin\theta \sin 2\theta}$$

if the relative power of reflexion P_s and the absolute F_s is known for NaCl (220) the desired F-values for Cu_2O may be calculated from

$$F^2_{[hkl]} = K \frac{P_{[hkl]}}{j} \frac{\sin\theta \sin 2\theta}{1+\cos^2 2\theta}$$

where

$$K = \frac{N_s^2}{N^2} \frac{\mu\rho}{\mu_s\rho_s} \frac{F_s^2 j_s}{P_s} \frac{1+\cos^2 2\theta}{\sin\theta_s \sin 2\theta_s}$$

and N is the number of atoms per unit volume; j, the number of reflecting planes; θ, the angle of reflexion; μ, the absorption coefficient; ρ, the density; F, the structure factor; P, the power of reflexion. The subscript s refers to NaCl. Absolute F-values for NaCl have not been determined for copper radiation. There is evidence,[5] however, for the fact that if the radiation used is not too close to the characteristic radiation of an element the atomic F-curve as a function of $(\sin\theta/\lambda)$ is independent of the wave-length λ. On this assumption the structure factor $F_{[NaCl\,220]}$ has been assigned the same value as for the $K\alpha$ radiation of molybdenum, which has been found to be[6] $F = 62.48$.

Values for the absorption coefficient were found by using Jönsson's general formula.[7] The coefficients used are:

Material	μ	ρ
NaCl	161.3	2.16
Cu_2O	113.6	5.88

The greatest uncertainty in determining the absolute F-values probably lies in assigning values to the absorption coefficient.

Cuprous oxide has a cubic structure containing 2 molecules of Cu_2O to the unit cell. The oxygens are in a body centered cubic arrangement, with the

[4] A. H. Compton, X-Ray and Electrons. (New York 1926) p. 131.
[5] E. Wagner and H. Kulenkampf, Ann. d. Physik **68,** 369 (1922).
[6] R. W. James and E. M. Firth, Proc. Roy. Soc. **A117,** 62 (1927).
[7] E. Jönsson, Uppsala Univers. Arsskrift (1928).

copper atoms arranged in tetrahedra around the oxygen atoms. For this type of structure the structure factor $F_{[hkl]}$ for the plane $[hkl]$ is given by the following equation[8]

$$F_{[hkl]} = Fo(1 + e^{\pi i(h+k+1)}) + F_{Cu}(e^{\pi i/2(h+k+1)} + e^{\pi i/2(h-k-1)} + e^{\pi i/2(-h-k+1)} + e^{\pi i/2(-h+k-1)})$$

where F_O and F_{Cu} are the atomic scattering factors for oxygen and copper. By means of this expression the relation between F_O and F_{Cu}, which are to be determined, and the structure factor F can be found for any reflexion.

Experimental Results

Table I gives the measured values of relative intensity, the structure factor F as determined from them, and the value of F in terms of F_O and F_{Cu}.

Table I.

Plane	$(\sin\theta)/\lambda$	Int.	F	Structure factor F:
110	0.164	17.1	11.7	$2F_O$
111	.202	288.	73.3	$4F_{Cu}$
200	.233	100.	58.9	$4F_{Cu}-2F_O$
220	.331	85.0	58.6	$4F_{Cu}+2F_O$
311	.388	68.3	44.8	$4F_{Cu}$
222	.406	14.1	36.8	$4F_{Cu}-2F_O$
NaCl 220		69.0	62.48	$(4F_{Na}+4F_{Cl})$

From these values of F the best values for F_{Cu} and F_O are found by graphically constructing smooth curves of $4F_{Cu}+2F_O$, $4F_{Cu}-2F_O$, F_{Cu} and F_O against $(\sin\theta/\lambda)$ such that the measured point will lie on these curves.

Table II gives the values of F_{Cu} and F_O thus determined:

Table II.

$(\sin\theta)/\lambda$	F_O	F_{Cu}	F(determined from F_O and F_{Cu}
0.104	5.9		11.8
.202	5.5	18.3	73.2
.233	(5.0)	(16.4)	(55.6)*
.331	3.4	12.9	58.4
.388	2.6	11.2	44.8
.406	2.4	10.4	36.8

* This value is 6 percent lower than the measured value of F_{200}. The presence of CuO in the sample is responsible for the measured F being too great.

Fig. 1 shows graphically a comparison between the values of F_{Cu} for Cu_2O and metallic copper. F_{Cu} for Cu_2O is shown as a full line, and black circles, and F_{Cu} from copper metal[1] as crosses. The F curves being plotted against $(\sin\theta/\lambda)$.

[8] H. Ott, Handbuch der Expermentalphysik. Vol. VII, part 2. (Leipzig 1928) p. 270.

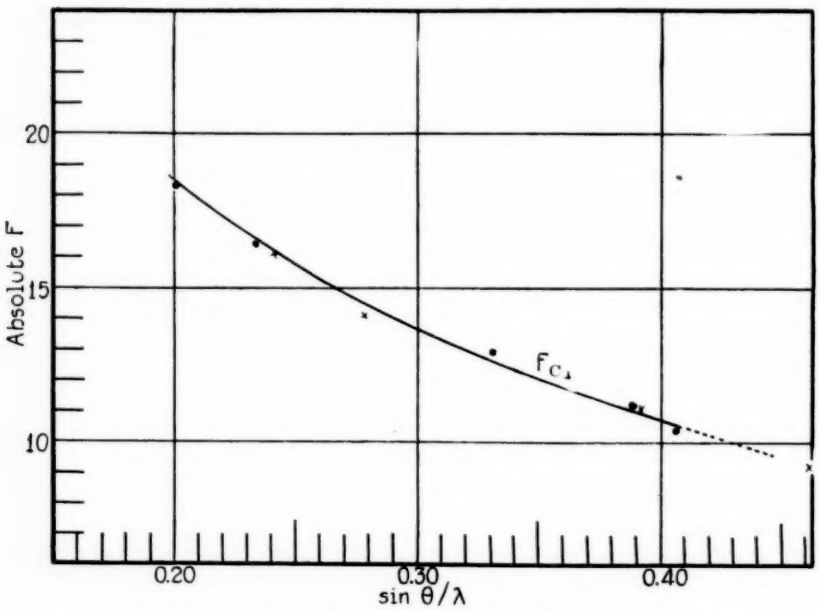

Fig. 1. The F-curves of copper atoms from Cu_2O and metallic copper.

Fig. 2 gives the same comparison for F_O from Cu_2O and NiO. The full curve and black circles showing the F curves for oxygen in Cu_2O. The crosses that for oxygen[2] in NiO.

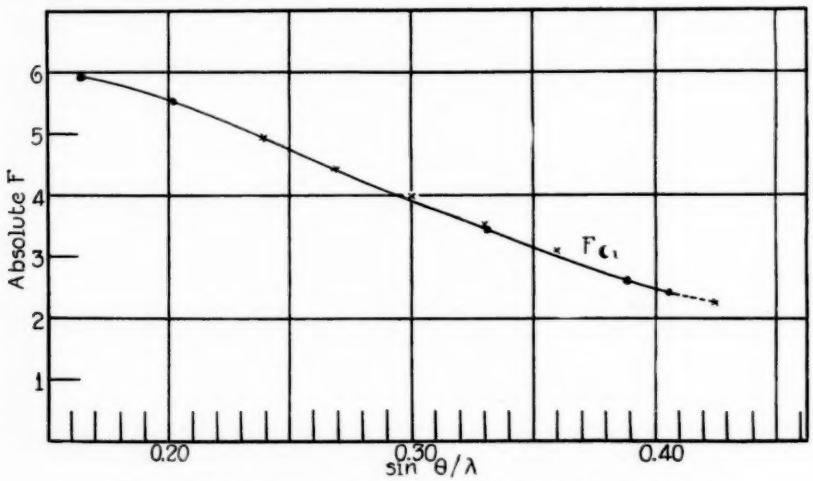

Fig. 2. The F-curves of oxygen atoms from Cu_2O and NiO.

Both the F_{Cu}-curve and F_O-curve are within the limits of the accuracy of the determination, the same for Cu_2O as for metallic copper and NiO.

In conclusion I wish to thank Dr. R. W. G. Wyckoff to whom I am indebted for the use of his powder spectrometer, and for invaluable aid and advice in carrying out this work.

THE ANALYSIS OF PHOTOELECTRIC SENSITIVITY CURVES FOR CLEAN METALS AT VARIOUS TEMPERATURES

By R. H. Fowler
Temporarily, Laboratory of Physics, University of Wisconsin

(Received May 28, 1931)

Abstract

An elementary theory is developed for the effect of temperature on the photoelectric sensitivity of a clean metal near the threshold. It is shown that the results observed by various workers for silver, gold, tantalum, tin, and potassium can be fairly completely accounted for by the effect of the temperature on the number of electrons available for extraction according to the distribution law of Sommerfeld's theory of metals. This is in agreement with the conclusions of Lawrence and Linford based on much less extensive data. A graphical method is given enabling the whole of the observed curves near the threshold for all temperatures to be used in determining the threshold itself thus avoiding an arbitrary extrapolation to zero current. At present the fundamental theory of the effect survives in two forms both of which are used as alternatives here, with nearly equal success. Until one or the other can be eliminated it is not possible to determine thresholds closer than about 1 percent.

§1. Introduction

A SERIES of studies have recently been made of the photoelectric sensitivity of very carefully cleaned metal surfaces to very carefully monochromatized light, by a number of workers in the Department of Physics of the University of Wisconsin. Detailed accounts of this work, embodying results which have been on hand here for over a year have been or will be published elsewhere in this journal. The experiments establish with considerable accuracy the relative number of electrons ejected from the metal, per quantum of light absorbed[1] as a function of the frequency of the light and the temperature of the metal. The precautions required in rendering the light sufficiently monochromatic and the surface sufficiently clean are exceedingly elaborate and cannot be discussed here.[2] They are such that one can only suppose, at least as a natural first approximation, that the observed curves do really yield to us a true representation of the ideal photoelectric sensitivity of the *clean* metal at various temperatures to *monochromatic* light of various frequencies. Typical curves for silver[3] and gold[4] are shown in Fig. 1, and for tantalum[5] in Fig. 2.

[1] The experiments actually determine the current per unit incident light intensity and are controlled so as to detect any change of reflection coefficient as a function of the temperature. No significant changes occurred for the small frequency range in which we are here interested; therefore there is no need to distinguish between electrons per quantum absorbed and current per unit incident intensity.

[2] Besides the various authors' own papers quoted below, a general account has been given by Mendenhall, Science **73,** 107 (1931).

[3] Winch, Phys. Rev. 37,1263 (1931).

[4] Morris, Phys. Rev. 37,1269 (1931).

[5] Cardwell, Private communication.

It is at once clear from these curves that there is no sharp threshold value of ν_0; especially at the higher temperatures the photoelectric sensitivity tails off gradually at lower frequencies, and the sensitivity curve can be followed out to a frequency which depends primarily on the sensitivity of the detecting apparatus. The question then arises whether the shape of these curves, especially near the threshold, cannot be simply accounted for in terms of the temperature effect on the electron distribution in the metal. The observed curves bear obvious characteristics suggesting this origin rather than any change in work function with temperature. It is of course necessary, however, to examine possible temperature effects which may arise from the form of

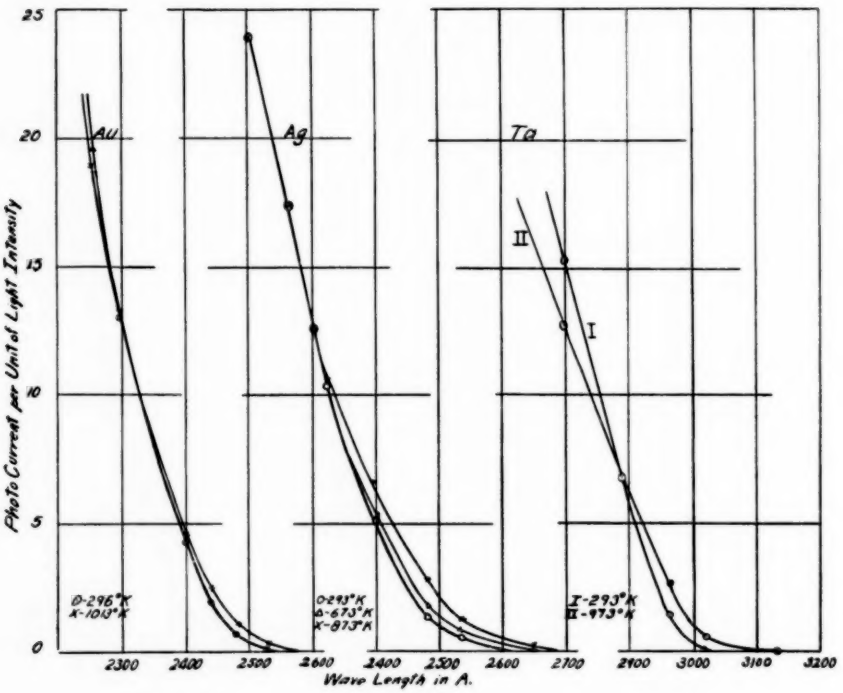

Fig. 1A. Fig. 1B. Fig. 2.

the boundary transmission coefficient $D(W)$, or from the form of the absorption coefficient of electrons of given energy for light of given frequency, so far as these functions are known. Probably it is more correct to fuse them together and regard their combined effect as a transition probability that under the action of light of unit intensity and frequency ν an electron originally in a given stationary state in the metal shall become a photo-electron with energy greater by $h\nu$. It may be stated at once that *the observed results for silver, gold, tin,*[6] *potassium (one temperature),*[7] *and tantalum appear to be completely accounted for by the change of distribution of the electrons with the temperature.* The excellent agreement between the forms of the observed and

[6] Goetz, Phys. Rev., **33**, 373 (1929).

[7] Lawrence and Linford, Phys. Rev. **36**, 482 (1930).

theoretical curves allows the use of a convenient graphical method for determining the true threshold from the general form of the whole family of sensitivity curves, which is thus of considerably greater certainty than any obvious method of extrapolating the observed curves to zero photoelectric current. At the same time, the whole effect here examined makes a precise determination of threshold almost impossible without a really exhaustive and reliable theory of the photoelectric effect.

Though any attempt to reinvestigate in detail the theory of the photoelectric effect would obviously be out of place in this paper, it is necessary to consider what corrections to this simple calculation are likely to be required by a more complete theory. We are interested here only in the form of the sensitivity curves in the immediate neighborhood of the threshold, and therefore factors like powers of ν in the transition probability can all be omitted, though they are of course of first class importance for a more general study of the whole sensitivity curve. It is only factors like $(\nu-\nu_0)^s$ where ν_0 is the threshold frequency which really matter to us. There are at present two not entirely consistent theories which we shall describe more closely later. According to one of these, the transition probability introduces no important factor and leaves unaltered the elementary theory of the form of the sensitivity curve near the threshold. According to the other, there is an extra factor introduced, of the form $(\nu-\nu_0)^{-1/2}$, which slightly modifies the shape and the temperature dependence. We therefore analyse the observations here according to both theories. The variation in the curves and their temperature dependence is about the limit of what the observations will stand. Excellent fitting is obtained on both theories, but that obtained with the simplest theory is slightly the better. Observations over a wider temperature range would probably allow one to discriminate between the theories.

In Figs. 1 and 2 we have shown curves for silver, gold, and tantalum because the tantalum sensitivity curves, in addition to behavior near the threshold similar to the curves for silver, show a new feature—a temperature-dependent general slope as they straighten out, instead of an asymptotic coalescence. There are symptoms of the same effect, but much less marked, for gold. Possible explanations of this are mentioned below, but they seem hardly satisfactory, and at present it is wisest to record this feature as not yet explained. It is important to see if it can be correlated with any special feature in the thermionic emission formula and this experiment will be undertaken by Dr. Cardwell.

The precise hypothesis which succeeds so well in correlating the observed effect near the threshold is that the photoelectric sensitivity or number of electrons emitted per quantum of light absorbed is to a first approximation proportional to the number of electrons per unit volume of the metal *whose kinetic energy normal to the surface augmented by $h\nu$ is sufficient to overcome the potential step at the surface.* We may call this number the number of *available* electrons. As we have said, this number as a function of ν and T near the threshold is left unaltered by one of the two current theories.

Before these results were finally written up, I became acquainted with a

paper by Lawrence and Linford[7] on the effect of strong electric fields on the photoelectric threshold (the Schottky lowering of the work function), in which they point out incidentally that the form of their curves (at room temperature only) near the threshold can be satisfactorily accounted for by the same assumption. The results here recorded are in entire agreement with theirs, but since this discussion is concerned with the analysis of somewhat elaborate data at many temperatures specially obtained for this purpose, it appears desirable to present them in full, with this acknowledgment of anticipation.

§2. The Number of Available Electrons

In a gas of electrons obeying the Fermi-Dirac statistics the number of electrons per unit volume having velocity components in the ranges u, $u+du$, v, $v+dv$, and w, $w+dw$ (u normal to the surface) is given by the well-known formula

$$n(u, v, w)dudvdw = 2\left(\frac{m}{h}\right)^3 \frac{dudvdw}{e^{\{\frac{1}{2}m(u^2+v^2+w^2)-\epsilon^*\}/kT}+1} \tag{1}$$

where ϵ^* is to be adjusted so that the total number of electrons per unit volume has the correct value. To a first approximation ϵ^* is constant and equal to the energy of the electron level of highest energy which is filled at the absolute zero. This approximation is to be expected to be a good one over a wide range of temperature.[8] The number per unit volume $\tilde{n}(u)du$ with velocity component normal to the surface in the range u, $u+du$ is given by

$$\begin{aligned}\tilde{n}(u)du &= 2\left(\frac{m}{h}\right)^3 du \int_0^\infty \int_0^{2\pi} \frac{\rho d\rho d\theta}{e^{\frac{1}{2}m(u^2+\rho^2)-\epsilon^*\}/kT}+1}, \\ &= \frac{4\pi kT}{m}\left(\frac{m}{h}\right)^3 \log\left\{1+e^{(\epsilon^*-\frac{1}{2}mu^2)/kT}\right\}du. \end{aligned} \tag{2}$$

We shall denote the total height of the potential step at the boundary by χ_0 and write $\chi=\chi_0-\epsilon^*$, so that to the usual approximation χ is the thermionic work function.

We first experimented with the hypothesis that the number of available electrons was the number with sufficient *total* energy to escape, after the addition $h\nu$ to the usual energy. We may call this number N_A. Then obviously

$$\begin{aligned} N_A &= 8\pi\left(\frac{m}{h}\right)^3 \int_{\frac{1}{2}m\rho^2=\chi_0-h\nu}^\infty \frac{\rho^2 d\rho}{e^{(\frac{1}{2}m\rho^2-\epsilon^*)/kT}+1} \\ &= 4\pi\left(\frac{m}{h}\right)^3\left(\frac{2kT}{m}\right)^{3/2} \int_0^\infty \frac{\{y+(\chi_0-h\nu)/kT\}^{1/2}}{e^{y+(\chi-h\nu)/kT}+1}dy. \end{aligned}$$

This expression can be simplified without spoiling its adequacy. For since we are concerned with values of $h\nu$ near the threshold ($h\nu \doteqdot \chi$), $h\nu-\chi$ is comparable with kT, while $\chi_0-h\nu$ is always large. It is therefore a sufficiently good

[8] Fowler, Statistical Mechanics, pp. 541–599 (Cambridge, 1929).

approximation to neglect y in $\{y+(\chi_0-h\nu)/kT\}^{1/2}$; the error in so doing can easily be investigated exactly if desired. Thus

$$N_A = \frac{4\pi(2mkT)^{3/2}}{h^3}\left(\frac{\chi_0 - h\nu}{kT}\right)^{1/2}\int_0^\infty \frac{dy}{e^{y+(\chi-h\nu)/kT}+1},$$
$$= \frac{4\pi(2m)^{3/2}}{h^3}kT(\chi_0 - h\nu)^{1/2}\log\{1+e^{(h\nu-\chi)/kT}\}. \tag{3}$$

As $T\to 0$ this reduces to the form

$$N_A \propto (\chi_0 - h\nu)^{1/2}(h\nu - \chi) \qquad (h\nu > \chi), \tag{4}$$
$$= 0 \qquad (h\nu < \chi). \tag{4'}$$

At the threshold $h\nu=\chi$, $N_A \propto T$.

While such a formula for the number of available electrons presents some of the characteristic features of the curves of Figs. 1, 2, it is at once evident that it is not of the correct form. The observed variation with T near the threshold is clearly faster than that predicted, and still more, no reasonable extrapolation of the observed curves to zero temperature can be adapted to (4), which is practically a straight line cutting the axis of zero sensitivity at a finite angle. More detailed examination soon proved conclusively that the whole predicted form was wrong. We therefore passed on to the examination of the hypothesis described in §1, which is of course more reasonable *a priori* and which has proved completely successful.

On this hypothesis the number of available electrons N_B will obviously be given by the formula

$$N_B = \int_{\frac{1}{2}mu^2=\chi_0-h\nu}^\infty \bar{n}(u)du$$
$$= \frac{2\pi kT}{m}\left(\frac{2kT}{m}\right)^{1/2}\left(\frac{m}{h}\right)^3\int_0^\infty \frac{\log\{1+e^{-y+(h\nu-\chi)/kT}\}}{\{y+(\chi_0-h\nu)/kT\}^{1/2}}dy.$$

Just as before we can approximate to this, and obtain with sufficient accuracy

$$N_B = \frac{2\sqrt{2}\pi m^{3/2}}{h^3}\frac{k^2T^2}{(\chi_0 - h\nu)^{1/2}}\int_0^\infty \log\{1+e^{-y+(h\nu-\chi)/kT}\}dy. \tag{5}$$

This integral cannot be evaluated in finite terms except when $h\nu=\chi$, but we may obtain convenient expansions for it from which its values can be rapidly computed,

(i) When $(h\nu-\chi)/kT=\mu\leq 0$ the logarithm may be expanded and integrated term by term. Then

$$N_B = \frac{2\sqrt{2}\pi m^{3/2}}{h^3}\frac{k^2T^2}{(\chi_0 - h\nu)^{1/2}}\left[e^\mu - \frac{e^{2\mu}}{2^2}+\frac{e^{3\mu}}{3^2}-\cdots\right] \qquad (\mu\leqq 0). \tag{6}$$

(ii) When $(h\nu-\chi)/kT=\mu\geq 0$

$$\int_0^\infty \log(1+e^{-y+\mu})dy = \int_0^\mu \log(1+e^{-y+\mu})dy + \int_0^\infty \log(1+e^{-y'})dy',$$

$$= \frac{\pi^2}{12} + \frac{1}{2}\mu^2 + \int_0^\mu \log(1+e^{-y''})dy''.$$

The logarithm may be expanded and integrated term by term giving

$$\int_0^\infty \log(1+e^{-y+\mu})dy = \frac{\pi^2}{6} + \frac{1}{2}\mu^2 - \left[e^{-\mu} - \frac{e^{-2\mu}}{2^2} + \frac{e^{-3\mu}}{3^2} - \cdots\right].$$

Thus

$$N_B = \frac{2\sqrt{2}\pi m^{3/2}}{h^3}\,\frac{k^2T^2}{(\chi_0 - h\nu)^{1/2}}\left[\frac{\pi^2}{6} + \frac{1}{2}\mu^2 - \left\{e^{-\mu} - \frac{e^{-2\mu}}{2^2} + \frac{e^{-3\mu}}{3^2} - \cdots\right\}\right]$$
$$(\mu \lessgtr 0). \tag{6'}$$

When $T \to 0$

$$\left.\begin{aligned} N_B &\propto \frac{(h\nu - \chi)^2}{(\chi_0 - h\nu)^{1/2}} && (h\nu > \chi) \\ &= 0 && (h\nu < \chi) \end{aligned}\right\}. \tag{7}$$

When $h\nu = \chi$, $N_B \propto T^2$.

The analysis of the observations described in the next section will be made on the assumption that the photoelectric current I per quantum of light absorbed is proportional to N_B.

§3. First Analysis of the Observations

It will be observed at once that if $I \propto N_B$ and N_B is given by (6) and (6') then

$$\frac{I(\chi_0 - h\nu)^{1/2}}{T^2} = Af(\mu) = Af\left(\frac{h\nu - \chi}{kT}\right), \tag{8}$$

where A is an unknown constant independent of ν and T and

$$\left.\begin{aligned} f(\mu) &= e^{\mu} - \frac{e^{2\mu}}{2^2} + \frac{e^{2\mu}}{3^2} - \cdots && (\mu \leqq 0) \\ &= \frac{\pi^2}{6} + \frac{1}{2}\mu^2 - \left[e^{-\mu} - \frac{e^{-2\mu}}{2^2} + \frac{e^{-3\mu}}{3^2} - \cdots\right] && (\mu \gtrless 0) \end{aligned}\right\}. \tag{9}$$

Further, when $h\nu = \chi$ approximately, then $\chi_0 - h\nu = \epsilon^*$ approximately and to a first approximation $(\chi_0 - h\nu)^{1/2}$ is constant. For example if ν changes 15% away from a threshold ν_0 corresponding to about 4 electron-volts, $\chi_0 - h\nu$ which is of the order of 10 volts will change by 6% and $(\chi_0 - h\nu)^{1/2}$ by 3% only. A sufficiently exact analysis can therefore be made as follows:—

Taking logarithms of (8), we have

$$\log\frac{I}{T^2} = B + \phi\left(\frac{h\nu - \chi}{kT}\right) \tag{10}$$

B being independent of temperature and frequency. The theoretical curve $\phi(\mu)$ can be plotted as a function of μ. It is shown in Fig. 3. For each observed curve of photoelectric current we plot log (I/T^2) from the observed values against the variable $h\nu/kT$, the scales of the logarithms and of $h\nu/kT$ or μ being the same. By adjustment of origin we then bring the observed curve of log (I/T^2) into coincidence with the theoretical curve of $\phi(\mu)$. But in doing so all the curves for one metal for different temperatures should normally fit the theoretical curve for the same shift of logarithmic origin, so long that is as B does not depend on T. The actual value of this shift is of no importance, but the $h\nu/kT$ shift gives the threshold ν_0 or χ/h since $h\nu_0/kT$ is the scale

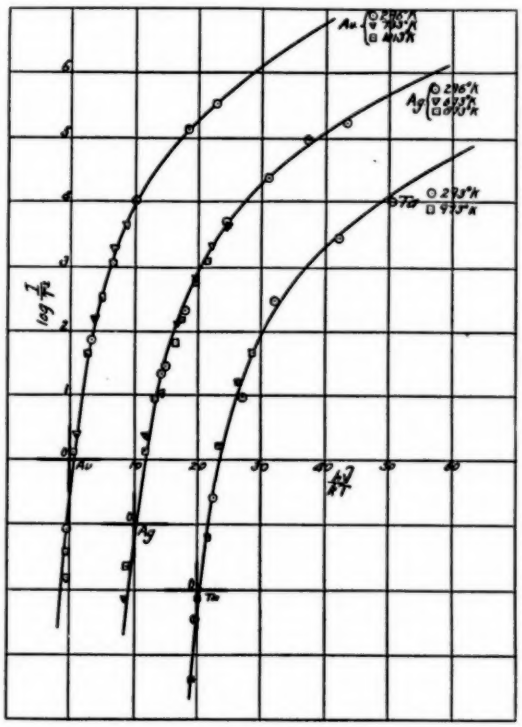

Fig. 3.

point on the observed curve coinciding with $\mu=0$ on the theoretical curve. The values of ν_0 so determined should, if the theory were exact, be independent of the temperature. Fig. 3 shows the agreement obtained in this way for silver, gold and tantalum. In the case of tantalum, where the observations show that B must have changed with the temperature, the vertical shifts used were forced to differ by the amount required to take up the change in B. For the other curves equal vertical shifts were imposed for all temperatures for any one metal. The suspicion of crossing observed for gold could be removed by a negligible correction.

It will be seen at once that the general agreement so obtained is remarkably good. The points for all temperatures can be reduced to a single smooth

curve except perhaps for one or two irregularities in tantalum. The thresholds determined from the horizontal shifts which should theoretically be independent of the temperature are given below.

Ag

°K	$h\nu_0/kT$	λ_0, A	χ, volts	
296	184.8	2620	4.71	averages $\lambda_0=2600$
673	82.2	2590	4.76	$\chi=4.74$
873	63.3	2590	4.75	

Au

°K	$h\nu_0/kT$	λ_0, A	χ, volts	
296	191.0	2530	4.86	averages $\lambda_0=2510$
733	78.0	2500	4.92	$\chi=4.90$
1013	56.5	2500	4.92	

Ta

°K	$h\nu_0/kT$	λ_0, A	χ, volts	
293	162.5	3010	4.10	averages $\lambda_0=2990$
973	49.5	2970	4.14	$\chi=4.12$

Though the small variation in λ_0 goes in the same direction and is of about the same amount for all three metals, it is extremely doubtful if it is really significant.

The results for tin and potassium give equally good fits with the theoretical curve; Lawrence and Linford have already pointed this out for their potassium results. From Goetz's observations on tin the results are as follows.

Sn

Substance	°K	$h\nu_0/kT$	λ_0, A	χ, volts	λ_0. Goetz
β-tin	358	142.5	2810	4.39	2740
γ-tin (1)	483	103.0	2880	4.28	2820
liquid	673	72.0	2955	4.17	2925

(1) Observations rather irregular.

There is here a decided change of threshold with temperature, or rather presumably with crystalline form and on melting. It would be interesting to confirm this result with other meltable metals. The size and direction of the changes in χ compared with the variations for the other metals are such that we can be confident that the effect is real. The differences between our λ_0 and Goetz's are due to the use by him of an empirical method of extrapolating to zero current.

§4. Attempts at a More Exact Theory

A proper theory of the photoelectric effect must calculate quantum mechanically the chance that an electron in a definite state of motion inside the metal shall "pick up" a quantum $h\nu$ and appear in a new state of motion as a

photoelectron. Such a theory was first attempted by Wentzel[9] and his theory has been improved by Houston[10] and by himself[10]; Its theoretical basis hardly appears to be entirely satisfactory in its original form. Apparently more satisfactory discussions have more recently been given by Fröhlich[11] and by Tamm and Schubin.[12] It does not appear even now that their interpretations of their theoretical formulae are entirely reliable, but the general principle of the calculation seems to be correct. This newer theory can be presented for our purposes in an elementary manner, a knowledge of which I owe to conversations with Professor Frenkel.

From an electron with kinetic energy $\frac{1}{2}mu^2$ normal to the surface, an escaping photoelectron can be created with energy normal to the surface $\frac{1}{2}mu^2+h\nu$. The work of Fröhlich and of Tamm and Schubin seems to show that the problem can be discussed one-dimensionally, the other velocity components being without effect. We shall be content to assume this hardly obvious result for our elementary presentation. The probability of this event will be proportional to the intensity of the light, and the dominating factor in the calculation of any such probability is always

$$\left| \int \Psi_1^* V \Psi_0 d\omega \right|^2,$$

where the integration is over the configuration space of the electron, V is the perturbing electromagnetic potential of the light in operator form, and Ψ_0, Ψ_1 are the properly normalized wave-functions for the electron in its initial and final states. Now Ψ_0 for the initial state is of the form

$$(ae^{2\pi ipx/h} + a^* e^{-2\pi ipx/h}) e^{-2\pi iWt/h}$$

inside the metal (constant potential energy), and dies away exponentially in the region where the potential energy exceeds the total energy. The a and a^* are adjusted to normalize Ψ_0 for one electron in the metal and do not depend on ν. On the other hand Ψ_1 representing one actually emerging electron must be normalized to represent an *emergent flux* of one electron and the external wave function is therefore of the form

$$\frac{1}{W'^{1/4}} e^{2\pi i(p'x - W't)/h},$$

where

$$W' = \tfrac{1}{2}mu^2 + h\nu - \chi_0 > 0. \tag{11}$$

It appears that this $W'^{1/4}$ is the only factor with a sensitive dependence on ν. Over the small light frequency ranges in which we are here interested, factors such as powers of ν itself are of slight interest. One may therefore expect the probability of emergence to contain a factor

[9] Wentzel, Probleme der Modernen Physik, Leipzig 1928 p. 79 Sommerfeld's Festschrift).
[10] Quoted by Lawrence and Linford (loc. cit) from private communications.
[11] Fröhlich, Ann. d. Physik **7**, 103 (1930).
[12] Tamm and Schubin, Zeits. f. Physik **68**, 97 (1931).

$$\frac{1}{(\frac{1}{2}mu^2 + h\nu - \chi_0)^{1/2}}$$

and no other factors of great importance. A detailed investigation confirms this.

On referring to (2) we now see that, provided nothing else has been overlooked, the photoelectric current should be proportional near the threshold to

$$\frac{4\pi kT}{m}\left(\frac{m}{h}\right)^3 \int_{\frac{1}{2}mu^2\chi_0 - h\nu}^{\infty} \frac{du}{(\frac{1}{2}mu^2 + h\nu - \chi_0)^{1/2}} \log\left\{1 + e^{(\epsilon^* - \frac{1}{2}mu^2)/kT}\right\},$$

which can be reduced, omitting constants of proportionality to

$$P = \frac{T^{3/2}}{(\chi_0 - h\nu)^{1/2}} \int_0^{\infty} \frac{dy}{\sqrt{y}} \log(1 + e^{\mu - y}), \tag{12}$$

where as before

$$\mu = \frac{h\nu - \chi}{kT}.$$

According to (12) therefore, we shall have a photoelectric current which as $T \to 0$ takes the form

$$P \propto \begin{cases} \dfrac{(h\nu - \chi)^{3/2}}{(\chi_0 - h\nu)^{1/2}} & (h\nu > \chi), \\ & (h\nu < \chi). \end{cases} \tag{13}$$

When $h\nu = \chi$, $P \propto T^{3/2}$. These forms are not a priori impossible. Equation (13) agrees with equation (6″) of Tamm and Schubin to the approximation to which we are working here. To analyse the experiments we have to plot

$$\log\left\{I\frac{(\chi_0 - h\nu)^{1/2}}{T^{3/2}}\right\}$$

against $h\nu/kT$ and compare it with the theoretical curve $\log f(\mu)$ where

$$f(\mu) = \int_0^{\infty} \frac{dy}{\sqrt{y}} \log(1 + e^{\mu - y}) dy. \tag{14}$$

When $\mu \leq 0$

$$f(\mu) = \sqrt{\pi} \sum_{n=1}^{\infty} \frac{(-1)^{n-1}}{n} e^{n\mu}. \tag{15}$$

When $\mu > 0$ there is no simple expansion available but there is the asymptotic expansion good for $\mu \geq 7$ or thereabouts.

$$f(\mu) \sim \frac{4}{3}\mu^{3/2} + \frac{\pi^2}{6}\frac{1}{\mu^{1/2}} + \frac{2}{\mu^{5/2}}\frac{1\cdot 3}{2^2}\sum_{n=1}^{\infty}\frac{(-1)^{n-1}}{n^4} + \frac{2}{\mu^{9/2}}\frac{1\cdot 3\cdot 5\cdot 7}{2^4}\sum_{n=1}^{\infty}\frac{(-1)^{n-1}}{n^6} + \cdots \tag{16}$$

On the other hand the corrected results of Wentzel and Houston quoted above give no additional factor sensitive to ν and therefore yield sensitivity curves near the threshold essentially in agreement with the N_B of Eq. (7). Their revised theories have however, so far as I am aware, not yet been published. We shall analyse the experimental results again according to the formulae of this section without further theoretical discussion.

§5. Second Analysis of the Observations

The method of analysis is the same as that of §3. The results for silver, gold and tantalum are shown in Fig. 4. It is perhaps just possible to decide, on inspecting fairly large scale plots, that the fit is less good than the fit obtained in §3. The fit obtainable for tin and potassium is distinctly less good than the fit obtainable according to §3 but of course these data are not so suitable for accurate discussion. The threshold values are given below.

Ag

°K	$h\nu_0/kT$	λ_0, A°	χ, volts	
296	186.7	259_5	4.75	averages $\lambda_0=2580$
673	82.9	2570	4.79	$\chi=4.78$
873	63.8	2570	4.79	

Au

°K	$h\nu_0/kT$	λ_0, A°	χ, volts	
296	192.2	2520	4.89	averages $\lambda_0=2500$
733	78.5	248_5	4.95	$\chi=4.93$
1013	56.7	2490	4.94	

Ta

°K	$h\nu_0/kT$	λ_0, A°	χ, volts	
293	163.8	298_5	4.13	averages $\lambda_0=2970$
973	50.0	2950	4.18	$\chi=4.16_5$

As with the results of §3 there is little or no significant variation to be detected here. The different methods of extrapolating to zero temperature (as it were) give values of λ_0 differing by about 20 A° and values of χ differing by about 0.04 volts. Until we can decide which theory must be preferred, there must remain this amount of uncertainty in the determination of the threshold.

§6.

The change of slope which leads to the intersection of the sensitivity curves for tantalum and perhaps for gold has yet to be considered. It is a change of about 20% for tantalum, and it is tempting to try to correlate it with the factor $(\chi_0-h\nu)^{-1/2}$ which occurs in both theories for the sensitivity. This factor is essentially $(\epsilon^*)^{-1/2}$ and to interpret the change of slope in this way without change of χ we should have to suppose that ϵ^* and χ_0 both increase equally with the temperature[12] by about 40%. This is most unlikely! It remains to be seen whether a more exact theory will give other factors of

this type, so that the effect could be accounted for by a smaller and more reasonable change. On the experimental side, it is desirable to know not only

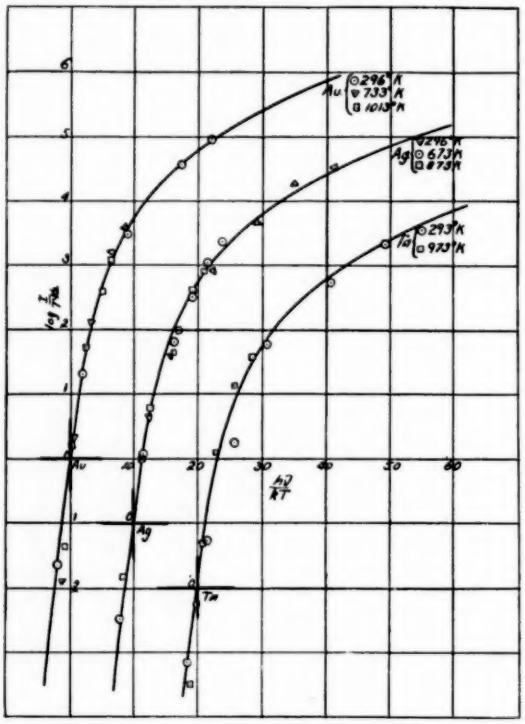

Fig. 4.

whether this change correlates with some peculiarity in the thermionic emission, but also whether the more normal behaviour is that of silver with no such effect, or gold with a very small one.

§7. Conclusion

In conclusion it seems fair to maintain that the temperature effect observed in the photoelectric sensitivity of all three metals (except for the change of slope for tantalum) is a result of the temperature effect on the distribution of the electrons among their various levels in the metal and that no other primary changes are taking place at these temperatures. We may also be confident that further study of the effect especially (if possible) over a wider temperature range and in connection with the thermionic emission will help to throw considerable light on the theory of metals.

It is a pleasure to thank Professor Mendenhall for the opportunity to become acquainted with the experimental work on this subject, afforded by a temporary post in his department, and Messrs. Winch and Morris for their generous assistance in the analysis of the experimental material, both their own, and of other observers.

[13] In view of the definition of ϵ^* this must be interpreted to mean that some change takes place, e.g., an increase in the number of free electrons such that if the new state were extrapolated back to zero temperature we should require a larger value of ϵ^*.

RELATIVISTIC THEORY OF THE PHOTOELECTRIC EFFECT PART I. THEORY OF THE *K*-ABSORPTION OF X-RAYS

By Harvey Hall

PART II. PHOTOELECTRIC ABSORPTION OF ULTRAGAMMA RADIATION

By Harvey Hall and J. R. Oppenheimer
University of California, Berkeley

(Received May 7, 1931)

Abstract

Part I: A strict theory of the absorption of x-rays is developed on the basis of relativistic quantum electrodynamics. The theory is applied to the absorption of x-rays by a Dirac electron in the field of a nucleus. Corrections to the non-relativistic theory are appreciable only for heavy elements, where the present calculations give a *K*-discontinuity twenty percent smaller than the earlier ones. The agreement with experiment is not improved.

Part II: The theory is applied to the calculation of the absorption of quanta whose energy is larger than the proper energy mc^2 of the electron. The cross section for absorption is here given approximately by

$$\sigma \backsim 2 \times 10^{-22} Z^5 \lambda.$$

This result is applied to account for the excess absorption over that predicted by the Klein-Nishina formula found experimentally for the gamma-rays of ThC'' by Chao and Tarrant. The theory is in fairly good agreement with experiment for Cu, but disagrees violently with it for Pb. An examination of the approximations made in deriving and applying the theoretical result shows that they cannot have introduced this discrepancy. There is thus a definite conflict between electrodynamical theory and experiment.

Introduction

THE photoelectric cross section for absorption, σ, is connected with the mass absorption coefficient μ, by the relation $\mu = \sigma/\rho$. Various quantum theoretic derivations of σ have been given; in addition to these the literature contains interesting and graphic solutions treating such problems as distribution in angle of the photoelectrons, group velocity of the waves representing the photoelectric current, and besides these the theory has been applied to shells higher than the *K*-shell. We refer to a few of these papers collectively[1]—due to the difference of treatment, or to the difference in the problem treated we shall make few explicit references.

The problem under discussion may be considered that of a hydrogenic

[1] Wentzel, Zeits. f. Physik **40,** 574; **41,** 828 (1926); Oppenheimer, Zeits. f. Physik **41,** 268 (1926); Phys. Rev. **31,** 349 (1928); Beck, Zeits. f. Physik **41,** 443 (1926); Suguira, J. de Physique **8,** 113 (0000); Sommerfeld and Schur, Ann. d. Physik **4,** 413 (1930); Schur, Ann. d. Physik **4,** 433 (0000); Froehlich, Ann. d. Physik **7,** 109 (4930); Stobbe, Ann. d. Physik **7,** 661 (1939); Szczeniowski, Phys. Rev. **35,** 347 (1930); Bethe, Ann. d. Physik **4,** (1930); T. Muto, I.P.C.R., Tokyo (1931).

atom in its normal state, interacting with a light-quantum field which induces transitions to hyperbolic orbits. This problem, strictly speaking, has one answer—the complete relativistic solution; but for convenience the problem is divided into two parts. If the region of interest does not involve photo-electron velocities that are too great, it is justifiable to assume that the non-relativistic model will suffice.

This is the model employed by Nishina and Rabi,[2] and involves simply the solution of the Schroedinger equation. This result could be expected to hold for those elements for which the binding in the K-shell is not great enough to necessitate bombardment by quanta whose wave-length are short compared to the size of the K-shell, but it should be added that neither this nor the relativistic result should be expected to hold for very light elements, since here the assumption that the effects of the more external electrons are negligible is invalid. We mention that except for very light elements the Nishina-Rabi result is in accord with experience.

To obtain a formula theoretically more general than that of Nishina and Rabi necessitates a complete solution of the relativistic problem. This in the present state of the theory means describing the atom with Dirac's linear Hamiltonian, using retarded potentials and the relativistic theory of the light-quantum field.

Attempts in this direction have not been numerous. It is not difficult to include retardation and evaluate the integrals if a Schroedinger wave equation describes the atom, and this has been done by at least two writers. Although it presents an analytic problem of some interest such a discussion is of course incomplete. An additional contribution has recently been made[3] in which the author employs Dirac wave functions but neglects retardation in discussing transitions for wave-lengths between λ_0 for the K-limit, and $\lambda_0/2$.

In the case of obtaining a solution of the more difficult relativistic problem, we should be interested in comparing it with two sets of experimental data. (1) Although agreement between the Nishina-Rabi result and experiment is qualitatively pretty good there are discrepancies which make a better quantitative check desirable. Consequently we should concern ourselves in seeing whether relativitity properly corrects the non-relativistic theory, and to this end we should compare our result with empirical data for the K-limit and the region immediately adjoining it.* (2) Recent data from the region of gamma and cosmic rays have made it appear not impossible that our previous assumption, that the cross section for absorption is too small to be observable for light as hard as gamma rays, may be unjustified, and that in reality the photoelectric absorption is comparable with the scattering in this region.

[2] Nishina and Rabi, Verh. d. Deut. Phys. Ges. **9**, 6 (1928).

[3] Roess, Phys. Rev. **37**, 533 (1931).

* Such a comparison has been made by Roess (Ref. 3). Since, as will appear in this paper, including the retarded potentials does not improve the accuracy over his model at the K-absorption limit we have not considered it valuable to make the further calculations away from the limit.

Work contributing along these lines has been done by Chao,[4] Tarrant,[5] Gray[6] and Meitner and Hupfeld. In particular the experiments of Chao could be accounted for if the ratio of σ for lead, to the Klein Nishina cross section for scattering[7] were about 0.5 for $\lambda = 4.7$X.U. In the course of the discussion considerably more will be said concerning the latter problem. For the present let us develop the general integrals and dispose of the discussion of the K-limit.

PART I. THEORY OF THE K-ABSORPTION OF X-RAYS

The cross section for absorption.

The Hamiltonian for our problem consists of three terms. The term for the atom

$$H_0{}^m = (\mathbf{s}' \cdot \mathbf{p}) - e\phi + mc^2\Gamma_0$$

we take from Weyl.[8] $\mathbf{s}'$ is a matrix (analogous to Dirac's α matrix) and will be given later. ϕ is the hydrogenic scalar potential Ze/r. Γ_0 is a matrix[9]; it will not be needed explicitly.

Let a wave function for the normal state of the atom given by this Hamiltonian be ψ_0; let the corresponding energy be $h\nu_0$. Further, let a complete set of wave functions for the energy $h\nu = h\nu' + h\nu_0 > 0$, be ψ_m; we need the index m because there are many states with the same energy, to which a photoelectric transition is possible. Let the ψ_m be normalized to $d\nu$. Then the cross section for photoelectric absorption of a quantum of frequency ν, with vector of propagation parallel to z, and with the electric vector plane-polarized in the x-y plane parallel to the unit vector $\mathbf{e}$, is given by[10],*

$$\sigma = \sum_m \frac{4\pi e^2 c}{h\nu} \left| \int \bar{\psi}_m (\mathbf{e} \cdot \mathbf{s}') \psi_0 \sin(\kappa z + \beta) d\tau \right|^2 . \tag{1}$$

[4] Chao, P.N.A. **16,** (1930).

[5] Tarrant, Proc. Roy. Soc. **A128,** 345 (1930).

[6] Gray, Proc. Roy. Soc. **A130,** 524 (1931).

[7] Klein, Nishina, Zeits. f. Physik **52,** 853 (1928).

[8] Weyl, Gruppentheorie u. Quantenmechanik, p. 175.

[9] Reference 8, p. 172.

[10] See for instance J. R. Oppenheimer, Phys. Rev. **35,** 461, par. 3, where the analogous result is derived for series transitions from the Heisenberg-Pauli theory. The extension to transitions in the continuous spectrum is trivial.

* The quantum which we are here considering is represented by a standing electromagnetic wave. The physics of our problem would make it more desirable to work with a progressive wave in which the momentum of the quantum was directed along the positive z-axis. In particular the use of such a wave would give an asymmetry in the direction of photoelectric emission about the $x-y$ plane; whereas from formula (1) we obtain a symmetrical result (see Eq. (17)). This may be interpreted as the photoelectric emission produced by a half unit intensity of radiation propagated in the positive z-direction, plus that from a half unit intensity of radiation propagated in the negative z-direction. The total value of the cross section integrated over all the angles is of course correctly given by (1). It would be possible to work directly with a relativistic extension of Dirac's light quantum theory (cf. e.g. I. Waller, Zeits. f. Physik **61,** 1930). When we start, however, with Maxwell's theory, and quantize according to the method of Heisenberg and Pauli we are led directly to the use of standing waves. It is not hard to modify the treatment of Heisenberg and Pauli; but it has seemed desirable to us to use the results of the strict theory in their most accessible form.

Here the coordinate z is to be measured from the center of mass of the atom; the phase constant β is introduced to take account of the fact that this center of mass may be anywhere between the crest and the trough of our electromagnetic wave. In our results we are to average over β. Further $\mathrm{K}=2\pi\nu/c$. We write for convenience

$$\Gamma = \kappa z + \beta.$$

We introduce two components of $\mathbf{s}'$[11]

$$s_x' = \begin{pmatrix} 0 & 1 & 0 & 0 \\ 1 & 0 & 0 & 0 \\ 0 & 0 & 0 & -1 \\ 0 & 0 & -1 & 0 \end{pmatrix}, \quad s_y' = \begin{pmatrix} 0 & -i & 0 & 0 \\ i & 0 & 0 & 0 \\ 0 & 0 & 0 & i \\ 0 & 0 & -i & 0 \end{pmatrix}. \tag{2}$$

Let us define the integral in Eq. (1) to be I^0. And further as there are two normal states we will identify one of them with the index α, and the other with β. $I^{0^2}=I_\alpha{}^{0^2}+I_\beta{}^{0^2}$. Then,

$$I_\alpha{}^0 = \frac{e_x}{2}(I_\alpha{}^R + I_\alpha{}^L) - \frac{ie_y}{2}(I_\alpha{}^R - I_\alpha{}^L)$$

$$= \frac{e_x - ie_y}{2} I_\alpha{}^R + \frac{e_x + ie_y}{2} I_\alpha{}^L$$

where

$$I_\alpha{}^R = \int \bar{\psi}_k(s_x' + is_y')\psi_\alpha{}^0 \sin\Gamma d\tau \tag{3}$$

$$I_\alpha{}^L = \int \bar{\psi}_k(s_x' - is_y')\psi_\alpha{}^0 \sin\Gamma d\tau.$$

Then multiplying $I_\alpha{}^0$ by its complex conjugate, the cross product term drops out because the selection rules for the two integrals are different. Averaging over all directions of e_s, we obtain

$$I_\alpha{}^{0^2} = \tfrac{1}{4}(I_\alpha{}^{R^2} + I_\alpha{}^{L^2}).$$

This equation may be interpreted as a verification of the fundamental notion[12] that out of circularly polarized light we may build up a non-polarized beam, that has the same properties as a non-polarized beam built up from plane-polarized light in which the electric vector may have all possible directions. An exactly similar relation holds for $I_\beta{}^0$. In addition it may be shown by using the wave functions associated with s', that $I_\beta{}^L=I_\alpha{}^R$, $I_\alpha{}^L=I_\beta{}^R$. Consequently we may write

$$I^{0^2} = \tfrac{1}{2}(I_\alpha{}^{R^2} + I_\beta{}^{R^2}).$$

We have then from Eq. (1)

[11] Reference 8, p. 172.

[12] Dirac, The Principles of Quantum Mechanics, Ch. I.

$$\sigma_\alpha + \sigma_\beta = \sum_k \frac{2\pi e^2 c}{h\nu}[I_\alpha{}^{2R}(k) + I_\beta{}^{2R}(k)].$$

The superscript R is to indicate one kind of polarization. Since we shall be interested in only one kind, R will not be written in explicitly from now on.

$$\sigma = \tfrac{1}{2}(\sigma_\alpha + \sigma_\beta) = \frac{\pi e^2 c}{h\nu} \sum_k (I_\alpha{}^2(k) + I_\beta{}^2(k)). \tag{4}$$

I_α is defined by Eq. (3), and I_β by a similar equation.

The wave functions.

In the following Weyl's wave functions and quantum numbers will be used.[13] The normal states α and β are specified by the quantum numbers $k=1$, $m=0$; $k=1$, $m=-1$ respectively. Both I_α and I_β will give rise to transitions into states of positive and negative values of k, and in each case $\Delta m=1$. The meaning of the quantum numbers j and m can briefly be given as follows. The total angular momentum of the electron in units of $h/2\pi$ is given by $M^2=k^2-1/4=j(j+1)$, where, in accordance with the customary meaning, j is the coupled angular momentum of spin and orbit. $k=\pm(j+1/2)\neq 0$. $k<0$ corresponds to states where spin and orbit are anti-parallel; while for $k>0$ spin and orbit are parallel, except for $k=1$ when the orbital angular momentum is zero. m is analogous to the magnetic quantum number, but is integral. The z-component of the total angular momentum is $h(m+1/2)/2\pi$.

The wave functions for the normal states may be obtained directly out of Weyl.[14] Only their components necessary to express I_α and I_β will be given here.

$$\left.\begin{aligned} &\alpha;\ k=1,\ m=0: \quad \psi_2{}^0 = -\psi_4{}^0 = i\alpha \sin\theta e^{i\phi} \\ &\beta;\ k=1,\ m=-1: \psi_2{}^0 = \bar{\psi}_4{}^0 = 1+\rho_1 - i\alpha\cos\theta \end{aligned}\right\} \cdot N_0 e^{-rb} r^{\rho_1-1}$$

α equals the fine structure constant times the atomic number $=2\pi e^2 Z/hc$
b equals the reciprocal of the first Bohr radius $=4\pi^2 me^2 Z/h^2$

$$\rho_1 = (1-\alpha^2)^{1/2}, \ [\text{In general, } \rho = (k^2-\alpha^2)^{1/2}]$$
$$1/N_0 = 4[\pi(1+\rho_1)\Gamma(1+2\rho_1)(2b)^{-1-2\rho_1}]^{1/2}.$$

Weyl's solutions[15] may be expressed in terms of better known functions in their dependence on θ.

$$r\psi_1 = e^{im\phi}(vq + iwp)$$
$$r\psi_2 = e^{i(m+1)\phi}[v(p - q\cos\theta) - iw(q - p\cos\theta)]\csc\theta$$

ψ_3 and ψ_4 are respectively ψ_1 and ψ_2 with the sign of iw changed
$q=\sin^{-m}\theta$ times the sum of Weyl's P and Q.
$p=\sin^{-m}\theta$ times the difference of Weyl's P and Q

[13] For a more complete statement of the formal role of the quantum numbers than is given in this paragraph one should consult par. 40 of reference 8.

[14] Reference 8, pp. 177–178.

[15] Reference 8, p. 184.

Then it is not hard to find that p and q are proportional to Ferrer's[15] $P_k^m(\cos\theta)$, and $P_{k-1}^m(\cos\theta)$ respectively, and then to show that

$$r\psi_1 = e^{im\phi}\left[vP_{k-1}^m(\cos\theta) + i\omega\frac{k-m}{k+m}P_k^m(\cos\theta)\right]$$

$$r\psi_2 = -\frac{e^{i(m+1)\phi}}{k+m}\left[vP_{k-1}^{m+1}(\cos\theta) + i\omega P_k^{m+1}(\cos\theta)\right].$$

v and w are the radial functions as in Weyl. Making the appropriate changes they are identical with the solutions given by Gordon.[17] We take over Gordon's solutions, and since we are interested in the continuum only, we make the convention $(1-\epsilon^2)^{1/2} = +i(\epsilon^2-1)^{1/2}$. The wave functions then become

$$\begin{aligned} r\psi_1(k) &= cNe^{im\phi}\left[(k+m)(\epsilon+1)^{1/2}\,x\,P_{k-1}^m(\cos\theta)\right. \\ &\quad \left. + i(k-m)(\epsilon-1)^{1/2}yP_k^m(\cos\theta)\right] \\ r\psi_2(k) &= -cNe^{i(m+1)\phi}\left[(\epsilon+1)^{1/2}\,x\,P_{k-1}^{m+1} + i(\epsilon-1)^{1/2}yP_k^{m+1}(\cos\theta)\right] \end{aligned} \qquad 5(a, b)$$

for positive k. The functions for negative k we distinguish by a prime, indicating that the sign of k has been changed in Eqs. (5, a, b) and that the absolute value of k is considered:

$$\begin{aligned} r\psi_1'(-k) &= -cN'e^{im\phi}\left[(k-m)(\epsilon+1)^{1/2}\,x'P_k^m\right. \\ &\quad \left. + i(k+m)(\epsilon-1)^{1/2}y'P_{k-1}^m\right] \\ r\psi_2'(-k) &= cN'e^{i(m+1)\phi}\left[(\epsilon+1)^{1/2}\,x'P_k^{m+1} + i(\epsilon-1)^{1/2}y'P_{k-1}^{m+1}\right]. \end{aligned} \qquad 5(c, d)$$

In each case to obtain ψ_3 change the sign of iy in ψ_1. The same connection holds between ψ_4 and ψ_2.

In the above expressions the quantities occurring are defined as follows:

$$\begin{aligned} f = x + iy &= e^{i\gamma}r^\rho e^{-ik_0 r}F(\rho+1+in, 2\rho+1, 2ik_0 r) \\ e^{2i\gamma} &= (\rho+in)/(k-ib/k_0) \\ f' = x' + iy' &= f(-|k|) = ie^{i\gamma'}(e^{-i\gamma}f) \\ e^{2i\gamma'} &= +(\rho+in)/(k+ib/k_0) \\ F(\alpha,\beta,x) &= \sum_{\sigma=0}^{\infty}\frac{\Gamma(\alpha+\sigma)\Gamma(\beta)}{\Gamma(\beta+\sigma)\Gamma(\alpha)\sigma!}x^\sigma \\ \epsilon &= E/mc^2. \end{aligned}$$

The following conservation law holds between the energy of the incident light, the energy of the electron in the normal state, and the energy of the photoelectron:

$$\kappa' + \rho_1 = \epsilon, \text{ where } \kappa' = h\nu/mc^2$$

$$k_0 = 2\pi mc(\epsilon^2-1)^{1/2}/h$$

$$n = b\epsilon/k_0.$$

[16] Whittaker and Watson, Modern Analysis, p. 323.

[17] Gordon, Zeits. f. Physik **48,** 11 (1928).

The normalization is carried out by the Weyl-Hellinger method.

The asymptotic expression of $f(k)$ for large r is

$$f \sim 2h_1 e^{ik_0 r} r^{in}$$

where,

$$h_1 = \frac{e^{i\gamma}\Gamma(2\rho+1)e^{-\pi n/2}e^{-\pi\rho i/2}}{2\Gamma(\rho+in)\,|\,2k_0\,|^{\rho-in}}.$$

Therefore, using

$$r\psi_1 = A_1 x + iB_1 y$$

$$r\psi_1 \sim G_1 e^{ik_0 r} r^{in} + \text{complex conjugate},$$

$G_1 = h_1(A_1 + iB_1)$, and A_1 is the coefficient of x in the expression for $r\psi_1$ of Eq. (6).

The normalization is now performed as follows. We use the above expression for ψ_1, and find

$$\lim_{\Delta\nu\to 0} \int_0^\infty \bar{\psi}_1 \left\{ \int_{\Delta\nu} \psi_1 d\nu \right\} r^2 dr.$$

The sum of these expressions for all four components of ψ is then integrated over the angles and set equal to unity.

One takes the asymptotic expression for ψ since the contribution over any finite part of the radial integration vanishes. This is the physical assertion that the relative time an electron (in a hyperbolic orbit) spends near the nucleus is negligible.

The normalization is further simplified by the smoothness of the integrand in the integral over $d\nu$; all factors involving ν except the exponential may be considered constant, since we will go to the limit $\Delta\nu \to 0$. One obtains

$$\int r^2 \bar{\psi}_1 \left\{ \int_{\Delta\nu} \psi_1 d\nu \right\} dr = \frac{d\nu}{dk_0} \pi\,|\,G_1\,|^2 + 0(\Delta\nu).$$

On completing the normalization

$$c^2 = \frac{8\pi m\epsilon(2k_0)^{2\rho-1}e^{\pi n}\,|\,\Gamma(\rho+1+in)\,|^2}{h\Gamma^2(2\rho+1)}$$

$$N^2 = \frac{(k-m-1)!}{4\pi\epsilon(k+m)!}\,\frac{2k+1}{(4k+1)\epsilon+1}$$

$$N'^2 = \frac{(k-m-1)!}{8\pi\epsilon(k+m)!}.$$

Let $N_1 = cN$, $N_1' = cN'$

As a guide in discussing the integrals, before actually expressing them, the physical meaning of the transitions that I_α and I_β of Eq. (3), and the analogous equation, correspond to, can be mentioned here. $I_a(\pm 1)$ will not exist as

there are no states such that $|k| - m - 1 < 0$, and for I_α m changes from zero to one. This will assert itself when I_α is seen to contain a factor $(k-1)$. $I_\beta(1)$, since it gives the probability of a transition involving a final state of zero orbital angular momentum, one might expect to be small. It must certainly be a term that approaches zero as the frequency of the incident light approaches zero, for the transition could not occur without some correction not considered in deriving the Schroedinger cross section. It turns out that this transition does occur, and is induced by the retardation factor; its probability is small of the order $(\kappa/b)^2$.

Expression of the integrals.

Using Eqs. (2) and (3) we may write

$$I_\alpha(k) = 2\int (\bar{\psi}_1 k\psi_2{}^{0,\alpha} - \bar{\psi}_3 k\psi_4{}^{0,\alpha}) \sin\Gamma d\tau \tag{6}$$

$$= 4\pi i\alpha N_0 N_1 (k+m)(\epsilon+1)^{1/2} \int_0^{2\pi}\int_0^{\pi}\int_0^{\infty} e^{i\phi(1-m)} d\phi r^{\rho_1} e^{-rb} x$$

$$\sin\theta P_{k-1}{}^m(\cos\theta) \sin\Gamma \sin\theta dr d\theta.$$

This gives immediately $m=1$. We employ the following representation of a wave.[18]

$$\sin\Gamma = \left(\frac{2\pi}{(\kappa r)^3}\right)^{1/2} \csc\theta \sum_{\sigma=0}^{\infty} (\sigma + 3/2) P_{\sigma+1}{}^1(\cos\theta) \sin\left(\frac{\pi\sigma}{2} + \beta\right) \tag{7}$$

$$J_{\sigma+3/2}(\kappa r)$$

integrate over θ, and use the following relation between Bessel functions and confluent hypergeometric functions

$$J_{k-1/2}(\kappa r) = \frac{(\kappa r/2)^{k-1/2} e^{-i\kappa r}}{\Gamma(k+\frac{1}{2})} F(k, 2k, 2i\kappa r).$$

The result is

$$I_\alpha(k) = \frac{-4\pi^{3/2} N_0 N_1 \alpha k(k^2-1)(\epsilon+1)^{1/2}(\kappa/2)^{k-2} \sin\left(\frac{\pi k}{2} + \beta\right)}{\Gamma(k+\frac{1}{2})}$$

$$\int_0^{\infty} e^{-r(b+i\kappa)} x r^{k+\rho_1-2} \cdot F(k, 2k, 2i\kappa r) dr.$$

It will be convenient in discussing this and the remaining integrals to express x and y in the explicit forms that will now be given. Using the recursion formula

$$\alpha F(\alpha+1, \gamma+1, x) = (\alpha-\gamma)F(\alpha, \gamma+1, x) + \gamma F(\alpha, \gamma, x),$$

[18] Reference 16, p. 383 (the expression in the reference should be multiplied by two).

we may write

$$x = \frac{\rho e^{-i\gamma'} e^{-ik_0 r} r^\rho}{(\rho^2 + n^2)^{1/2}} [F(\rho + in, 2\rho, 2ik_0 r) + gF(\rho + in, 2\rho + 1, 2ik_0 r)]$$

where the following definitions hold: $\gamma' = \tan^{-1} n/\rho - \gamma$,

$$g = \frac{1}{2\rho}\left[k - \rho + i\alpha\left(\frac{\epsilon - 1}{\epsilon + 1}\right)^{1/2}\right] \to 0\left(\frac{\alpha^2}{4k^2}\right), \text{ as } k_0 \to 0.$$

By finding the real and imaginary parts of $e^{-ik_0 r} F(\rho+1+in, 2\rho+1, 2ik_0 r)$, y may be found.

$$y = \frac{r^\rho e^{-ik_0 r}}{(\rho^2 + n^2)^{1/2}} [pF(\rho + in, 2\rho, 2ik_0 r) + qrF(\rho + 1 + in, 2\rho + 2, 2ik_0 r)]$$

where,

$$p = \left[\frac{1}{2}\left(\rho^2 - \rho k + \frac{\alpha^2 \epsilon}{\epsilon - 1}\right)\right]^{1/2} \to 0\left[\frac{\alpha^2}{2(\epsilon - 1)}\right]^{1/2}, \text{ as } k_0 \to 0$$

$$q = \frac{b\epsilon\left[\frac{1}{2}\left(\rho^2 - \rho k + \frac{\alpha^2\epsilon}{\epsilon - 1}\right)\right]^{1/2} + \rho k_0\left[\frac{1}{2}\left(\rho^2 + \rho k + \frac{\alpha^2\epsilon}{\epsilon + 1}\right)\right]^{1/2}}{\rho(2\rho + 1)}$$

$$\to 0\left[\frac{b^2\alpha^2}{2\rho^2(2\rho + 1)^2(\epsilon - 1)}\right]^{1/2}, \text{ as } k_0 \to 0$$

$$y' = y(-k).$$

To obtain x' we use the relation $2x = f + \bar{f}$, and the formula

$$F(\alpha + 1, \gamma, x) - F(\alpha, \gamma, x) = \frac{x}{\gamma} F(\alpha + 1, \gamma + 1, x)$$

and thus obtain

$$x' = -e^{i\gamma'} r^\rho e^{-ik_0 r}\left[\frac{k_0 r}{2\rho + 1} F(\rho + 1 + in, 2\rho + 2, 2ik_0 r) + jF(\rho + in, 2\rho + 1, 2ik_0 r)\right]$$

where,

$$j = \frac{\rho - k + i\alpha\left(\frac{\epsilon - 1}{\epsilon + 1}\right)^{1/2}}{2i(\rho + in)}.$$

We may now write out the integrals arising from the two normal states α and β. Before doing so, in order to save writing, we call attention to the factor $\sin(\pi k/2 + \beta)$ that will occur in front of each term. Each term will ul-

timately have its absolute value squared, when we must average over the phases β. In each case the average value of $\sin^2(\pi k/2+\beta)$ will be $1/2$, and to indicate this we now write $1/2$ for each of these factors.

Then,

$$I_\alpha(k) = \frac{-(2\pi)^{3/2}i\alpha N_1 N_0 k(k^2-1)(\epsilon+1)^{1/2}(\kappa/2)^{k-2}e^{-i\gamma'\rho}}{\Gamma(k+\frac{1}{2})(\rho^2+n^2)^{1/2}} \cdot [S(\mu-2,\, k,\, a,\, 2\rho) + gS(\mu-2,\, k,\, a,\, 2\rho+1)] \tag{8(a)}$$

$$I_\alpha(-k) = \frac{-4\pi^{3/2}i\alpha N_1' N_0 k(k^2-1)(\epsilon+1)^{1/2}(\kappa/2)^{k-1}}{\Gamma(k+3/2)} \left[\frac{k_0}{2\rho+1}S(\mu,\, k+1,\, a+1,\, 2\rho+2) + jS(\mu-1,\, k+1,\, a,\, 2\rho+1)\right] \tag{8(b)}$$

$$\begin{aligned} I_\beta(k) = {} & \frac{-(2\pi)^{3/2}i\alpha N_1 N_0 k(\kappa/2)^{k-2}}{\Gamma(k+\frac{1}{2})(\rho^2+n^2)^{1/2}} \Big\{ \frac{k\alpha(\epsilon+1)^{1/2}\kappa^2 e^{-i\gamma'}}{4k^2-1}[S(\mu,\, k+1,\, a,\, 2\rho) \\ & + gS(\mu,\, k+1,\, a,\, 2\rho+1)] - \alpha e^{-i\gamma'}(\epsilon+1)^{1/2}\rho(k-1) \\ & [S(\mu-2,\, k-1,\, a,\, 2\rho) + gS(\mu-2,\, k-1,\, a,\, 2\rho+1)] \\ & + \frac{(1+\rho_1)(\epsilon-1)^{1/2}\kappa^2}{2k+1}[pS(\mu,\, k+1,\, a,\, 2\rho) \\ & + qS(\mu+1,\, k+1,\, a+1,\, 2\rho+2)]\Big\} \end{aligned} \tag{8(c)}$$

$$\begin{aligned} I_\beta(-k) = {} & \frac{-2(2\pi)^{3/2}iN_0 N_1' k(\kappa/2)^{k-1}}{\Gamma(k+\frac{1}{2})(\rho^2+n^2)^{1/2}} \Big\{ -\frac{(\rho^2+n^2)^{1/2}\kappa^2\alpha(\epsilon+1)^{1/2}(k+1)e^{i\gamma}}{(2k+1)^2(2k+3)} \\ & \cdot\left[\frac{k_0}{2\rho+1}S(\mu+2,\, k+2, a+1,\, 2\rho+2) + jS(\mu+1,\, k+2,\, a,\, 2\rho+1)\right] \\ & + \frac{(\rho^2+n^2)^{1/2}k\alpha(\epsilon+1)^{1/2}e^{i\gamma'}}{2k+1}\left[\frac{k_0}{2\rho+1}S(\mu,\, k,\, a+1,\, 2\rho+2)\right. \\ & \left. + jS(\mu-1,\, k,\, a,\, 2\rho+1)\right] \\ & - (1+\rho_1)(\epsilon-1)^{1/2}[p'S(\mu-1,\, k,\, a,\, 2\rho) \\ & + q'S(\mu,\, k,\, a+1,\, 2\rho+2)]\Big\} \end{aligned} \tag{8(d)}$$

where,

$$S(A,\, k,\, a,\, 2\rho) = \int_0^\infty e^{-r(b+i\kappa+ik_0)} r^A F(k,\, 2k,\, 2i\kappa r) F(a,\, 2\rho,\, 2ik_0 r)\, dr \tag{9}$$

and, $\mu = \rho+\rho_1+k$, $a = \rho+in$

The other quantities S are obtained from this by appropriate changes in the parameters.

By expanding both of the confluent functions in this integral in powers of r, integrating over r, and then summing first over powers of $2i\kappa$, one obtains an infinite series, each term of which contains a hypergeometric function. To the latter apply the formula

$$F(\alpha, \beta, \gamma, x) = (1 - x)^{-\beta} F\left(\gamma - \alpha, \beta, \gamma, \frac{-x}{1 - x}\right)$$

and then use the definition

$$F(\alpha, \beta, \gamma, x) = B^{-1}(\beta, \gamma - \beta) \int_0^1 u^{\beta-1}(1 - u)^{\gamma-\beta-1}(1 - xu)^{-\alpha} du.$$

We now define

$$S = \frac{2i\kappa}{b + i\kappa + ik_0}, \quad t = \frac{2ik_0}{b + i\kappa + ik_0}.$$

It is then seen by summing under the sign of integration in the expression obtained as just indicated, that

$$S(\mu - 2, k, a, 2\rho) = \frac{(S/2i\kappa)^{\mu-1}\Gamma(\mu - 1)}{(1 - s)^k B(k, k)}$$
$$\int_0^1 (u - u^2)^{k-1}\left(1 + \frac{su}{1 - s}\right)^{\mu-2k-1} F\left(a, \mu - 1, 2\rho, t + \frac{tsu}{1 - s}\right) du.$$

To the hypergeometric function in the integrand we apply

$$F(\alpha, \beta, \gamma, x) = (1 - x)^{\gamma-\alpha-\beta} F(\gamma - \alpha, \gamma - \beta, \gamma, x)$$

so

$$F\left(a, \mu - 1, 2\rho, t + \frac{tsu}{1 - s}\right)$$
$$= \left[1 - t\left(1 + \frac{su}{1 - s}\right)\right]^{2\rho-\mu-a+1} F\left(\bar{a}, 2\rho - \mu + 1, 2\rho, \tau\left(1 + \frac{su}{1 - s}\right)\right).$$

It follows that

$$S(\mu - 2, k, a, 2\rho) = \frac{(S/2i\kappa)^{\mu-1}\Gamma(\mu - 1)(1 - t)^{2\rho-\mu-a+1}}{(1 - s)^k B(k, k)} \cdot$$
$$\int_0^1 (u - u^2)^{k-1}\left(1 + \frac{su}{1 - s}\right)^{\mu-2k-1}\left[1 - \frac{stu}{(1 - s)(1 - t)}\right]^{2\rho-\mu-a+1} \tag{10}$$
$$F\left(\bar{a}, 2\rho - \mu + 1, 2\rho, t\left(1 + \frac{su}{1 - s}\right)\right) du.$$

All of the remaining integrals S may again be obtained from this one by making suitable changes in the parameters.

We shall now treat explicitly the problem at the K-limit.

Let us introduce the following quantities

$$\delta = 2k + 1 - \mu$$
$$\delta' = 2\rho - \mu + 1.$$

Rewriting Eq. (10)

$$S(\mu - 2, k, a, 2\rho) = \frac{(s/2i\kappa)^{\mu-1}\Gamma(\mu-1)(1-t)^{\delta'-a}}{(1-s)^k B(k,k)} \cdot \tag{10'}$$

$$\int_0^1 (u-u^2)^{k-1}\left(1+\frac{su}{1-s}\right)^{-\delta}\left(1-\frac{stu}{(1-s)(1-t)}\right)^{\delta'-a} F\left(\bar{a}, \delta', 2\rho, t\left(1+\frac{su}{1-s}\right)\right)du, \text{ for } |s| \sim 0(\alpha).$$

This integral is now evaluated by taking the factors $(1+su/1-s)^{-\delta}$ and $F(a, \delta', 2\rho, t(1+su/1-s))$ outside of the sign of integration and giving u its average value $1/2$.[19] It is then immediate that

$$S(\mu - 2, k, a, 2\rho) = \frac{(s/2i\kappa)^{\mu-1}\Gamma(\mu-1)(1-t)^{\delta-a}}{(1-s)^k}$$

$$\left(\frac{1-s}{1-s/2}\right)^{\delta} F\left(a, \delta', 2\rho, t\left(\frac{1-s/2}{1-s}\right)\right) \cdot F\left(a-\delta', k, 2k, \frac{st}{(1-s)(1-t)}\right) \tag{10''}$$

It would be possible now to discuss this S as a function of κ, to determine its contribution to the wave-length law, *et cetera*. However, this paper is concerned with a discussion of σ at the K-absorption limit, and we propose at this point to reduce our expressions so they will apply only for $k_0=0$. (The K-limit).

Letting k_0 approach zero we see after making a simple confluence in each hypergeometric function of Eq. (10) that

$$S(\mu - 2, k, a, 2\rho) = \frac{(s/2i\kappa)^{\mu-1}\Gamma(\mu-1)e^{-\beta}}{(1-s)^k(1-\bar{s}/2)^{\delta}} F(k, 2k, \beta\bar{s}) F\left(\delta', 2\rho, \beta\left(1-\frac{\bar{s}}{2}\right)\right) \tag{11}$$

where β is defined as $\beta = 2b/(b+i\kappa)$. The remaining integrals are evaluated in exactly the same way (see appendix). In this case, however, where $k_0=0$ the work may be shortened by going to the limit in Eq. (10'). Corresponding to the factors $(1-su)^{-\delta}$ and $F(\delta', 2\rho)$ in the integral just discussed, other factors will occur where δ and δ' will be increased or decreased by one or two. In all cases it will be legitimate for our purposes to proceed in the same way, putting u average equal $1/2$.

Thus the equations analogous to Eq. (11) may be written down. These expressions are substituted into Eqs. (8; a, b, c, d) and the square of the ab-

[19] See appendix Part I.

solute value of each $I(\pm k)$ is taken. Then on multiplying by the proper normalizing factor in each case, one obtains the following expressions:

$$I_\alpha^2(k) = H(k)(k^2-1)\,|\,F(k, 2k, \beta\bar{s})\,|^2\Big[F(\delta', 2\rho) + \frac{k-\rho}{2\rho}F(1+\delta', 2\rho+1)\Big]^2 \tag{12, a}$$

$$I_\alpha^2(-k) = H(k)\,\frac{32(\kappa/2)^2b^2\mu^2(\mu-1)^2F^2(k+1)}{(2k+1)^2(2\rho+1)^2(2\rho)^2(b^2+\kappa^2)^2}\Big[F(\delta', 2\rho+2) + \frac{k-\rho}{2}F(\delta', 2\rho+1)\Big]^2 \tag{12, b}$$

$$\begin{aligned} I_\beta^2(k) = H(k)\,\frac{b^4}{(b^2+\kappa^2)^2}\Big\{&(k-1)\Big[F(\delta', 2\rho) + \frac{k-\rho}{2\rho}F(1+\delta', 2\rho+1)\Big]F(k-1) \\ &- \frac{k\mu(\mu-1)(\kappa\,|\,b)^2F(k+1)}{4k^2-1}\Big[F(\delta'-2, 2\rho) + \frac{k-\rho}{2\rho}F(\delta'-1, 2\rho+1)\Big] - \frac{(1+\rho_1)\mu(\mu-1)(\kappa/b)^2F(k+1)}{2\rho(2k+1)} \\ &\Big[F(\delta'-2, 2\rho) + \frac{F(\delta'-1, 2\rho+2)}{\rho(2\rho+1)(1+a^2\kappa^2)}\Big]\Big\}^2 \end{aligned} \tag{12, c}$$

$$\begin{aligned} I_\beta^2(-k) = \frac{H(k)(2\kappa)^2\mu^2(\mu-1)^2b^6}{(2\rho+1)^2(2\rho)^2(b^2+\kappa^2)^4}\Big\{&\frac{(k+1)(\mu+1)(\mu+2)(\kappa/b)^2}{(2k+1)^2(2k+3)}F(k+2) \\ &\cdot\Big[F(\delta', 2\rho+2) + 0\Big(\frac{\alpha^2}{30}\Big)\Big] - \frac{kF(k)}{2k+1}\Big[F(\delta', 2\rho+2) \\ &+ \frac{(k-\rho)(2\rho+1)(1+a^2\kappa^2)}{2\mu}F(\delta', 2\rho+1)\Big) \\ &+ \frac{(1+\rho_1)F(k)}{2\rho}\Big[F(\delta', 2\rho+2) \\ &+ \frac{\rho(2\rho+1)(1+a^2\kappa^2)}{\mu}F(\delta'-1, 2\rho)\Big]\Big\}^2 \end{aligned} \tag{12, d}$$

where,

$$H(k) = \frac{8\pi^4N_0^2km(2b)^{2\rho-1}\alpha^2\Gamma^2(\mu-1)(\kappa/2)^{2k-4}}{h\Gamma^2(k+\frac{1}{2})\Gamma^2(2\rho)(b^2+\kappa^2)^{\mu-1-\delta}\,b^{2\delta}\,e_1^{\,4l+a^2\kappa^2}}$$

$a=1/b$, $F(k+m)$ is an abbreviation for $F(k+m, 2k+2m, \beta s)$. Also, the argument of the F's in the brackets has been left out. This argument is $\beta(1-\bar{s}/2)$

in all cases. e_1 is the base of the natural logarithms. We now rewrite Eq. (4), where ν is now the frequency of the K-absorption limit. $\nu=(1-\rho_1)mc^2/h$.

$$\sigma = \frac{\pi e^2}{(1-\rho_1)mc}\left\{\sum_{k=1}^{\infty}[I_\beta^2(k)+I_\beta^2(-k)]+\sum_{k=2}^{\infty}[I_\alpha^2(k)+I_\alpha^2(-k)]\right\}. \quad (13)$$

By going to the limit $c\to\infty$ one easily sees that $I_\alpha^2(k)=3I_\beta^2(k)=0$ unless $k=2$; and $I_\beta^2(-k)=(2/3)I_\alpha^2(2)$ if $k=1$. In this way it becomes obvious that in the absence of spin forces the contributions from the two normal states are equal, and any asymmetry between them vanishes, as it must. Furthermore, for c infinite we have

$$\sigma = \alpha a^2\frac{2^9\pi^2}{3e_1^4Z}.$$

As given by Eq. (13) and Eqs. (12), σ, according to our approximations, is correct to within 3 percent for $Z<68$. For $Z>68$ the error may increase, but due to the nature of these approximations we should obtain a fair estimate at least, for all Z.

Results.

Calculations using Eqs. (12) and (13) yield the results of Table I at the K-limit.[20] As indicated, these values of σ are less than those given by the Schroedinger theory, and, with one exception, grow more discrepant with increasing Z. The Schroedinger theory gave fairly good results but was itself slightly low.

TABLE I.

Z	1	11	19	37	55	79
$Z^2\sigma 10^{18}$	6.3	6.3	6.2	5.9	6.0	5.2
$10^{18}Z^2\sigma_{SCH}$	6.3	—	—	—	—	—

From data in Roess' paper his τ_κ at the K-limit is from 0.3 percent to 14.6 percent less than the Schroedinger result, for effective Z roughly from 11 to 80. In approximately the same range our result is lower than the Schroedinger result from about 0.3 to 20 percent.

We may say that in this case the more precise model which includes the retarded potentials (Roess does not include the retardation factor in his integrals) does not improve the comparison with experiment, and if anything makes it slightly worse.*† This discrepancy between theory and experiment must be attributed to the inaccuracy of a model which neglects all electrostatic interactions.

[20] It is unfortunate in comparing our results with those of Roess (reference 4) that these calculations are for different values of Z than those he has used. However, due to the obvious inaccuracy of the theory even in this case where retardation is included, and as shown by our results, it does not seem necessary to make a further comparison between our results than can be done qualitatively.

Part II. Photoelectric Absorption of Ultragamma Radiation

Introduction.

In order to discuss the problem mentioned in the introduction to this paper under (2), we should now be obliged to consider the quantities S defined by Eq. (9), for large κ. That such a consideration leads to a grave difficulty it is the purpose of the present section to point out. The nature of this difficulty can be elucidated in a considerably simplified case. Let us in Eq. (9) set $\alpha=0$ and $n=0$. Eq. (9) can then be written, after a simple substitution,

$$S(2k-1,\, k,\, k,\, 2k) = \left(\frac{\kappa k_0}{4}\right)^{-k+1/2} \Gamma^2(k+\tfrac{1}{2}) \int_0^\infty e^{-rb} J_{k-1/2}(\kappa r) J_{k-1/2}(k_0 r)\, dr.$$

The integral in this equation can now be evaluated[21] with the result

$$\int e^{-rb} J_{k-1/2}(\kappa r) J_{k-1/2}(k_0 r)\, dr = \frac{(\kappa k_0)^{-1/2}}{\pi} Q_{k-1}\left(\frac{\epsilon}{k_0'}\right). \tag{14}$$

In order to evaluate σ it is necessary to find $\Sigma_k I^2$. This sum does not converge uniformly in k; that is the value of k for which the contribution of the terms is a maximum, increases as κ increases. We are thus faced with one of two problems: (a) That of finding the expansion of $Q_k(x)$ about $x=1$, necessarily uniform in k, or, (b) That of finding an asymptotic expansion for $Q_k(x)$, for k large, which is uniform as $x \to 1+0$.

Either of these problems, after considerable study of the contour integral, and of the differential equation, we believe to form a major analytical difficulty; and that the answer to (b) is probably not to be found by the method of steepest descents. It should further be remarked that even in the case problem (a) or (b) is resolved, that, due to the non-uniformity of the function $\Sigma_k I_\alpha^2$, it is not unlikely that the function I_α will be such as to make the sum over k difficult, if not impossible.

Just this difficulty persists if n and α are retained in Eq. (9), and, although the analysis is more complicated, the answer would be forthcoming if this simpler case could be treated. In the face of this we have been forced to leave the solution in this form.

This difficulty, and in fact most of the complication encountered in this physically simple problem, can be regarded as having been introduced by the

---

* Roess explains that his τ_k, which is assertedly computed for a one-electron atom, does not need to be doubled to give the total absorption of the two K-electrons. A closer examination of Roess' work, shows, however, that his τ_k gives the absorption of an atom in which both normal states are filled, whereas our σ gives the absorption for an atom with one electron, which is with equal probability to be found in either of the two normal states.

† As remarked in the footnote of page 2, no treatment of the wave-length dependence is to be given in this paper. However, it has been verified that retardation does not change the dependence on wave-length in any critical way, and that as nearly as the curve may be described at all by assigning a specific exponent to λ this exponent is never much different from 3. Roess found that the relativistic theory, when retardation was not included, gave something closer to a λ^3 law than was given by the previous less exact theories applied to the K-shell.

[21] G. N. Watson, Theory of Bessel Functions, p. 389.

resolution of the waves representing states in the continuum into spherical harmonics, in order to obtain a solution of Dirac's equation. In the relativistic theory the problem of the hydrogen atom is no longer separable in parabolic coordinates, so that wave functions representing hyperbolic orbits, which take the relativistic change of mass with velocity into account, and which are otherwise analogous to Gordon's wave functions,[22] are not known. We see graphically that the trouble arises from the fact that for very hard radiation there is a strong directional selection for the photoelectrons, while due to the non-separability of the wave equation in any coordinate system that allows this condition to be useful, we are forced to recompose waves resolved into spherical harmonics by solving the above stated problem.

Now for $b/\kappa << 1$ the translational energy of the photoelectrons becomes very large, and we should not expect in the limit of $b/\kappa \sim 0$ that the effect of binding on the photoelectrons would play a very great role. We thus feel tempted to neglect altogether the binding of the photoelectrons, and to apply for their wave functions in the continuum relativistic plane waves.

In neglecting the binding of the photoelectrons we are setting the two quantities n and b/κ equal to zero; the neglect of b/κ will always be justified for sufficiently hard radiation, but for the application to the gamma rays of ThC'' the effect of terms $1/\kappa'$ is appreciable, as we shall see in our formulas (18) and (19). The neglect of n does not become justified as $\kappa' \to \infty$ and we have taken particular care to verify that this effect is inappreciable for light elements, and can introduce even for lead at the very most a factor of three. To do this we have *inter alia* so modified the wave functions that they have the correct asymptotic behavior for an electron moving in the field of the nucleus. This modification introduces a term in the exponent of the wave functions, in addition to the $ik_0 r$ term of the plane waves, of the form $in \cdot \log k_0 r$. The result of this investigation is given in the footnote to Eq. (17), and justifies the approximation involved in neglecting the binding entirely.

It would appear impossible to improve substantially this calculation except by a strict evaluation of the cross section by the method outlined in the first paragraph of this section.

Derivation of the results.

We distinguish the two sets of wave functions in the continuum by the labels α' and β'; each set corresponds to a different orientation of spin.

$$\left.\begin{aligned} \psi_1{}^{\alpha'} &= 1 + \epsilon + k_{0z}' \\ \psi_2{}^{\alpha'} &= k_{0x}' + ik_{0y}' \\ \psi_3{}^{\alpha'} &= 1 + \epsilon - k_{0z}' \\ \psi_4{}^{\alpha'} &= -(k_{0x}' + ik_{0y}') \end{aligned}\right\} \cdot Ne^{i(k_0 \cdot r)}$$

$$\psi_1{}^{\beta'} = \bar{\psi}_2{}^{\alpha'},\ \psi_2{}^{\beta'} = \psi_3{}^{\alpha'},\ \psi_4{}^{\beta'} = -\bar{\psi}_1{}^{\alpha'},\ \psi_4{}^{\beta'} = \psi_1{}^{\alpha'}$$

$$(\bar{\psi}^{\alpha'} \cdot \psi^{\beta'}) = 0$$

ϵ as before is the energy in units mc^2. k_0' is the momentum in units mc.

[22] Gordon, Zeits. f. Physik **48,** 180 (1928).

There will be four integrals I corresponding to transitions between the two initial and the two final states. They are $I^{\alpha\alpha'}$, $I^{\alpha\beta'}$, $I^{\beta\alpha'}$, $I^{\beta\beta'}$, and are defined as in Eq. (6) by the equation

$$I^{\alpha\alpha'} = 2\int (\bar{\psi}_1{}^{\alpha'}\psi_2{}^{0,\alpha} - \psi_3{}^{\alpha'}\psi_4{}^{0,\alpha}) \sin\Gamma d\tau. \tag{15}$$

By use of the wave equations for the normal states already given, and those adopted for the final states, we have from Eq. (15)

$$I^{\alpha\alpha'} = 4i\alpha N_0 N(1+\epsilon)\int e^{-i(k_0 r)} \sin\theta e^{i\phi} r^{\rho_1-1} e^{-rb} \sin\Gamma d\tau$$

$$I^{\alpha\beta'} = 0$$

$$I^{\beta\alpha'} = 4N_0 N\int \{k_{0z}'(1+\rho_1) - i\alpha(1+\epsilon)\cos\theta\} e^{-rb} r^{\rho_1-1} \sin\Gamma e^{-i(k_0 r)} d\tau$$

$$I^{\beta\beta'} = -4N_0 N(k_{0x}' + ik_{0y}')(1+\rho_1)\int e^{-i(k_0 r)} e^{-rb} r^{\rho_1-1} \sin\Gamma d\tau.$$

By the same method of normalization given previously we obtain, normalizing to $dvd(\cos w)d\phi$,

$$N^2 = \frac{mk_0}{2h\pi(1+\epsilon)}.$$

Consider $I^{\alpha\alpha'}$. Writing $\sin\Gamma$ in the exponential form,

$$I^{\alpha\alpha'} = 2\alpha N_0 N(1+\epsilon)[e^{i\beta} I_1 - e^{-i\beta} I_2]$$

where,

$$I_1 = \int (x + iy) e^{-rb} r^{\rho_1-2} e^{-ir(k_0-\kappa)} d\tau$$

$$I_2 = I_1(-\kappa).$$

Next multiplying $I^{\alpha\alpha'}$ up by its complex conjugate and averaging over the phases β, we find that

$$|I^{\alpha\alpha'}|^2 = 4\alpha^2 N_0{}^2 N^2 (1+\epsilon)^2 [|I_1|^2 + |I_2|^2].$$

Let us now evaluate the expression I_2. To do this it is convenient to transform to coordinates whose z-axis has the direction of the vector $k_0+\kappa$. We define the angle w and the quantity p by the following relations

$$\begin{aligned}(k_0+\kappa)^2 &= k_0{}^2 + \kappa^2 - 2k_0\kappa\cos\omega \\ &= p^2.\end{aligned} \tag{16}$$

We transform the integrand according to the scheme

	x'	y'	z'
x	l_1	l_2	l_3
y	m_1	m_2	m_3
z	n_1	n_2	n_3

and obtain

$$I_2 = (l_3 + im_3) \int r^{\rho_1+1} e^{-rb-irp\cos\theta} \cos\theta \sin\theta dr d\theta d\phi .$$

Integrating first over the angles we soon find that*

$$I_2 = \frac{\pi^{3/2} i(l_3 + im_3)\Gamma(\rho_1 + 3)}{\Gamma(5/2)} \frac{p}{(p^2 + b^2)^{\rho_1+3/2}} F\left(\frac{\rho_1+3}{2}, \frac{1-\rho_1}{2}, \frac{5}{2}, -\frac{p^2}{p^2+b^2}\right).$$

The remaining integrals are obtained similarly, and after a few easy calculations, and using the relation

$$\sigma(w) = \frac{\pi e^2 c}{h\nu}\{ | I^{\alpha\alpha'} |^2 + | I^{\alpha\beta'} |^2 + | I^{\beta\alpha'} |^2 + | I^{\beta\beta'} |^2 \}$$

one finds that†

$$\sigma(w) = \frac{4\pi^2 e^4 Z\alpha \Gamma^2(\rho_1 + 2)}{h^3 \nu} \cdot \frac{(2b)^{1+2\rho_1}}{(1+\rho_1)\Gamma(1+2\rho_1)} \frac{mk_0}{1+\epsilon}$$
$$\cdot \left\{ (1+\rho_1)^2 k_0^2 (f_{3+}^2 + f_{3-}^2) + \frac{(1+\epsilon)^2(\rho_1+2)^2}{9} (p_+^2 f_{5+}^2 + p_-^2 f_{5+}^2) \right\} \quad (17)$$

$$f_{M\pm} = F\left(\frac{\rho_1+3}{2}, \frac{1-\rho_1}{2}, \frac{M}{2}, \frac{p_\pm^2}{p_\pm^2 + b^2}\right) \cdot (p_\pm^2 + b^2) - \frac{\rho_1+3}{2}$$

where p_+ is the p defined by Eq. (16); $p_- = p_+(\pi - w)$.

The above expression for $\sigma(w)$ gives the distribution in angle about the direction of κ. The range of w is $0-\pi$. The hypergeometric function with $M = 5$ varies slowly, as can be seen from a continuation of the function about $1-x$. Similarly in the other case, $M = 3$. (See appendix, Part II.)

The angular dependence is then seen to be given, nearly, by the factor

$$\left\{ \left(1 + \frac{1}{k_0'^2}\right)^{1/2} - \cos w \right\}^{-4}$$

and the steepness of the curve when k_0 and κ are nearly parallel is apparent. For κ infinite it is therefore justified to give both hypergeometric functions their values when k_0 and κ are parallel, in the angular integration. Even for $\kappa' = 5$, as it is for ThC'' gamma rays, it may be shown that the error introduced by this procedure is completely negligible (less than 2 percent). With this understanding we may proceed with the integration over the angles; to do so it is necessary to find

$$\sigma = \int \sigma(w) d\cos w d\phi .$$

* These integrals may be evaluated in terms of elementary functions but we prefer to express them as is here done.

† If the modification due to binding be carried through, its effect can be seen, approximately, by substituting $\rho_1 + in$ for ρ_1 in this formula (excepting of course N_0).

The result of this integration is

$$\sigma = \frac{\pi\alpha_0^2 a_0^2}{4} \frac{\Gamma^2(\rho_1+2)}{(1+\rho_1)\Gamma(1+2\rho_1)} \frac{1}{1+\epsilon}\left[\frac{2\alpha_0^2}{\kappa'(\epsilon-k_0')}\right]^{\rho_1+2}$$
$$\cdot Z^{3+2\rho_1}\left\{(\rho_1+2)\left[\frac{(1+\rho_1)k_0}{(\rho_1+2)\kappa} F\left(\frac{3+\rho_1}{2}, \frac{1-\rho_1}{2}, \frac{3}{2}; x\right)\right]^2 \right. \tag{18}$$
$$\left. + (\rho_1+1)\left[\frac{(\rho_1+2)(1+\epsilon)}{3(\rho_1+1)\kappa^1} F\left(\frac{3+\rho_1}{2}, \frac{1-\rho_1}{2}; \frac{5}{2}, x\right]^2\left(1-\frac{2}{3}\alpha^2\right)\right\}.$$

For κ infinite, this result becomes

$$x=(k_0'-\kappa')^2/2\kappa'(\epsilon-k_0')$$
$$\sigma = \frac{\pi a_0^2}{16} \frac{\Gamma^2(\rho_1+2)(2\alpha_0)^{2\rho_1+6}}{(1+\rho_1)\Gamma(1+2\rho_1)} \cdot \frac{Z^{3+2\rho_1}}{\epsilon}\left\{\frac{(1+\rho_1)^2}{2+\rho_1} F^2\left(\frac{1-\rho_1}{2}, \frac{3+\rho_1}{2}, \frac{3}{2}; 1-\alpha^2\right)\right.$$
$$\left. + \frac{(2+\rho_1)^2}{9(1+\rho_1)} F^2\left(\frac{1-\rho_1}{2}, \frac{3+\rho_1}{2}, \frac{5}{2}; 1-\alpha^2\right)\left(1-\frac{2}{3}\alpha^2\right)\right\}. \tag{19}$$

For light elements we may set $\alpha=0$ and obtain

$$\sigma \sim \frac{88\pi a_0^2 \alpha_0^8 Z^5}{3\epsilon}. \tag{20}$$

This formula is radically different from that we should obtain by an extrapolation of the experimental law for softer x-rays, or the earlier non-relativistic calculations. These agree in giving for σ, more or less roughly, it is true,

$$\sigma_S = 10^{-2} Z^4 \lambda^3 \tag{21}$$

whereas we find

$$\sigma \sim 1.9 \times 10^{-22} Z^5 \lambda. \tag{22}$$

For the gamma-rays of ThC'' our result gives a much larger absorption than the extrapolated value (21).[23a] In contrast with the extrapolated formula, (22) gives a photoelectric absorption which falls off almost as slowly with decreasing wave-length as the scattering from a free electron,

$$(\sigma)_{KN} \sim 10^{-15}\lambda \log \epsilon.$$

This result and (18) and (19) are what we must compare with experiment. For sufficiently hard radiation we may use (19) with complete confidence; for the gamma-rays of ThC'', (18) and (19) give appreciably different results, and we shall use the strict result (18).

[23a] One may understand this result physically; the reason for the rapid decrease in σ with $\lambda(\lambda^3)$ in the theory of absorption of ordinary x-rays is that the nucleus has to take up more and more momentum as the frequency of the quantum increases. For very hard light the electrons which are ejected in the direction of the γ-ray beam acquire a momentum which differs from that of the quantum by a constant amount: the momentum which the nucleus has to take up does not increase indefinitely with the energy of the quantum. For this reason we should expect the true value of σ to lie, for hard radiation, higher than the value extrapolated from (21).

Comparison with experiment.

The formulas just given apply only to the K-electrons of a naked nucleus. In using them to obtain the total photoelectric absorption from an atom we shall apply the customary procedure, which may be justified only qualitatively, of supposing each electron in the atom to move in the field of an appropriately screened nucleus. We take the screening constants directly from the spectroscopic values given by Ruark and Urey.[24] There appears to be no more satisfactory treatment of the problem which does not involve a complicated study of the wave functions for all the electrons. It is in this connection of extreme importance to note that the discrepancy between theory and experiment which we find for the absorption of the gamma-rays of ThC'' by Pb, persists even if we neglect entirely the absorption of all but the two K-electrons.

We take therefore the total photoelectric cross section of the atom

$$\sigma_A = \sum_i n_i \sigma(Z - s_i) \tag{23}$$

where $\sigma(Z\text{-}s)$ is the absorption given by (18) for an electron bound to a nucleus of charge $e(Z-s)$, where further n_i is the number of electrons in the atom with screening constant s_i, and where the summation is to be taken over all the electrons of the atom.

The simplest way to compare σ_A with experiment is to find its ratio to the cross section for scattering given by the Klein-Nishina formula. We therefore compute the ratio *R per electron* of the photoelectric cross section to the Klein-Nishina[25] cross section for scattering, (σ) K.N. For ThC'' gamma-rays, this ratio is

$$R = \frac{(\sigma_A/Z)}{(\sigma_E)_{KN}}, \text{ for } \lambda = 4.7\ X.U. \tag{24}$$

Chao[26] and Tarrant[27] have observed the total absorption of these gamma-rays of ThC'' in a number of elements, and agree in finding it greater than the value predicted by the Klein-Nishina formula. From their data the quantity R may be directly found. There are of course several possible explanations of the excess absorption which Chao and Tarrant find, an excess absorption which is more marked for the heavier elements. On the other hand the binding of the electrons will surely modify the scattering; it will also give rise to a photoelectric absorption; further, the electrons of the nucleus may absorb or scatter appreciably such hard radiation. (The increase, and according to Chao it is a regular increase, with Z would on this view be hard to understand.) It is here our purpose to discover what part of the effect observed by Chao and Tarrant can be ascribed to photoelectric absorption.

[24] Ruark and Urey, Atoms, Molecules and Quanta, (McGraw-Hill), p. 259.
[25] Reference 7, or see reference 5.
[26] Reference 5.
[27] Reference 5.

Carrying out this comparison, we find from (18), (23), and (24) for Cu

$$R - 1 = 0.08$$

Chao finds for Cu 0.11, and Tarrant 0.12. A set of typical results is given in Table II.

TABLE II.

Z	Obs. Chao	Obs. Tarrant	$R-1$
13	0.06	0.12	0.002
29	.11	.12	.08
30	.11	.006	.08
50	.21	.21	1.3
82	.42	.34	14.

The agreement of this computed value for the photoelectric absorption in Cu with the excess absorption over that given by the Klein-Nishina formula experimentally found by Chao and Tarrant, is in some ways satisfactory, and suggests that the experimental absorption can, even for this very hard radiation, be explained by the photoelectric absorption and scattering of extra-nuclear electrons. There are, however, very serious difficulties with this interpretation which arise from the following circumstance. Our computed photoelectric absorption increases very much more rapidly (Z^5) with atomic number than that found by Tarrant and Chao. Chao finds roughly a linear dependence on Z; Tarrant, whose values do not agree at all well with those of Chao, finds no regular dependence on Z at all for the excess absorption. (This is what we should expect if the absorption were primarily nuclear.) Our theoretical values for the photoelectric effect give therefore, a smaller a correction for the light elements (e.g. A1) than is needed to explain the empirical values; whereas for heavier elements, like Pb, the theoretical correction is over 25 times too large. It must be emphasized that the empirical values are by no means certain; only in the case of lead, where both Tarrant and Chao find a value very much smaller than the theoretical, can we be sure of a definite discrepancy between theory and experiment.

An examination of the error introduced into our calculations by a partial neglect of the binding of the photoelectrons has convinced us that correction for this error could hardly bring our results into accord with experiment. Only in the case of lead could this correction be appreciable, and even there it should not change our result by more than a factor of three. We believe that a precise calculation based on the strict formula, Eq. (9), would also lead to results that could not be reconciled with the experiments. They would fail to agree with Chao's measurements because of too fast an increase with atomic number; and they would disagree with Tarrant's not only in this, but in giving a quite regular dependence on Z. For if the dependence on Z is really as irregular as that found by Tarrant, the effects can hardly be of extra-nuclear origin, and the photoelectric effect computed by us should be only a small part of the excess absorption observed; whereas for large Z it is in fact greater. We believe, therefore, that the application of the present electrodynamical theory to the absorption of very hard light does not give correct results.

There are of course grounds for distrusting the theory in this application, because the energy of the light involved is many times the proper energy of the electron. It is because we seem to have here another breakdown of present electrodynamical theory that we have insisted so much on this comparison with experimental results by no means unambiguous. It is to be hoped that a more complete and rigorous solution of the theoretical problem will be found in the future, and it is very much to be desired that the experiments be repeated and improved.

Appendix

Part I.

To the first order in α^2

$$\delta = \frac{\alpha^2}{2}\left(1+\frac{1}{k}\right)$$

$$\delta' = \frac{\alpha^2}{2}\left(1-\frac{1}{k}\right).$$

Since the error involved in this procedure will be of interest to us only for the case $k_0=0$, we shall justify the approximation only for this case. It is clear, however, that a similar process will be possible in other restricted parts of the range of k_0.

From Eqs. (12) one sees that the largest contribution to σ comes from the first term of I_α for $k=2$. For $k=2$, $F(\delta', 2\rho, \beta(1-\bar{s}u))$ of Eq. (10′) converges to within 0.007 of its value in two terms ($\alpha<1/2$); this value is practically independent of $s\sim i\alpha$. Therefore, in a heuristic way we take this factor outside the integral. Now expanding the other factor of interest,

$$(1-\bar{s}u)^{-\delta} = 1+\delta\bar{s}u+\frac{\delta(1+\delta)}{2}(\bar{s}u)^2+\cdots$$

we integrate term by term. In the resulting series

$$B(k_1k)F(k_12k, \beta\bar{s}) + \delta B(k+1, k)F(k+1, 2k+1, \beta\bar{s})+\cdots$$

the ratio of the first two terms gives u average. We find $|\bar{u}|$ slightly greater than $1/2$ (the imaginary part of u average can be neglected), but for our purposes putting average $u=1/2$ in the factors that have been removed is convenient, and should entail an error of less than $1/2$ percent, since the series for the second factor converges to within 0.01 of its value in three terms for $|u|=3/4$, and the same upper limit on α.

In the remaining integrals the approximation is not always such a good one in the integral itself. Fortunately, however, when in place of the factors above we have the factors $F(\delta'\pm1)$, or $(1-\bar{s}u)^{\pm1-\delta}$, or similar ones with 2 in place of 1, then, either the approximation just happens to be right to a fair accuracy, or else the integral being considered belongs to a term of σ which is already small because of a factor $(\kappa/b)^2$, or $(\alpha/2)^2$. For example: the other large terms in σ, by Eqs. (12), come from $I_\beta(+2)$, $I_\beta(-1)$. The largest term

in $I_\beta(+2)$ comes from $S(\mu-2, k-1, a, 2\rho)$. The $F(\delta')$ factor in this integral is again the same as the one we have just discussed, but the other factor is $(1-\bar{s}u)^{2-\delta}$. The series obtained by expanding this expression converges in four terms to 0.15 of its value, if $|u|$ average is near $1/2$. Again integrating term by term, and finding the necessary ratios of the confluent functions in the succeeding terms, we find that putting $|\bar{u}| = \bar{u}^2 = \cdots = 1/2$ introduces an error <0.02 in this integral.

The remaining large term arises from $I_\beta(-1)$. $S(\mu, k, a+1, 2\rho+2)$ and $S(\mu-1, k, a, 2\rho)$ contribute to this term. The question involved in the first of these is the same as in the term just discussed. The latter involves $(1-\bar{s}u)^{1-\delta}$, and $F(-1, 2\rho, \beta(1-\bar{s}u))$, since $\delta'=0$ for $k=1$. In this case it is better to expand both of these factors under the sign of integration, and obtain

$$c_0 + c_1 u + c_2 u^2 + \cdots .$$

Then in a similar way one finds $\bar{u}$, $\bar{u}^2$, $\cdots$. The F in this case vanishes as $\alpha \to 0$.

Now in the contribution to σ, $I_\beta^2(+2)$ has roughly the weight $1/6$, and $I_\beta^2(-1)$ the weight $1/3$. On squaring we must double the estimated errors. We find that for $k_0=0$, $\alpha<1/2$ the error in σ should be less than 3 percent. The error for small Z should be almost entirely negligible—in general all of our errors vanish with α.

Part II.

The formula for continuation gives in this case,

$$F\left(\frac{\rho_1+3}{2}, \frac{1-\rho_1}{2}, \frac{5}{2}, \frac{p^2}{p^2+b^2}\right)$$

$$= \frac{\Gamma\left(\frac{1}{2}\right)\Gamma\left(\frac{5}{2}\right)}{\Gamma\left(\frac{2-\rho_1}{2}\right)\Gamma\left(\frac{4+\rho_1}{2}\right)} F\left(\frac{\rho_1+3}{2}, \frac{1-\rho_1}{2}, \frac{1}{2}, \frac{b^2}{p^2+b^2}\right)$$

$$- 2\frac{\Gamma\left(\frac{1}{2}\right)\Gamma\left(\frac{5}{2}\right)}{\Gamma\left(\frac{\rho_1+3}{2}\right)\Gamma\left(\frac{1-\rho_1}{2}\right)}\left(\frac{b^2}{p^2+b^2}\right)^{1/2} F\left(\frac{2-\rho_1}{2}, \frac{4+\rho_1}{2}, \frac{3}{2}, \frac{b^2}{p^2+b^2}\right).$$

The difference of this F from unity is seen to be negligible except for the heaviest elements (e.g. Pb), even when $\boldsymbol{k}_0$ and $\boldsymbol{\kappa}$ are parallel. It is to be noted, however, that the correction is in the direction to decrease F, but the decrease in F^2 is not more than 8 percent for lead.

The continuation of $F(\rho_1+3/2, 1-\rho_1/2, 3/2; p^2/p^2+b^2)$ shows that again in this case F changes slowly, and *exceeds* the value unity about 10 percent for Pb when $\boldsymbol{k}_0$ and $\boldsymbol{\kappa}$ are parallel.

TRANSMISSION OF ELECTRONS THROUGH POTENTIAL BARRIERS

By N. H. Frank and L. A. Young[1]
Massachusetts Institute of Technology

(Received May 22, 1931)

Abstract

It is shown that the application of the Wentzel-Kramers-Brillouin approximate solution of the wave equation to problems of the transmission of electrons through potential barriers leads to simple derivations of formulas for the transmission coefficient. This method may be applied systematically to potential barriers of arbitrary form.

1. NUMEROUS examples of the transmission of electrons through potential barriers may be found in the literature in connection with the theory of radioactive disintegration and emission of electrons from metals. In those cases in which the wave equation does not admit of elementary solutions the calculations become lengthy and laborious and it has been found necessary to introduce asymptotic properties of the solutions in order to arrive at results of physical interest. We have found that the same end results can be obtained by the use of the Wentzel-Kramers-Brillouin approximate solution of the wave equation. The calculations are much simplified and can be extended systematically to any problems of this type.

2. The W.K.B. solution possesses enough similarity to classical behaviour so that the physical interpretation of every step of the calculation is self-evident, yet it also possesses properties which are typically wave-mechanical.[2] If the one-dimensional wave equation be written in the form

$$\psi''(x) + (E - V(x))\psi(x) = 0 \tag{1}$$

the W.K.B. fundamental solutions may be written

$$\psi(x) = (E - V)^{-1/4} e^{\pm i \int (E-V)^{\frac{1}{2}} dx}. \tag{2}$$

This approximation is invalid in the neighborhood of values of x for which $E - V(x) = 0$, that is, where the classical kinetic energy vanishes. In regions where $E - V(x) > 0$ the solutions have an oscillatory character while in those regions where $E - V(x) < 0$ they behave as real exponentials. In order to have an approximate solution valid throughout the range of x we must know the correspondence between solutions of the oscillatory type in one region and those of the exponential type in an adjoining region. "Connection formulas" have been given by Kramers and Zwaan.[3] They require that

[1] National Research Fellow, Mass. Inst. of Technology and Harvard University.

[2] G. Wentzel, Zeits. f. Physik **38,** 518 (1926); L. Brillouin, C. R., Juli, 1926; H. A. Kramers, Zeits. f. Physik **33,** 828 (1926); L. A. Young and G. E. Uhlenbeck, Phys. Rev. **33,** 1154 (1930)

[3] H. A. Kramers, reference 2; A. Zwaan, Utrecht Dissertation, 1929.

$$(V-E)^{-1/4}e^{+\int(V-E)^{1/2}dx} \longleftrightarrow (E-V)^{-1/4}\cos\left\{\int(E-V)^{1/2}dx-\frac{\pi}{4}\right\}$$
$$(V-E)^{-1/4}e^{-\int(V-E)^{1/2}dx} \longleftrightarrow 2(E-V)^{-1/4}\cos\left\{\int(E-V)^{1/2}dx+\frac{\pi}{4}\right\}. \tag{3}$$

The above integrals are to be taken between the limits x and x_1 $(E-V(x_1)=0)$ in such a way that the integrals are always positive. Since we are always interested in travelling waves we shall use an alternative form of the above.

$$(E-V)^{-1/4}e^{+i\int(E-V)^{1/2}dx} \longleftrightarrow (V-E)^{-1/4}\left\{(i)^{1/2}e^{+\int(V-E)^{1/2}dx}+\tfrac{1}{2}(-i)^{1/2}e^{-\int(V-E)^{1/2}dx}\right\}$$
$$(E-V)^{-1/4}e^{-i\int(E-V)^{1/2}dx} \longleftrightarrow (V-E)^{-1/4}\left\{(-i)^{1/2}e^{+\int(V-E)^{1/2}dx}+\tfrac{1}{2}(i)^{1/2}e^{-\int(V-E)^{1/2}dx}\right\} \tag{4}$$

In the neighborhood of $x=x_1$ we may replace $E-V(x)$ by a linear function of x and use exact solutions which are expressible in terms of Bessel functions of order 1/3.

3. We shall first consider a case treated by Fowler and Nordheim,[4] that of an electron escaping from a metal into a uniform accelerating field (Fig. 1). We must consider the following cases: (a) $E>V_0$; (b) $E<V_0$; (c) $E=V_0$. Case (a).

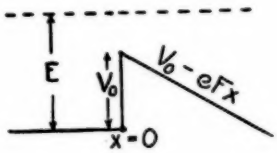

Fig. 1.

For $x<0$ we write for the incident electron beam

$$\psi_i = p^{-1/2}e^{ipx} \quad p=\frac{2\pi}{\lambda}=\frac{2\pi}{h}(2mE)^{1/2} \tag{5}$$

for the reflected beam

$$\psi_r = bp^{-1/2}e^{-ipx}. \tag{6}$$

For $x>0$ we use the W.K.B. solution for an emerging wave

$$\psi_t = cy^{-1/4}e^{+i\int_0^x y^{1/2}dx} \tag{7}$$

where

$$y = p^2 - p_0^2 + \alpha x;\ p_0 = \frac{2\pi}{h}(2mV_0)^{1/2}$$

$$\alpha = \frac{8\pi^2 meF}{h^2}.$$

The constants b and c are normalization factors and ψ_i is normalized for unit "current." At $x=0$ $>\!<$ $\psi_i+\psi_r=\psi_t$ and $\psi_i'+\psi_r'=\psi_t'$

[4] R. H. Fowler and L. Nordheim, Proc. Roy. Soc. **A119**, 173 (1928).

$$\begin{aligned} 1 + b &= cp^{1/2}y_0^{-1/4} \\ 1 - b &= cp^{-1/2}\{y_0^{1/4} + i\alpha y_0^{-5/4}/4\} \\ y_0 &= (y)_{x=0}. \end{aligned} \tag{8}$$

The transmission coefficient is defined as the ratio of transmitted to incident current i.e.

$$T = c\bar{c}$$

from Eqs. (8) we find immediately

$$T = \frac{4py_0^{1/2}}{[p + y_0^{1/2}]^2 + \left[\frac{\alpha}{4y_0}\right]^2} \tag{9}$$

or in terms of energies

$$T = \frac{4(E(E - V_0))^{1/2}}{[E^{1/2} + (E - V_0)^{1/2}]^2 + \frac{e^2F^2}{16\kappa^2(E - V_0)^2}} \qquad \kappa^2 = \frac{8\pi^2 m}{h^2}. \tag{10}$$

For an arbitrary $V(x)$ $(V(x) < V_0)$ the transmission coefficient may be obtained by replacing in (9) α by $(8\pi^2 m/h^2)(dV/dx)_{x=+0}$.

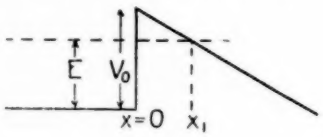

Fig. 2.

Case (b).

For this case it is convenient to normalize the transmitted "current" rather than the incident to unity. We have

$$\left.\begin{aligned} \psi_i &= ap^{-1/2}e^{ipx} \\ \psi_r &= bp^{-1/2}e^{-ipx} \end{aligned}\right\} \quad x < 0 \tag{11a}$$

$$\psi_t = y^{-1/4}e^{i\int_{x_1}^{x} y^{1/2}dx} \quad x > x_1.$$

With the help of (4) we find for the region $0 < x < x_1$

$$\begin{aligned} \psi &= z^{-1/4}\{(i)^{1/2}e^{+\int_{x_1}^{x} z^{1/2}dx} + \tfrac{1}{2}(-i)^{1/2}e^{-\int_{x_1}^{x} z^{1/2}dx}\} \\ z &= -y. \end{aligned} \tag{11b}$$

Boundary conditions at $x = 0$ yield

$$\begin{aligned} a + b &= p^{1/2}z_0^{-1/4}\{(i)^{1/2}A_+ + \tfrac{1}{2}(-i)^{1/2}A_-\} \\ a - b &= -ip^{-1/2}z_0^{-1/4}\left\{((i)^{1/2}A_+ - \tfrac{1}{2}(-i)^{1/2}A_-)z_0^{1/2}\right. \\ &\qquad \left. + \frac{\alpha}{4z_0}\left((i)^{1/2}A_+ + \frac{(-i)^{1/2}}{2}A_-\right)\right\} \end{aligned} \tag{12}$$

where

$$A_+ = e^{+\int_{x_1}^{0} z^{1/2} dx}$$
$$A_- = e^{-\int_{x_1}^{0} z^{1/2} dx}. \tag{13}$$

Elimination of b from the above allows the evaluation of $a\bar{a}$. We find

$$a\bar{a} = \tfrac{1}{4} p z_0^{-1/2} A_+^2 \left\{ \left(1 + \frac{\alpha}{8pz_0} A_-^2 - \frac{1}{2p} z_0^{1/2} A_-^2 \right) + \left(\frac{z_0^{1/2}}{p} + \frac{\alpha}{4pz_0} - \frac{1}{2} A_-^2 \right) \right\}. \tag{14}$$

Examination of the relative orders of magnitudes of the bracketed terms shows that terms containing A_-^2 are negligible. The error introduced by dropping these terms increases as $E \to V_0$ but in this case the entire approximation becomes invalid since the critical point x_1 approaches $x=0$ where boundary conditions must be satisfied.

Due to our altered normalization the transmission coefficient for this case is

$$T = (a\bar{a})^{-1} = \frac{4pz_0^{1/2} A_-^2}{p^2 + \left(\frac{\alpha}{4z_0} + z_0^{1/2} \right)^2}. \tag{15}$$

We have

$$z = p_0^2 - p^2 - \alpha x$$
$$z_0 = p_0^2 - p^2$$
$$A_-^2 = e^{-4(p_0^2 - p^2)^{3/2}/3\alpha}.$$

We obtain, therefore

$$T = \frac{4(E(V_0 - E))^{1/2} e^{-4\kappa(V_0 - E)^{3/2}/3eF}}{E + \left(\frac{eF}{4\kappa(V_0 - E)} + (V_0 - E)^{1/2} \right)^2} \tag{16}$$

It is easy to see that for all values of the electric field F obtainable in practice the term in F can be neglected giving

$$T = \frac{4(E(V_0 - E))^{1/2}}{V_0} e^{-4\kappa(V_0 - E)^{3/2}/3eF} \tag{17}$$

in agreement with the final results of Fowler and Nordheim.[4] Eq. (15) may be generalized for an arbitrary $V(x)$ ($V(x) < V_0$) just as in the case of Eq. (9).

Case (c).

This case cannot be treated by the W.K.B. approximate method but it is easy to treat it exactly in the following manner. For $x<0$ we write as usual

$$\psi_i = p^{-1/2} e^{ipx} \quad \psi_r = b p^{-1/2} e^{-ipx}. \tag{18}$$

For $x>0$ we have the wave equation

$$\psi_t'' + \alpha x \psi_t = 0. \tag{19}$$

The solution of this equation for small values of x which represents an outgoing beam for large x may be written:

$$\psi_t = c(1 - \beta e^{-i\pi/3}x) \tag{20}$$

where

$$\beta = \frac{\Gamma\left(\frac{2}{3}\right)}{\Gamma\left(\frac{4}{3}\right)}\left(\frac{\alpha}{9}\right)^{1/3} = \frac{\Gamma\left(\frac{2}{3}\right)}{\Gamma\left(\frac{4}{3}\right)}\left(\frac{\kappa^2 eF}{9}\right)^{1/3}. \tag{21}$$

The boundary conditions at $x=0$ yield

$$\begin{aligned} 1 + b &= cp^{1/2} \\ 1 - b &= -ic\beta p^{-1/2}e^{-i\pi/3}. \end{aligned} \tag{22}$$

The transmission coefficient

$$T = 1 - b\bar{b} = \frac{4p\beta \sin\frac{\pi}{3}}{p^2 + \beta^2 + 2p\beta \sin\frac{\pi}{3}} \tag{23}$$

It is easy to show that the above expression is still valid for more general potentials if F is taken as the field at $x=0$.

4. As our next example we will consider a potential barrier with external retarding field of the type indicated in Fig. 3.

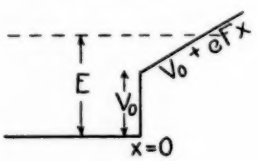

Fig. 3.

It is clear that in this case there will be no transmitted current and that only electrons possessing energies greater than V_0 will contribute appreciably to the charge density for $x>0$. Only these electrons will be considered. As usual we write for the incident and reflected beams ($x<0$).

$$\psi_i = p^{-1/2}e^{ipx} \quad \psi_r = bp^{-1/2}e^{-ipx}.$$

For $x>x_1$ where $x_1=(E-V_0)/eF$ we write for the transmitted electrons (no current!)

$$\begin{aligned} \psi_t &= \frac{de^{-\int_{x_1}^{x} z^{1/2}dx}}{2z^{1/4}} \\ z &= -y \\ y &= p^2 - p_0^2 - \alpha x. \end{aligned} \tag{24}$$

Making use of the connection Eqs. (3) we find for the region $0<x<x_1$.

$$\psi = dy^{-1/4}\cos\left\{\int_x^{x_1} y^{1/2}dx + \frac{\pi}{4}\right\}. \tag{25}$$

This represents a stationary wave in this region. Boundary conditions at $x=0$ give

$$\begin{aligned} 1+b &= dp^{1/2}y_0^{-1/4}\cos A \\ 1-b &= -idp^{-1/2}y_0^{-1/4}\left\{\frac{\alpha}{4y_0}\cos A + y_0^{1/2}\sin A\right\} \end{aligned} \tag{26}$$

where

$$A = \int_0^{x_1} y^{1/2}dx + \frac{\pi}{4} = \frac{2}{3\alpha}y_0^{3/2} + \frac{\pi}{4}$$

we find

$$d\bar{d} = \frac{4y_0^{1/2}}{p\left\{\cos^2 A + \frac{1}{p^2}\left(\frac{\alpha\cos A}{4y_0} + \sin A\right)^2\right\}}. \tag{27}$$

Since A varies extremely rapidly with p we may take the average values of the trigonometric terms in the denominator to obtain

$$\overline{(d\bar{d})}_{(\Delta p)} = \frac{8y_0^{1/2}}{p\left\{1+\frac{1}{p^2}\left(\frac{\alpha^2}{16y_0^2}+1\right)\right\}}. \tag{28}$$

The average charge density over the range Δp is

$$\psi\bar{\psi}_{(\Delta p)} = \overline{(d\bar{d})}_{\Delta p}y^{-1/2}\cos^2\left\{\int_x^{x_1} y^{1/2}dx + \frac{\pi}{4}\right\}. \tag{29}$$

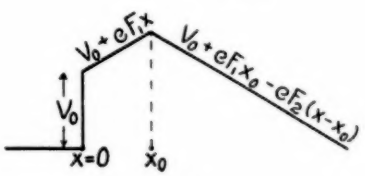

Fig. 4.

Since the space periodicity is approximately λ, the de Broglie wave-length, we may replace $\cos^2\left\{\int_x^{x_1} y^{1/2}dx+\pi/4\right\}$ by $1/2$ to obtain

$$\psi\bar{\psi}_{(\Delta p,\Delta x)} = \frac{4(y_0/y)^{1/2}}{p\left\{1+\frac{1}{p^2}\left(\frac{\alpha^2}{16y_0^2}+1\right)\right\}}. \tag{30}$$

The above results allow a complete discussion of the following case (Fig. 4).

This form of potential curve approximates the space charge condition in vacuum tubes. The retarding field acts effectively to increase the work function.

5. In conclusion we shall consider two cases where the form of potential barrier is modified by an image field. The first example is illustrated by Fig. 5. For $x<x_0$ $V(x)=0$ and for $x>x_0$ $V(x)=V_0-e^2/4x$. Nordheim[5] determines x_0 by $V_0=e^2/4x_0$. We can find the transmission by using the generalization of Eq. (9).

$$T=\frac{4py_0^{1/2}}{[p+y_0^{1/2}]^2+\left[\frac{\alpha}{4y_0}\right]^2}=\frac{4E}{4E+\left(\frac{V_0^2}{\kappa e^2 E}\right)^2}=\frac{1}{1+\frac{V_0^4}{16RhE^3}} \tag{31}$$

It is interesting to note that Rh, the ionization energy of hydrogen, enters naturally because of the occurrence of a hydrogenic potential in the wave equation. This formula is valid for $E\geqq V_0$ since $y>0$ throughout the finite region of x. Anyone who has attempted to follow Nordheim's calculations will

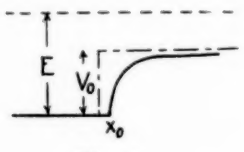

Fig. 5.

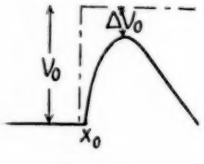

Fig. 6.

see immediately the advantages of the method used here. As our last example we will consider the example of image field plus a uniform accelerating field (Fig. 6). For $x<x_0$ $V(x)=0$ for $x>x_0$

$$V(x)=V_0-\frac{e^2}{4x}-eFx$$

$$\Delta V_0=+(e^3F)^{1/2}.$$

The generalization of (9) for all electrons possessing energies greater than $V-\Delta V_0$ gives

$$T=\frac{4E^{1/2}\left(E+\frac{e^3F}{4V_0}\right)^{1/2}}{\left\{E^{1/2}+\left(E+\frac{e^3F}{4V_0}\right)^{1/2}\right\}^2+\left\{\frac{e^3F-4V_0^2}{4\kappa\left(E+\frac{e^3E}{4V_0}\right)}\right\}^2}. \tag{32}$$

It is hoped that these examples will indicate the advantages of the use of the W.K.B. approximation in problems of this type and will suffice to facilitate its application to other cases of interest.

[5] L. Nordheim, Proc. Roy. Soc. **A121,** 626 (1928).

Λ-TYPE DOUBLING AND ELECTRON CONFIGURATIONS IN DIATOMIC MOLECULES

By Robert S. Mulliken and Andrew Christy
Ryerson Physical Laboratory, University of Chicago

(Received May 20, 1931)

Abstract

Van Vleck's equations for Λ-type and spin doubling in $^1\Pi$, $^2\Sigma$, and $^2\Pi$ states are restated in convenient form for application to empirical data, explicit equations being given for each component separately in a Λ-type or spin doublet. The equations have been applied to a wide variety of data on many molecules, including data on $^2\Pi$ states corresponding to numerous intermediate coupling cases between *a* and *b*, and have been found to fit excellently (cf. Figs. 1–4). Incidentally this has made possible a revision of the hitherto doubtful assignment of *J* values for the Q_2 lines in the $^2\Pi$, $^2\Sigma$ bands of CaH, and has permitted identification of the ^SR branch. Empirical values of the coefficients in Van Vleck's equations have been obtained for many molecules, and are given in Tables I and II.

From the observed values of these constants further confirmation of Van Vleck's theoretical results is obtained. In most of the molecules examined a Π and a Σ state are found which stand to each other in the relation called "pure precession" by Van Vleck, or something similar; that is, the Π and the Σ state act as if they had electron configurations essentially alike in all respects except that one electron has $\lambda=0$ in the Σ state but $\lambda=1$ in the Π state, or vice versa. The existence of such relations strongly indicates that the *n* and *l* values previously assigned to outer electrons in hydrides have almost the same well-defined significance as they would in an atom formed by *uniting* the H nucleus with the heavier nucleus. For example, in the normal ($^2\Sigma$) and first excited ($^2\Pi$) state of CdH, with configurations $\ldots 5s\sigma^2 5p\sigma$ and $\ldots 5s\sigma^2 5p\pi$, the present evidence shows that the last electron really behaves like a $5p$ atomic electron, even though the normal ($^2\Sigma$) state is formed with a small energy of formation from a normal Cd atom ($\ldots 5s^2$, ^1S) and a normal H atom ($1s$, ^2S). Another type of case, in which a close similarity of the electron orbits to two *separate* atoms is evident, is one which is found in He_2, Li_2, and Na_2. In He_2 the $1s\sigma^2 2p\sigma 3p\sigma$, $^3\Sigma_g^+$ and the $1s\sigma^2 2p\sigma 2p\pi$, $^3\Pi_g$ states act as if the relation of pure precession were fulfilled. This is presumably because the $3p\sigma$ election acts essentially like $2p\sigma$, the $3p\sigma$ and $2p\pi$ both becoming $2p$ on dissociation of the molecule.—In the CaH molecule an interesting complicated case, earlier discussed by Watson, occurs in which strong *l*-uncoupling and spin uncoupling occur simultaneously in a $^2\Pi$ state. The theory accounts well for the observed relations in this case (Figs. 2, 3, 4).

Introduction

THE theory of Λ-type doubling, as developed by Kronig and especially by Van Vleck for $^1\Pi$, $^2\Pi$ and other states of diatomic molecules,[1] has interesting possibilities of application to which not much attention has been given. It is capable of giving helpful clues to the interpretation of band structures and to electron configurations. In a recent paper[2] on the SiH bands, the quali-

[1] R. de L. Kronig, Zeits. f. Physik **50**, 347, 1928 (*singlet states*); J. H. Van Vleck, Phys. Rev. **33**, 467–506 (1929).

[2] R. S. Mulliken, Phys. Rev. **37**, 733 (1931).

tative theory has been used in this way. In the present paper, further qualitative applications of the theory are made, as well as quantitative tests. The closely related theory of spin doubling in $^2\Sigma$ states[1] is also tested and applied. As a result of this work, experimental confirmation of certain details of the theory is obtained,[3] and evidence in regard to the electron configurations of various molecules is secured.

Before proceeding to the application of the theory, it will be helpful to summarize the equations for the widths $\Delta\nu$ of Λ-type doublets in $^1\Pi$ and $^2\Pi$ states and of spin doublets in $^2\Sigma$ states. The equations can be made considerably more useful by giving explicitly the *sign* as well as the magnitude of the $\Delta\nu$'s. This was not done by Van Vleck, although the proper results are contained implicitly in his work.

For Λ-type doubling, the following definition of $\Delta\nu$ (in cm^{-1}) will be used here

$$\Delta\nu_{dc}(J) = T_d(J) - T_c(J). \tag{1}$$

This expression, rather than $T_c(J) - T_d(J)$, has been chosen because it is usually positive. The reasons why $T_d - T_c$ is usually positive, but sometimes negative, form one of the subjects of this paper. The symbol T(term) means E/hc, where E is the total energy. The definitions of c and d rotational levels in Λ-type doubling will be found in a recent article in Reviews of Modern Physics.[4] These definitions were chosen primarily for singlet and case b states, the assignment of the designations c and d for the levels of case a states then being determined on the basis of an adiabatic correlation with case b. This method of assignment for case a seemed advisable because of the many examples of states intermediate between cases a and b, and because of the frequent occurrence of case a states which go over with increasing J into case b. The examples of $^2\Pi$ states discussed below are largely of these types.

For $^2\Sigma$ and also for case b $^2\Pi$ states, the following definition will be used

$$\Delta\nu_{12}(K) = T_1(K) - T_2(K), \tag{2}$$

where $J = K + \frac{1}{2}$ for T_1 and $J = K - \frac{1}{2}$ for T_2.

Review of Theoretical Relations For $^1\Pi$ and Other Case b Π States

For any $^1\Pi$ state, Van Vleck finds[5,6]

$$\begin{aligned} T_d(K) &= T_0 + B_v K(K+1) - 2C + (C + C_1)K(K+1) + \cdots; \\ T_c(K) &= T_0 + B_v K(K+1) - 2C + (C + C_2)K(K+1) + \cdots. \end{aligned} \tag{3}$$

[3] The main features of the theory are in striking agreement with experiment.[1]

[4] For definitions of c and d levels in Λ-type doubling, of positive and negative rotational levels, of Σ^+ and Σ^- states, and of even and odd (g and u) electronic states, cf. R. S. Mulliken, Rev. Modern Physics, **3**, 91–95 and 146–7 (1931).

[5] Cf. Eq. (44) of Ref. 1. Here we have used K instead of J (Van Vleck's j), which is permissible since $K \equiv J$ in singlet states. The correlation of the component involving C_1 with T_d is not given explicitly in Van Vleck's paper, but can be seen by a study of the development given there, according to a private communication from Van Vleck.

[6] All coefficients such as C, C_1 and quantities such as ν, $\Delta\nu$, are given here in spectroscopic units (cm^{-1}), although in Van Vleck's paper C, C_1, etc. are in ergs and ν is in $sec.^{-1}$

Hence, as was also shown by Kronig,[1]

$$\Delta\nu_{dc}(K) = qK(K+1), \text{ with } q = C_1 - C_2. \tag{4}$$

In Eqs. (3) and (4), C and C_2 may be expected usually to be much smaller than C_1. These coefficients are given[7] by

$$\begin{aligned} C &= -4\Sigma_{(\text{all } v \text{ values of all } {}^1\Delta \text{ states})} \left| BL_y(\Delta, \Pi) \right|^2/\nu(\Delta, \Pi), \\ C_1 &= 8\Sigma_{(\text{all } v \text{ values of of all } {}^1\Sigma^+ \text{ states})} \left| BL_y(\Pi, \Sigma^+) \right|^2/\nu(\Pi, \Sigma^+), \end{aligned} \tag{5}$$

while C_2 is like C_1 except that the summation is over all ${}^1\Sigma^-$ states.[4] [In the case of a molecule composed of two atoms of the same element, the summations need be taken only over ${}^1\Delta_g$ and ${}^1\Sigma_g$ states if the ${}^1\Pi$ is a ${}^1\Pi_g$, or over ${}^1\Delta_u$ and ${}^1\Sigma_u$ states if it is ${}^1\Pi_u$.] In these equations $\nu(\Pi, \Sigma^+)$ is the frequency (cm^{-1}) corresponding to any ${}^1\Pi \rightarrow {}^1\Sigma^+$ transition from the given ${}^1\Pi$ state and v value to any ${}^1\Sigma^+$ state and v value, and is taken as positive or negative according as the ${}^1\Pi$ level is above or below the ${}^1\Sigma^+$ level; $\nu(\Delta, \Pi)$ has an analogous meaning. The expression $BL_y(\Pi, \Sigma^+)$ denotes the matrix component, corresponding to a ${}^1\Pi$, ${}^1\Sigma^+$ transition involving the given ${}^1\Pi$ state, of the quantity BL_y, B being $h/8\pi^2\mu cr^2$ and L_y being one of the components L_x and L_y of the resultant electronic orbital angular momentum vector $\boldsymbol{L}$ perpendicular to the electric axis (the component parallel to the axis is represented by the quantum number Λ). Approximately, at least if v is small in the Π state, B can be treated as a constant (equal to B_v of the Π state), and the summation over different v values in each Σ^+ or Δ state in Eqs. (5) can be set equal to unity. This gives[8]

$$C_1 \sim 8B_v^2\Sigma_{(\text{all } {}^1\Sigma^+ \text{ states})} \left| L_y(\Pi, \Sigma^+) \right|^2/\nu(\Pi, \Sigma^+), \tag{5a}$$

with corresponding equations for C and C_2. In Eq. (5a), $\nu(\Pi, \Sigma^+)$ should be a suitably weighted mean of the ν's which would correspond to transitions between the given Π level with its given v to various v values of the Σ^+ state. (This means ν can be determined in the manner described below in the first paragraph of "calculation of p_0, q_0, and γ_0 for pure precession.") If the interaction between spin (S) and orbital electronic motion is very small, as in Hund's case b, the results just given for ${}^1\Pi$ and ${}^1\Sigma$ states obviously apply also to Π and Σ states in general.

In the summations given for C_1 or C_2 (let us assume for the moment that $C \sim 0$), it often happens that one term is much larger than all the rest because ν is unusually small or because the BL_y matrix component is much larger for one ${}^1\Sigma$ state than for all the rest. If one matrix component predominates over all others, we have Van Vleck's case of **"pure precession,"** or something similar to it. In this case we may sometimes think of $\boldsymbol{L}$ as precessing uniformly and corresponding to a well-defined quantum number. The ${}^1\Pi$ and

[7] Cf. Eq. (45) of Ref. 1. L_y (same as Van Vleck's l_y) is used here, since it is identical for singlet states with Van Vleck's P_y (y component of total electronic angular momentum), and since L_y rather than P_y is needed in equations for ${}^2\Pi$ states (cf. Eqs. 9, 10). The arguments of BL_y and of ν have been abbreviated here in a way that is used by Van Vleck later in his paper, but which is also convenient for ${}^1\Pi$ states.

[8] Cf. pp. 478–9, Eqs. (23)–(24), footnote 39, and p. 488 of Ref. 1.

the corresponding $^1\Sigma$ state then share this L and differ only in that $\Lambda=1$ for $^1\Pi$ and $\Lambda=0$ for $^1\Sigma$. But usually matters are more complicated, so that we should not think of L as being a well-defined quantum number for the molecule as a whole. The case of pure precession can, however, still be fulfilled if even just one electron has a well-defined l. If the sum of the λ values for all other electrons is zero, then Λ is equal to the λ value of this one electron. If this special electron has $l=1$, then according as it has $\lambda=1$ or 0, we have a $^1\Pi$ or a $^1\Sigma$ state; and we have a relatively very large matrix component for BL_y (Π, Σ) in Eq. (5) or (5a). Similarly if it has $l=2$, we have a $^1\Delta$, a $^1\Pi$, and a $^1\Sigma$ state, for which $L_y(\Delta, \Pi)$ and $L_y(\Pi, \Sigma)$ are both large, and C is comparable with C_1. When more than one electron has pure precession, similar but more complicated cases are also possible.

The existence of well-defined l's is to be expected in the case of outer electrons whose orbits approximate those in the atom which would be obtained by uniting the two nuclei. This situation occurs especially in the case of hydrides where the charge on the H nucleus is much smaller than the effective charge on the other nucleus, and (for one electron) in excited states of such molecules as H_2 and He_2, where the orbit-dimensions of the excited electron greatly exceed the distance between the nuclei. As will be shown later, Λ-type doubling relations indicating well-defined l's are also found for electrons whose orbits are nearly the same as if the two atoms were separate, and we again have a case which will here be classified under the heading "pure precession," although it is not the same as Van Vleck's pure precession.

If the case of pure precession applies approximately to an electron which determines Λ, all other electrons being in closed shells (or else one or more of them in σ orbits differing in l or n from the precession electron), then[9]

$$C = -B_v^2(l^2 + l - 2)/\nu(\Delta, \Pi), \text{ and } C_1 = 2B_v^2 l(l+1)/\nu(\Pi, \Sigma), \tag{6}$$

while $C_2=0$, since the conditions stated just before Eqs. (6) can be fulfilled only for Σ^+ states. If $l=1$, of course $C=0$. For any value of l, Eq. (6) gives for q of Eq. (4),

$$q = 2B_v^2 l(l+1)/\nu(\Pi, \Sigma) \tag{7}$$

Eqs. (6) and (7) would also apply, with L instead of l, in case L should be a well-defined quantum number. In this case, Σ^- as well as Σ^+ states are possible. If the Σ state is Σ^-, we have $C_1=0$, while C_2 is given by the second part of Eq. (6) and the expression for q in Eq. (7) must be preceded by a minus sign. Eqs. (6) and (7) involve the assumption that B_v is independent of Λ for the states concerned in the pure precession.[9] This is to be expected only in the *ideal* case of pure precession. When it is not true, the correct procedure would seem to be to use B_v of the Π state in Eqs. (6) and (7), and then for $\nu(\Pi, \Sigma)$ to use the value which would be obtained if B_v were the

[9] Cf. Ref. 1, Eq. (46) and pp. 488–9. Professor Van Vleck kindly pointed out to us the necessity of modifying Eqs. (6) and (7) when there is independent precession of l's of more than one electron of given n and l. The argument leading up to Eq. (7a) was also suggested by him.

same for the Σ as for the Π state (cf. later section,—$p109$,—on "calculation of p_0, q_0, and γ_0 for pure precession").

According to the conditions stated in introducing Eq. (6), Eqs. (6) and (7) are applicable to pairs of states such as the following: $(A)np\sigma$, $^2\Sigma^+$ and case b $(A)np\pi$, $^2\Pi$; $(A)(m\sigma)(np\sigma)$, $^1\Sigma^+$ and $(A)(m\sigma)(np\pi)$, $^1\Pi$. Often, however, we have cases such as the following, with two, three, or more electrons alike in n and l: $(A)np\sigma^2$, $^1\Sigma^+$ and $(A)np\sigma np\pi$, $^1\Pi$; $(A)np\sigma^2np\pi$, $^2\Pi$ and $(A)np\sigma np\pi^2$, $^2\Sigma^+$, $^2\Sigma^-$, $^2\Delta$, $^4\Sigma^-$, and $np\pi^3$, $^2\Pi$; and so on. In the case of *two* electrons alike in n and l, and giving a $^1\Sigma^+$ state (σ^2) and a $^1\Pi$ state ($\sigma\pi$), it is easily shown that in the limiting case of *independent* pure precession of their l's (and approximately in the actual case, unless there is a well-defined L), the values of C_1 and q are just *twice* those given by Eqs. (6) and (7). The proof is as follows.[9] Suppose we designate by $l_y(\sigma, \pi)$ the value of the l_y matrix element which one gets in Eq. (5a) for pure precession for the case of a single electron fulfilling the conditions stated before Eq. (6). Suppose further that we designate by $l_y(\sigma^2, \sigma\pi)$ the corresponding matrix element for the above case of two electrons alike in n and l. Letting ψ_0 and ψ_1 represent wave-functions, neglecting spin, corresponding respectively to the two cases $\lambda=0$ and $\lambda=1$ (σ and π), we have

$$l_y(\sigma, \pi) = \int l_y\psi_0\psi_1^*d\tau,$$

$$l_y(\sigma^2, \sigma\pi) = \int (l_{y_1}+l_{y_2})\left[\psi_0(1)\psi_0(2)\right](1/2^{1/2})\left[\psi_0(1)\psi_1(2)+\psi_0(2)\psi_1(1)\right]^*d\tau_1d\tau_2.$$

The second relation is true on the assumption of a vanishingly small interaction between the two electrons, but should usually hold fairly well in the actual case, unless there is a well-defined L. The integral reduces to $(1/2^{1/2})\left[\int l_{y_1}\psi_0(1)\psi_1^*(1)d\tau_1+\int l_{y_2}\psi_0(2)\psi_1^*(2)d\tau_2\right]$, which is $2/2^{1/2}$ times the integral representing $l_y(\sigma, \pi)$. Hence $\left|l_y(\sigma^2, \sigma\pi)\right|^2=2\left|l_y(\sigma, \pi)\right|^2$. From this the statement above as to the values of C_1 and q follows. That is:

$$(\sigma^2, \sigma\pi): q = 4B_v^2l(l+1)/\nu(\Pi, \Sigma) = C_1. \tag{7a}$$

In cases where the number of electrons with given n and l is greater than one or two, more complicated relations may in general be expected. If, however, the Σ and Π states have respectively the configurations $\sigma\pi^4$ and $\sigma^2\pi^3$ (closed shells *minus* one σ or π electron), it is fairly evident that Eqs. (6) and (7) apply just as to the case where only one σ or π electron is *present* outside of closed groups.

$^1\Sigma$ *states.* In connection with Eqs. (3), (5), (5a), (6), the following equation for $^1\Sigma$ states is of interest.[10]

$$T(K) = T_0 + B^*K(K+1) + \cdots,$$

where

[10] This is obtained from the equation for $^2\Sigma$ states (Eq. 15 below) by dropping the terms in the latter which depend on electron spin.

$$B^* = B_v - 8\Sigma_{(\text{all } {}^1\Pi \text{ states})} \left| BL_y(\Pi, \Sigma) \right|^2 / \nu(\Pi, \Sigma) \tag{8}$$

In the case of pure precession, the summation in Eq. (8), like C_1 or C_2 of Eq. (5), becomes identical with C_1, or with C_2, in the case of a Σ^- state, of Eq. (6).

Review of Theoretical Relations in $^2\Pi$ and $^2\Sigma$ States

For the general intermediate case between *a* and *b* Van Vleck obtains for $^2\Pi$ states an equation for the term values that includes the effects of spin doubling and Λ-type doubling simultaneously. Van Vleck's equation, which involves an expansion that gives a good approximation if $|A| << |\nu(\Pi, \Sigma)|$, is as follows:[11]

$$\begin{aligned} T(J) = {} & T_0 + B_v\{(J+\tfrac{1}{2})^2 - 1 \pm \tfrac{1}{2}X\} + \tfrac{1}{2}\{o + \tfrac{1}{2}p^* + q^*(J+\tfrac{1}{2})^2\} \\ & \pm \tfrac{1}{2}X^{-1}\{(2-Y)(o+\tfrac{1}{2}p^*+q^*) + (p^*+2q^*)(J-\tfrac{1}{2})(J+3/2)\} \\ & + [\pm]\tfrac{1}{2}(J+\tfrac{1}{2})\{[\pm 1 + X^{-1}(2-Y)](\tfrac{1}{2}p+q) \\ & + 2X^{-1}q(J-\tfrac{1}{2})(J+3/2)\} + \cdots . \end{aligned} \tag{9}$$

The first term $T_0+B_v\{\cdots\}$ in Eq. (9) is nothing other than the familiar Hill and Van Vleck term, which correctly represents the energy, taking care of the effects of spin uncoupling, in the absence of *l*-uncoupling. The latter, which is the cause of Λ-type doubling, gives rise to the remaining terms in Eq. (9). In Eq. (9) the upper (+) sign in the case of a $\pm$ sign refers to T_2 levels, the lower (−) sign to T_1 levels, except that in the case of the *bracketed* $[\pm]$ sign, the + sign refers to T_d levels, the − sign to T_c levels. It will be seen that Eq. (9) really contains equations for all of the four kinds of levels T_{2d}, T_{2c}, T_{1d}, and T_{1c}. [It should be recalled that T_2 corresponds to $^2\Pi_{1\frac{1}{2}}$ in regular case *a*, to $J=K-\frac{1}{2}$ in case *b*, and to $^2\Pi_{\frac{1}{2}}$ in inverted case *a*, while T_1 corresponds to $^2\Pi_{\frac{1}{2}}$ in regular case *a*, to $J=K+\frac{1}{2}$ in case *b*, and to $^2\Pi_{1\frac{1}{2}}$ in inverted case *a*.] In Eq. (9), X stands for the *positive square root* of $[Y(Y-4)+(J+\frac{1}{2})^2]$, with $Y=A/B_v$, where A is the coefficient of the coupling energy between S and the orbital electronic motion.

The coefficient q in Eq. (9) has exactly the same meaning as in Eqs. (4)–(5), except of course that $^2\Sigma$,$^2\Pi$ are meant here instead of $^1\Sigma$, $^1\Pi$; q^* stands for $C_1+C_2=q+2C_2$. The coefficient p^* means $a_1+a_2=p+2a_2$, while p is given by

$$p = a_1 - a_2, \tag{10}$$

where

$$a_1 = 8\Sigma_{(\text{all } v \text{ values of all } {}^2\Sigma^+ \text{ states})}[1/\nu(\Pi, \Sigma^+)] \{(\text{Real part of } [AL_y(\Pi, \Sigma^+)BL_y(\Sigma^+, \Pi)]\}, \tag{10a}$$

[11] Eq. (9) is obtained from Van Vleck's Eq. (61) as follows. First μ, μ^*, η, etc. in Eq. (61) of Ref. 1 are replaced according to Van Vleck's Eqs. (58). In doing this, each μ has a double value ($\mu=\theta\pm\zeta$), which gives Λ-type doubling. On investigation, it proves that $\mu=\theta+\zeta$ has to be associated with the *d* levels when there is a + sign (T_2) in Eq. (61), but with the *c* levels when there is a − sign (T_1) in Eq. (61), i.e. $\mu=\theta+\zeta$ corresponds to T_{2d}, and T_{1c}. Similarly, $\mu=\theta-\zeta$ corresponds to T_{2c}, and T_{1d}. When due account is taken of the $\pm$ signs which give T_1 or T_2, and of those which give T_c or T_d, and when suitable abbreviations are introduced, Eq. (9) results.

with a corresponding summation, involving $^2\Sigma^-$ states, for a_2. The coefficient o in Eq. (9) is given by

$$o = \Sigma_{(\text{all } r \text{ values of all } ^2\Sigma \text{ states})} [1/\nu(\Pi, \Sigma)] \mid AL_y(\Pi, \Sigma) \mid ^2. \tag{11}$$

[In case the molecule is composed of two atoms of the same element, the summations for a_1, a_2, or o need be taken only over $^2\Sigma_g$ or only over $^2\Sigma_u$ states, according as the $^2\Pi$ state is $^2\Pi_g$ or $^2\Pi_u$.]

It should be pointed out that Eq. (9) was derived[1] under the assumption that interactions of the $^2\Pi$ state under consideration with $^2\Delta$ states are negligible in comparison with interactions with $^2\Sigma$ states. This is usually but by no means always true: cf. Eqs. (3), where the interactions with $^1\Delta$ states are taken care of by the terms involving C. To remedy this deficiency, further terms should be added to Eq. (9), but the form of these is not yet known. Another deficiency in Eq. (9) is the fact that it takes no account of the variation of the moment of inertia of a molecule with J. This can be removed probably nearly perfectly by replacing B_v wherever it appears, explicitly or (in Y, X, o, p, and q) implicitly, by $B_{v,\,s}$ as given by Eqs. (24) ahead.

In the same way that Eq. (5a) was obtained as an approximation to Eq. (5), one gets

$$a_1 \sim 8AB_v\Sigma_{(\text{all } ^2\Sigma^+ \text{ states})} \mid L_y(\Pi, \Sigma^+) \mid ^2/\nu(\Pi, \Sigma^+). \tag{10b}$$

If we have approximately the case of "pure precession," the expressions for q and p can be simplified, giving

$$q = 2B_v{}^2l(l+1)/\nu(\Pi, \Sigma),\ p = 2AB_vl(l+1)/\nu(\Pi, \Sigma) \tag{12}$$

Eqs. (12) hold under the same provisos as Eqs. (6) and (7) and apply only for Σ^+ states. If there is pure precession of an L, this should appear instead of l in Eq. (12). With an L, the Σ state may be Σ^-, and in this case a minus sign must be inserted on the right side of each Eq. (12). Under the provisos which apply to Eq. (7a), the right hand side of each Eq. (12) must be multiplied by a factor 2 (cf. Eqs. 7 and 7a).

If one puts $A \sim +\infty$ or $-\infty$ in Eq. (9), one gets for $A \sim +\infty$ in the T_1 case and for $A \sim -\infty$ in the T_2 case, corresponding respectively to regular and inverted $^2\Pi_{\frac{1}{2}}$, equations which can be written as follows:

$$T(J) = \text{Const.} + B_vJ(J+1) \mp [\pm]\tfrac{1}{2}p(J+\tfrac{1}{2}) + \cdots. \tag{13}$$

The upper sign in $\mp$ applies when A is positive, the lower when it is negative, while the upper sign in $[\pm]$ applies to T_d, the lower to T_c. The constant is different for A positive than for A negative. Eq. (13) shows that in case a $^2\Pi_{\frac{1}{2}}$ states, the correction terms corresponding to Λ-type doubling are practically equal and opposite for $T_c(J)$ and $T_d(J)$.

Experimentally it is easier to study the doublet separations $\Delta\nu_{dc}$ than the terms themselves. From Eq. (9) the following expression can be obtained immediately (cf. Eq. 1):

$$\Delta\nu_{dc}(J) = [(\tfrac{1}{2}p+q)(\pm 1 + 2X^{-1} - YX^{-1}) + 2qX^{-1}(J-\tfrac{1}{2})(J+3/2)](J+\tfrac{1}{2}) \tag{14}$$

In Eq. (14) the + sign in ± 1 refers to T_2 levels, the − sign to T_1 levels. For case a $^2\Pi_{\frac{1}{2}}$ states this reduces (cf. Eq. 13) to

$$\text{Case } a\ ^2\Pi_{\frac{1}{2}}: \Delta\nu_{dc} = \pm\, p(J+\tfrac{1}{2}) + \cdots . \tag{14a}$$

Here the − sign applies when A is positive, the + when it is negative.

If in Eq. (14) we put $A \sim -\infty$ in the T_2 case or $A \sim +\infty$ in the T_1 case, and suitably expand, both results can be expressed[12] by

$$\text{Case } a\ ^2\Pi_{1\frac{1}{2}}: \Delta\nu_{dc} = \pm\, (p/Y^2 + 2q/Y)(J-\tfrac{1}{2})(J+\tfrac{1}{2})(J+3/2) + \cdots , \tag{14b}$$

the + sign applying when A is positive, the − sign when it is negative. [The *term* equations for $^2\Pi_{1\frac{1}{2}}$, analogous to Eq. (13) for $^2\Pi_{\frac{1}{2}}$, are more complicated and less interesting, and so are not given here.]

In real case a ($|Y| >> 1$, but not infinite), Eq. (14a) gives wide Λ-type doublets, since p is approximately proportional (cf. Eq. 12) to $AB_v = B_v^2 Y$, while Eq. (14b) gives narrow doublets, since $(p/Y^2 + 2q/Y)$ is approximately proportional to $B_v^3/A = B_v^2/Y$ (cf. Eqs. 12, 10, 10a). Since p (and so p/Y^2) may be expected to have practically always the same sign as $2q/Y$ (cf. Eqs. 4, 5, 5a, 10, 10a, 10b) for a given $^2\Pi$ state, Eqs. (14a) and (14b) show that $\Delta\nu_{dc}$ should practically always have opposite signs for a $^2\Pi_{\frac{1}{2}}$ and its corresponding $^2\Pi_{1\frac{1}{2}}$ state in case a. In practice, $\Delta\nu_{dc}$ is commonly negative for $^2\Pi_{\frac{1}{2}}$ in case a and positive for $^2\Pi_{1\frac{1}{2}}$; the reasons for this will be discussed shortly. A study of the behavior of Eq. (14) shows that, for states which are near case a for low J values but go over to case b with increasing J, $\Delta\nu_{dc}$ finally changes sign in the case of the $^2\Pi_{\frac{1}{2}}$ levels (cf. Fig. 1). Thus for large enough J it has the same sign for T_1 and T_2 levels, as is required in case b.

Spin doubling in $^2\Sigma$ *states.* For $^2\Sigma$ states, Van Vleck finds[13]

$$T = T_0 + O + B^* K(K+1) + \tfrac{1}{2}\gamma[J(J+1) - K(K+1) - S(S+1)] + \cdots , \tag{15}$$

where of course $S = \frac{1}{2}$. In Eq. (15),

$$\left.\begin{aligned} O &= -\Sigma_{(\text{all } ^2\Pi \text{ states})}[\,|\,AL_y(\Pi,\Sigma)\,|\,^2/\nu(\Pi,\Sigma)], \\ B^* &= B_v - 8\Sigma_{(\text{all } ^2\Pi \text{ states})}[\,|\,BL_y(\Pi,\Sigma)\,|\,^2/\nu(\Pi,\Sigma)], \end{aligned}\right\} \tag{16}$$

$$\text{and } \gamma = 8\Sigma_{(\text{all } ^2\Pi \text{ states})}[1/\nu(\Pi,\Sigma)]\{\text{Real part of } [AL_y(\Pi,\Sigma)BL_y(\Sigma,\Pi)]\} \tag{17}$$

[12] The equation given here for case a $^2\Pi_{\frac{1}{2}}$ is the same, except for the precise specification of the sign, as the equation given by Van Vleck (cf. Ref. 1, Eqs. 49, 56). Eq. (14b) corresponds to Van Vleck's Eqs. (50, 51), $-2q/|Y|$ here corresponds to Van Vleck's b, − except that Eq. (14b) contains a term $p/Y|Y|$ neglected by Van Vleck. Actually this term is of the same order of magnitude as the term $2q/|Y|$, as can be seen by considering the case of pure precession (Eq. 12 above), and remembering that $Y = A/B$.

[13] Eq. (15) is easily obtained from Van Vleck's Eq. (65),— cf. his Eq. (67),—by amalgamating the terms $-(1/4)\gamma \pm \frac{1}{2}h\Delta\nu$, with the + sign for $J = K - \frac{1}{2}$; hcT_0 is the same as Van Vleck's E. Here we have defined γ so that it is the *negative* of Van Vleck's a'. As Van Vleck remarks, γ in Eqs. (15) and (18) should really be replaced by $\gamma + a''$, where $\frac{1}{2}a''\,[J(J+1) - K(K+1) - S(S+1)]$ is the energy of the spin S in the magnetic field produced by the rotation of the nuclei. Van Vleck states that a'' is of the order of m/μ times the coefficient A (m and μ are respectively the electronic mass and the reduced mass of the nuclei), and shows that one then expects $|a''| < |\gamma|$. Although it would be difficult to prove, it seems probable that a'' is usually negligible compared with γ, and we shall so assume in this paper.

[In case the molecule is composed of two atoms of the same element, the summations need be taken only over all $^2\Pi_g$ or over all $^2\Pi_u$ states, according as the $^2\Sigma$ state is $^2\Sigma_g$ or $^2\Sigma_u$.] From Eq. (15) one finds (cf. Eq. 2),

$$\Delta\nu_{12}(K) = \gamma(K + \tfrac{1}{2}). \tag{18}$$

If for a particular $^2\Sigma$ and $^2\Pi$ state the case of "pure precession" holds, then, at least if the provisos applying to Eqs. (6) and (7) are fulfilled, the summation for γ in Eq. (18) reduces to a single term, and this one term becomes identical, if B_v is the same for two states, with the single term to which the summation for p reduces. Since $p = a_1 - a_2$, and since $a_2 = 0$ for Σ^+ states, this single term is one of the terms of a_1 (cf. Eq. (10a)). In this case (cf. Eq. (12)) we have

$$\gamma = p = 2AB_v l(l+1)/\nu(\Pi, \Sigma) \tag{19}$$

At the same time, O of Eqs. (15), (16) becomes equal to $-o$ of Eqs. (9), (11), and $B^* - B_v$ to q of Eq. (9).

Spin doubling at high J in $^2\Pi$ *states.* If A is not too large, the rotational levels of a $^2\Pi$ state become approximately of case b type when J is large enough. It is of interest to consider the form of the doublet separation $\Delta\nu_{12}(K)$ for this case. $\Delta\nu_{12}(K)$ can be obtained here by taking $T_1(K) - T_2(K) = T_1(J_1) - T_2(J_2)$, where $J_1 = K + \frac{1}{2}$ and $J_2 = K - \frac{1}{2}$. If the Λ-type doubling is negligible, we need only the Hill and Van Vleck formula,—the term $T_0 + B_v\{\cdots\}$ in Eq. (9),—and from this get

$$HVV,\ \Delta\nu_{12}(K) = B_v[(2K+1) - \tfrac{1}{2}(X_1 + X_2)], \tag{20a}$$

where

$$X_1 = X(J_1) = [Y(Y-4) + 4(K+1)^2]^{1/2}, \text{ and}$$
$$X_2 = X(J_2) = [Y(Y-4) + 4K^2]^{1/2}.$$

Often, however, the effects of Λ-type doubling are not negligible. Using the complete Eq. (9) to get $\Delta\nu_{12}(K)$, one obtains for the case that $8K^2 >> Y^2$, after a considerable amount of algebraic manipulation including an expansion, the following simple approximate relation:

$$\Delta\nu_{12}(K) = [HVV, \Delta\nu_{12}(K)] - \tfrac{1}{2}(p^* \pm p)(K + \tfrac{1}{2}) + \cdots, \tag{20b}$$

where the + sign in $\pm$ refers to the d levels, the − sign to the c levels. Recalling that $p^* = a_1 + a_2$, $p = a_1 - a_2$, we find that if the $^2\Pi$ state interacts mainly only with one or more $^2\Sigma^+$ states, so that $a_2 = 0$ (cf. Eq. 10a), we have $p^* = p$, and

$$\Delta\nu_{12c}(K) = [HVV, \Delta\nu_{12}(K)] + \cdots, \tag{20c}$$
$$\Delta\nu_{12d}(K) = [HVV, \Delta\nu_{12}(K)] - p(K + \tfrac{1}{2}) + \cdots. \tag{20d}$$

If the interaction is mainly with $^2\Sigma^-$ states, we have $a_1 = 0$ and the left-hand sides of Eqs. (20c) and (20d) should be interchanged. As will be shown later in this paper, the condition that the $^2\Pi$ state interacts mainly only with $^2\Sigma^+$ or with $^2\Sigma^-$ states—in fact mainly with just *one* $^2\Sigma$ state, usually a $^2\Sigma^+$ state,—seems to be practically always fulfilled.

Hence it is to be expected that, for sufficiently large K values, $\Delta\nu_{12}(K)$ will usually be given by the Hill and Van Vleck equation (20a) for the c rotational levels, but will *differ* from this for the d rotational levels approximately

by the amount $-p(K+\frac{1}{2})$. This last quantity, it will be noted, is essentially the same as $\Delta\nu_{dc}$ of regular case a $^2\Pi_{\frac{1}{2}}$. In the case of pure precession involving the $^2\Pi$ and a $^2\Sigma^+$ state, a case which is usually closely approximated, the quantity $-p(K+\frac{1}{2})$ is exactly the same, except for sign, as the quantity $\gamma(K+\frac{1}{2})$ which gives $\Delta\nu_{12}(K)$ for the $^2\Sigma$ state (cf. Eqs. 18, 19).

The relations stated in the preceding paragraph, which hold when there is pure precession between a $^2\Pi$ and a $^2\Sigma^+$ state, have an interesting physical explanation.[14] In terms of the vector model and old quantum theory, we have, say, an l vector which for small J values precesses around the electric axis giving $\Lambda=0$ ($^2\Sigma$ state) or $\Lambda=1$ ($^2\Pi$ state). The rotation of the molecule, however, causes a partial uncoupling of l. At the same time there is an uncoupling of S in the $^2\Pi$ state. The l-uncoupling produces an average component of l along the axis of rotation, i.e. essentially along K. In the limit of complete uncoupling, l is oriented with reference to R, now the quantum number of nuclear rotation, in such a way that $K-R=+l$ for the $^2\Sigma$ levels if for small J values the $^2\Pi$ is above the $^2\Sigma$, $K-R=0$ for the T_c levels of $^2\Pi$, and $K-R=-l$ for the T_d levels of $^2\Pi$ if the $^2\Pi$ is above the $^2\Sigma$. If the $^2\Sigma$ is above the $^2\Pi$, $K-R=-l$ goes with $^2\Sigma$, $K-R=+l$ with $^2\Pi^d$. For partial uncoupling, we may assume that l has a component, which we may call ρ, parallel to K, with values proportional to $\pm l$, 0, and $\mp l$ for $^2\Sigma$, $^2\Pi^c$, and $^2\Pi^d$.

The spin doubling $\Delta\nu_{12}$ in $^2\Sigma$ states can be explained, following Kemble and Van Vleck, as caused by the interaction of the electron spin with the component of the magnetic field of l corresponding to ρ[1,14], the linear variation of $\Delta\nu_{12}$ with $K+\frac{1}{2}$ corresponding to a proportionality of ρ approximately to K. The spin doubling in $^2\Pi$ states is ordinarily explained by the interaction of the spin with the component of the magnetic field of l corresponding to Λ. The variation of the spin doublet width $\Delta\nu_{12}$ with J caused by spin uncoupling is then given by the Hill and Van Vleck formula. But this neglects the possibility of l-uncoupling. When there is appreciable l-uncoupling, the ρ component of the magnetic field may become important and contribute to $\Delta\nu_{12}$. If from the total $\Delta\nu_{12}$ we deduct the $\Delta\nu_{12}$ calculated according to Hill and Van Vleck,[14a] the residuum should correspond to the interaction of the spin with ρ, and, from the considerations of the preceding paragraph, should for the $^2\Pi^c$ levels be approximately zero, but for the $^2\Pi^d$ levels should be approximately equal but opposite in sign to the doubling in the correlated $^2\Sigma$ state. [All this applies for the case that the $^2\Sigma$ state is $^2\Sigma^+$, but analogous statements can be made if it is $^2\Sigma^-$.] These conclusions are in agreement with the formal results given by Eqs. (20c), (20d), and (18), (19).

[14] Cf. F. Hund, Zeits. f. Physik **52,** 606 (1929); W. W. Watson, Phys. Rev. **34,** 1010 (1929) and Ref. 19; R. S. Mulliken, Rev. Modern Physics **2,** (1930), pp. 99–100, Fig. 13, and especially Ref. 44a and Section (2) at top of p. 107; also corrections in **2,** 506–7 (1930). The part of $\Delta\nu_{12}(K)$ arising from the magnetic field of the ρ component of l is that corresponding to the coefficient γ in Eqs. (33)–(36) of the two references of Mulliken just cited.

[14a] If the l-uncoupling is very large, so that the component of l parallel to the electric axis becomes appreciably less than the original Λ, the Hill and Van Vleck part of $\Delta\nu_{12}$ should of course be somewhat less than that calculated by their formula. This, however, does not affect the qualitative relations to be expected.

One cannot expect to demonstrate the relations just discussed except in cases where simultaneously (1) A is fairly large so as to give easily measurable $\Delta\nu_{12}$'s; (2) the spin uncoupling is fairly complete at moderate J(A must not be *too* large); (3) the l-uncoupling is large at moderate J. This set of conditions is rarely fulfilled, but a good example of it is found in the CaH molecule (cf. Fig. 4, inset), which will be further discussed later in this paper.

A result, usually overlooked,[14] of the preceding considerations, is that $\Delta\nu_{12}(K)$ does not necessarily asymptotically approach zero with increasing K in $^2\Pi$ states. The above argument shows that this asymptotic approach to zero is usually to be expected in the T_c levels, but that in the T_d levels, $\Delta\nu_{12}(K)$ may go to a minimum and then increase again (ρ negative, $^2\Pi$ above $^2\Sigma^+$, if $A>0$) or may go through zero and increase again with opposite sign (ρ positive, $^2\Pi$ below $^2\Sigma^+$, if $A>0$). The latter behavior is observed in CaH (cf. Fig. 4).

Empirical Verification of the Theory, with Applications to Interpretation of Band Structures

It is of interest to compare the equations given above with experimental data, and to seek to determine and interpret the coefficients p, q, and γ. As Van Vleck has earlier shown, experimental data are in excellent agreement

Table I. Λ-*Type doubling in case b'* Π *states (all* $^1\Pi$, *except* $^3\Pi$ *in* He_2).

Molecule	Probable Elec. Configuration	Elec. Config. of Interacting State	B^*_v Values Π^d	Σ	$\nu_0(\Pi,\Sigma)$	$\nu(\Pi,\Sigma)$	q_0 calc'd for "pure precession"	q_0 obs'd
H_2	$1s\sigma 2p\pi[C]$; $v=0$	$1s\sigma 2p\sigma[B]$	30.0	19.45	+9003	8130	+0.425	+0.7
	1		29.0			9050	0.348	0.6
	2		27.2			10100	0.289	0.6
BH	$\cdots 2s\sigma^2 2p\sigma 2p\pi$	$\cdots 2s\sigma^2 2p\sigma^2$	11.938	11.80	+23074	23070	+0.0246 (Eq. 7) +0.0192 (Eq. 7a)	+0.03
AlH	$\cdots 3s\sigma^2 3p\sigma 3p\pi$; $v=0$	$\cdots 3s\sigma^2 3p\sigma^2$	6.08	6.33	+23471	23430	+0.0050 (Eq. 7) +0.0120 (Eq. 7a)	+0.0057
	1		5.46			21960	0.00545 (Eq. 7) 0.0109 (Eq. 7a)	0.0050
He_2	$1s\sigma^2 2p\sigma 2p\pi$	$1s\sigma^2 2p\sigma 3p\sigma$	7.34	6.85	−6107	−6150	−0.035	−0.024
Li_2	$\cdots 2s\sigma 2p\pi$	$\cdots 2s\sigma 3p\sigma$	0.553	0.495	+6373	6250	+0.00017	+0.00020
Na_2	$\cdots 3s\sigma 3p\pi$	$\cdots 3s\sigma 4p\sigma$	0.1254	0.1085	+5295	5280	+0.0000118	+0.000013

Explanation and Notes. For each Π state given there seems to be one definite Σ state which stands to it in the relation of "pure precession," as is indicated by the fact that this assumption gives calculated values of q_0 in rather good agreement with the observed values. The observed q_0 values given (obtained in accordance with Eqs. 4 and 27), and the B^*_v values given, are for $v=0$ unless otherwise indicated. The calculated q_0 values are from Eq. (7) or (7a), using B_v of the Π state, and using for $\nu(\Pi,\Sigma)$ not the value $\nu_0(\Pi,\Sigma)$ corresponding to the transition between the levels $v=0$ of the Π and Σ states, but a somewhat different ν estimated by projecting vertically downward (or upward) from the $U(r)$ curve of the Π state to that of the Σ state (cf. text, p. 109). *In addition to the examples given, several nearly perfect cases of pure precession exist in the* $1s\sigma^2 2p\sigma nd(\sigma,\pi,\delta)$ *states of* He_2, others in H_2. The uncoupling in these cases is so great, however, that Van Vleck's equations do not hold well. A number of further examples of $\cdots np\pi$, $^1\Pi$ and $^3\Pi$ states in He_2 are also known which do obey Eq. (4).

The B^*_v values given are related to the true B_v values as follows: $B^*_v=B_v+(C+C_1)$ for $^1\Pi^c$ (T_c terms of $^1\Pi$), $B^*_v=B_v+(C+C_2)$ for $^1\Pi^d$ (cf. Eq. 3), while for $^1\Sigma$ states $B^*_v=B_v-C_3$, where C_3 represents the summation given in Eq. (8). Usually the B^*_v values are empirically more directly obtained for the Π^d than for the Π^c levels, hence in the table they are given for the former. The B^*_v values for Π^c can, however, be obtained simply by subtracting the observed q_0 value from B^*_v of Π^d. For pure precession with $l=1$, and a $^2\Sigma^+$ state, $C=0$, $C_2=0$, and $C_1=-C_3=q_0$. Hence for the T_c levels, $B^*_v=B_v$ is expected in this (usual) case.

The experimental data used were from the following sources: H_2, T. Hori, Zeits. f. Physik **44,** 845–6 (1927); B_v of the $^1\Sigma$ state is as calculated by H. Hyman, Phys. Rev. **36,** 187 (1930); BH, W. Lochte-Holtgreven and E. S. Van der Vleugel, Nature **127,** 236 (1931); R. F. Paton and G. M. Almy (private communication; cf. abstract No. 129, Washington Meeting American Phys. Soc., 1931); AlH, E. Bengttson and E. Hulthén, Zeits. f. Physik **52,** 275 (1928); E. Bengtsson and R. Rydberg, Zeits. f. Physik **59,** 546(1930); He_2, G. H. Dieke, S. Imanishi and T. Takamine, Zeits. f. Physik **57,** 305 (1929); W. E. Curtis, Proc. Roy. Soc. **A 118,** 157 (1928); W. E. Curtis and A. Harvey, Proc. Roy. Soc. **A 125,** 484 (1929); Li_2, K. Wurm, Zeits. f. Physik **58,** 562; **59,** 35 (1929); Na_2, F. W. Loomis and R. W. Wood, Phys. Rev. **32,** 223 (1928), and W. R. Fredrickson, Phys. Rev. **34,** 207 (1929).

TABLE II. *Λ-Type doubling in* $^2\Pi$ *states and spin doubling in* $^2\Sigma$ *states.*

Molecule	State	Probable Elec. Configuration	A	B_v or B^*_v	$Y=A/B_v$	$\nu_0(\Pi,\Sigma)$	$\nu(\Pi,\Sigma)$	Calc'd (pure precession) p_0	Calc'd (pure precession) γ_0	Calc'd (pure precession) q_0	Obs'd p_0	Obs'd γ_0	Obs'd q_0
BeH	$^2\Sigma^+$	$1s\sigma^2 2s\sigma^2 2p\sigma$		10.16		20032	20040		0.00399			0	
	$^2\Pi$	$1s\sigma^2 2s\sigma^2 2p\pi$	1.97	10.30	0.191		20030	0.00405		0.0212	—		0.0142
MgH	$^2\Sigma^+$	$\cdots 3s\sigma^2 3p\sigma$		5.70		19217	19310		0.0414			very small	
	$^2\Pi$	$\cdots 3s\sigma^2 3p\pi$	35	6.0	5.74		19070	0.0449		0.00780	0.04		0.002
	$^2\Pi$	$\cdots 3s\sigma^2 4p\pi$	4?	6.1	0.7?						—		0.021
CaH	$^2\Sigma^+$	$\cdots 4s\sigma^2 3d\sigma$		4.23		14432			(cf. text)			0.045	
	$^2\Pi$	$\cdots 4s\sigma^2 4p\pi$	79.6	4.29	18.5		−1320	−1.04		−0.056	−0.704		−0.067
	$^2\Sigma^+$	$\cdots 4s\sigma^2 4p\sigma$		4.40		−1322	−1320		−1.06			−0.945 or −0.543 (cf. Fig. 3)	
ZnH	$^2\Sigma^+$	$\cdots 4s\sigma^2 4p\sigma$		6.54		23429	23820		0.374			0.248	
	$^2\Pi$	$\cdots 4s\sigma^2 4p\pi$	341.5	7.31	46.7		23160	0.431		0.0092	0.277		0.004
	$^2\Sigma^+$	$\cdots 4s\sigma 4p\sigma^2$		3.4		−5811							
CdH	$^2\Sigma^+, v=0$	$\cdots 5s\sigma^2 5p\sigma$		5.32		22778	23000		0.926			0.59	
	1			5.04			23050		0.875			0.54	
	2			4.71			23500		0.802			0.48	
	3			4.32			25000		0.692			0.40	
	4			3.81			25900		0.589			0.30	
	$^2\Pi, v=0$	$\cdots 5s\sigma^2 5p\pi$	1001	5.99	167		22090	1.090		0.0065	0.62		0.0004
	1			5.75	174		22600	1.019		0.0058	0.44		0.0004
	$^2\Sigma^+, v=0$	$\cdots 5s\sigma 5p\sigma^2$		2.91		−5581						(Cf. Fig. 3)	
	1			2.79									
	4			2.59									
HgH	$^2\Sigma^+, v=0$	$\cdots 6s\sigma^2 6p\sigma$		5.39			28700		2.77			2.08	
	1			4.94			27500		2.65			1.78	
	2			4.35			29200		2.19			1.27	
	3			3.25			31400		1.52			0.75	
	4			1.45			31400		0.68			0.00	
	$^2\Pi_{1/2}, v=0$	$\cdots 6s\sigma^2 6p\pi$	3684	6.58	560	{24933	23730	3.79		0.0068	3.26		—
	$^2\Pi_{\frac{1}{2}}, v=0$					{28617	27410						
	$^2\Pi_{1/2}, v=1$		3684	6.36	580		{23900	3.64		0.0063	2.84		—
	$^2\Pi_{\frac{1}{2}}, v=1$						{27590						
	$^2\Sigma^+, v=0$	$\cdots 6s\sigma 6p\sigma^2$		4.09		−8943 from $^2\Pi_{1/2}$, $v=0$						0.95? (cf. Fig. 3)	

TABLE II. (*Cont.*)

Molecule	State	Probable Elec. Configuration	A	B_v or B^*_v	$Y=A/B_v$	$\nu_0(\Pi,\Sigma)$	$\nu(\Pi,\Sigma)$	Calc'd (pure precession) p_0	Calc'd (pure precession) γ_0	Calc'd (pure precession) q_0	Obs'd p_0	Obs'd γ_0	q_0
CH	$^2\Pi$	$\cdots 2p\sigma^2 2p\pi$	+28.4	14.207	+2.0		$\left\{\begin{matrix}-26270\\-31810\end{matrix}\right.$	+0.0614 −0.0507	(See text)	$\left\{\begin{matrix}+0.0307\\-0.0253\end{matrix}\right\}$	+0.032		+0.037
	$^2\Delta$	$\cdots 2p\sigma 2p\pi^2$		14.60									0.000
	$^2\Sigma^-$	$\cdots 2p\sigma 2p\pi^2$		12.62		−25715	−25180	(See text)	−0.0564	(See text)		−0.01(?)	
	$^2\Sigma^+$	$\cdots 2p\sigma 2p\pi^2$		14.24		−31810	−31810		−0.0508			0	
SiH	$^2\Pi$	$\cdots 3p\sigma^2 3p\pi$	+144	7.4	+19.5						0.049		0.0154
OH	$^2\Pi$	$\cdots 2p\sigma^2 2p\pi^3$	−138	18.47	−7.45		−32710	+0.311		−0.0417	+0.231		−0.038
	$^2\Sigma^+, v=0$	$\cdots 2p\sigma 2p\pi^4$		16.95		−32410	−32060		+0.292			+0.22	
	1			16.00			−30620		+0.289			+0.21	
HCl^+	$^2\Pi, v=0$	$\cdots 3p\sigma^2 3p\pi^3$	−637	9.80	−66.6		−29780	+0.839		−0.0126	+0.563		−0.0057
	$v=1$			9.46	−67.4		−28080	+0.859		−0.0128	+0.52		−0.0057
	$^2\Sigma^+, v=0$	$\cdots 3p\sigma 3p\pi^4$		7.25		−28195	−23550		+0.893			+0.58	
	1			7.00			−20510		+0.956			+0.58	
	2			6.75			−17860		+1.02			+0.57	
N_2^+	$^2\Sigma^+_g$	$\cdots 3p\sigma^2 2p\pi^4 3d\sigma$		1.922								$\lvert<0.005\rvert$(?)	
	$^2\Sigma^-_u$	$\cdots 3p\sigma 2p\pi^4 3d\sigma^2$		2.074								+0.016 (?)	
BO	$^2\Sigma^+$	$\cdots 3p\sigma^2 2p\pi^4 3d\sigma$		1.779		+23584						<0.005	
	$^2\Pi$	$\cdots 3p\sigma^2 2p\pi^3 3d\sigma^2$	−123	1.408	−87						+0.022		−0.00019
	$^2\Sigma^+$	$\ldots 3p\sigma 2p\pi^4 3d\sigma^2$		1.512		−19281						?	
NO	$^2\Pi, v=2$	$\cdots 2p\pi^4 3d\pi$	+124	1.648	+75	−44132					+0.015		+0.00035
	$^2\Sigma^+$	$\cdots 2p\pi^4 3s\sigma$		1.971								$\lvert<0.02\rvert$	
	$^2\Pi$	$\cdots 2p\pi^3 3d\pi^2$	+32	1.118	+28.6	+1308					0.00 (probably)		
O_2^+	$^2\Pi_g, v=8$	$\cdots 2p\pi^4 3d\pi$	+195	1.530	+128						+0.020		+
	$^2\Pi_u, v=0$	$\cdots 2p\pi^3 3d\pi^2$	+8	1.043							very small		very small

Explanation and Notes. The general remarks under Table I in the main also apply here. The observed values of p_0, q_0, and γ_0 are obtained in accordance with Eqs. (14), (18), (26), (27), or also (14a), (14b) for pronounced case *a*. The calculated values are from Eqs. (12), (19). In calculating p_0, B_v of the corresponding Π state is used, in calculating γ, B_v of the corresponding Σ state; $\nu(\Pi,\Sigma)$ is obtained in either case by vertical projections from the state whose coefficient is to be calculated to the $U(r)$ curve of the other state involved in the "pure precession" (cf. text). The electron configurations given are largely from R. S. Mulliken, Phys. Rev. **33,** 737 (1929).

The B^*_v or B_v values given in the table are always B^*_v values in the case of $^2\Sigma$ states. Here $B^*_v = B_v - C_3$, where C_3 is a quantity given by Eq. (16). For pure precession with $l=1$, C_3 should be the same as q_0 of the $^2\Pi$ state, (or $-q_0$ in the case of a $^2\Sigma^-$ state). For case *b* $^2\Pi$ states, the table gives B^*_v values of $^2\Pi^d$, just as Table I gives B^*_v values of $^1\Pi^d$ (cf. Notes to Table I); the case *b* states in Table II are those of BeH, MgH (upper $^2\Pi$), CH and OH. For case *a* $^2\Pi$ states, Table II gives approximately the true B_v values, obtained by averaging the B^* values B^*_1 and B^*_2 corresponding to the $^2\Pi_{1/2}$ and $^2\Pi_{1\frac{1}{2}}$ states.

The experimental data used were from R. S. Mulliken, Phys. Rev. **32,** 388 (1928); **33,** 507 (1929) and sources there cited, and from the following original or secondary sources:

1. BeH, W. W. Watson and A. E. Parker, Phys. Rev. **37,** 167 (1931).
2. MgH, R. W. B. Pearse, Proc. Roy. Soc. **A 122,** 442 (1929).
3. CaH, E. Hulthén, Phys. Rev. **29,** 97 (1927); R. S. Mulliken, Phys. Rev. **30,** 138 (1927); W. W. Watson and W. Bender, Phys. Rev. **35,** 1513 (1930).
4. ZnH, upper $^2\Sigma$ state, E. Bengtsson and E. Hulthén, Faraday Soc. Proc. **25,** 751 (1929).
5. CdH, E. Svensson, Zeits. f. Physik **59,** 333 (1930).
6. HgH, E. Hulthén, Diss. Lund, 1923; Zeits. f. Physik **32,** 32 (1925); **50,** 319 (1928).
7. CH, T. Hori, Zeits. f. Physik **59,** 91 (1929); and references cited in R. S. Mulliken, Phys. Rev. **30,** 785 (1927).
8. SiH, R. S. Mulliken, Phys. Rev. **37,** 733 (1931).
9. OH, G. H. Dieke, Proc. Acad. Sci. Amsterdam **28,** 174 (1925); G. M. Almy, Phys. Rev. **35,** 1495 (1930).
10. HCl^+, M. Kulp, Zeits. f. Physik **67,** 7 (1931).
11. N_2^+, M. Fassbender, Zeits. f. Physik **30,** 73 (1924); R. S. Mulliken, Phys. Rev. **30,** 138 (1927).
12. BO, A. Elliott: Diss. Utrecht, 1930; W. Scheib, Zeits. f. Physik **60,** 73 (1930).
13. NO, M. Guillery, Zeits. f. Physik **42,** 127 (1927).
14. O_2^+, D. S. Stevens, Abstract No. 134, Washington Meeting Am. Phys. Soc. 1931. The signs (+) of p_0 and q_0 for the lower $^2\Pi$ are based on the very probable assumption that this is $^2\Pi_g$ as given in the table and on the safe assumption that the observed rotational levels have ψ functions which are symmetrical in the nuclei.

with the relations predicted by the theory for $^2\Sigma$ and $^2\Pi$ states in the limiting cases *a* and *b*, and for $^1\Pi$ states. Our purposes here include (1) a study of the applicability of Van Vleck's general equation (our Eq. 9 or 14) to $^2\Pi$ states in the intermediate cases between *a* and *b*, and (2) determination of the magnitudes and signs of the coefficients p, q, and γ for a number of molecular states. In a following section we shall examine more carefully than has been done before whether the values of p, q, and γ are in agreement with what would be expected theoretically from our knowledge of the electron levels of the molecules in question; and conversely, we shall use the values of p, q, and γ as a means of getting information about electron configurations or other properties of electron levels.

Tables I and II give the sign and magnitude of q of Eq. (4) for some $^1\Pi$ states, of p and q for several $^2\Pi$ states (cf. Eqs. 10, 14) and of γ for a number of $^2\Sigma$ states (cf. Eq. 18). [Really, values of p_0, q_0, and γ_0 are given in the tables. The relation of these to p, q, and γ is explained in the next section.] The sources of data are given in the notes to the tables. The values of p and q given in Tables I and II, where they differ from those given or implied in an earlier paper[15] dealing briefly with similar subject matter, are to be taken as superseding the latter. In preparing Tables I and II, much care has been taken to obtain correct signs and magnitudes of p, q, and γ, but it is not unlikely that some errors are present.

Modification of theoretical formulas to take care of variation of mean moment of inertia with J and with v. In the course of the work we found that, while the forms of Van Vleck's equations are such as to fit the experimental data nearly always extremely well for low and moderate J values, rather large deviations seem to occur when data for high J values are used. Now in all Van Vleck's equations there appears as a factor the matrix element BL_y or $|BL_y|^2$, in which $B=h/8c\pi^2 I$, where $I(=\mu r^2)$ represents the moment of inertia. Approximately, it is seen to be possible to take out B as a factor and set it equal to B_v(cf. e.g. Eq. 5a). In the case of a non-vibrating molecule, we have $B=B_e=h/8c\pi^2\mu r_e^2=h/8c\pi^2 I_e$ in the limit of zero angular velocity of rotation. But if the molecule rotates, it stretches slightly, or if the rotation is very fast, it stretches considerably, i.e., r becomes greater than r_e. From the way in which Van Vleck's BL_y and B are defined, it is clear that allowance should be made, in applying his equations, for the effect of such stretching on B and BL_y.

For a non-vibrating diatomic molecule with $\Lambda=0$ and $S=\frac{1}{2}$ the kinetic energy of rotation is given[16] by

$$P_\phi^2/2\mu r^2 = [P_\phi^2/2\mu r_e^2](r_e/r)^2 = hcB_eK(K+1)[1/(1+\xi)^2], \qquad (21)$$

where P_ϕ is the angular momentum, equal to $K(K+1)h/2\pi$ according to quantum theory, while $\xi=(r-r_e)/r_e$, a quantity which is a measure of the stretching by rotation.

[15] R. S. Mulliken, Phys. Rev. **33**, 507 (1929).

[16] Cf. e.g. R. S. Mulliken, Ref. 14, p. 65.

If ξ is not too large, we may assume that the stretching takes place against a force whose potential energy is given by

$$U(r) = a^*\xi^2/2, \text{with } a^* = 4\pi^2c^2\omega_e^2\mu r_e^2 = hc\omega_e^2/2B_e, \tag{22a}$$

$c\omega_e$ being the frequency of infinitesimal classical vibrations about $r=r_e$. In this case, it is easily found [16] that ξ is given by

$$\xi = u^2K(K+1), \text{where} \tag{22b}$$

$$u^2 = 4B_e^2/\omega_e^2 = -D_e/B_e, \tag{22c}$$

D_e being a coefficient determinable from an analysis of the rotational energy levels. Ordinarily $u^2 \ll 1$. Eqs. (22a), (22b) show how r increases with K.

Assuming Eq. (22a), one can write, according to Eqs. (21), (22b),

$$\begin{aligned} B_K &\equiv h/8\pi^2c\mu r^2 = B_e/(1+\xi)^2 \\ &= B_e/[1+u^2K(K+1)] \sim B_e[1-2u^2K(K+1)+\cdots]. \end{aligned} \tag{23}$$

On adding to the kinetic energy of rotation as given by Eqs. (21) and (23), the potential energy $U(r)$ given by Eq. (22a), and dividing by hc, one gets the ordinary rotational spectroscopic term $F(K)$. The result can be reduced[16] to:

$$F(K) = B_eK(K+1) + D_eK^2(K+1)^2 + \cdots.$$

For a vibrating molecule, one gets essentially the same results, in particular

$$B_{v,K} = h/8\pi^2c\mu\overline{r_v^2} \tag{24a}$$

$$\sim B_v/[1+u^2K(K+1)] \tag{24b}$$

$$\sim B_v[1-2u^2K(K+1)+\cdots] \tag{24c}$$

$$F(K) = B_vK(K+1) + D_vK^2(K+1)^2 + \cdots. \tag{25}$$

Eq. (24a) defines a kind of mean r for any vibrational state[16a]. Since in practise B_v usually decreases with increasing v, this mean r increases with v.

For molecules with $\Lambda>0$ or $S>0$ the rotational term $F(K)$ becomes more complicated than the form given by Eq. (25), but the variation of B_v with the rotational quantum number is always given with sufficient accuracy by Eq. (24b) or (24c). Often J rather than K, or something slightly different from both, is needed in Eqs. (24), but this makes very little difference in the result.

Proper allowance can now evidently be made, in Van Vleck's equations, for rotational stretching by using $B_{v,K}$ instead of B_v. Since $B_{v,K}$ varies with K, the coefficients p, q, and γ in Van Vleck's equations should likewise vary with K. The coefficients p and γ, which according to the theory involve BL_y, should vary with K in the same way that $B_{v,K}$ does, while q, which according to the theory involves $|BL_y|^2$, should vary in the same way that $(B_{v,K})^2$ does. In other words, we expect, for any given value of v,

[16a] Cf. R. T. Birge, Nat. Research Council Report on Molecular Spectra, p. 112, Eq. (48).

$$p = p_0/[1 + u^2K(K+1)\,] \sim p_0[1 - 2u^2K(K+1) + \cdots], \quad (26a)$$

$$\gamma = \gamma_0/[1 + u^2K(K+1)] \sim \gamma_0[1 - 2u^2K(K+1) + \cdots], \quad (26b)$$

$$q = q_0/[1 + u^2K(K+1)]^2 \sim q_0[1 - 4u^2K(K+1) + \cdots]. \quad (27a)$$

Likewise for varying v and fixed K we may reasonably expect

$$p_0 \text{ and } \gamma_0 \text{ proportional to } B_v, \quad (26c)$$

$$q_0 \text{ proportional to } B_v^2 \quad (27b)$$

Since $u \ll 1$, it is of course only when K or J is large that p, q, and γ differ appreciably from p_0, q_0, and γ_0. *The coefficients* p_0, q_0, and γ_0 given in *Tables I and II have been mainly determined from data for low and moderate J values, where the effect of the stretching of the molecule on p, q, and* γ *is still negligible.* Eqs. (26) and (27) have been used mainly only to explain the variation of these coefficients with J which is observed at high J values. In some cases, however, the values of the coefficients have been adjusted slightly in order to give better agreement at high J values.

In applying Eqs. (26) and (27), either of the two forms $(4B_e^2/\omega_e^2$ or $-D_e/B_e)$ of the quantity u^2(cf. Eq. 22c) may be used. The choice depends on the relative accuracy, or on the existence, of available data for D_e and ω_e. In the following work, sometimes the one, sometimes the other choice has been found best.

A particularly good example of the effect of the variation of q with K is seen in the case of BeH (Fig. 2). Here we have a case $b\ ^2\Pi$ state to which Eq. (4) applies. According to Eq. (4) , if q is a constant, $\Delta\nu_{dc}(K)$ should be proportional to $K(K+1)$. Actually, $\Delta\nu_{dc}$ goes to a maximum as K increases to large values, then shows a tendency to decrease. But this behavior can probably be completely accounted for (cf. Fig. 2, caption) by the variation of q with K which is predicted by the foregoing considerations. In other molecules, similar behavior of $\Delta\nu_{dc}$ can always be partly accounted for in the same way, although usually some deviations from the simple Van Vleck formulas still remain to be accounted for in other ways. These will be discussed later.

The proportionality of p, γ, and q to B_v or B_v^2 which is predicted by Eqs. (26c) and (27b) is found to be at least qualitatively fulfilled in all cases (cf. Tables I and II) except those of certain states where there are strong perturbations (upper $^2\Sigma$ states of CdH, HgH in Fig. 3) and where one would not expect the equations to hold.

Determination of coefficients p_0, q_0, *and* γ_0. It will be well at this point to explain how one obtains the doublet separations $\Delta\nu_{dc}$ and $\Delta\nu_{12}$ used as a basis for the determination of p_0, q_0, and γ_0 of Tables I and II. For the way in which the $\Delta\nu_{12}$'s are determined (and the uncertainties involved in some cases), the reader may be referred to some earlier papers.[17] The problem of determining the $\Delta\nu_{dc}$'s resolves itself into two parts, namely determination of the *signs* and of the *magnitudes* of these quantities.

[17] Cf. R. S. Mulliken, Phys. Rev. **30**, 138, 1927 ($^2\Sigma$, $^2\Sigma$ bands); Phys. Rev. **30**, 785, 1927 and **32**, 388, 1928 ($^2\Pi$,$^2\Sigma$ and $^2\Sigma$, $^2\Pi$ bands), also the figures in Ref. 4.

The sign of $\Delta\nu_{dc}$ for the rotational levels of any Π state can always be determined if combinations of the Π state with a Σ state are known, and if it is known whether the Σ state is a Σ^+ or a Σ^- state. Since the + or − character of every rotational level is then known for the Σ state (cf. Ref. 4, Fig. 17), and since the selection rule $+\longleftrightarrow-$ is obeyed (cf. Ref. 4, p. 96) in all band lines (with very rare exceptions resulting from the influence of electric fields), one can determine the + or − character of each rotational level of the Π state. This makes it possible to assign the theoretically defined labels c and d to each level, and so, the positions of the levels having been determined from analysis of the band structure, to determine the sign of $\Delta\nu_{dc}$. Reference to Figs. 17, 25, 28 of Ref. 4 will help to make the method clear.

The above method obviously depends on knowing whether the Σ state used in the process is a Σ^+ or Σ^- state. This cannot be determined empirically, but can nearly always be decided with practical certainty on theoretical grounds. Nearly always in dealing with $^1\Sigma$ and $^2\Sigma$ states, one encounters Σ^+ states. Σ^- states cannot occur except in the case of molecules having two (or an even number of) π electrons which are not in closed shells (or in similar cases, never yet found, involving δ, ϕ electrons). Thus a knowledge of its electron configuration is usually sufficient to determine whether a Σ state is Σ^-.

In the case of every state listed in Tables I and II, with one exception (SiH, see below), Π, Σ bands have been analyzed and the electron configuration of the Σ state is known with practical certainty, at least to the extent that is necessary to establish whether it is Σ^+ or Σ^-. In only *one* case, that of CH, is a Σ^- state involved; here the $^2\Pi$ combines with a $^2\Sigma^-$ and also with a $^2\Sigma^+$ state[18] both of which are derived from the same electron configuration $\ldots 2p\sigma 2p\pi^2$; supplementary considerations in regard to dissociation products here make it probable that the lower of the two $^2\Sigma$ states is $^2\Sigma^-$ and the upper $^2\Sigma^+$, and thus make it possible to fix the sign of $\Delta\nu_{dc}$ in the $^2\Pi$ state. The $^2\Pi$ state of SiH is known only from $^2\Delta$, $^2\Pi$ bands.[2] Such bands are always incapable of fixing the sign of $\Delta\nu_{dc}$. The probable close analogy of SiH to CH makes it probable, however, even with due regard for the possibilities involved in Eqs. (5), that p and q have the same sign in the $^2\Pi$ of SiH as in that of CH; this then serves to fix the sign of $\Delta\nu_{dc}$.

In determining the *magnitude* of $\Delta\nu_{dc}$, the procedure is usually simplest in the case of $^2\Delta$,$^2\Pi$ and $^2\Pi$,$^2\Delta$ bands. Here the doublet separations are usually negligible in the $^2\Delta$ states (this can always be checked, if doubtful, by a study of combination relations), and one gets $\Delta\nu_{dc}$ directly:

$$\Delta\nu_{idc} = R_{icid}(J) - R_{idic}(J) = Q_{id}(J) - Q_{ic}(J) = P_{icid}(J) - P_{idic}(J),$$

where $i = 1$ or 2,—cf. Fig. 26 of Ref. 4.

In determining $\Delta\nu_{dc}$ from Π, Σ or Σ, Π bands (cf. Figs. 17, 25, 28 of Ref. 4, also Ref. 17), one gets for instance

$$[R(J) - Q(J)] - [Q(J+1) - P(J+1)] = \Delta\nu_{dc}(J) + \Delta\nu_{dc}(J+1) \quad (28)$$

[18] Cf. T. Hori, Zeits. f. Physik **59**, 918, 1929.

in the case of a $^1\Pi,^1\Sigma^+$ or $^2\Pi_{\frac{3}{2}},^2\Sigma^+$ or $^2\Pi_{1\frac{1}{2}},^2\Sigma^+$ transition. One may write

$$\Delta\nu_{dc}(J) + \Delta\nu_{dc}(J+1) \sim 2\Delta\nu_{dc}(J+\tfrac{1}{2}), \tag{29}$$

i.e. one gets in this way not the real doublet separation $\Delta\nu_{dc}(J)$ for actual values of J, but instead the separations $\Delta\nu_{dc}(J+\frac{1}{2})$ for a set of fictitious J values half way between the members of the set of real J's. These quantities are, however, just as useful in determining p and q as the $\Delta\nu_{dc}(J)$'s would be.

$^2\Pi$ *states intermediate between cases a and b.* Before discussing the interpretation of the values of p_0, q_0, and γ_0 given in Tables I and II, we shall consider in some detail the applicability of Eq. (14) to several examples of $^2\Pi$ states intermediate between cases *a* and *b*, and the way in which the coefficients p_0 and q_0 were determined from experimental data. The examples chosen are the $^2\Pi$ states of ClH^+, OH, CH, CaH, SiH, ZnH, and HgH. A and B_v, hence Y of Eq. (14), are already known for these states from previous work. The empirical data on $\Delta\nu_{dc}(J)$ are obtained from $^2\Pi$, $^2\Sigma$ or $^2\Sigma$, $^2\Pi$ bands except in the case of SiH, where the $^2\Delta$, $^2\Pi$ bands are used.

Given a set of $\Delta\nu_{dc}$ data for each of the two sets of levels T_1 and T_2 or of the two substates $^2\Pi_{\frac{3}{2}}$ and $^2\Pi_{1\frac{1}{2}}$ of a $^2\Pi$ state, one can often determine p_0 and q_0 independently for each set or substate. The values so determined should according to the theory be the same, at least very nearly, for the two sets. One can also use the data on both substates simultaneously so as to determine a p_0 and q_0 which apply to both.

Using the latter method, it will be seen that Eq. (14) predicts the following relation:

$$\Delta\nu_{2dc}(J) - \Delta\nu_{1dc}(J) = (p+2q)(J+\tfrac{1}{2}) + \cdots. \tag{30}$$

Here $\Delta\nu_{2dc}$ refers to the T_2 levels, $\Delta\nu_{1dc}$ to the T_1 levels. On examining the data for the examples mentioned above, it was found that $\Delta\nu_{2dc}-\Delta\nu_{1dc}$ is accurately proportional to $(J+\frac{1}{2})$ up to moderate J values, but that considerable deviations from this proportionality set in for high J values. Thus for small and moderate J values the quantity p_0+2q_0 could be accurately determined from the data. The behavior of $\Delta\nu_{2dc}-\Delta\nu_{1dc}$ at high J values was always at least partly accounted for by means of Eqs. (26) and (27).

Next, by taking $\Delta\nu_{2dc}(J)+\Delta\nu_{1dc}(J)$, a more complicated expression than Eq. (30) is obtained, which depends largely on q and to a lesser extent (except for small J) on $(p+2q)$. By correcting for the terms involving $(p+2q)$, a set of empirical quantities proportional to $q(J-\frac{1}{2})(J+\frac{1}{2})$ $(J+3/2)$ is obtained. These give q, and the value of p then follows.

Values of p_0 and q_0 determined as just outlined are given in Tables I and II, while in Figs. 1 and 2 are shown theoretical curves for $\Delta\nu_{dc}(J)$ corresponding to Eqs. (14), (26), (27) for several of the molecular states whose p_0 and q_0 values are given in Table II. The empirical values of $\Delta\nu_{dc}(J)$ or $\Delta\nu_{dc}$ $(J+\frac{1}{2})$ are shown by small circles. It will be seen that the agreement is excellent, except in some cases for high J values. The disagreements at high J values would be worse if the variation of p and q with J had not been taken into account (cf., e.g., Fig. 2). Possible explanations of the remaining dis-

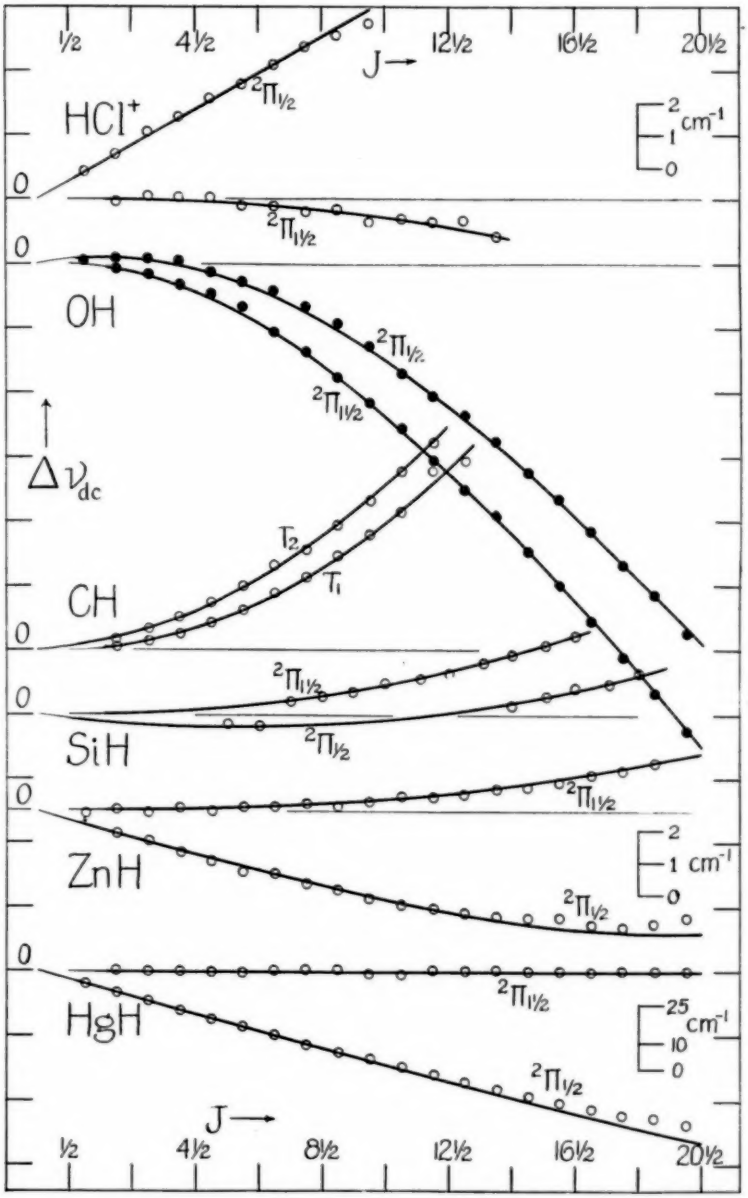

Fig. 1. Comparison of experimental data, indicated by circles, with theoretical curves drawn according to Eq. (14) for $\Delta\nu_{dc}(J)$ for $^2\Pi$ states of several hydride molecules having a variety of values of the parameter $Y=A/B$. The scale used is the same for all the molecules except HgH. Two further examples are shown in Fig. 2. The coefficients p_0, q_0 used in drawing the theoretical curves were chosen so as to fit the experimental data as well as possible. They are the "observed" values given in Table II. The slight variation in p and q for high J values (cf. Eqs. 26, 27) has been taken into account in drawing the theoretical curves for HgH, ZnH, and OH; the quantity $u^2=4B_e^2/\omega_e^2$ in Eqs. (26), (27) has been calculated using experimental ω values, or in the case of ZnH a value estimated from the empirical relation $\omega_e/B_e\sim$constant, using for the constant the value which is found in CuH.

crepancies will be taken up later. Empirical values of γ_0 are given in Table II, while Fig. 3 gives observational data for $\Delta\nu_{12}(K)$ for several examples of $^2\Sigma$ states.

Applications of theory to interpretation of band structure (SiH, CaH). The quantitative agreement of the data for SiH with Eq. (14) confirms the conclusions, reached in a previous paper[2] on the basis of a qualitative use of the same theory, as to the interpretation of the $^2\Delta$,$^2\Pi$ bands of SiH. Eq. (14) has also been used here to clear up an uncertainty as to the numbering of the lines of the Q_2 branch in the $^2\Pi$, $^2\Sigma$ bands of CaH. The numbering of the Q_1 lines in these bands was recently revised by Watson and Bender[19] on the basis of combination relations involving a previously undiscovered $^0P_{12}$ branch. This made it possible for them to determine also the quantities

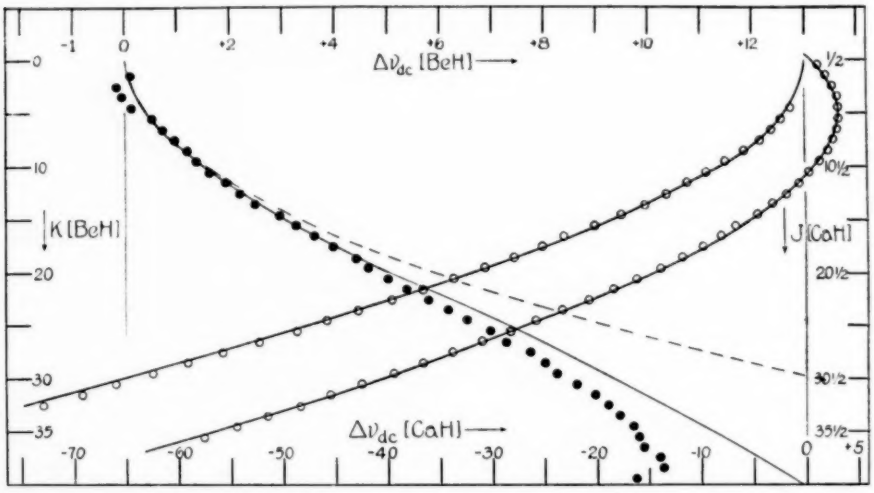

Fig. 2. Comparison of experimental data with theoretical curves for $\Delta\nu_{dc}$ for $^2\Pi$ states of BeH and CaH. Eqs. (14), (26), and (27) were used for CaH; the u value needed in Eqs. (26), (27) was calculated using $\omega = 1300$, estimated (by means of the relation $\omega_e/B_e \sim$ constant) from the observed ω_e value[20] of the normal $^2\Sigma$ state. Eq. (4) and the exact form of Eq. (27) were used for BeH, which is case b and acts practically like a $^1\Pi$ state. The importance of using Eq. (27) for q instead of assuming a constant q in Eq. (4) is shown here. The dashed curve represents Eq. (4) drawn for $q = q_0$, while the full curve assumes a varying q in accordance with Eq. (27). The remaining discrepancy between the full curve and the experimental points can be attributed to the failure of the simple relation $U(r) = a^*\xi^2/2$ (cf. Eq. 22a) and consequently of Eq. (22b) at high K values. As is indicated by the course of the T values[26] themselves at the highest observed K values, the molecule stretches considerably more rapidly than in Eqs. (22a), (22b). Hence (cf. Eq. 23) $B_{v,K}$ and so q should, as observed, diminish more rapidly at the highest K values than Eq. (27) demands. In obtaining u in Eq. (27), the relation $u^2 = -D_e/B_e$ has been used for BeH, with experimental values[26] of D_e and B_e. (In other cases shown in Figs. 1–3, the same effects as in BeH exist at high J values, but are not nearly so large.)

$\Delta\nu_{1dc}(J+\frac{1}{2})$ corresponding to the $^2\Pi_{\frac{1}{2}}$ sub-state. From these data we determined p_0 and q_0 of Eq. (14), and then used them to calculate the quantities $\Delta\nu_{2dc}$ applicable to the $^2\Pi_{1\frac{1}{2}}$ state. Knowing these and the frequencies of the

[19] W. W. Watson and W. Bender, Phys. Rev. **35**, 1513 (1930).

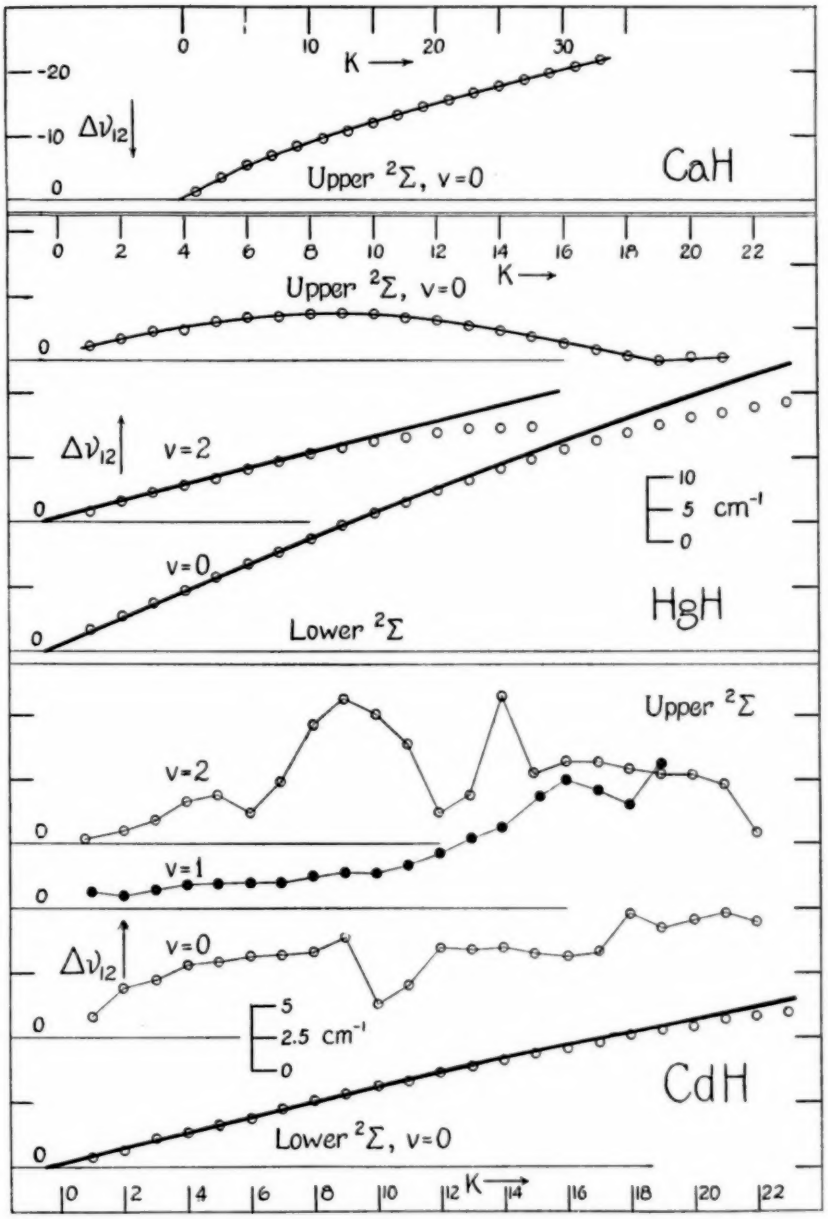

Fig. 3. Spin doublet separations $\Delta\nu_{12}(K)$ in $^2\Sigma$ states (cf. Eqs. 2, 18). The circles represent experimental values. The *heavy* curves (only for CdH, lower $^2\Sigma$, $v=0$ and for HgH, lower $^2\Sigma$, $v=0$ and 2) are theoretical curves corresponding to Eq. (18), (26). The coefficient γ_0 of these theoretical equations has been chosen in each case to give a best fit to the experimental data, while the quantity $u^2=4B_e^2/\omega_e^2$ needed in the second equation has been calculated using the experimental B_v values (Table II) and ω values ($\omega_{\frac{1}{2}}=1374$ for CdH, $\omega_0=1308$ for HgH). The considerable deviations of the experimental points from the calculated curves for high K values in HgH are tentatively attributed to changes in the electronic wave functions, hence in γ_0, with increasing K.

band-lines $P_2(J)$ and $R_2(J)$, it was possible to predict the positions of the band-lines $Q_2(J)$ with sufficient accuracy to determine the correct numbering of these lines.[20] From the P_2, Q_2, and R_2 branches, accurate values of $\Delta\nu_{2dc}$ were now obtained, and from the data on $\Delta\nu_{1dc}$ and $\Delta\nu_{2dc}$ improved p_0 and q_0 values were determined in the usual way.

As a check on the numbering of the Q_2 lines, the positions of the hitherto unassigned lines of the weak branch ${}^SR_{21}$ have been calculated on the basis of Eqs. (31) and (32).[21]

$$ {}^SR_{21}(J) = R_2(J) - \Delta\nu_{2dc}(J+1) + T_2''(J) - T_1''(J) \qquad (31) $$

$$ = Q_2(J+1) + T_2''(J-1) - T_1''(J-1). \qquad (32) $$

The ${}^SR_{21}$ lines were calculated from Eq. (32), except for $J = \frac{1}{2}, 1\frac{1}{2}, 2\frac{1}{2}$, where Eq. (31) had to be used owing to the absence of data on $Q_2(J)$. In Eq. (31), *calculated* values of the small quantities $\Delta\nu_{dc}(J+1)$ were used. For R_2 and Q_2 in Eqs. (31) and (32), empirical ν data were used directly, while the other quantities in these equations were obtained by suitable additions and subtractions of measured ν's.

Measurements on a second-order grating plate of the CaH bands (taken by Dr. P. S. Delaup in this laboratory in connection with his work on the Zeeman effect of these bands) disclosed a set of lines having appropriate intensity relations[22] and agreeing excellently in position with the values calculated for the ${}^SR_{21}$ branch (cf. Table III).

TABLE III. ${}^SR_{21}$ *Lines in* (0,0) *Band of* ${}^2\Pi,{}^2\Sigma^+$ *System of CaH.*

J	Calc'd ν	Obs'd ν	Int.	J	Calc'd ν	Obs'd ν	Int.
$\frac{1}{2}$	14,479.08	14,479.32	5	$6\frac{1}{2}$	14,573.43	14,573.46	2 (dif)
$1\frac{1}{2}$	493.33	493.42	2	$7\frac{1}{2}$	590.57	Masked by Q_1 $(39\frac{1}{2})$	
$2\frac{1}{2}$	508.29	Masked by $R_1(9\frac{1}{2})$		$8\frac{1}{2}$	608.59	608.55	1−
$3\frac{1}{2}$	523.75	523.87	1	$9\frac{1}{2}$	626.81	626.62	1−
$4\frac{1}{2}$	539.89	Masked by $R_1(12\frac{1}{2})$		$10\frac{1}{2}$	645.02	644.89	1−
$5\frac{1}{2}$	556.53	Masked by atomic line					

Interpretation of Results in Relation to Electron Configurations

The values of p_0, q_0 and γ_0 given in Tables I and II have a significant bearing on the question of the forms of the electron orbits or of the wave functions for the molecules concerned. That the values of p_0, q_0, and γ_0 depend on these can be seen from Van Vleck's theoretical equations for them (cf. Eqs. 4, 5, 5a; 10, 10a, 10b; 17). In the simple case that a Σ and a Π state are to each other in the relation of "pure precession" (cf. discussion in two paragraphs preceding Eqs. 6 and 7), simple theoretical expressions can be given for p_0, q_0, and γ_0 (cf. Eqs. 6, 7, 7a, 12, 19).

[20] As a result of the revised numbering of the Q_2 branches, the positions of the Q_2 (and ${}^QP_{21}$) lines shown in Fig. 30a of Ref. 4 should be revised, and in such a way (cf. Fig. 4 of the present paper) that the Q_1 and Q_2 branches *do not cross.*

[21] The correctness of these equations can be seen from Fig. 28 of Ref. 4.

[22] Cf. Ref. 4, pp. 140–141; also cf. data on the ${}^SR_{21}$ branch in the ${}^2\Sigma^+,{}^2\Pi$ bands of OH (R. S. Mulliken, Phys. Rev. **32**, 410, 1928).

Van Vleck pointed out in his paper[1] that the observed values of p, q and γ commonly are of an order of magnitude corresponding well to the case of pure precession. We now find that something like pure precession seems to be almost quantitatively fulfilled in most of the molecular states studied here. This rather surprising result appears to carry with it the important conclusion that in these molecules the electrons commonly have well-defined quantum numbers n and l having the same significance as in atoms. In some cases, in particular the hydrides, these quantum numbers n and l are those corresponding to the atom which would be obtained if the two nuclei could be united. In other cases, the n and l which are significant are found to be those which would exist if the two atoms were completely separated. The various relations which exist in different cases can best be brought out by a discussion of examples.

Calculation of p_0, q_0, γ_0 for pure precession. First, however, something needs to be said in regard to the method of obtaining the *calculated* values of p_0, q_0, and γ_0 in Tables I and II. The first step, in the case of a Π state, is to see whether there is a neighboring Σ state such that, using Eqs. (7), (7a), (12) with $\nu_0(\Pi, \Sigma)$, p_0 and q_0 come out roughly in agreement with the observed values. [By $\nu_0(\Pi,\Sigma)$ is mean the difference in E/hc between the level $v=0$ of the Π state and that of the Σ state.] In nearly all cases it turns out that just one such state is known, and that the agreement is good. The calculated values of p_0 and q_0 are then revised by replacing $\nu_0(\Pi, \Sigma)$ by a quantity $\nu(\Pi, \Sigma)$ obtained by projecting vertically downward (or upward, if the Σ level is above the Π) from the level $v=0$ of the Π state (or from the level $v=v$, if one wishes to calculate p_0 and q_0 for $v>0$) to the $U(r)$ curve of the Σ state. [In projecting "from the level $v=v$," one may take a suitably weighted average of the two values of $\nu(\Pi, \Sigma)$ obtained by projecting from the two points of intersection of the level $v=v$ with the $U(r)$ curve of the Π state.] If B_v is the same for the Π and Σ states, as it should be in the ideal case of pure precession, then $\nu(\Pi, \Sigma)$ for $v=0$ is practically the same as $\nu_0(\Pi, \Sigma)$. In some cases, however, e.g. that of the $1s\sigma 2p\pi$, $^1\Pi$ state of H_2, the two quantities are far from being equal. In the case of a $^2\Pi$ state with a large case a doublet separation, a separate value of $\nu(\Pi, \Sigma)$ must be used for $^2\Pi_{1/2}$ and $^2\Pi_{3/2}$.

In calculating γ for a $^2\Sigma$ state, the procedure is similar. The quantity $\nu(\Pi, \Sigma)$ is obtained by projecting upwards (or downwards) from the level $v=0$ (or $v=v$) of the $^2\Sigma$ state to the $U(r)$ curve (or curves) of the $^2\Pi$ state.—It should be noted that ν in *all* the equations used in this paper is to be taken as positive or negative according as the Π state is above or below the corresponding Σ state.

Hydrides with one outer p electron. The states listed in Tables I and II for H_2, BeH, MgH, ZnH, CdH, and HgH include a Σ and a Π state whose previously assigned electron configurations[23] might lead one to expect the case of pure precession. In each case, the most loosely bound electron is supposed to be in an np orbit, which when $\lambda=0$ ($np\sigma$) gives the Σ state, when $\lambda=1$ ($np\pi$)

[23] Cf. R. S. Mulliken, Phys. Rev. **33**, 738 (1929); also F. Hund, Ref. 25 and elsewhere.

gives the II state. In each case the values of p_0 and q_0 calculated for the II state, and of γ_0 calculated for the $^2\Sigma$ state, agree remarkably well with the observed values. In nearly every case the calculated values are somewhat larger than the observed values, as would ordinarily be expected, since the ideal case of pure precession corresponds to the largest possible mutual influence of a Σ and a II state. In CaH also we have a $^2\Sigma$ and a ^{2}II state which show the same relations, together with other interesting features; discussion of this molecule will be postponed to a later section.

Observed values larger than calculated values may probably be attributed largely to the fact that Eqs. (7), (12), and (19) are really somewhat too simplified to give accurate results when v is small and when at the same time there is a possibility of having very small values of v(II, Σ) for individual vibrational levels. In calculating, for instance, Λ-type doubling coefficients for a II state, one should use a summation over all v values of the Σ state,[8] as in Eq. (5) except that here we assume that only one Σ state need be considered. Of course if all the vibrational levels of the Σ state are *above* the given v level of the II state, Eqs. (7) and (12) should always hold well when we have pure precession. But if the zero level of the Σ state is *below* that of the II state, then some of the terms in the summation may have very small v(II, Σ)'s which may have an important effect on p_0 and q_0, even if BL_v is small. Usually these terms should tend to increase $|p_0|$ and $|q_0|$, since those v's which have the same sign as the single weighted mean v of Eqs. (7) and (12) should on the whole have larger BL_v's than those with opposite sign.

Associated with such cases as those under discussion there should be irregularities in the mode of dependence of $\Delta\nu_{dc}$ (and of T_c and T_d themselves) on v and on J (*perturbations*). A good example of a state showing irregular $\Delta\nu_{dc}$'s (larger than those calculated by Eq. 7) is the $1s\sigma 2p\pi$, ^{1}II state of H_2. Similarly, except that here the case of pure precession is not at all approximated, the large and irregular $\Delta\nu_{12}$'s and the perturbed terms in the upper $^2\Sigma$ states of CdH and of HgH may be ascribed to their very close proximity to the higher vibrational levels of the ^{2}II state.

The agreements of observed and calculated values of p_0, q_0, and γ_0 in Tables I and II even as to *order of magnitude* are very significant, since without a strong tendency toward the case of pure precession, even such agreements would not be expected. The actual observed agreements are so good as to leave little doubt that the case of pure precession is very often pretty closely approximated. This gives strong support to the views of Hund and of Mulliken, who have maintained that the "electron configurations" (or "electron orbits," or "wave-functions") in these molecules are really closely similar to those of the "united-atom" which would be obtained if the two nuclei were united, and radically different, in respect to one at least of the outer electrons, from the wave-functions which would exist if the molecule acted merely like two somewhat modified atoms. (The view that a molecule can nearly always be regarded as consisting merely of somewhat modified atoms seems to be widespread among those who have used the separated atoms as a starting point for the calculation of molecular properties).

An example will make the point clearer. We know beyond reasonable doubt[24] that the normal $^2\Sigma$ state and the $^2\Pi$ state of HgH are related to the states of their separated atoms as follows:

$$\text{Hg}, \cdots 6s^2, {}^1S + \text{H}, 1s, {}^2S \rightarrow \text{HgH}, {}^2\Sigma^+ (+ 0.37 \text{ volts})$$

$$\text{Hg}, \cdots 6s6p, {}^3P + \text{H}, 1s, {}^2S \rightarrow \text{HgH}, {}^2\Pi (+ 1.8 \text{ volts}).$$

If in the molecule the H electron were still essentially a $1s$ electron, we could write

$$\text{HgH}, {}^2\Sigma^+ : \cdots (6s\sigma^2)\sigma 1s; \quad \text{HgH}, {}^2\Pi : (6s\sigma 6p\pi)\sigma 1s.$$

The electron configurations of the Σ and the Π state would here be essentially the same except for the replacement of a $6s\sigma$ Hg electron present in the Σ state by a $6p\pi$ Hg electron in the Π state. But a $6s\sigma$ and a $6p\pi$ orbit, differing in l, are not related in such a way as to give pure precession, and the experimental evidence from the p_0, q_0, and γ_0 values in favor of pure precession could not be understood.

If, however, we suppose that the $1s$ orbit of the H electron has been completely changed when the molecule is formed, becoming a $6p\sigma$ electron in the case of the $^2\Sigma$ state, and a $6s\sigma$ electron in the case of the $^2\Pi$ state, we have

$$\text{HgH}, {}^2\Sigma^+ : 6s\sigma^2 6p\sigma; \quad \text{HgH}, {}^2\Pi : 6s\sigma^2 6p\pi.$$

Now if the symbols $6s\sigma$, $6p\sigma$, $6p\pi$ really have quite definitely the meaning which they would have for the united-atom (Tl) under the influence of the electric field of a proton, we should expect the case of pure precession to be fulfilled, otherwise not. Comparison of the observed and calculated values of p_0, q_0, and γ_0 for HgH shows that pure precession is actually nearly fulfilled. In some of the other molecules of the same type, the agreement is even better than in HgH. It seems remarkable that in a molecular state like the $^2\Sigma$ normal state of HgH, whose energy of formation from its atoms is only 0.37 volt, the transformation of the wave-function from that of Hg+H toward that of the united-atom has been so complete as to give the observed close approximation to pure precession. It is also worthy of note that this thoroughgoing transformation takes place regardless of the fact that, according to conventional valence theory, no valence bond exists in this $^2\Sigma$ state of HgH.

Several interesting minor points, some of them giving considerable added support to the preceding conclusions, remain to be discussed.

Let us begin with the data on H_2. Here one notes an unusually large difference in the B_v values of the $^1\Sigma_u$ and $^1\Pi_u$ states which here give the pure precession. The U(r) curve of the $^1\Sigma$ state lies rather close below that of the $^1\Pi$ state for small r values, and the two curves should come together at $r=0$. For large values of r the curves go far apart, but as $r \rightarrow \infty$, they finally come together again. An approximate diagram of these curves, and a partial ex-

[24] Cf. R. S. Mulliken, Phys. Rev. **36**, 1449 (1930) for HgH curves, and E. Svensson, Zeits. f. Physik **59**, 349 (1930) for CdH. The curves given must, however, not be taken as more than roughly correct.

planation of their behavior, will be found in an article by Hund.[25] Probably the $^1\Sigma$ state departs markedly from united-atom conditions as r becomes fairly large, corresponding to a tendency of the $2p\sigma$ electron in H_2 to become a $1s$ electron (of $H^+ + H^-$), although actually it finally goes over as $r \to \infty$ into a 2-quantum electron of an H atom. For large r values, therefore, one cannot expect to find pure precession approximated, but if we calculate q_0 for the $^1\Pi$ state, for small values of v, we have r small enough so that conditions are near those of the united-atom. The fact that the observed q_0's are actually larger than those calculated for pure precession, and the irregularities in the $\Delta\nu_{dc}$'s as functions of v and K, have already been explained earlier in this section.

In BeH, γ_0 of the $^2\Sigma$ state is too small to measure, as would be expected, even for pure precession, from the calculated γ_0. In the $^2\Pi$ state (a good example of case b, with p_0 negligible), the observed q_0 is about two thirds the calculated, indicating that the case of pure precession is fairly well fulfilled. The mere fact that the observed q_0 is positive shows (cf. Eqs. 4, 5, 5a) that the $^2\Pi$ interacts principally with the $^2\Sigma$ state below it if, as is almost certain, this is $^2\Sigma^+$. (There is in all probability only *one* $^2\Sigma$ state below the $^2\Pi$). Similar remarks apply to MgH, ZnH, CdH, HgH. Of course $^2\Sigma^-$ states above the $^2\Pi$ would tend to make q_0 positive, but they are not often likely to be important.

The peculiarities in behavior of the rotational levels of the $^2\Pi$ state of BeH for large values of K, which Watson[26] attributed to a more or less complete uncoupling of an l vector, are here found to be explained by the variation of the moment of inertia with K. Thus the fact that the Λ-type doublet widths no longer increase in proportion to $K(K+1)$ for large K values can be explained in this way (cf. caption of Fig. 2). Likewise the fact that the rotational energy itself increases much less rapidly for large K values[26] than it would if given by $B_vK(K+1)$ alone is completely explained by the ordinary rotational stretching of the molecule, which is taken care of by added terms[27] beginning with $D_vK^2(K+1)^2$ as in Eq. (25). Thus there is no evidence in BeH of any large, much less of complete, rotational uncoupling of an l, even at the highest K values where the molecule is apparently approaching dissociation because of rotational instability. In making the calculations with Eqs. (22c) and (27), we have used $u^2 = 1.005\text{x}10^{-4}$, calculated from the experimental B and D values[27] $B_0 = 10.30$, $D_0 = -1.038\text{x}10^{-3}$.

According to Watson and Parker,[27] $\Delta\nu_{dc}(K)$ is negative in BeH for the lowest K values, for both T_1 and T_2 levels, then becomes positive and remains so (cf. experimental points in Fig. 2). According to Eq. (14), however, and in view of the small value of A/B which exists here, there is no possibility, for either T_1 or T_2 levels, that $\Delta\nu_{dc}$ can change sign at small K values (cf.

[25] Cf. F. Hund, Zeits. f. Physik **63,** 719–751 (1930), especially pp. 741–2 and Fig. 5. Hund does not refer specificially to a tendency toward $H^+ + H^-$, although this is apparently involved in the tendency, which accounts for the low energy of this $^1\Sigma$ state at large r, of the $2p\sigma$ electron to become atomic $1s$.

[26] W. W. Watson, Phys. Rev. **34,** 1010 (1929); also Ref. 27, p. 173–4.

[27] W. W. Watson and A. E. Parker, Phys. Rev. **37,** 167 (1931).

theoretical curve in Fig. 2). It seems necessary to attribute the small observed negative values to experimental error.

Judging from the observed value of p_0 for the lower $^2\Pi$ state of MgH, the case of pure precession is well fulfilled there. The observed value of q_0 is, however, low, but the observed values of $\Delta\nu_{dc}$ are so small that the experimental p_0 and especially q_0 are not at all accurate. The upper $^2\Pi$ state of MgH, which is case *b*, has a relatively large positive value of q_0, suggesting that this $^2\Pi$ state stands approximately in the relation of pure precession to a $^2\Sigma^+$ state (. . . $3s\sigma^2 4p\sigma$) lying perhaps some 4000 cm^{-1} below it. Data on such a state seem not to be recorded in the literature.

For ZnH, CdH, and HgH, the data are accurate and extensive. As already noted, a relation of pure precession between the normal $^2\Sigma$ state and the $^2\Pi$ state is well fulfilled. The values of p_0 are accurately known experimentally, while those of q_0 are too small, relative to p_0, to be determined experimentally, except roughly in the case of ZnH. For $v=0$, the values of p_0 of $^2\Pi$ and of γ_0 of $^2\Sigma$ are nearly as large as those calculated for pure precession. The agreement with the calculated values is poorest in HgH, presumably because of the very small energy of dissociation of the $^2\Sigma$ state. The quantities p_0 and γ_0 are nearly equal, especially in ZnH and CdH, as they should be for pure precession.

In CdH and HgH we have data on p_0 and γ_0 for several values of v. According to Eqs. (26c) and (27b), p_0 and γ_0 should be proportional to B_v, but actually they decrease faster with v than B_v does (cf. observed and calculated values in Table II). This suggests that the case of pure precession is less and less well fulfilled as v increases. A natural explanation is that, as v increases, the electronic wave-functions become, on the average, more and more like those of two atoms, thus departing more and more (cf. discussion of HgH several paragraphs back) from the united-atom-like forms corresponding to pure precession.

Further evidence in regard to the effect of increased separation of the nuclei in causing departure from pure precession might be sought in a study of the $\Delta\nu_{dc}$'s for large values of J, where the molecule is considerably stretched by rotation. Here we use Eqs. (26), (27). In BeH we found that Eq. (27), with a varying q but *constant* q_0 holds fairly well up to rather large K values (Fig. 2). When plots for p and γ as functions of J and K are made for ZnH, CdH, and HgH, however, it turns out that for large J values not only p and γ but p_0 and γ_0 as well, diminish somewhat with increasing J (cf. Figs. 1, 3). Qualitatively, this can be accounted for by an increasing departure from pure precession as the molecule stretches and becomes more like two atoms.

We have so far not mentioned here the $^2\Sigma$ states which lie a short distance above the $^2\Pi$ states of ZnH, CdH, and HgH. These show large and often irregular $\Delta\nu_{12}$'s, corresponding mainly to large positive γ_0 values which, however, vary with K and v. An inspection of the $U(r)$ curves of these $^2\Sigma$ states[24] snows that they cross those of the $^2\Pi$ states of Table II. The crossing takes place in a region of low vibrational quantum numbers of the $^2\Sigma$ state and moderately high vibrational quantum numbers of the $^2\Pi$ states. The doubling

in the $^2\Sigma$ states can probably be attributed mainly to interaction with these $^2\Pi$ levels.

The large size of the γ_0's is well explained by the smallness of the ν values without assuming that the BL_v's are at all comparable with those corresponding to pure precession. The irregularities of the $\Delta\nu_{12}$'s, together with observed irregularities of the term values T_1 and T_2 themselves, evidently result from the occurrence of unusually large interaction terms resulting from unusually small $\nu(\Pi, \Sigma)$ values for particular v, K values. In other words, we may speak of perturbations. The case is apparently rather similar to that in the red CN bands.[28] It deserves further study, although this is beyond the scope of the present paper.

Hydrides with two or more outer p electrons. In BH and AlH (Table I) there seems to be a fairly good approach to pure precession for the normal ($^1\Sigma^+$) state and the $^1\Pi$ state. In this case, unlike that of HgH, pure precession is equally to be expected for nearly-united-atom ($\cdots 3p\sigma^2, {}^1\Sigma$ and $\cdots 3p\sigma 3p\pi, {}^1\Pi$) and for separated atoms (Al, $\cdots 3p\sigma$, from ^2P, plus H, $1s$, and Al, $\cdots 3p\pi$, from ^2P, plus H, $1s$). In the nearly-united case, however, Eq. (7a) with $l=1$ applies (or if an L exists, Eq. 7 with $L=2$), while Eq. (7) with $l=1$ should apply in the separated case. The calculated q values are larger for the united-atom cases. The observed q values agree better with the separated-atoms case.

In OH there seems again to be a good example of pure precession. Particularly striking are the close agreement of p_0 with γ_0, and of the ratio p_0/q_0 with A/B_v, just as expected for pure precession. Nevertheless, the observed values of p_0, q_0 and γ_0 are decidedly less than the calculated ones. This case is interesting for the fact that A and ν are both negative, giving a positive p_0 and γ_0 but a negative q_0,—observed as well as predicted. The existence of a relation of pure precession between the $^2\Sigma$ and $^2\Pi$ of OH is perhaps assisted by the fact that there can be no other low-energy states; the next lowest states involve the displacement of a $2s\sigma$ electron to a $2p\sigma$ or $2p\pi$ orbit (which should require a large energy change), or of an electron to a 3-quantum orbit.

In HCl^+, whose electron configuration is analogous to that of OH, analogous relations exist for p_0, q_0, and γ_0, although the departures of the observed values from those calculated for pure precession are greater.

In CH we have a low $^2\Pi$ state (probably the normal state, unless perhaps a $^4\Sigma^-$ is lower), which from its electron configuration (cf. Table II) should apparently stand in the relation of pure precession to *three* other states, a $^2\Sigma^-$, a $^2\Delta$, and a $^2\Sigma^+$, all known empirically. The $^2\Delta$ state presumably cannot affect p_0 and q_0, but one might expect the latter to be determined by both the $^2\Sigma^-$ and the $^2\Sigma^+$ states. The $^2\Sigma^+$, since $\nu(\Pi, \Sigma)$ is negative, would according to Eq. (12) tend to make p_0 and q_0 negative, but the $^2\Sigma^-$, because it is Σ^- but at the same time has a negative ν, would tend to make p_0 and q_0 positive. One might expect to calculate p_0 and q_0 each as the sum of two contributions, a positive term from the $^2\Sigma^-$, largely cancelled by a negative one from the $^2\Sigma^+$. The observed values, however, do not agree with the values so calculated. Even

[28] Cf. J. E. Rosenthal and F. A. Jenkins, Proc. Nat. Acad. Sci. **15**, 381 (1929).

greater discrepancies are encountered when one compares observed values of γ_0 for the $^2\Sigma^-$ and $^2\Sigma^+$ states with those calculated from Eq. (19). [For the $^2\Sigma^-$ state, $\gamma = -p = +2AB_v \cdots$]. But these results should not cause surprise, since as we have already seen (cf. discussion before and after Eq. 7a), the usual equations are not applicable to electron configurations like those present here in CH.

The relations in the $^2\Pi$ state of SiH are probably analogous to those in CH, but the $^2\Sigma$ levels are not yet known experimentally.

Molecules with a p electron belonging to one atom. In the case b' II states of $He_2(^3\Pi)$, Li_2 and $Na_2(^1\Pi)$, we find the relation of pure precession well fulfilled toward certain neighboring states. The existence of this relation would not be expected from the electron configurations given in Table I. Although in each case the Σ differs from the Π state only in having a $p\sigma$ electron instead of a $p\pi$ electron, the principal quantum number n is not the same for the two, but is in each case one unit higher for the $p\sigma$. There can be hardly any doubt that this is true. In He_2, for example, we have already one $2p\sigma$ electron (a $2p\sigma 1s$, i.e. a promoted $1s$, electron); for the $^3\Sigma$ state here in question the other $p\sigma$ electron *must* according to the Pauli principle have a different value of n.

Apparently, however, this difference in n does not interfere seriously with the existence of "pure precession." But this is after all not difficult to understand. In the case of He_2, for example, the energy of the $\cdots 3p\sigma\ ^3\Sigma$ state is only a little above that of the $\cdots 2p\pi\ ^3\Pi$ state, and we believe that for $r \to \infty$ the electron in question becomes in both cases a $2p$ electron of one of the atoms, i.e., we have $3p\sigma 2p$ and $2p\pi 2p$. The small energy difference (much less than that between a 2- and a 3-quantum atomic orbit) indicates that the part of the wave-function corresponding to the $3p\sigma$ is really not much different from that which $2p\sigma$ would give in a helium atom. In other words, the electron orbits in the He_2 molecule are not very much different from those in the two atoms (He, $1s^2$+He, $1s2p$, ^3P) before union. Hence we get a strong interaction between the two states having $\cdots 3p\sigma 2p$ and $\cdots 2p\pi 2p$, agreeing well with the case of pure precession. Analogous relations exist in Li_2 and Na_2, although in these cases the $\cdots (n+1)p\sigma np$ is below the $\cdots np\pi np$, a fact which is faithfully reflected in the sign of q_0, and which is also signalized (as is reasonable) by a very close agreement of the q_0 values with those calculated for pure precession.

In the examples just discussed we apparently have the Λ-type doublet separations agreeing with those calculated for pure precession *because the wave-function of the molecule approximates that of two separate atoms*, whereas if the wave-functions were nearly as in the united-atom, we could not expect such agreement. This relation is the exact opposite of that found in molecules such as ZnH, CdH, HgH, where we saw that wave-functions resembling those of the separate atoms could not give pure precession, while wave-functions like those of the united atom do give it.

These results give strong support to the idea that among molecules there exist, for the outer electrons, examples of all stages of transformation of the electronic wave-functions from those of two separate atoms nearly to those

of the united-atom. Examples of the first stage are found in loosely-bound molecules; an intermediate stage may be expected in stable states of firmly bound molecules like N_2; and the last stage is found in firmly-bound molecules with very unequal nuclei, notably among the hydrides.

Interpretation of the electron states of CaH. We have left the CaH molecule until the last, since it shows several interesting features. Beginning with the normal $^2\Sigma$ state, we notice that the observed γ_0 is only about one fourth that calculated on the assumption of a relation of pure precession between this state and the $^2\Pi$ state, whereas in the similar molecules ZnH, CdH, HgH, the observed γ_0 is not far below the calculated.

Furthermore, the observed p_0 and q_0 of the $^2\Pi$ state are negative, showing that this state interacts with a $^2\Sigma^+$ state *above* it. [The possible alternative of interaction with a $^2\Sigma^-$ state below it is too improbable from the standpoint of electron configurations.] Further, p_0 agrees well in value and has the same sign as γ_0 of a $^2\Sigma$ state which lies only 1320 cm^{-1} above the $^2\Pi$. Finally, the observed values of p_0, q_0, and γ_0 from the $^2\Pi$ and the upper $^2\Sigma$ (evidently $^2\Sigma^+$) states agree well with those calculated assuming a relation of pure precession between them with $l=1$ (cf. Table II). In view of the smallness of $|\nu(\Pi, \Sigma)|$, the agreement is surprisingly good (cf. the case of H_2 in Table I). The fact that B_v is practically the same for the $^2\Pi$ and $^2\Sigma^+$ states is no doubt important here, since it tends to cause $v=0$ of $^2\Pi$ to interact almost exclusively with $v=0$ of the $^2\Sigma^+$, and $v=0$ of $^2\Sigma^+$ with $v=0$ of $^2\Pi$.

In a previous paper,[23] it was suggested that the normal $^2\Sigma$ state of CaH is $\cdots 4p\sigma$, as in ZnH, and that the $^2\Pi$ and upper $^2\Sigma$ states are $\cdots 4p\pi$ and $\cdots 3d\sigma$. But in view of the relations stated in the preceding paragraphs, it seems evident that the upper $^2\Sigma$ is $\cdots 4p\sigma$, in which case it seems reasonable to assume that the normal $^2\Sigma$ is $\cdots 3d\sigma$. In the Ca atom, the $3d$ electron is almost as firmly bound as the $4p$, and apparently in CaH, the $3d\sigma$ is much *more* firmly bound than $4p\sigma$. This is presumably because $\lambda=0$ in $3d\sigma$ makes the $3d$ orbit penetrating. Even so, it is surprising that $\cdots 4p\sigma$ is above $\cdots 4p\pi$, but this may perhaps be attributed partly to a quantum mechanical repulsion between the states with $\cdots 3d\sigma$ and $\cdots 4p\sigma$. The fairly large γ_0 of the $\cdots 3d\sigma$ state may be attributable to the existence of a pure precession relation with a $\cdots 3d\pi$ state which probably lies above the $\cdots 4p\pi$. A quantum-mechanical repulsion between these two II states may help to account for the fact that the $\cdots 4p\pi$ lies below the $\cdots 4p\sigma$. Possibly, however, the $\cdots 3d\pi$ lies below the $\cdots 4p\pi$ and is involved in some new infrared bands.[29]

As for dissociation products, there seems to be no reason to doubt that

[29] B. Grundström and E. Hulthén (Nature **125,** 634, 1930) give data on the *C* system of bands, whose final level is the normal $^2\Sigma$ state of CaH. The observed hand-heads can be represented by the equation $\nu=28{,}290+(1423\ v'-24.7v'^2)-(1273\ v''-22.1\ v''^2$.) The four observed vibrational levels of the lower state can be represented accurately by a linear function of v. Using a linear extrapolation as in the Birge and Sponer method, the energy of dissociation is 2.28 volts. Making a liberal allowance for actual departure of $G(v'')$ from linearity, 1.5 volts appears to be a reasonable value. Further data on CaH are given in a new paper by B. Grundström, Zeits. f. Physik, **33,** 235 (1931).

the $\cdots 4s\sigma^2 4p\pi$ and $\cdots 4s\sigma^2 4p\sigma$ both dissociate to give a normal H atom and a $\cdots 4s4p$, ^3P excited Ca atom, and that the $\cdots 4s\sigma^2 3d\sigma$ normal state gives a normal H and a normal Ca atom ($\cdots 4s^2$, ^1S). Since the interval $^2\Sigma$ (normal) to $^2\Pi$ is 1.78 volts, and the interval $^2\Sigma$(normal) to $^2\Sigma(\cdots 4p\sigma)$ is 1.94 volts, while the interval $4s^2$, ^1S to $4s4p$, ^3P in the Ca atom is 1.87 volts, it is evident that the energy of dissociation of the $^2\Pi$ state is only 0.09 volts more, that of the upper $^2\Sigma$ state 0.07 volts less, than that of the normal $^2\Sigma$. In other words, the energy of dissociation is nearly equal in these three cases. Its value for the normal state may be roughly estimated[30] as about 1.5 volts.

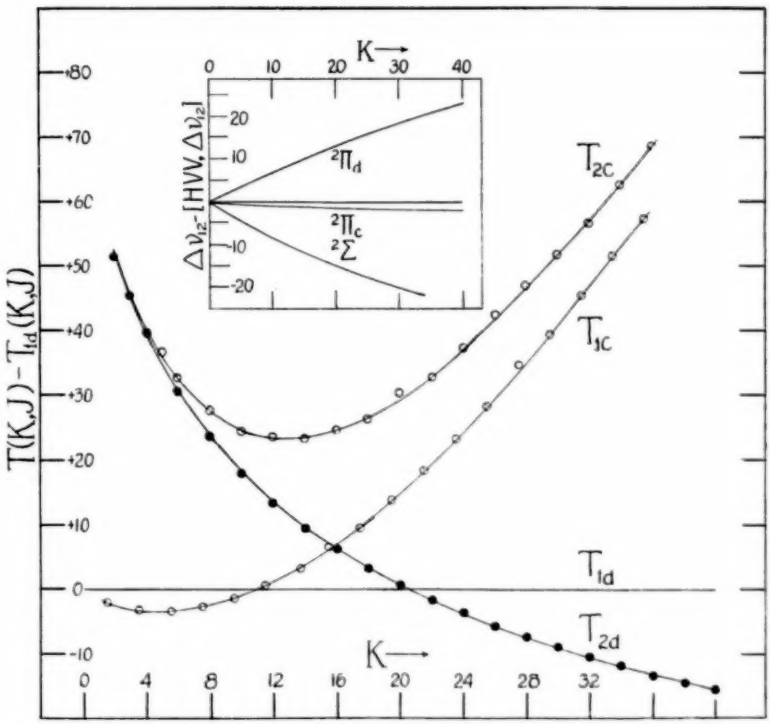

Fig. 4. Main figure: relative term values for the four sets of rotational levels T_{2c}, T_{1c}, T_{1d}, T_{2d} of the $^2\Pi$ state of CaH. All the term values are shown *relative* to the T_{1d} levels, $T_{1d}(J)$ being arbitrarily taken as zero. Inset: Spin doublet widths $\Delta\nu_{12}(K)$ for upper $^2\Sigma$ state of CaH (cf. also Fig. 3) and corrected spin doublet widths $\Delta\nu_{12}(K) - [\mathrm{HVV}, \Delta\nu_{12}(K)]$ for the c and d sets of $^2\Pi$ levels. HVV, $\Delta\nu_{12}(K)$ means the doublet width which would be calculated according to Hill and Van Vleck's equation, taking only spin uncoupling into account. The *deviations* from this, $\Delta\nu_{12} - [\mathrm{HVV}, \Delta\nu_{12}]$ represent secondary effects of l-uncoupling (cf. Eqs. 18, 19, 20c, 20d).

The $\cdots 4p\sigma$, $^2\Sigma$ state of CaH shows a peculiar curve for $\Delta\nu_{12}(K)$. It begins with nearly a straight line of slope -0.945, then for higher K values breaks over to another nearly straight line of slope -0.543 (cf. Fig. 3). In ordinary cases one finds a single straight line, $\Delta\nu_{12}(K) = \gamma(K + \frac{1}{2})$, up to high K values where γ begins to vary appreciably with K (cf. normal $^2\Sigma$ states of CdH and HgH in Fig. 3). In abnormal cases like the upper $^2\Sigma$ states of CdH and HgH, the irregular variations of $\Delta\nu_{12}$ with K are classified under the heading of per-

turbations, i.e. are ascribed to the influence of various individual levels whose $\nu(\Pi, \Sigma)$ happens to be very small. Very likely a similar explanation applies here, although perhaps a tendency toward case c for low K values might be held responsible.

The relative spacings of the four energy levels T_{1c}, T_{2c}, T_{1d}, T_{2d} as functions of K for the $^2\Pi$ state are interesting. They are shown in Fig. 4, which represents a revision of a somewhat similar figure by Watson, who has also given an interpretation of the uncoupling phenomena in this and the related $^2\Sigma$ state along the same general lines as here.[26,19] The positions of all the above four levels should be given by Eq. (9). This has not been tested directly here, but it has been shown that the doublet separations $\Delta\nu_{1dc}$ and $\Delta\nu_{2dc}$ are in accordance with Eq. (9),—cf. Eq. (14) and Fig. 2,—and that the doublet separations $\Delta\nu_{12d}(K)$ and $\Delta\nu_{12c}(K)$, also $\Delta\nu_{12}(K)$ of the $^2\Sigma$ state, show predicted behavior for high K values (cf. Fig. 4 inset, Eqs. 20c, 20d, and discussion following these equations).

The size of $\Delta\nu_{12}(K)$ in the $^2\Sigma$ state, and of $\Delta\nu_{12}(\text{corr.}) = \Delta\nu_{12}(K) - [\text{HVV}, \Delta\nu_{12}(K)]$ in the $^2\Pi$ states, permits ρ to be estimated somewhat directly, since we may expect these $\Delta\nu_{12}$ quantities to be equal to $A\rho$, where A is the known coupling constant obtained from the separation of the $^2\Pi_{\frac{1}{2}}$ and $^2\Pi_{1\frac{1}{2}}$ levels at low J values. From the observed values of $\Delta\nu_{12}$ or $\Delta\nu_{12}(\text{corr.})$ at $K = 33$, namely -22 for the $^2\Sigma$ state and $+20$ for the $^2\Pi^d$ state, together with the value $A = 80$, we conclude that the component of l along the direction of K is about 0.25. It seems rather remarkable, for such large uncoupling, that the Van Vleck formulas agree as well as they do with the experimental data. A careful re-examination of data on the Zeeman effect[19] of the $^2\Pi \rightarrow {}^2\Sigma$ and $^2\Sigma \rightarrow {}^2\Sigma$ bands of CaH in relation to the above conclusions might be of interest.

Molecules N_2^+, BO, NO, O_2^+. Data on these and similar molecules are not very abundant. The existing data give no clear indication of the existence of relations of pure precession between known states of these molecules. The absence of such relations is, however, in agreement with the probable electron configurations.

The opposite signs of p_0 and q_0 in the $^2\Pi$ state of BO are in agreement with the requirements of the theory for an inverted $^2\Pi$. The fact that p_0 is positive indicates, since A is negative, that the interacting Σ state or states lie above the $^2\Pi$, so as to make $\nu(\Pi, \Sigma)$ negative. The observed values of p_0 and q_0 indicate that if there is a relation of pure precession, the interacting $^2\Sigma$ state is a $^2\Sigma^+$ state lying somewhat higher than the upper of the two known Σ states. This state, which is unknown experimentally, should presumably have the electron configuration $\cdots 3p\sigma^2 2p\pi^3 3d\sigma 3d\pi$.

The fact that p_0 and q_0 have the same sign in the case of the $^2\Pi$ normal state of NO is in agreement with what the theory requires for a regular $^2\Pi$. The fact that p_0 and q_0 are positive[30] shows, since A is positive and $\nu(\Pi, \Sigma)$ is

[30] The information that p_0 and q_0 are positive for the normal state of NO depends on the assumption that the $^2\Sigma$ state given in Table II (upper level of the γ bands) is $^2\Sigma^+$. This is very probable from a consideration of electron configurations. If, however, it were $^2\Sigma^-$, we should have to conclude that p_0 and q_0 are negative; and from this, that the $^2\Pi$ state interacts princi-

necessarily negative, that the $^2\Pi$ state interacts principally with a $^2\Sigma^-$ state, and not with the well known $^2\Sigma^+$ state listed in Table II (upper state of the γ bands). A $^2\Sigma^-$ state which should probably lie not very far above the $^2\Sigma^+$ state just mentioned, and whose electron configuration would correspond to a relation of pure precession with the normal $^2\Pi$ state, would be one with the configuration $\cdots 3d\sigma 2p\pi^4 3d\pi^2$. Such a state would probably have a large r_e like the upper $^2\Pi$ state, and so probably cannot be identified with the upper level of either the δ or ϵ bands of NO, one at least of which is $^2\Sigma$.

In the case of the O_2^+ bands it has been possible to determine the signs as well as the magnitudes of p_0 and q_0 if the very probable assumption is made that the normal state is $\cdots 3d\pi$, $^2\Pi_g$ as given in the table. Since in O_2 only levels symmetrical in the nuclei are present,[4] only positive rotational levels can be present in an even (g) state.[4] This requirement, in connection with the experimental data, suffices to determine the sign of $\Delta\nu_{dc}$. The result, that p_0 and q_0 are positive in the normal state of O_2^+, agrees with that observed[30] in NO, and may be taken as evidence in support of the even (g) character of normal O_2^+ and of the assigned electron configuration $\cdots 3d\pi$ for the normal states of O_2^+ and NO. In the case of the upper state of O_2^+, p_0 and q_0 are too small to determine. By analogy, it is very likely that p_0 and q_0 are also very small in the upper $^2\Pi$ state of NO. These coefficients cannot be directly determined for the upper $^2\Pi$ of NO from the available data, except that it can be said that, if p_0 of the lower state is $+0.015$, p_0 of the upper $^2\Pi$ is either $+0.03$ or ± 0.00. The analogy to O_2^+ now makes the latter value the more probable.

In conclusion, we take pleasure in acknowledging our indebtedness to Professor J. H. Van Vleck for helpful discussions and correspondence.

---

pally with $^2\Sigma^+$ states above it. Thus whether we assume the upper level of the γ bands to be $^2\Sigma^+$ or $^2\Sigma^-$, we must conclude that it does not stand in a relation of pure precession to the $^2\Pi$ state. This conclusion in turn gives strong support to the original assumption that the $^2\Sigma$ state in question is not $^2\Sigma^-$, since a low $^2\Sigma^-$ could hardly be other than the one with the configuration . . . $3d\sigma 2p\pi^4 3d\pi^2$, which *should* stand in the relation of pure precession to the normal $^2\Pi$.

THE INVERSE-CUBE CENTRAL FORCE FIELD IN QUANTUM MECHANICS*

By George. H. Shortley
Palmer Physical Laboratory, Princeton University

(Received May 22, 1931)

Abstract

The problem of the motion of a particle in an inverse-cube central force field is fully treated by quantum mechanics and the results compared with the classical theory. Taking the effective radial potential energy as S/r^2, although the solutions for negative energy for $0 \geqq S \geqq -h^2/32\pi^2\mu$ satisfy the usual boundary conditions, they can not be admitted because the Hamiltonian is not Hermitian in these solutions. This corresponds to taking $(l+\frac{1}{2})^2$ in place of $l(l+1)$ as the analogue of the square of the classical angular momentum. If we do this, we get a complete analogy between the classical and quantum mechanically allowed solutions, with no quantization. The solutions involve Bessel functions of both real and imaginary orders with both real and imaginary arguments.

1. CLASSICALLY, considerable interest has attached to the problem of the motion of a particle in a central-force field falling off inversely as the cube of the distance. This force law occupies a somewhat special position mathematically, and is one of the three for which the forms of the various possible orbits may be expressed in terms of circular functions. It was studied in particular by Roger Cotes, and the orbits are sometimes known as Cotes' spirals.[1] Quantum mechanically, this problem is of particular interest because of the complete lack of quantization, the variety of Bessel functions to which the solution leads, the peculiar rôle played by the angular momentum value $(l+\frac{1}{2})^2$, and the necessity for careful consideration of the conditions which an allowed solution must satisfy.

Let a particle of mass μ be acted on by a radial force of $2S'/r^3$, so that the potential energy is

$$V = \frac{S'}{r^2},$$

where S' is negative for an attractive force, positive for a repulsive.

We have the Schrödinger equation

$$\Delta\psi + \frac{8\pi^2\mu}{h^2}\left[W - \frac{S'}{r^2}\right]\psi = 0,$$

which, on being separated in polar coördinates, yields, as in any central-force problem

* This paper was presented at the New York meeting of the American Physical Society, February 27, 1931.

[1] Roger Cotes, Harmonia Mensurarum, Cambridge, 1722, pp. 31–35, 98. For a modern discussion of this problem see, for example, Lamb's Dynamics, p. 266 ff.

$$\psi = \left(\frac{(2l+1)(l-|m|)!}{4\pi(l+|m|)!}\right)^{1/2} \frac{R(r)}{r} \sin^{|m|}(\theta) P_l^{|m|}(\cos\theta) e^{im\phi},$$

where $mh/2\pi$ specifies the z component of angular momentum; $l(l+1)h^2/4\pi^2$ the square of the total angular momentum, and $R(r)$ satisfies the equation

$$R'' + \frac{8\pi^2\mu}{h^2}\left[W - \frac{S'}{r^2} - \frac{h^2}{8\pi^2\mu}\frac{l(l+1)}{r^2}\right]R = 0.$$

This is the equation for one-dimensional motion in the r-coördinate under a potential energy $V_r = S/r^2$, where the effective radial force constant

$$S = S' + \frac{1}{2\mu} l(l+1) \frac{h^2}{4\pi^2}. \tag{1}$$

We then have the radial equation

$$R'' + k[W - S/r^2]R = 0, \qquad \text{where } k = 8\pi^2\mu/h^2. \tag{2}$$

In this the change of variable

$$\rho = (kW)^{1/2} r \tag{3}$$

and the substitution

$$R(r) = |\rho|^{1/2} Z_\nu(\rho) \tag{4}$$

give for $Z_\nu(\rho)$ the standard form of Bessel's equation

$$\rho^2 Z_\nu''(\rho) + \rho Z_\nu'(\rho) + (\rho^2 - \nu^2) Z_\nu(\rho) = 0, \tag{5}$$

where the order ν is related to S by

$$\nu = (\tfrac{1}{4} + kS)^{1/2}. \tag{6}$$

The boundary conditions which must be satisfied[2] are that at the origin ψ shall not become infinite so rapidly as $1/r$, and that it shall remain at infinity. This requires $R(r)$ to be zero at the origin and allows it to become infinite at a rate r at infinity.

We see that since the energy W occurs only in the argument of the Bessel function we have no quantization, but only continuous spectra of energy levels.

The quantum-mechanical probability that the particle be between r and $r+dr$ is proportional to $|R(r)|^2 dr$, which may be compared with the classical radial probabilities obtained by writing

$$W = \frac{S'}{r^2} + \frac{1}{2}\mu\dot{r}^2 + \frac{M^2}{2\mu r^2} = \frac{S}{r^2} + \frac{1}{2}\mu\dot{r}^2, \tag{7}$$

where $S_c = S' + M^2/2\mu$, and the probabilities of the different values of r are proportional to

$$\frac{1}{\dot{r}} = \frac{dt}{dr} = r\left(\frac{\mu}{2(r^2W - S_c)}\right)^{1/2}. \tag{8}$$

[2] See Dirac, Quantum Mechanics, pp. 143–4.

§2. It is seen that the Bessel function of the radial factor (4) has an imaginary argument for $W<0$, and an imaginary index for $S<-1/4k$. In this case classically the particle spirals in from a maximum radius $(S_c/W)^{1/2}$ to the origin, along the path

$$\frac{1}{r} = \left(\frac{W}{S_c}\right)^{1/2} \cosh\left(\frac{(-2\mu S_c)^{1/2}}{M}\,\theta\right),$$

increasing its radial velocity to infinity at the origin, as may be readily seen from an energy diagram. If we write $\rho = i\kappa = (-kW)^{1/2}r$, we get as the normalized classical probability that ρ be between ρ and $\rho+d\rho$

$$\frac{1}{(-kS_c)^{1/2}}\,\frac{\rho}{(-kS_c-\rho^2)^{1/2}}\,d\rho. \tag{9}$$

Quantum mechanically we have, if $\nu = in$,

$$R(r) = \rho^{1/2}Z_{in}(i\rho). \tag{10}$$

Very little work has been done on such a Bessel function, but we can determine its characteristics in a manner indicated by Bôcher,[3] using a form of Bessel's equation given by Riemann-Hattendorf.[4] If we write $t=\log|\kappa|$, $Z_\nu(\kappa)$ satisfies the equation

$$\frac{d^2Z}{dt^2} + (\kappa^2-\nu^2)Z = 0, \tag{11}$$

and so $Z_{in}(i\rho)$ satisfies

$$\frac{d^2Z}{dt^2} - (\rho^2+n^2)Z = 0. \tag{12}$$

From this we see that for $\rho<n$, d^2Z/dt^2 has always the opposite sign from Z, so that the solution oscillates from $t=-\infty$ $(\rho=0)$ to $\rho=n$. For $\rho>n$, the second derivative has the same sign as ρ and by proper choice of the phase near $t=-\infty$, we can find one solution which falls exponentially to zero as $\rho\to\infty$. Since $\rho=n$ is the classical limit of motion for $S_c=S+1/4k$, this is just as expected. For $\rho\to 0$, $t\to-\infty$, the equation becomes that for $\sin(nt-\text{const.})$ $=\sin(n\log\rho-\text{const.})$. This gives an infinity of oscillations near the origin of constant amplitude at the start; making the average probability start as ρ, as does the classical probability. Further, the de Broglie wave-length of $\sin(n\log\rho)$ for small ρ is $2\pi\rho/n$, or, in ordinary units, $2\pi r/n$. This is seen to correspond exactly with the classical $h/\mu\dot{r} = 2\pi r/(-kS_c)^{1/2}$ for $S_c=S+1/4k$. Although we cannot ascertain the quantum mechanical probabilities in more detail than this, it is quite certain that the average of the normalized probability curve will follow the classical probability curve (9) closely almost to the classical limit where the classical probability becomes infinite and the

[3] Bôcher, Annals of Math. **6**, 137 (1891–2).

[4] Riemann-Hattendorf, Partielle Differentialgleichung, Braunschweig, 1876, p. 266 ff.

quantum mechanical curve starts falling exponentially to zero. This is probably the first instance which has been pointed out of the occurrence of a continuity of energy levels with a closed orbit and quadratically integrable ψ function.

For positive energies in this case ($S<-1/4k$), classically the particle spirals in from infinity to the origin, with its radial velocity asymptotically constant for large distances, but increasing to infinity at the origin, along the path

$$\frac{1}{r} = \left(-\frac{W}{S_c}\right)^{1/2} \sinh\left(\frac{(-2\mu S_c)^{1/2}}{M}\,\theta\right).$$

The clasical probabilities of being between R and $R+dR$ are proportional to

$$\frac{R}{(R^2 - kS_c)^{1/2}}\,dR. \tag{13}$$

Quantum mechanically, our solution takes the form

$$R(r) = R^{1/2}Z_{in}(R) \tag{14}$$

with R real. This Bessel function $Z_{in}(R)$ satisfies

$$\frac{d^2Z}{dt^2} + (R^2 + n^2)Z = 0, \tag{15}$$

from which we see that d^2Z/dt^2 and Z always have opposite signs, so that the solution oscillates all the way from $t=-\infty$ to $+\infty$. Near $R=0$ we get exactly the same behavior as for solution (10) above, but for $R \gg n$, Eq. (15) becomes the equation for $R^{-1/2}$ sin (R+const.), whereas Eq. (12) became that for $\rho^{-1/2}e^{-\rho}$. This makes the radial factor (14) approach sin (R+const.) for large R, giving a constant average probability and a proper de Broglie wave-length exactly to correspond with the constant classical velocity. Here we should expect that in the whole range from 0 to ∞, the average of $R^2(r)$ will follow closely the classical probability curve (13) and that $R(r)$ will have approximately the proper de Broglie wave length to correspond to the classical velocity, just as we have seen these conditions to hold at both ends of the range.

The case $S<-1/4k$, $W=0$ demands special consideration. Here classically we get the equiangular spiral

$$\frac{1}{r} = \exp\left\{\frac{(-2\mu S_c)^{1/2}}{M}\,\theta\right\},$$

with a radial probability proportional to r(since $\dot{r} \propto 1/r$). Quantum mechanically Eq. (2) becomes $r^2R'' - kSR = 0$, giving the solutions

$$R(r) = r^{1/2} \sin(n \log r + \text{const.}), \tag{16}$$

whose square increases as r, agreeing with the classical probability, and

whose de Broglie wave-length as calculated from the slope of the n log r curve is $2\pi r/n$, agreeing exactly with the classical $h/\mu\dot{r}$ for $S_c = S + 1/4k$.

So for all W, with $S < -1/4k$, we get solutions oscillating infinitely rapidly near the origin to correspond to the classical infinite velocity, and good probability and wave-length agreements with the classical theory throughout if we compare S with $S_c - 1/4k$. We further can obtain from these solutions a good approximation to the amplitude and rate of oscillation of a Bessel function of imaginary index throughout its range.

§3. When we consider the range of S between 0 and $-1/4k$ for negative W, we have the well-known Bessel function of real order ν between $1/2$ and 0, and imaginary argument. The particular solution[5] $K_\nu(\rho)$ falling exponentially to zero at infinity starts at the origin as $\rho^{-\nu}$ (as log ρ for $\nu = 0$), and so because of the factor $\rho^{1/2}$,

$$R(r) = \rho^{1/2} K_\nu(\rho) \tag{17}$$

is zero at the origin and formally satisfies all the boundary conditions. However, these solutions remain everywhere positive, and so neither they nor the eigendifferentials $\int_W^{W+\Delta W} R_W(r)dW$ are orthogonal for different W. For this reason their physical significance as stationary states is questionable, although from considerations purely of the Schrödinger equation the probability of the particle's being at each point is definitely specified for every W. Because of this non-orthogonality the matrix of H in these solutions is neither diagonal nor Hermitian.

The theory of the eigenvalues of Hermitian operators has been completely investigated by von Neumann.[6] Let H be a linear operator which can be applied to a number of functions

$$\psi_1, \psi_2, \psi_3 \cdots \tag{18}$$

and their linear combinations in such a way that the Hermitian condition

$$\int \bar{\psi}_1 H\psi_2 = \int \overline{\bar{\psi}_2 H\psi_1} = \int \overline{H\psi}_1 \psi_2 \tag{19}$$

is satisfied. In general, the field of operation of H can be extended to other functions

$$\psi_1', \psi_2', \psi_3' \cdots \tag{20}$$

and their linear combinations, so that (19) holds for the total set (18), (20). If the field of operation of H is extended in this way as far as possible, one obtains a set of functions which is everywhere dense, and H has[7] a spectrum whose eigenfunctions and eigendifferentials are *included* in (18), (20), and which form a *complete* set of functions. These eigenfunctions or eigendifferentials are therefore orthogonal in the usual way, so the usual statistical interpretations may be made.

[5] See Watson, Theory of Bessel Functions, p. 78.

[6] J. v. Neumann, Math. Ann. **102**, 49 (1929).

[7] von Neumann finds one exception.

Now it is clear in our case that the field of operation of H can be extended at most to *one* of the functions (17), because (19) does not hold for *two* of them or their eigendifferentials. Hence the rest of our solutions must form a complete set, and solutions (17) must be linear combinations of our other solutions, and therefore not stationary states of energy.

This means that we must be able to express the solutions

$$r^{1/2}K_\nu(\rho) = r^{1/2}K_\nu([-kW_1]^{1/2}r), \qquad 0 \leqq \nu < \tfrac{1}{2}$$

for negative W_1 as combinations of the eigendifferentials

$$\int_W^{W+\Delta W} r^{1/2}J_\nu([kW]^{1/2}r)dW$$

arising from the solutions $r^{1/2}J_\nu(\kappa)$ which hold for positive W (see §4). This expansion is known[8]:

$$r^{1/2}K_\nu([-kW_1]^{1/2}r) = \int_0^\infty \frac{1}{2(W-W_1)}\left(-\frac{W}{W_1}\right)^{\nu/2} \cdot r^{1/2}J_\nu([kW]^{1/2}r)dW \quad (21)$$

and so bears out the theory completely.[9]

This situation is related in an interesting fashion to the question of the quantum mechanical analogue of resultant angular momentum. The value $S=0$ corresponds, from Eq. (1), to the force constant

$$S' = -\frac{1}{2\mu}l(l+1)\frac{h^2}{4\pi^2}, \qquad (S=0) \quad (22)$$

[8] See Watson, Reference 5, p. 425.

[9] The algebra of the general theory contains inherently the requirement that all operators be Hermitian, and so the general theory eliminates these eigenvalues in the following way: Making use of the commutator $(1/r)p_r - p_r(1/r) = h/2\pi i r^2$, we may write the Hamiltonian in the form

$$H = \bar{A}A = \left(\frac{p_r}{(2\mu)^{1/2}} + \frac{i\alpha}{r}\right)\left(\frac{p_r}{(2\mu)^{1/2}} - \frac{i\alpha}{r}\right) = \frac{1}{2\mu}p_r^2 + \frac{S}{r^2},$$

where α is real and $S=\alpha^2+\alpha/k^{1/2}$. This form for the Hamiltonian is possible only for $S \geqq -1/4k$, since the expression $\alpha^2+\alpha/k^{1/2}$ has an absolute minimum at $-1/4k$ for α real. Now since $H\psi(W) = W\psi(W)$, we have

$$\int\bar{\psi}(W)H\psi(W) = W\int\bar{\psi}\psi = \int\bar{\psi}\bar{A}A\psi = \int\overline{A\psi}A\psi > 0$$

since the integral of a function times its complex conjugate is necessarily positive. Hence W is necessarily positive whenever H can be written in this form, that is, for $S \geqq -1/4k$. Thus we see that in terms of the general theory the usual boundary conditions on Schrödinger's ψ are necessary but not sufficient, and must be supplemented by an orthogonality requirement.

Langer and Rosen, Phys. Rev. **37,** 658 (1931), conclude that the fundamental requirement for an allowed solution is the equality of the "Hamiltonian Integral" $J = \int[(h^2/4\pi^2)T(q, \partial\psi/\partial q) + V\psi^2]d\tau$ and the energy. This is equivalent to the introduction of the Hermitian requirement and accomplishes the elimination of this band of energies since J here is divergent at the origin.

The solution of the central field problem for non-integral l, which led Jaffé (Zeits. f. Physik **66,** 770 (1931)) to conclude that ψ must be finite and continuous, may be eliminated on the same grounds of non-orthogonality as our solutions above. Requiring $\psi(=R(r)/r)$ to be finite at the origin would eliminate almost all of our solutions!

while the value $S=-1/4k$ corresponds to

$$S' = -\frac{1}{2\mu}(l+\tfrac{1}{2})^2\frac{h^2}{4\pi^2}. \qquad (S = -1/4k) \qquad (23)$$

Now classically, the force constant

$$S' = -\frac{1}{2\mu}M^2 \qquad (S_c = 0)$$

divides those values of S_c for which all values of W are allowed from those for which only positive values of W are allowed, and quantum mechanically, this same rôle is played by (23), so in the sense of comparing the allowed energy ranges with classical theory, $(l+\frac{1}{2})^2h^2/4\pi^2$ is to be taken as the

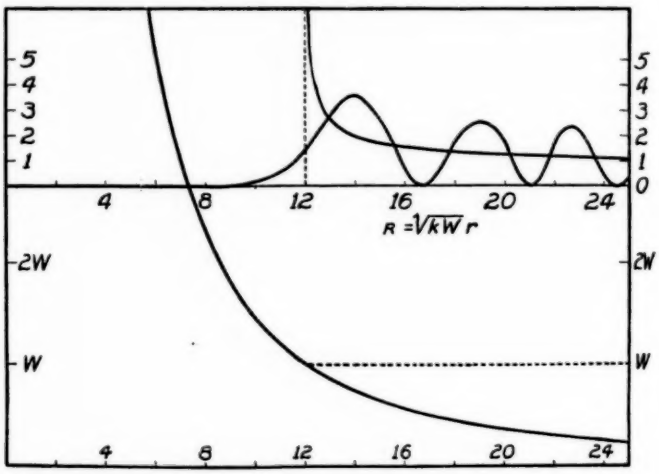

Fig. 1. Probability curves for $\nu=12$. Lower curve is the radial potential energy $S/r^2\approx 144W/R^2$. Upper curves compare the quantum mechanical probability $\pi RJ^2_{12}(R)$ with the classical $R/(R^2-144)^{1/2}$.

analogue of the square of the angular momentum. So we should compare $S+1/4k$ with the classical S_c, in which case our correspondence is complete in every respect.

§4. For positive S_c and W, classically the particle moves from $R=(kS)^{1/2}$ to ∞, rapidly approaching a constant velocity, along the path

$$\frac{1}{r} = \left(\frac{W}{S_c}\right)^{1/2}\cos\left(\frac{(2\mu S_c)^{1/2}}{M}\,\theta\right),$$

with radial probabilities given by Eq. (13), which has an average value one.

Quantum-mechanically for $S\geqq -1/4k$, $W>0$, we get

$$R(r) = \pi^{1/2}R^{1/2}J_\nu(R), \qquad 0 \leqq \nu \qquad (24)$$

with the ordinary Bessel functions whose properties are well known.[10] This solution remains very small almost until $\kappa = \nu$, the classical limit for $S_c = S + 1/4k$, after which it oscillates to infinity, approaching $2^{1/2} \sin(\kappa + \text{const.})$, with the proper de Broglie wave-length and average probability one. The average of this probability curve follows the classical curve very closely as expected. One point of interest is that the case $S_c = 0$, giving a constant radial velocity, would seem to correspond better to $S = 0$, which gives $R(r) = \pi^{1/2}\kappa^{1/2}J_{1/2}(\kappa) = 2^{1/2} \sin \kappa$, than to $S = -1/4k$, which involves $J_0(\kappa)$; however, for these small values of S one cannot expect too good a comparison. Fig. 1 shows the good agreement between the probability curves for $\nu = 12$, and it is just such an agreement, for large $|S|$, that we would expect with the solutions involving the imaginary Bessel functions previously discussed.

As in the classical case, these results are only as yet of academic interest; it would be pleasing if such pretty mathematical results were to find an application to atomic physics. I wish to thank Professors Condon, Wigner, and Robertson of Princeton University for helpful discussions concerning this problem.

[10] For the limited range $0 \leqq \nu < \frac{1}{2}$, the solution with the Bessel function of the second kind, $Y_\nu(\kappa)$, also formally satisfies the boundary conditions, since it starts as $\kappa^{-\nu}$. We might expect this solution to be eliminated just as was the quadratically-integrable solution for negative energies which started in the same way in the same band of S. Orthogonality considerations are rather difficult, but the reasonable requirement that the Hamiltonian integral J converge in any finite range—in particular in a range about a singularity or infinity of the potential function—would eliminate these solutions, since for the solution $\kappa^{1/2}Y_\nu(\kappa)$, J does not converge at the origin, whereas for $\kappa^{1/2}J_\nu(\kappa)$ it does. See footnote (9).

THE SPECTRUM OF DOUBLY IONIZED CARBON, C_{III}

By I. S. Bowen
California Institute of Technology

(Received May 16, 1931)

Abstract

With new experimental data 54 lines of C_{III} have been classified. A large number of these lines involve terms in which both valence electrons are excited. The ionization potential deduced from this classification is 47.7 volts. The classification of a few additional C_{II} lines is also given. These analyses fix the relative position of the singlets and triplets in C_{III} and the doublets and quartets in C_{II}.

THE spectrum of carbon was obtained with a vacuum spectrograph using as a source a vacuum spark between graphite electrodes. The electrodes were cut from graphite tubes that had been especially purified by the Acheson Graphite Company for Dr. King of the Mount Wilson Observatory. The particular sample used had been glowed out at a high temperature in the vacuum furnace by Dr. King. This treatment, Dr. King reports, gives material that is spectroscopically pure. The lines arising from the various stages of ionization were differentiated by varying the capacity and self induction in the spark circuit.

Table I. *Triplet lines in* C_{III}.

Int.	λ Vac.	ν	Series designation	Int.	λ Vac.	ν	Series designation
0	319.24	313244	$2s2p^3P-2s7d^3D$	0	818.18	122222	$(2p)^2\,{}^3P_2-2s3p^3P_2$
1	327.12	305698	$2s2p^3P-2s6d^3D$	9	1174.922	85112.0	$2s2p^3P_1-(2p)^2\,{}^3P_2$
				8	1175.261	85087.5	$2s2p^3P_0-(2p)^2\,{}^3P_1$
3	341.14	293135	$2s2p^3P-2s5d^3D$	3	1175.577	85064.6	$2s2p^3P_1-(2p)^2\,{}^3P_1$
				9	1175.711	85054.9	$2s2p^3P_2-(2p)^2\,{}^3P_2$
4	360.59	277323	$2s2p^3P-2p3p^3P$	8	1175.988	85034.9	$2s2p^3P_1-(2p)^2\,{}^3P_0$
				9	1176.359	85008.1	$2s2p^3P_2-(2p)^2\,{}^3P_1$
2	363.81	274869	$2s2p^3P-2p3p^3S$				
				4	1426.50	70101.6	$2s3d^3D-2p3d^3P$
1	366.15	273112	$(2p)^2\,{}^3P-2p5d^3D$				
				4	1427.89	70033.4	$2s3p^3P_{1,2}-2p3p^3P_2$
2	369.40	270709	$2s2p^3P-2p3p^3D$	2	1428.23	70016.7	$2s3p^3P_{1,0}-2p3p^3P_1$
				2	1428.56	70000.6	$2s3p^3P_{2,1}-2p3p^3P_{1,0}$
5	371.73	269012	$2s2p^3P-2s4d^3D$				
				3	1477.70	67672.7	$2s3d^3D-2p3d^3D_{2,1}$
5	389.05*	257036	$2s2p^3P-2s4s^3S$	2	1478.21	67649.4	$2s3d^3D-2p3d^3D_2$
0	397.85	251351	$(2p)^2\,{}^3P-2p4d^3P$	1	1480.03	67566.2	$2s3p^3P-2p3p^3S$
3	399.71	250181	$(2p)^2\,{}^3P-2p4d^3D$	3	1576.48	63432.5	$2s3s^3S-2p3s^3P_2$
				2	1577.28	63400.3	$2s3s^3S-2p3s^3P_1$
7	459.532	217613	$2s2p^3P_{1,0}-2s3d^3D$	2	1577.95	63373.4	$2s3s^3S-2p3s^3P_0$
7	459.643	217560	$2s2p^3P_2-2s3d^3D$				
				4	1619.98	61729.2	$2s3p^3P_{1,0}-2s4d^3D$
4	493.49	202638	$(2p)^2\,{}^3P-2p3d^3P$	4	1620.62	61704.8	$2s3p^3P_2-2s4d^3D$
5	499.493	200203	$(2p)^2\,{}^3P-2p3d^3D$	4	1922.98	52002.6	$2s3d^3D-2s4f^3F$
				3	1923.33	51993.2	$2s3d^3D-2s4f^3F$
7	538.108	185836	$2s2p^3P_{1,0}-2s3s^3S$				
7	538.318	185764	$2s2p^3P_2-2s3s^3S$	3	4648.70	21511.4	$2s3s^3S-2s3p^3P_2$
				2	4651.46	21498.6	$2s3s^3S-2s3p^3P_1$
3	609.00	164204	$(2p)^2\,{}^3P_{1,0}-2p3s^3P_{2,1}$	1	4652.65	21493.1	$2s3s^3S-2s3p^3P_0$
4	609.29	164125	$(2p)^2\,{}^3P_{2,1}-2p3s^3P_{2,1,0}$				

I. Analysis of Triplet Lines

A few of the triplet lines of C_{III} were classified by Bowen and Millikan.[1] It has however become evident that the 2297A line identified by them as $(2s)^2{}^1S-2s2p^3P_1$ is too intense to be classified in this way. Fowler and Selwyn[2] have also pointed out that the 1931A line identified as $2s3d^3D-2s4f^3F$ is in reality a C_I line and has suggested instead the line at 1923A for this transition.

The triplet lines which have been classified with the aid of the more complete data now available are given in Table I. The term values deduced from them are given in Table II. A surprising fact, that is brought out by this analysis, is the great strength of the lines involving terms in which both valence electrons are excited.

Table II. *Triplet term values in* C_{III}.

$2s3s^3S$	147896	$2s2p^3P_0$	333740	$2s3d^3D$	116100	$2s4f^3F$	64102
		$2s2p^3P_1$	333717				
$2s4s^3S$	76664	$2s2p^3P_2$	333660	$2s4d^3D$	64680		
		$2s3p^3P_0$	126402.9	$2s5d^3D$	40565		
		$2s3p^3P_1$	126397.4				
		$2s3p^3P_2$	126384.6	$2s6d^3D$	28002		
				$2s7d^3D$	20456		
		$2p3s^3P_0$	84523	$(2p)^{2}P_0$	248682	$2p3d^3P$	45998
		$2p3s^3P_1$	84496	$(2p)^{2}P_1$	248652		
		$2p3s^3P_2$	84464	$(2p)^{2}P_2$	248605	$2p3d^3D_{2,1}$	48427
						$2p3d^3D_3$	48451
				$2p3p^3S$	58827		
				$2p3p^3P_0$	56397		
				$2p3p^3P_1$	56383	$2p4d^3P$	−2708
				$2p3p^3P_2$	56357		
				$2p3p^3D$	62991	$2p4d^3D$	−1538
						$2p5d^3D$	−24469

II. Analysis of Singlet Lines

Unfortunately it has not been found possible to obtain as definite and clear cut an identification of many of the singlet lines as might be desired. However since not only the relative positions of the singlet and triplet terms of C_{III} but also the relationship between the terms of different multiplicity in C_{II} and C_I are dependent on the values of the singlet terms it seems wise to

Table III. *Singlet lines in* C_{III}.

Int.	λ Vac.	ν	Series designation	Int.	λ Vac.	ν	Series designation
5	386.20*	258933	$(2s)^2\,{}^1S-2s3p\,{}^1P$	6	1247.391	80167	$2s2p\,{}^1P-(2p)^2\,{}^1S$
2	409.30*	244320	$2s2p\,{}^1P-2s5d\,{}^1D$	2	1308.75*	76409	$(2p)^2\,{}^1S-2s3p\,{}^1P$
3	450.74*	221857	$2s2p\,{}^1P-2s4d\,{}^1D$	2	1531.74*	65285	$2s3p\,{}^1P-2s4d\,{}^1D$
5	574.287*	174129	$2s2p\,{}^1P-2s3d\,{}^1D$	10	2297.59	43524	$2s2p\,{}^1P-(2p)^2\,{}^1D$
2	884.52*	113055	$(2p)^2\,{}^1D-2s3p\,{}^1P$	4	5697.6*	17551.3	$2s3p\,{}^1P-2s3d\,{}^1D$
10	977.031	102351	$(2s)^2\,{}^1S-2s2p\,{}^1P$				

[1] Bowen and Millikan, Phys. Rev. **26,** 310 (1925).

[2] Fowler and Selwyn, Proc. Roy. Soc. **A118,** 40 (1928).

TABLE IV. *Singlet term values in* C_{III}.

$(2s)^2\,{}^1S$	386480	$2s2p\,{}^1P$	284129	$2s3d\,{}^1D$	110000
		$2s3p\,{}^1P$	127551	$2s4d\,{}^1D$	62266
				$2s5d\,{}^1D$	39809
				$(2p)^2\,{}^1S$	203962
				$(2p)^2\,{}^1D$	240605

make available the most probable identifications that can now be made. These lines are given in Table III and the terms fixed by them in Table IV.

Note added June 1, 1931. When the singlet lines were originally classified two possible arrangements of the lines were found. These were identical for the lines caused by transitions between the terms arising from the $(2s)^2$, $2s2p$ and $(2p)^2$ configurations but differed for the lines connecting these terms with higher terms. The first of these arrangements was discarded because of the very anomalous rations that it yielded for the separations between the terms of the $(2p)^2$ configuration of C_{III} and of the $(2p)^3$ configuration of C_{II} as discussed below.

Recently however Bengt Edlén (Nature **127** p. 744, 1931) using the exceedingly efficient grazing incidence spectrograph at Uppsala has been able to obtain these lines in N_{IV} and O_V as well as in C_{III}. The progression to these from the spectra of B_{II} already known, unambiguously shows that in spite of the anomalies mentioned above the first arrangement must be the correct one. The tables of lines and term values have been modified accordingly. All changes in the classification of lines have been marked with an asterisk.

III. Additional Lines in C_{II}

The doublets and quartets have been quite completely analysed by Fowler[3] by Bowen[4] and by Fowler and Selwyn.[5] The new experimental material now available makes it possible to identify a few additional lines that are of importance in fixing the relationships between the doublets and quartets. These lines are given Table V. The identification of the lines caused by

TABLE V. *Additional lines in* C_{II}.

Int.	λ Vac.	ν	Series designation	Int.	λ Vac.	ν	Series designation
1	516.8	193498	$2s(2p)^{2}P-2s2p6d\,{}^1D$	3	600.39	166558	$2s(2p)^{2}\,{}^4P-2s2p4s\,{}^1P$
3	531.91	188002	$2s(2p)^{2}P-2s2p5d\,{}^1P$	4	1065.89	93818.3	$2s(2p)^{2}\,{}^2D_3-(2p)^3\,{}^2P_2$
				4	1066.14	93796.3	$2s(2p)^{2}\,{}^2D_2-(2p)^3\,{}^2P_1$
3	532.75	187705	$2s(2p)^{2}P-2s2p5d\,{}^1D$				
				3	1720.37	58127.0	$2s(2p)^{2}\,{}^2P_1-(2p)^3\,{}^2P_2$
0	547.27	182725	$2s(2p)^{2}P-2s2p5s\,{}^1P$	3	1721.01	58105.4	$2s(2p)^{2}\,{}^2P_1-(2p)^3\,{}^2P_1$
				4	1721.67	58083.1	$2s(2p)^{2}\,{}^2P_3-(2p)^3\,{}^2P_2$
3	562.51	177775	$2s(2p)^{2}P-2s2p4d\,{}^1P$	2	1722.24	58063.9	$2s(2p)^{2}\,{}^2P_2-(2p)^3\,{}^2P_1$
					λ air		
5	564.63	177107	$2s(2p)^{2}P-2s2p4d\,{}^1D$	2	2885.47*	34646.3	$2s2p3p\,{}^4P_3-2s2p4d\,{}^4D_4$

* From Fowler and Selwyn[5].

[3] Fowler, Proc. Roy. Soc. **A105,** 299 (1924).
[4] Bowen, Phys. Rev. **29,** 231 (1927), and **34,** 534 (1929).
[5] Fowler and Selwyn, Proc. Roy. Soc. **A120,** 312 (1928).

transitions from terms of the $(2p)^3$ configuration, i.e., the ^2P term here fixed and the ^2D determined by Fowler and Selwyn, is very definite as shown by the irregular doublet law relationships indicated in Table IV. The classification of the lines involving the ^4S term of this same configuration is likewise confirmed by irregular doublet law considerations given in a previous paper.[4]

TABLE VI. *Irregular doublet law relationships confirming the identification of* $(2p)^3$ *configuration of* C_{II}.

$2s(2p)^2\ ^2P_2-(2p)^3\ ^2P_2$			$2s(2p)^2\ ^2P_2-(2p)^3\ ^2D_3$		
C_{II}	58083.1	26337.1	C_{II}	[6]39796.46	17289
N_{III}	[4]84420.2	23886	N_{III}	[6]57085.7	17344
O_{IV}	[4]108306		O_{IV}	74430	
$2s(2p)^2\ ^2D_3-(2p)^3\ ^2P_2$			$2s(2p)^2\ ^2D-(2p)^3\ ^2D$		
C_{II}	93818.3	35564	C_{II}	[6] 75531.0	26520
N_{III}	[4]129382.3	32711	N_{III}	[6]102051	26183
O_{IV}	[4]162093		O_{IV}	128234.1	

The additional quartet combinations here given determine longer series of terms than were available in previous analyses. When these are taken into account it indicates that the quartet term values given by Fowler and Selwyn should be decreased by about 500 cm^{-1}.

IV. Relationships between Terms of Different Multiplicity in C_{III} and C_{II}

As was pointed out above the identification of the singlet lines and in particular the higher series members on which the determination of series limits depends is rather uncertain. For this reason it is particularly important to obtain confirmatory evidence of the general correctness of the term values thus found.

One piece of evidence is found in the arrangement of the terms of the $(2p)^3$ configuration of C_{II}. If the C_{III} singlet terms are correctly fixed then the difference between $(2s)^{21}S$ and $2s2p^3P_1$ is 52763 cm^{-1}. Since the known doublet series of C_{II} converge to the $(2s)^{21}S$ term of C_{III} as a limit while the quartet terms are based on the $2s2p^3P$ term, the quartet term values should all be decreased by this difference to make them comparable to those of the doublets. When this shift is made, in addition to the correction of 500 cm^{-1} mentioned in the previous section, the ^4S term of the $(2p)^3$ configuration has a term value of 54525. Likewise the doublet identifications mentioned above fix the $^2P_2$ term of this configuration at 27909 while the $^2D_3$ term had previously been determined as 46196. This gives a ratio for $(^2D_3-{}^2P)/(^4S-{}^2D_3)=2.196$ as compared with 0.509 for the $(2s)^2(2p)^3$ configuration of O_{II} and 0.500 for N_I and 0.651 for S_{II}.

Similarly if we consider C_{III} directly and assume the correctness of the classification of the 2297A line and the 1247A line we find the ratio $(^1D-{}^1S)/(^3P_2-{}^1D)=4.580$ for the terms of the $(2p)^2$ configuration. This compares with 1.148 for the $(2s)^2(2p)^2$ configuration of O_{III} and 1.144 for N_{II}.

[6] Freeman, Proc. Roy. Soc. **A121,** 318 (1928).

As there are theoretical reasons for expecting these ratios to remain approximately constant it seems very unusual to find so anomalous values for these ratios in carbon. However the progressions found by Edlen are so convincing that it does not seem possible to arrive at any other values.

This fixes the ionization potential of C_{III} at 47.7 volts. The resonance potential of C_{III} is fixed at 6.51 volts with the resonance line $(2s)^2\,{}^1S - 2s2p\,{}^3P_1$ occurring at $\nu = 52763$ cm^{-1} or $\lambda = 1895$A. Since the transition probability of this line is very small it should appear very faintly if at all. This coupled with the very large uncertainty in position will make it very difficult to locate. Similarly the resonance potential of C_{II} comes out of 5.32 volts and the resonance lines i.e. $(2s)^2 2p^2P - 2s(2p)^2\,{}^4P$ should appear at $\nu = 43111$ cm^{-1} or $\lambda = 2320$A. Again the lines will be very faint and the positions uncertain.

THE ELECTRO-OPTICAL KERR EFFECT IN GASES

By E. C. Stevenson and J. W. Beams
University of Virginia

(Received May 26, 1931)

Abstract

The electric double refraction or Kerr electro-optical effect in CO_2 has been investigated as a function of the density and of the temperature. A method of study has been developed by means of which it is possible to work at several hundred atmospheres pressure and with high electric field strengths. The polarizing prisms and the Kerr cell are enclosed in the same pressure chamber thus eliminating errors due to strains in the windows. The double refraction of the emergent light is measured by means of a photoelectric cell arrangement. The Kerr constant B in CO_2 was found to vary with density over the range 0.08 to 0.18 gm/cm^3 by about the amount to be expected from theory. The temperature variation, also, was in approximate accord with theory. Preliminary results show an easily measurable effect in oxygen and nitrogen, the former being larger.

THE phenomenon of electric double refraction was discovered by J. Kerr[1] in 1875 and is usually known as the Kerr electro-optical effect. In his early experiments Kerr was able to establish the relationship connecting the magnitude of the double refraction with that of the electric field strength. Briefly, the law states that if n_1 and n_2 are the refractive indices for the components of the light vibrating parallel and perpendicular to the lines of force in the substance, respectively, their phase difference D in radians after passing through the electric field E is

$$D = \frac{2\pi l(n_1 - n_2)}{\lambda} = 2\pi B l E^2 \qquad (1)$$

where λ is the wave-length of the light, l is the length of the light path through the electric field, and B is called the Kerr constant. The latter, however, has been found to vary with different substances, wave-lengths, and temperatures.

The theory of the Kerr effect as developed by Langevin,[2] Born,[3] Raman and Krishnan,[4] and others[5] connects the Kerr constant B with the index of refraction, the dielectric constant, and the light scattering coefficient (depolarization constant); the last of which has been extensively studied by Rayleigh, Raman, and many others.[6]

The fundamental assumptions of this theory are that the molecules

[1] Kerr, Phil. Mag. **1,** 337 (1875); **7,** 85 (1879); **9,** 157 (1880).
[2] Langevin, Le Radium **7,** 249 (1910).
[3] Born, Ann. d. Physik **35,** 117 (1918).
[4] Raman and Krishnan, Phil. Mag. **3,** 713 (1927); Proc. Roy. Soc. **A117,** 1 (1927).
[5] R. de L. Kronig, Zeits. f. Physik **45,** 458, 508 (1927); **47,** 702 (1927); See Born and Jordon, Elementare Quantenmechanik 259, 1930.
[6] Gans, Wien-Harms, Handbuch der Experimental Physik **19,** 338–408 (1928).

possess an intrinsic optical and electrical anisotropy and hence, as a consequence of the orientative influence of the electric field upon the induced and permanent electrical doublets in the molecules, the substance as a whole becomes doubly refracting. It is shown[7,4] that

$$B \equiv B_m N = \frac{(n^2 - 1)(n^2 + 2)}{4n\lambda}\left(\frac{\epsilon + 2}{3}\right)^2 \frac{\theta_1 + \theta_2}{\alpha_0} \tag{2}$$

where N is the number of molecules per unit volume, λ is the wave-length of the light, n is the index of refraction with zero field strength, ϵ is the dielectric constant, α_0 is the polarizability. B_m as defined by the above relation will be called the Kerr constant per molecule. Further

$$\theta_1 = \frac{1}{45kT}[(a_{11} - a_{22})(b_{11} - b_{22}) + (a_{22} - a_{33})(b_{22} - b_{33}) + (a_{33} - a_{11})(b_{33} - b_{11})]$$

$$\theta_2 = \frac{1}{45k^2T^2}[(\mu_1^2 - \mu_2^2)(b_{11} - b_{22}) + (\mu_2^2 - \mu_3^2)(b_{22} - b_{33}) + (\mu_3^2 - \mu_1^2)(b_{33} - b_{11})],$$

where T is the absolute temperature, k is Boltzmann's constant, b_{11}, b_{22}, b_{33} are the moments induced in a molecule along its three principal axes of optical anisotropy by unit electrical force in the light wave acting along the three axes respectively. a_{11}, a_{22}, a_{33} are the moments induced in the same directions respectively by unit electrostatic force arising from the applied field, while μ_1, μ_2, μ_3, are the components of the permanent electric moment along these same directions.

It is obvious that the above theory, as well as any other that might at the present time be proposed, should be expected to hold strictly only in the case of gases or vapors, because our insufficient knowledge of the liquid and solid states does not permit us to determine definitely all the essential factors necessarily involved. Although the Kerr effect has been extensively studied in liquids, the data for gases is comparatively meager. However, where the data for gases are available, the agreement between theory and experiment is as good as the precision of the experiment will justify.[4,8] Nevertheless, there is need for better experimental data, especially on the way B varies with different factors, in order to subject the theory to a rigid test. With this accomplished, the Kerr effect can be utilized as a powerful tool in studying not only the structure of the molecules themselves, but the influences of the molecules on each other which occur in gases under high pressure, and in the liquid and solid states. We have, therefore, undertaken a study of the effect in gases as a function of the density and temperature.[9]

[7] Debye Marx Handbuch der Radiologie, 754, 1925.

[8] Szwessy, Handbuch der Physik **21,** 724–955 (1929).

[9] Beams and Stevenson, Phys. Rev. **35,** 1440 (1930); Stevenson and Beams, J.O.S.A. **21,** 147 (1931).

The scarcity of experimental data in the case of gases results from the fact that the effect in gases and vapors is very small compared to that in liquids and solids, and hard to measure with accuracy. Previously the most precise methods of measurement consisted in plane polarizing the incident light at 45° to the lines of force by means of a Nicol prism and analyzing the emergent elliptically polarized light by means of a Brace half-shade arrangement. The "Kerr cell" containing the gas under investigation was enclosed in a vessel with glass ends placed between the Nicol and the half-shade instrument. With this apparatus it is possible to work only at pressures in the neighborhood of one atmosphere because with greater pressure the resulting strains produce enough double refraction in the transparent windows to render the Brace half-shade method unreliable. This necessity of working in the region of atmospheric pressure makes the effect exceedingly small for most substances, because of the limitations set by the small densities and the low sparking potentials.

In the present work we have succeeded in developing a new experimental method by which it is possible to study the Kerr effect up to pressures of several hundred atmospheres and at field strengths many times the sparking

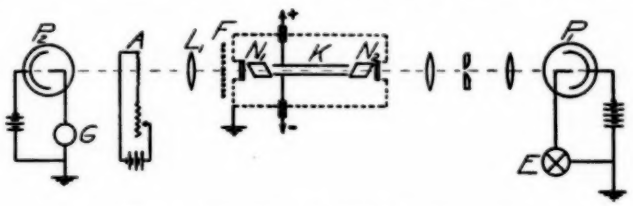

Fig. 1. Diagram of optical arrangement.

potential at atmospheric pressure. These conditions are accomplished by enclosing both polarizing and analyzing prisms together with the plates of the Kerr cell in a heavy pressure chamber with glass windows in the ends to permit the passage of light. The prisms under uniform pressure are not strained and no errors can be caused by strains in the windows. The increased pressure of the gas permits the use of very high field strengths because the sparking potential increases almost linearly with density according to Paschen's law.[10] This gives a very important advantage for, as can be seen from Eq. (1), the Kerr effect increases as the square of the field strength. The Brace half-shade method for measuring the double refraction was discarded because it not only required the measurement of small angles inside the tube but also depended upon the skill of the observer in matching light intensities. Instead, a photoelectric cell has been substituted which has given excellent results.

In Fig. 1 the arrangement of the optical parts is given. The light source A is a mercury arc or an incandescent lamp. A particular portion of the spectrum is selected by filters or a monochromator and the rays made parallel by the lens L_1. After being plane polarized by the polarizing prism N_1 they pass

[10] See J. J. Thompson, Conduction of Electricity through Gases, 2nd Edition p. 451, 1906.

between the oppositely charged parallel plates of the Kerr cell, through the analyzing prism N_2 and are finally brought to a focus on the surface of a vacuum photoelectric cell P_1. The latter is provided with a guard ring to prevent leakage and when used with a Swann electrometer E, was found to be linear for varying light intensities. The prism N_1 is set at a fixed angle with the plane of the plates such that the plane of vibration of the polarized light entering the cell is inclined at 45° to the direction of the lines of electric force between the plates. The prism N_2 may be oriented at any desired angle.

With N_1 and N_2 crossed and no field between the plates, no light enters the photoelectric cell and the rate of charge of the electrometer is zero except for an occasional small electrical or light leak for which a correction is made. When a potential is applied to the Kerr cell, the gas between the plates assumes the properties of a uniaxial crystal with its optic axis parallel to the lines of force. The light striking N_2 is therefore elliptically polarized and a small portion of the initial total intensity will pass on to the photoelectric cell. For particular settings of N_2 and the corresponding light intensities measured by the electrometer, the amount of double refraction in the Kerr cell can

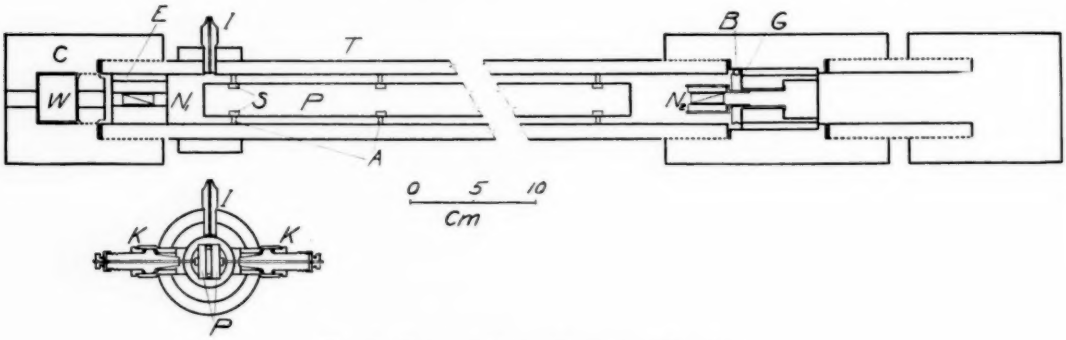

Fig. 2. Cross-sections of pressure chamber.

be calculated. Obviously, the intensity of the light source must remain constant, and to insure this, a second photoelectric cell P_2 and galvanometer are used to detect and correct for any fluctuations in A. The pressure chamber is indicated by the dotted enclosure.

In Fig. 2 are shown sections of the pressure tube. The barrel is a cold drawn steel tube of 3.8 cm inside diameter and walls 1.25 cm thick. The heavy caps on the ends contain plate glass windows 3 cm thick and 3 cm in diameter. The hole allowing passage of the light is 1.25 cm in diameter. The polarizing prism N_1 is mounted in the front end of the tube and the plates P are held in place by bakelite rings A. They are also insulated from each other by bakelite separators S. The plates used throughout this work were Starrett steel straight-edges 90 cm in length, 2.5 cm wide and 4 mm apart. The intermediate section F contains a worm and gear mounting BG for the analyzing prism N_2 by which it can be turned from the outside of the tube. Lead washers at all joints provide gas tight seals. Electrical connections to the plates are made by the use of ordinary spark plugs KK and the gas inlet is at I. Where the

gas inlet and spark plugs enter, the tube is reinforced by a steel ring shrunk on. Gases are admitted to the tube from commercial steel bottles through copper pressure tubing, and the pressures are measured on a special spring gauge with telescope mirror and scale attachment. This was calibrated by a dead-weight piston gauge. The densities were then calculated from the data of Amagat.[11]

Fig. 3 is a diagram of the method for obtaining and measuring the electric potential applied to the plates. One side of the secondary of a five-kilowatt x-ray transformer is grounded, while the other goes to two kenotrons in parallel. These charge the opposite sides of the condenser C through the resistances RR. The two sides of the condenser are connected to the plates of the

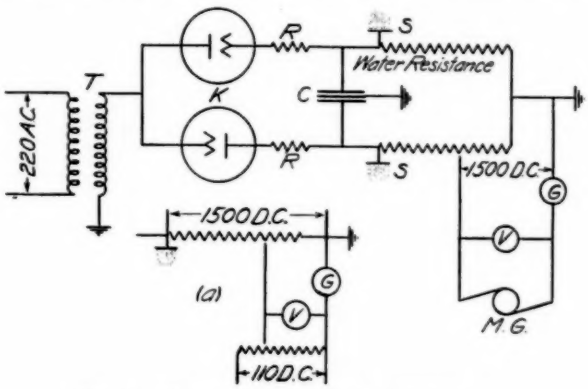

Fig. 3. Diagram of electrical arrangement.

Kerr cell and to the ends of a long continuous-flow water resistance. The water enters at ground potential, divides into two branches and is expelled through sprinklers at the end of each half. The use of sprinklers to break the stream obviates the need of a return path and thus reduces electrical leakage from the condenser. The total potentials are determined by a potentiometer method.[12] Voltage differences across segments of each half of the water resistances are balanced against a 1500 volt motor-generator set, the voltmeter V recording voltages directly and the galvanometer G being used only as a null instrument. Voltage readings across the segments are multiplied by the proper factors to give the total voltage across each half of the resistance. The multiplying factors are obtained by calibration in which the 1500 volt generator is connected across the half resistance and the voltage across the segments balanced against a 110 volt line source or batteries as shown in Fig. 3 (a). The potentials can be measured to 0.2 percent while the ripple was less than this. The temperature of the gas is controlled by immersing the whole tube in a water or oil bath regulated by a mercury in glass thermostat to less than 0.02 of a degree centigrade.

In order to determine D in Eq. (1) with the above apparatus it is only necessary to recall that the substance between the plates of the Kerr cell

[11] Amagat, Comptes Rendus, 663, 1885.
[12] Gunn, J.O.S.A. and R.S.I. **14**, 257 (1927).

takes the optical properties of a uniaxial crystal with the optic axis in the direction of the lines of electric force in the cell. Hence the intensity of light I passing the second or analyzing Nicol N_2 is[13]

$$I = [\cos^2(\alpha - \beta) - \sin 2\alpha \sin 2\beta \sin^2(D/2)] \tag{3}$$

where α and β are the angles that the planes of vibration of the transmited light of N_1 and N_2 make respectively with the lines of force. In the case where N_2 is crossed with respect to N_1 and the plane of transmission of N_1 makes an angle of 45° with the lines of force,

$$I_1 = I_0 \sin^2 \frac{D}{2}. \tag{4}$$

When the Nicols are parallel, $\alpha = \beta = 45°$, and

$$I_2 = I_0\left(1 - \sin^2 \frac{D}{2}\right). \tag{5}$$

Hence

$$\frac{I_1}{I_2} = \tan^2 \frac{D}{2} = \tan^2 \pi N B_m l E^2 \tag{6}$$

or

$$NB_m = \frac{1}{\pi l E^2} \tan^{-1} \left(\frac{I_1}{I_2}\right)^{1/2}. \tag{7}$$

Thus if the light intensities are measured by the above photoelectric cell method for conditions of crossed and uncrossed prisms I_0 is eliminated and NB_m can be determined. The accuracy attainable in measuring D by this method is as good as is needed at the present time for it is better than that with which it is possible to measure the other factors entering into Kerr's law. The principal difficulty in this measurement arises from the fact that I_1 is usually very much smaller than I_2 making it necessary to measure photoelectric currents of widely different orders of magnitude.

In this work, it was especially desired to study the variations of the Kerr constant per molecule, B_m, with density and with temperature, so that greater precision was obtained by holding as many of the factors as possible in Eq. (1) constant rather than determining their absolute magnitudes. Rewriting Eq. (4)

$$\sin^{-1}\left(\frac{I_1}{I_0}\right)^{1/2} = \pi B_n N l E^2 = \left(\frac{I_1}{I_0}\right)^{1/2} \text{(approximately)}. \tag{8}$$

(The error due to the above approximation is less than one part per thousand because of the smallness of D). If now T, I_0, l, λ and E are held constant and $\sin^{-1}(I/I_0)^{1/2}$ is plotted as a function of the density a straight line should result, provided B_m is independent of the density. Fig. 4 shows an example of

[13] See Wood, Physical Optics 320, 1923; Robertson, Physical Optics 290, 1929.

such a graph for a density variation from 0.08 to 0.18 gm/cm³. It will be observed that over this range the curve within the limits of experimental error is a straight line. However, the line should pass through the origin if B_m is completely independent of the density, but the experimental values show clearly that this is not the case. B_m must, therefore, vary with density. If the curve were extended either to larger or smaller densities it would no doubt

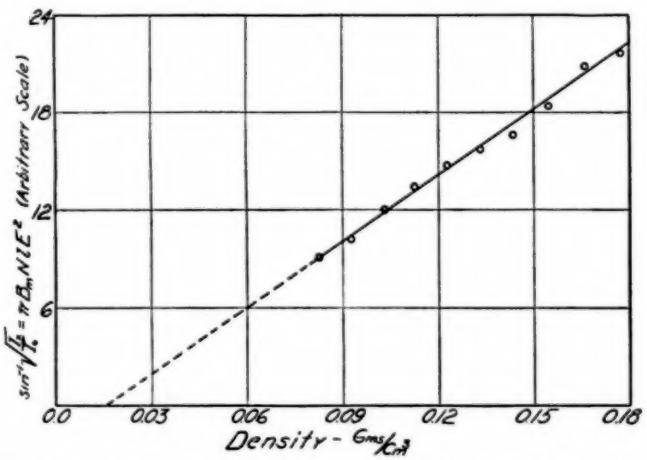

Fig. 4. Variation of the Kerr effect with density, temperature 34.3°C, λ4300–4700 A.

deviate from a straight line. It is interesting to compare this result with what should be expected from theory and the known behavior of the index of refraction and the dielectric constant.

Since CO_2 is non-polar θ_2 in Eq. (2) is zero and if we also substitute for α_0 the value $\alpha_0 = 3/4\pi N \cdot n^2 - 1/n^2 + 2$

$$B = B_m N \propto \frac{(n^2+2)^2(\epsilon+2)^2}{n\lambda T}. \tag{9}$$

From the data of Phillips[14] for the index of refraction of CO_2 and that of Keyes and Kirkwood[15] for the dielectric constant of CO_2 the values for n and ϵ can be obtained and the variation of $B_m N$ with density calculated. Fig. 5 shows a graph of $(n^2+2)^2 \cdot (\epsilon+2)^2/n\lambda T$ plotted against the density over the same interval as our experimental values in Fig. 4. It will be observed that the calculated values also lie on approximately a straight line, which, however, does not pass through the origin, but cuts the density axis at approximately the same value as the experimental curve in Fig. 4. In fact, the agreement between theory and experiment is as good as should be expected considering that there is some choice in the way the lines should be drawn. The index of refraction and dielectric constant data indicate that if we were to extend our measurements to higher densities the variation of B_m with density would be found quite marked. The fact that the relation expressed in Eq. (1) is not ap-

[14] Phillips, Proc. Roy. Soc. **A97**, 226 (1920).
[15] Keyes and Kirkwood, Phys. Rev. **26**, 754 (1930).

preciably changed by a variation in density indicates that the same causes which produce a variation in ϵ and in n with increasing ρ also produce the corresponding changes in B_m. However, as far as the writers know a satisfactory hypothesis concerning the changes in the structure of the molecule itself or its association with other molecules, resulting from increased density, has not been proposed that will quantatively explain all the experimental results. It will perhaps be necessary to extend the measurements to greater densities and to other gases before a clear understanding can be obtained.

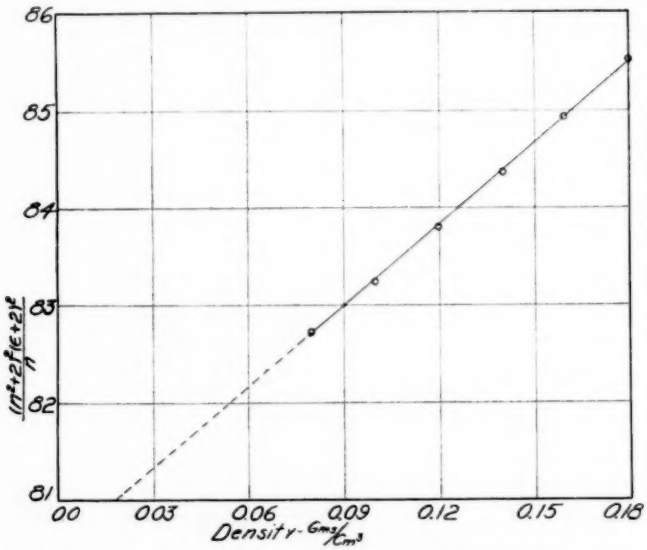

Fig. 5. Calculated variation of the Kerr effect with density from the data of Phillips, for n, and Keyes and Kirkwood, for ϵ.

Referring again to Eq. (9) it will be noticed that B should vary inversely as the absolute temperature holding the remaining factors constant. We have made preliminary measurements of the changes of B with temperature from 20° to 45°C and find that the results are in approximate agreement with theory.

We have also looked for the Kerr effect in oxygen and nitrogen and found it large enough to be measurable by the method. The effect is larger in oxygen than in nitrogen but we did not obtain satisfactory absolute values because of a fire with oxygen that terminated the experiment before it was complete. In hydrogen our preliminary results indicate that the effect is much smaller than in nitrogen.

THE RAMAN SPECTRA OF CERTAIN ORGANIC LIQUIDS

By Charles S. Morris
Mendenhall Laboratory of Physics, Ohio State University

(Received April 22, 1931)

Abstract

The Raman spectra of nineteen organic compounds chosen from different chemical series have been measured. Frequency shifts are given and a relationship is shown between certain frequency shifts and molecular structure. In particular the frequency shift $\Delta\nu = 1024$ cm^{-1} recurs with the C−C structure, likewise $\Delta\nu = 1613$ cm^{-1} is associated with C=C, $\Delta\nu = 1446$ cm^{-1} with 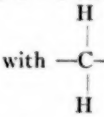 , $\Delta\nu = 2929$ cm^{-1} with 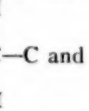 and $\Delta\nu = 3054$ cm^{-1} with . It is suggested that anti-Stokes lines may have slightly greater frequency shifts than the corresponding Stokes lines. A comparison between Raman frequency shifts and infrared absorption data is made.

Introduction

DATA on the incoherent scattering of light, as first observed by Raman,[1] give information about the energies associated with different states of vibration and rotation of molecules. It is evident, therefore, that a study of the scattering of light by organic molecules affords one means of advancing our knolwedge of the structure of these molecules. The possibility of correlating structural characteristics of organic molecules with frequency shifts observed in the Raman effect has been made highly probable by the work of Dadieu and Kohlrausch.[2] Certain special atomic groupings in the molecule, for example hydrogen bound to carbon or two carbons bound by a double bond, appear to have definite frequency shifts associated with them. The assignment of certain frequency shifts to definite types of molecular structure is further strengthened by the results obtained by Kettering, Shutts, and Andrews[3] in their investigations of the vibrations executed by mechanical models of various types of molecular structure. The mechanical vibrations produced in the models are in good agreement with those which would be postulated on the basis of observed frequency changes in the Raman effect.

Experimental

A high speed glass spectrograph was used, consisting of two 60° glass prisms 4×2.5 in, and two achromatic lenses of 6 in focal length and 2.5 in aperture. The dispersion obtained was 54A per mm at 4000A, 95A per mm at 4500A, and 145A per mm at 5000A. The slit width used was 0.1 mm.

[1] Raman, Ind. Jour. Phys. **2,** 387 (1928).
[2] Dadieu and Kohlrausch, Ber. d. Deut. Chem. Ges. **63,** II, 251 (1930).
[3] Kettering, Shutts, and Andrews, Phys. Rev. **36,** 531 (1930).

The source of radiation was a horizontal Cooper-Hewitt quartz mercury arc lamp. It was operated in a vertical position from a 125 volt d.c. generator in series with suitable inductances and resistances to give a steady current of about 2.2 amperes. The tube containing the liquid to be studied had the form indicated in Fig. 1. The exposed length of the column of liquid from *A* to *B* was 11 cm and the diameter of this portion of the tube 2.5 cm. This tube and the arc were surrounded by a cylindrical reflector. The bottom end of the tube was flattened and ground plane, care being taken to get this plane perpendicular to the axis of the tube. This precaution together with the fact that the index of refraction of the liquids used did not differ widely from that of the tube reduced to a minimum stray reflection from the walls of the tube into the spectrograph. The tube was painted with flat black paint at *A* and for about 10 cm at *B* to prevent undesirable reflections. The scattered light

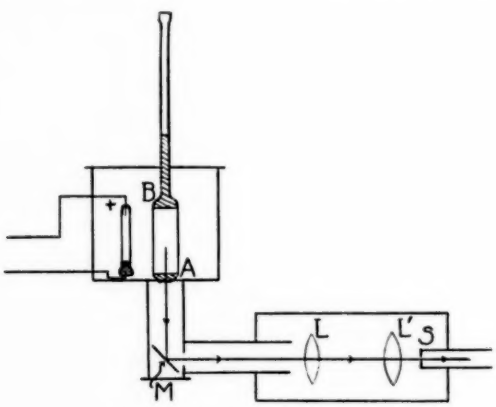

Fig. 1. Diagram of apparatus.

passed through the bottom end of the tube was reflected by the mirror, *M*, and focussed by means of the convex lenses *L* and *L'* on the slit of the spectrograph, *S*. Suitable shields and diaphragms were provided to prevent stray illumination from reaching the spectrograph. The mercury arc and the observation tube were cooled by blowing air against them. The temperature of the tube was kept at about 45° C.

Eastman Speedway plates were used with the time of exposure ranging from 1 to 4 hours. In most cases an exposure of 1 hour was sufficient to bring out all the lines which could be obtained. The plates were measured on a Zeiss comparator. The probable error of the sharper lines is approximately 0.5A at 4500A but for the more diffuse lines it reaches about 1.5A.

Results

In Table I are given the data for the nineteen organic compounds studied in this investigation. The Raman frequency shifts are expressed in vacuum wave-numbers, followed in each case by the average estimated intensity in parenthesis, and this in turn by the exciting line also in parenthesis. The estimated intensities are expressed on a 1 to 5 scale with 5 the greatest in-

TABLE I.

Substance Formula	Δν	Δν	Δν	Δν	Δν	Δν	Δν	Δν	Δν	Δν	Δν
ter-Amyl Chloride $(CH_3)-CH_2(CH_3)_2CCl$	378(4)(ad)	566(5)(ae)	618(1)(ae)	788(3)(ae)	922(2)(ae)	1150(4)(ae)	1207(3)(ade)	1451(3)(ace)	2929(3)(aegi)	2983(4)(aei)	
Benzyl Acetate $CH_3COOCH_2C_6H_5$	364(1)(d)	479(1)(e)	633(1)(d)	998(4)(ae)	1022(2)(def)	1602(1)(e)	2933(2)(ae)	3046(2)(ae)			
Benzyl Chloroacetate $CH_2ClCOOCH_2C_6H_5$	490(2)(e)	618(3)(ade)	808(2)(ae)	1009(3)(adef)	1150(1)(a)	1614(2)(ae)	3061(1)(acde)				
n-Butyl Acetate $CH_3COOC_4H_9$	629(1)(e)	1031(1)(e)	1440(1)(ae)	1686(1)(a)	2916(3)(ade)						
n-Butyl Formate $HCOOC_4H_9$	832(1)(ae)	912(1)(e)	1065(1)(e)	1314(1)(e)	1452(2)(ae)	1710(1)(a)	2734(3)(de)	2926(4)(aeh)			
-Butyraldehyde $CH_3(CH_2)_2CHO$	983(1)(a)	2915(2)(ae)	3032(1)(a)								
o-Chlorophenol ClC_6H_4OH	168(1)(a)	254(1)(a)	559(1)(ae)	680(1)(ae)	829(1)(ae)	890(1)(e)	1022(2)(ae)	1155(1)(a)	1585(1)(ae)	2138(1)(de)	3061(1)(adeg)
Cyclohexanol $(CH_2)_5CHOH$	783(3)(ae)	832(1)(de)	1080(4)(a)	1256(2)(de)	2887(3)(a)	2935(3)(ei)					
Cyclohexene C_6H_{10}	814(3)(ae)	1068(2)(ae)	1212(2)(e)	1254(2)(ae)	1426(2)(ae)	1643(2)(a)	2908(2)(adeg)	3005(2)(ad)			
p-Cymene $CH_3C_6H_4CH(CH_3)_2$	619(1)(de)	808(1)(a)	1195(1)(e)	1617(1)(a)	2720(1)(de)	2975(1)(ad)	3020(1)(ad)				
Dichloroacetic acid $CHCl_2COOH$	421(1)(a)	779(1)(a)	3025(1)(a)								
Ethyl Chloroacetate $CH_2CLCOOC_2H_5$	788(2)(e)	863(2)(e)	1186(1)(b)	2953(2)(ah)							
Ethylene Glycol $HOCH_2CH_2OH$	860(1)(ae)	1042(1)(e)	1225(1)(e)	1444(1)(e)	2873(3)(e)	2907(2)(a)					
Isoamyl Propionate $CH_3CH_2COOC_5H_{11}$	272(1)(a)	412(1)(a)	605(1)(a)	770(2)(ade)	827(2)(ae)	989(1)(a)	1078(1)(e)	1151(3)(ae)	1456(2)(ae)	1738(1)(a)	2925(4)(adeh)
n-Propyl n-Propionate $C_2H_5COOC_3H_7$	1077(1)(d)	1435(2)(e)	2924(3)(ae)								
Propylene Glycol $CH_3CHOHCH_2OH$	830(1)(ae)	919(1)(e)	1050(1)(e)	2918(2)(ae)							
Safrol $C_{10}H_{10}O_2$	594(1)(ade)	721(2)(ade)	816(2)(ade)	1107(1)(de)	1174(1)(d)	1248(1)(ade)	1303(1)(ae)	1624(1)(a)	2911(1)(ae)	3072(1)(ade)	
†Tetrachloroethylene $CCl_2:CCl_2$	239(4)(a)	347(2)(ae)	450(4)(ade)	513(2)(ae)	1575(5)(ae)						
1.2.4 Trichlorobenzene $C_6H_3Cl_3$	188(1)(a)	319(1)(a)	392(1)(a)	816(1)(a)	1030(1)(a)	1144(2)(a)	1229(2)(ad)	1573(2)(a)	1882(1)(e)	2235(1)(e)	3067(2)(ae)

† Numerical data given in part by Pringsheim and Rosen, Zeits. f. Physik **50**, 741(1928).

tensity. The intensity of the Hg line 4916A is assumed arbitrarily to have an intensity of 5 units on this scale. The wave-lengths of the exciting lines corresponding to each of the letters used in Table I are as follows,

	wave-length in A.U.	wave-number in cm^{-1}
a	4358	22938
b	4348	22994
c	4339	23038
d	4078	24516
e	4047	24705
f	3984	25093
g	3663	27290
h	3655	27354
i	3650	27388

Where the Raman frequency shift as tabulated in Table I is followed by two or more letters in parentheses, as (*a*, *d*, *e*), the meaning is that this Raman frequency shift was observed for the three exciting lines designated by the letters *a*, *d*, *e*, that is, for $\lambda = 4358$A, $\lambda = 4078$A and $\lambda = 4047$A. In such cases the frequency shift recorded is the mean of the values obtained from each of the exciting lines. Where only one letter in parentheses follows a Raman frequency shift this frequency shift was observed for this exciting line only.

Table II classifies certain frequency shifts as suggested by Dadieu and Kohlrausch.[2] The average values of frequency shifts here listed for particular structural characteristics are in close agreement with those given in the reference cited. In the case of n-butyl acetate the C = C structure does not occur, but there is however in this case an unexplained frequency shift of 1686 cm^{-1}

TABLE II.

Substance	$\Delta\nu$ C—C	$\Delta\nu$ 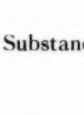	$\Delta\nu$ C=C	$\Delta\nu$ 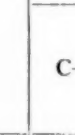	$\Delta\nu$ 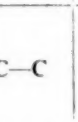
ter-Amyl Chloride $(CH_3)-CH_2(CH_3)_2CCl$		1451(3)		2929(3)	
Benzyl Acetate $CH_3COOCH_2C_6H_5$	998(4) 1022(2)		1602(1)	2933(2)	3046(2)
Benzyl Chloroacetate $CH_2ClCOOCH_2C_6H_5$	1009(3)		1614(2)		3061(1)
n-Butyl Acetate $CH_3COOC_4H_9$		1440(1)	1686(1)	2918(2)	
n-Butyl Formate $HCOOC_4H_9$		1452(2)		2926(4)	
n-Butyraldehyde $CH_3(CH_2)_2CHO$	983(1)			2915(2)	
o-Chlorophenol ClC_6H_4OH	1022(2)		1585(1)		3061(1)
Cyclohexanol $(CH^2)_5CHOH$	1080(4)			*2935(3)	
Cyclohexene C_6H_{10}	1068(2)		1643(2)	*2908(2)	
p-Cymene $CH_3C_6H_4CH(CH_3)_2$			1617(1)	2975(1)	3020(1)
Ethyl Chloroacetate $CH_2ClCOOC_2H_5$				2953(2)	
Ethylene Glycol $HOCH_2CH_2OH$	1042(1)	1444(1)		*2907(2)	
Isoamyl Propionate $CH_3CH_2COOC_5H_{11}$	989(1)	1456(2)		2925(4)	
n-Propyl n-Propionate $C_2H_5COOC_3H_7$		1435(2)		2924(3)	
Propylene Glycol $CH_3CHOHCH_2OH$				2918(2)	
Safrol $C_{10}H_{10}O_2$			1624(1)	*2911(1)	3072(1)
Tetrachloroethylene $CCl_2:CCl_2$			1575(5)		
1·2·4 Trichlorobenzene $C_6H_3Cl_3$	1030(1)		1573(2)		3067(2)
Average	1024	1446	1613	2929	3054

which does not differ greatly from the mean value of 1613 cm^{-1} attributed to C = C bond. A few cases were noted in which frequency shifts are missing for structural characteristics that do occur. It is probable that in these cases the corresponding Raman lines were produced but with intensity too weak to detect. In a few instances, as indicated by an asterisk in the table, frequency shifts are found without the corresponding molecular structure occurring. However in the great majority of cases similar frequency shifts are noted with the recurrence of similar molecular structures.

Table III gives a comparison of Raman frequency shifts with infrared absorption data for isoamyl-propionate and safrol. The column headed $\Delta\nu$ gives the average Raman frequency shifts, the column headed μ_λ gives the corresponding wave-lengths calculated from these frequency shifts, and the column headed μ_I gives the wave-lengths from observations on infrared

TABLE III.

Isoamyl Propionate			Safrol		
$\Delta\nu$	μ_λ	μ_I*	$\Delta\nu$	μ_λ	μ_I†
272	36.8		594	16.8	
412	24.3		721	13.9	13.9s
605	16.5				12.9s
770	13.0	13.2s	816	12.3	12.36s
827	12.1	12.3			11.67s
989	10.1				10.85s
		9.5s			10.06s
1078	9.27				9.62s
1151	8.69	8.6s	1107	9.03	9.12s
		7.5s			8.4s
		7.0	1174	8.52	
1456	6.87				8.15s
		5.9	1248	8.01	
1738	5.57		1303	7.67	
2925	3.42	3.5s			7.43
					6.82s
			1624	6.16	6.07
					5.78
			2911	3.43	3.42s
			3072	3.25	
					2.90
					2.58

* Weniger, Phys. Rev. [1] **31**, 388 (1910).

† Coblentz, Investigation of Infrared Spectra, Carnegie Institution of Washington, Pub. No. 35 (1905).

absorption. The letter *s* is used to indicate particularly strong infrared absorption. As has been noted by many observers a direct correspondence does not exist between Raman frequency shifts and infrared absorption data. This table gives a sample of results obtained in this investigation in which only an occasional near approach of values exists. This is in accord with theoretical considerations as has been shown by Langer and Meggers[4] and others.

An observation that seems worthy of mention is the appearance in the case of tetrachloroethylene of three anti-Stokes lines of frequency shifts -448 cm^{-1}, -349 cm^{-1}, -240 cm^{-1} with corresponding Stokes lines of frequency shifts 447 cm^{-1}, 348 cm^{-1}, 238 cm^{-1}. The shift of the anti-Stokes lines

[4] Langer and Meggers, B S. Jour. Research **4**, 711 (1930).

thus average slightly greater than the coresponding Stokes lines. In the accurate work of Langer and Meggers[4] a similar difference appears in the data on carbon tetrachloride and chloroform. These small differences by which the negative shifts exceed the positive may be due to a systematic error in measurement. However, the suggestion is here offered that perhaps we are observing a true difference such as might be expected to exist if a double electron shift takes place when the molecule is removed from its excited state to its normal state. More data accurately taken with high dispersion will need to be secured before final statement can be made on this point.

In conclusion the author wishes to express his appreciation to Professor Alpheus W. Smith for suggesting the problem and for his assistance in the work. He is also indebted to Dr. M. L. Pool for advice and helpful discussion as the work progressed.

NEW ABSORPTION BANDS OF AMMONIA, METHYL BROMIDE, METHYL IODIDE AND CARBON DIOXIDE IN THE INFRARED SPECTRUM

By W. W. Sleator
University of Michigan

(Received May 25, 1931)

Abstract

Work done with the recording spectrometer at the University of Michigan has shown near the wave-length 16.1μ an absorption band of ammonia not hitherto observed in detail, and bands due to methyl bromide and methyl iodide, near wave-lengths 16.4μ and 18.8μ respectively. It has also shown the strong absorption band due to carbon dioxide near 15μ to be more complex and extensive than has previously been indicated.

I. Introduction

THE cooperative work recounted here is preliminary to more precise and more extended investigations now going on, but seems of sufficient interest to merit a brief presentation. It has opened the way to observations of importance in infrared spectroscopy.

II. Apparatus

During a spectroscopic investigation with another purpose the author used the recording prism spectrometer constructed and described by Randall and Strong.[1] Already known spectra of the substances reported upon were used to calibrate the instrument and the new absorption bands were photographed incidentally. Auxiliary equipment comprised the gauge and pumps for evacuating the case in which the path of the radiation was entirely enclosed, and a Moll thermal relay, used ordinarily to give an amplifying factor of 20 to 50. The source of radiation was a platinum strip bent to form a V, heated by a current of about 28 amperes. The spectra of ammonia and carbondioxide were given by a 30° prism of potassium chloride silvered on the back, the other two by a prism of potassium bromide of about 60°, used with a Wadsworth and a Littrow mirror. The two slits were 0.2 mm wide. This means that in the region of 16μ the interval in the slit before the thermopile with the chloride prism was 0.045μ, or 1.7 waves per cm. For the bromide prism which has double the angle but whose material in this region has about six-tenths the dispersion, the slit corresponds to 0.038μ or 1.4 waves per cm.[2] Calibration was empirical. Known wave-lengths of emission and absorption lines were plotted against the position of the prism which moves uniformly with respect to the drum on which the photographic paper is carried. The

[1] H. M. Randall and John D. Strong, Rev. Sci. Inst., in press.

[2] Data on the dispersion of potassium bromide have recently been given by E. Grundelach, Zeits. f. Physik **66**, 775 (1930).

vertical lines appearing equally spaced in Fig. 1 and Fig. 3 have each a number representing a position of the prism and therefore a particular wave-length.

III. The Absorption Bands

Ammonia. An actual photographic record such as the apparatus produces, was submitted for Fig. 1. At the left side of the figure appear the details at the long wave end of the great absorption band of ammonia analysed by Barker[3] and given completely, from another photographic record, by Randall and Strong (reference 1). To the lines have been assigned the arbitrary

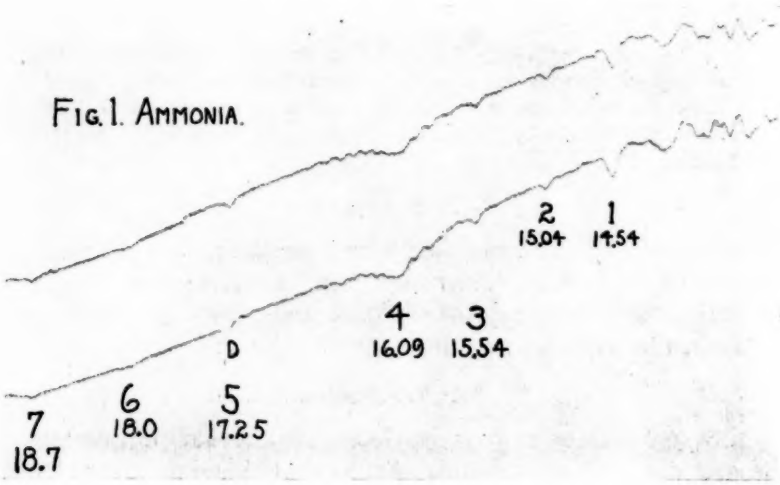

Fig. 1.

numbers 1 to 7, and wave-lengths are written on the figure. No. 4 at 16.09μ is evidently the center of a band which is in a state of resolution slightly showing the influence of rotation.[4] The absorption is due to ammonia at 68 cm pressure in a cell 12 cm long at about 30°C. The fine vertical lines one of which is labelled *D*, below the lower trace, represent the displacement or deflection which occurred when the shutter was closed, cutting off the entering radiation. These lines enable one to estimate the extent of the absorption. The center of line 4 represents about 40 percent. The fact that the lines slope generally toward the left is due to a drift of the zero, which was troublesome when these records were made, but has since been eliminated. The fact that two independent and successive curves are so closely parallel speaks for the reality of the absorption lines which appeared unmistakably on other records as well.

[3] E. F. Barker, Phys. Rev. **33,** 684 (1929).

[4] The center of No. 4 is shown, probably, as the sharp line marked *d* in Fig. 1, by Sir Robert Robertson and J. J. Fox, Proc. Roy. Soc. **A120,** 168, 193, 197 (1928). This band is considered by Robertson and Fox to be one member of a rotation series of which the band found at 63μ by Rubens and Wartenberg is the first term. The wave-length of *d* is given as 15.91μ.

Methyl bromide and methyl iodide. So many details, involving spectra of several other substances, appear on the same photographic record, that it was necessary to make ink tracings of the original for Fig. 2. From these the minute fluctuations noticeable in Fig. 1 have disappeared, but the tracing faithfully represents the significant details of the original. It represents them at least, in so far as comparison of several records permits one to distinguish significant from insignificant variations. The upper curve shows the absorption—about 50 percent at the highest, near 16μ—due to methyl bromide at 20 cm pressure in the 12 cm cell. The lower shows that due to methyl iodide

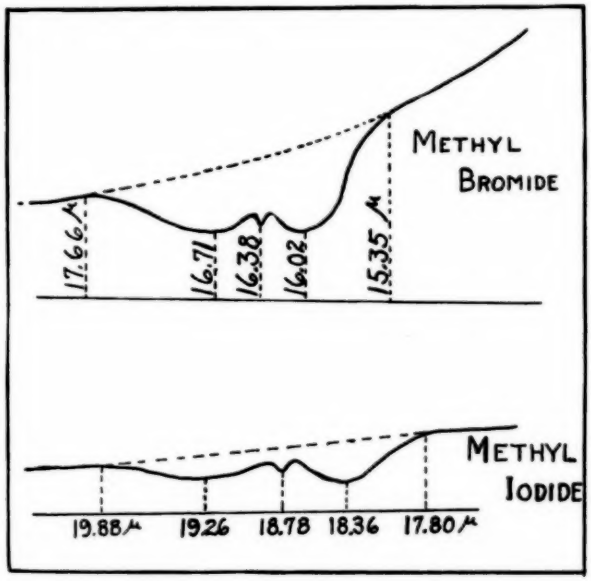

Fig. 2.

at 44 cm pressure in the same cell. The dotted vertical lines show how the deflection generally declines as wave-length increases, and the probable course of the record, had the gas been absent, is given by the dotted curve. The gases were at about 30°C. Those spectra were taken with the potassium bromide prism.

The infrared absorption spectra of the methyl halides have been investigated by Bennett and Meyer.[5] Their observations did not extend beyond 15μ, but according to the scheme shown in Fig. 4 of their paper the two bands given here belong to the *A* series. They have the same general appearance as the methyl chloride band whose center is at 13.65μ. As is shown in the case of methyl chloride the *P* branches in the new bands are of greater extent than the *Q* branches.

By means of Raman spectra Ball[6] has determined infrared wave-lengths for the absorption by methyl chloride, bromide and iodide. It was first

[5] Willard H. Bennett and Charles F. Meyer, Phys. Rev. **32,** 888 (1928).

[6] Gajendra Nath Ball, Zeits. f. Physik **66,** 257 (1930).

thought that these values could be used as points on the calibration curve of the potassium bromide prism. The wave-lengths were such, however, that either the curve had to be distorted beyond probability, or else many wave-lengths determined in this laboratory had to be discarded. Therefore these values were not relied upon. It is plain that for an infrared wave-length determined by the Raman effect the precision of measurement is less as the wave-length is greater. Recent work by Cleeton and Dufford[7] gives certain wave number differences observed in the Raman spectra of methyl bromide and methyl iodide as 603 and 534 respectively. These numbers correspond to the wave-lengths 16.58μ and 18.73μ.[8]

Carbon dioxide Fig. 3 shows three curves from a photographic record by the sylvite prism. For curve *A* the absorption cell, which is entirely within the spectrometer case, was empty. The general slope of the curve, like that

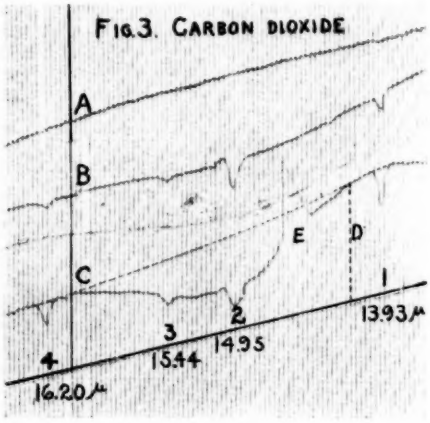

Fig. 3.

of the other two, is due to a drift of the zero. The fine fluctuations are due to Brownian motion, and perhaps in a small measure to vibrations of the building. These variations are absent when the amplifier is not used, and can be much stronger than here shown—easily of amplitude one or two centimeters—if the amplifying factor is high. The three curves appeared on the same sheet so that the vertical lines should be continuous. The paper was cut and glued for the sake of the order of the curves, and to diminish the diagram. Curve *B* shows the effect of carbon dioxide occupying the cell at 5 cm pressure. For curve *C* the pressure was 23 cm, the temperature in both cases about 30°C. It is plain that an increase in pressure tends to obscure the "zero branch," if such it be, at 14.95μ, while it accentuates the absorption at 13.93μ and 16.20μ. The deflections for curve *C* are shown by the dotted line *D* and

[7] C. E. Cleeton and R. T. Dufford, Phys. Rev. **37**, 362 (1931).

[8] A. Dadieu and K. W. F. Kohlrausch, J.O.S.A., **21**, 286, 297 (1931), give the wave numbers 594 and 522, corresponding to 16.84μ and 19.16μ, for methyl bromide and methyl iodide respectively, in the liquid state. These are wave number differences for anti-Stokes Raman lines.

the heavy base line. The dotted curve indicates as before the probable course of the record if the gas had been removed. At *E* some disturbance occurred which caused a temporary deflection; perhaps it was due to radio waves which penetrated out shielding. In the recent book by Schaefer and Matossi[9] this absorption band of carbon dioxide is shown as a strong band with principal maxima at about 14.8μ and 15.4 μ, very much as it has been known since the work of Burmeister. It was some what of a surprise to find this material absorbing radiation as is indicated in Fig. 3.

From consideration of different records for the same material, and of the definiteness with which certain lines appear at particular places on the photographic record, we may make some estimate of the precision of the wave-lengths here presented. For the center lines of methyl bromide and iodide, the lines of carbondioxide, and the lines numbered 1, 2 and 3 of ammonia, we should write the wave-lengths with the probable error $\pm 0.01\mu$. Line 4 of ammonia is naturally indefinite on account of its width and lines 5, 6 and 7 are not so precisely given.

For the long wave part of our calibration curve, on which the values of these wave-lengths depended, observations were made on the spectrum of water by L. R. Weber, using the recording spectrometer. Wave-lengths of some of these lines were measured by Norman Wright and H. M. Randall, using a large grating and residual rays from quartz. Wave-lengths of other lines were taken from observations on atmospheric absorption made with a combination spectrometer by E. K. Plyler. One of the lines of carbon dioxide and the center line of methyl bromide were measured directly with a grating by E. F. Barker and P. E. Martin. A very convenient material was acetylene, which furnished a wave-length determined by Levine and Meyer. In taking the photographic records the author has the efficient help of V. H. Fraenckel.

Note added June 29, 1931. Information now available, after the proof of this article had been read and returned, indicates that the values given for the wave-lengths in the ammonia spectrum are too great. These values are hereby withdrawn. The wave-length of the center of line No. 4, given as 16.09μ, is probably nearly 15.92μ. The values for the other materials are still believed to be correct

[9] Cl. Schaefer and F. Matossi, Das Ultrarote Spektrum, Springer, Berlin, 1930, p. 225.

THE TRANSMISSION OF VISIBLE LIGHT THROUGH FOG

By H. G. Houghton
Round Hill Research Division
Massachusetts Institute of Technology

(Received March 23, 1931)

Abstract

Measurements were made on the transmission of visible light through artificial fog which was produced by condensing low pressure steam in a chamber 300 cm long and about 25 cm square. Curves for several fog densities were obtained and they all indicated a definite maximum transmission at about 0.490μ. The relation between the transmission of light through fog and the fog density was found to be practically linear. The maxima obtained are not in agreement with the results of other investigators but a comparison of the particle sizes of the fogs used in this work with those of the fogs used by others leads to the conclusion that the shape of the transmission curve is dependent on the particular particle size or sizes of the fog on which the measurements are made.

DUE to the increasing importance of commercial aviation considerable experimental work has been done on the transmission of light through fog and it is now generally realized that no type of visible radiation possesses any marked fog penetrating powers. However, since complete lighting equipment is required in any event for night flying, it seems that advantage should be taken of even the small increase in visibility to be expected from the use of the proper type of light. Much of the existing experimental data on this problem are purely qualitative and depend to a large extent on individual judgment under special conditions. Such quantitative data as are available are somewhat difficult of analysis and of comparison because of the different conditions under which the measurements were made. The work described in this paper was undertaken with the hope of clarifying the problem and indicating the type of light most effective for fog penetration.

Due to the uncertainty of the occurrence of natural fogs and the desirability of controlling the density, all measurements were made on artificial fog. This also simplified the measurement of the density of the fog and the size of the fog particles. The fog was produced by condensing low pressure steam in a zinc-lined wooden chamber 300 cm long and about 25 cm square. At one end of this chamber were located the incandescent lamp light sources, the necessary optical systems and filters for obtaining various bands of wavelengths in the visible spectrum. At the far end of the chamber was located the detecting apparatus which consisted of a photoelectric cell, a two-stage direct current vacuum tube amplifier and a sensitive milliammeter.

In order to duplicate more closely natural fogs, no condensation nuclei were added, the steam condensing on the nuclei normally present in the air. The only apparent difference between artificial fog produced in this manner

and natural fog is the size of the fog droplets, the artificial fog being composed of somewhat smaller particles of more uniform size.

In a chamber of such small dimensions as the one described above, the density of the fog changes quite rapidly due to settling and condensation and it was found desirable to produce a new fog for each reading. It was, therefore, necessary to have a means for duplicating a given fog a number of times. Due to variations in humidity, temperature and the number and size of the condensation nuclei, it is not feasible to duplicate fogs by admitting a given amount of steam at a specified pressure. After some experimentation, it was decided that for the purposes of this work, a fog could be satisfactorily specified by the transmission of a standard light which is assumed to have a constant candle power and spectral distribution. In this paper fog density is defined as the ratio of the intensity of the standard light after passing through the fog to its initial intensity and is expressed as a decimal fraction. This method permits of a continuous reading of density. This is desirable since a dense fog may be formed and allowed to settle to the desired value thereby obtaining a more uniform and less turbulent fog.

Although a spectroscope or a source with conspicuous line spectra would probably have proved advantageous, an incandescent lamp source together with suitable gelatine filters was chosen because of their greater convenience, a choice justified by the small changes of transmission with wave-lengths. The pass bands of the filters used ranged in width from about 0.030 to 0.050 μ and the visible spectrum was fairly well covered with eight filter combinations. Certain of these filters had additional pass bands in the infrared which, however, did not affect the results because of the selective action of the photoelectric cell. The attenuation of the filters in the pass bands was so high that a 200 watt concentrated-filament lamp was required to obtain sufficient illumination. Some difficulty was experienced in obtaining a parallel beam from this source but this was finally accomplished by first focussing the light on a small iris which was in turn at the focus of a second collimating lens. This system exhibited some chromatic aberration but in view of the relatively narrow bands of wave-lengths used this was not considered detrimental.

A second light source was used to specify the fog density as described above. No filters were employed so it was possible to use a lamp of lower candle power which had a very small filament. To insure constant candle power this lamp was operated at somewhat under rated voltage from a storage battery. A simple, long focus lens system sufficed to produce a parallel beam with no appreciable chromatic aberration. Both lamps remained lighted at all times during the measurements in order to maintain a constant illumination. The beams were controlled by shutters which, for convenience, were arranged to be operated from the far end of the chamber where the measuring apparatus was located.

Some difficulty was experienced in finding a photoelectric cell which would be sensitive over the entire visible spectrum, many of them being useless above 0.500μ. One was finally obtained which was quite satisfactory

throughout the desired range and in addition cut off in the near infrared where some of the filters had extraneous pass bands. The cell was mounted behind a glass window at one end of the fog chamber and the light sources were adjusted so that each beam completely covered the cathode of the cell. In order to prevent condensation on the glass window a shutter was placed before it and so arranged that it was only opened while a reading was actually being taken. The filters were similarly protected by the shutters used for controlling the light beams.

The photoelectric currents were amplified to readable values by means of a two-stage direct current vacuum tube amplifier. In order to obtain sufficient stability and to prevent excessive extraneous pick-up the amplifier was constructed of the most stable circuit elements available and the circuit was so arranged that all batteries could be grounded as shown in Fig. 1. It

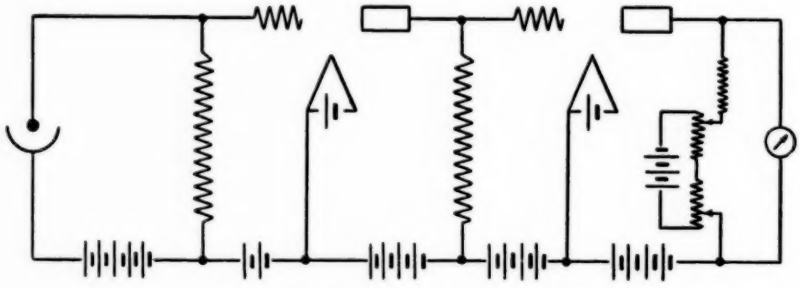

Fig. 1. Amplifier for photoelectric cell.

was also found desirable to ground the metal lining of the fog chamber and to shield the photoelectric cell and the first amplifier stage. The overall characteristic of light intensity on the photoelectric cell versus amplifier output current proved to be substantially linear but this curve was used as a calibration curve in all of the measurements.

The transmission of the light was expressed as the ratio of the intensity of the light transmitted through the fog to the initial intensity. In this way it was not necessary to measure absolute values of intensity. Runs were taken over the visible spectrum at a constant fog density. A curve may be obtained from these data by plotting the transmission ratio against an average wave-length for the filter combination used. Several such curves for different fog densities are given in Figs. 2, 3 and 4. It will be noted that each of these curves has a definite maximum at about 0.490μ. Sufficient data were taken in each case to eliminate any experimental errors. The possible effect of the previously mentioned infrared pass bands of some of the filters was tested by including additional filters which definitely excluded this region and no differences were noted in any case. There were no known pass bands in the ultraviolet but this region was effectively eliminated by the large amount of glass in the optical system.

Because of the finite width of the pass bands of the filters, the curves as given do not represent the true spectral transmission. The true curve would

have a somewhat sharper maximum but it happens that the filter used to obtain the point at 0.490μ has a very narrow pass band so that the error is not very great.

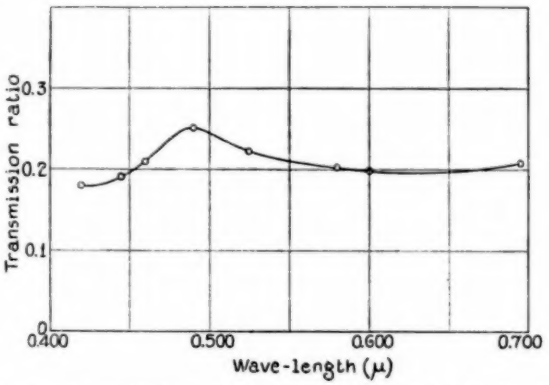

Fig. 2. Transmission of light through a fog of 0.20 density.

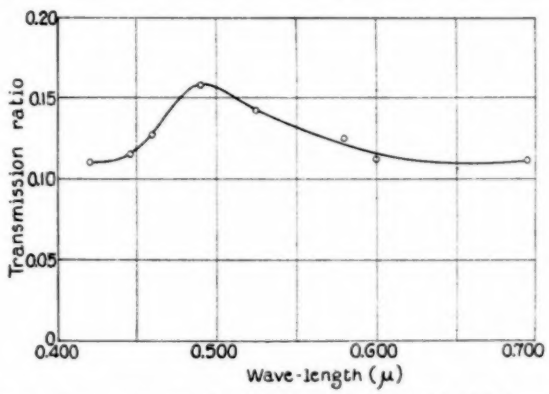

Fig. 3. Transmission of light through a fog of 0.125 density.

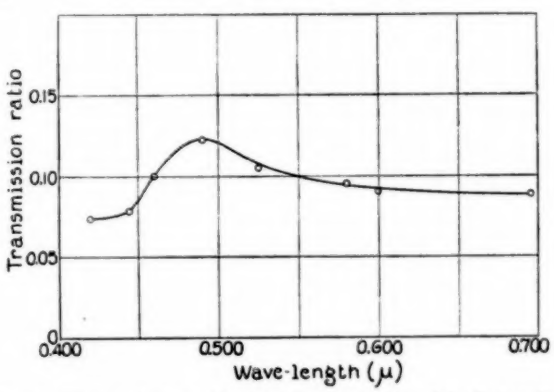

Fig. 4. Transmission of light through a fog of 0.10 density.

A second set of curves can be obtained from the same data by plotting transmission ratio against fog density for a given wave-length. Several such curves are given in Fig. 5. It will be noted that they are all practically linear

as is to be expected if the particles scatter independently although they must obviously pass through the point (1, 1). They are at least sufficiently linear to permit of reasonable extrapolation to fogs of less density than those used in this investigation.

Comparable measurements on the transmission of light through fog have been made by Utterback,[1] Granath and Hulburt,[2] and Anderson.[3] Utterback used artificial fog produced by the sudden expansion of moist air, but his measurements were made by means of a Macbeth illuminometer and so apparently include the sensitivity curve of the eye. This curve is so markedly peaked that it would effectively mask the transmission curve for the fog alone. This is borne out by the location of Utterback's maximum at 0.560μ which

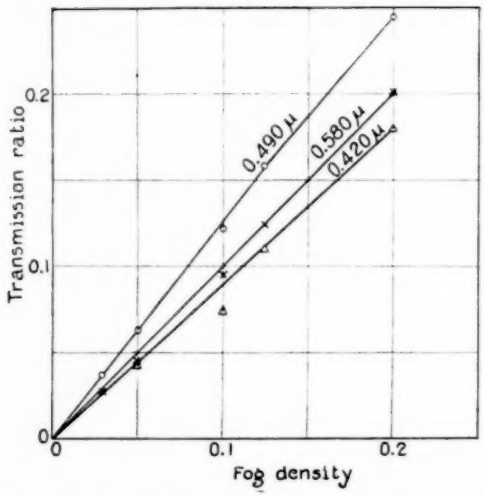

Fig. 5. The transmission of light of a single wave-length through fog as a function of fog density.

corresponds almost exactly to the accepted average value for the peak of the eye sensitivity curve. Granath and Hulburt made all of their measurements on natural fogs using a quartz spectrograph and a recording densitometer in the visible spectrum. The measurements were also extended into the infrared using relatively wide bands of radiation. Their results show no peaks, merely a gradual increase in transmission for the longer wave-lengths.

Anderson used artificial fog made with artificially introduced hygroscopic nuclei. His measurements were made with filters and a photoelectric cell much as described in this paper and in common with Granath and Hulburt he found no maximum transmission but merely a rise towards the red end. Anderson also gives curves similar to those of Fig. 5, which are also practically linear.

The attenuation of light by fog is probably due principally to scattering rather than absorption. The classical solution of this problem, when the

[1] C. L. Utterback, Trans. I. E. S. **14,** 133–140, No. 3 (1919).
[2] L. P. Granath and E. O. Hulburt, Phys. Rev. **34,** 140 (1929).
[3] S. H. Anderson, Aviation **28,** No. 19, May 10 (1930).

particles are small compared to the wave-length, was given by Lord Rayleigh[4] who found that the intensity of the scattered light varied inversely as the fourth power of the wave-length. This serves to explain the red sunsets and the red appearance of the sun when viewed through so-called "smoke fogs," but hardly applies to true fogs where the particles are larger than the wave-lengths of visible light.

The definite maxima of the curves obtained in this work and the total absence of any such peaks in the results of other investigators suggests a difference in the fogs used. The curves of Fig. 5 together with Anderson's similar results indicate quite definitely that it is not a question of the density of the fog. It appears reasonable to suppose that the size of the particles is a controlling factor in the location of the wave-length of maximum transmission and it was, therefore, decided to determine the size of the particles of the fogs used.

The method of corona measurements as employed by Kohler[5] and others for measuring the droplet size of natural fogs appeared to be a convenient means and an attempt was made to apply it to this problem. Either due to space limitations in the fog chamber, the small size of the particles or to imperfections of the apparatus, results from the corona measurements were entirely unsatisfactory. Furthermore, corona measurements give no indication of the distribution of particle size but merely an average value.

Recourse was next had to the microscope. Due to the transparency of the droplets and their rapid motion it is rather difficult to view them microscopically. It was found desirable to employ very intense transverse or dark field illumination. This type of illumination gives rise to various diffraction disks which make it possible to detect ultramicroscopic particles but which are somewhat confusing in the case of larger particles. With a little care it was found possible to identify definitely the fog droplets. Even with the lowest power objective which could be used the motion of the particles across the relatively limited field of view was so rapid that no size comparisons could be attempted. To reduce this motion a small glass chamber with sliding doors was fitted over the end of the objective. In this way, it was possible to trap a number of fog particles and hold them relatively still although there was still considerable motion due to eddies, settling, and possibly Brownian motion. Size comparisons were made by placing objects of known size in the eyepiece of the microscope. It was found that the droplets were quite uniform and ranged from about two to three microns in diameter. Attempts to photograph the particles were entirely unsuccessful due to the low illumination and the rapid motion of the particles.

Although no definite information is available, it seems that the particles of the natural fogs used by Granath and Hulburt and of Anderson's artificial fogs were larger than two or three microns. This leads to the conclusion that the shape of the transmission curve is largely dependent on the particle size

[4] Lord Rayleigh, Phil. Mag. **41,** 107–274 (1871).

[5] Hilding Kohler, Meddelanden Fran Stratens Meteorologist—Hydrografiska Anstalt **2,** No. 5 (1925).

of the fog used and, therefore, that any transmission curve is applicable only to the particular fog on which the measurements were made. Thus the results obtained in this work might well apply to a particular small particle natural fog or haze but would have no application whatsoever to larger particle fogs.

In view of the above it was decided to undertake a theoretical investigation of the problem which could be verified by these particular experimental results and then extended to other types of fog. The definite maxima of the experimental curves make them particularly suitable for this purpose. This theoretical work has been completed and is presented in another paper.

Apart from the transmission of the radiant energy through the fog there are other extremely important factors which affect the visibility of lights in fog. As previously noted, the sensitivity curve of the eye is so markedly peaked that a maximum of the magnitude obtained in this work would be completely masked. This would, of course, not apply to infrared or other radiations beyond the visible spectrum where other than visual means of detection are employed. In the case of visible light, the nature of the background against which the light is viewed is of the utmost importance. Thus, it appears certain that against the white background commonly produced by general illumination in fog, a red light would be much more effective than a white one. Apparently very little work has been done on this question of contrast and it seems that a study of the problem together with a proper consideration of the eye sensitivity curve would produce valuable results.

A THEORETICAL INVESTIGATION OF THE TRANSMISSION OF LIGHT THROUGH FOG

By J. A. Stratton and H. G. Houghton
Round Hill Research Division
Massachusetts Institute of Technology

(Received March 23, 1931)

Abstract

This theoretical investigation was undertaken in an attempt to explain some unexpected experimental results which are described in detail in another paper. The fog droplets are assumed to be dielectric spheres with an index of refraction of 1.33 and the development is based on the work of Mie and Debye on the pressure of light and the colors of colloidal solutions. The results show that the particle size of the fog is a controlling factor in the transmission characteristics of the fog. By assuming the appropriate particle size a theoretical transmission curve is obtained which closely corresponds to the experimental data. In conclusion, it is pointed out that the King formula is not applicable to the scattering of light by particles as large as fog drops.

THIS theoretical investigation of the transmission of light through fog was undertaken as a result of some rather unexpected and interesting experimental results which have been described in another paper. Instead of the gradual increase in transmission from the blue to the red end of the visible spectrum as observed by several experimenters, a definite maximum was found at about 0.490μ. Measurements showed that the particles of the fog used were somewhat smaller than would be expected in natural fog and in the artificial fogs employed by other investigators. It appeared reasonable to suppose that the observed maximum was dependent on the particle size of the fog and that for the larger particle fogs the maxima were beyond the range of the measurements or in regions where other factors are of greater importance. It is the purpose of this paper to obtain a theoretical confirmation of the experimental results with the hope of extending these results to other regions of the spectrum and to fogs having different particle sizes.

Although this particular problem has apparently not been treated heretofore, the general method of attack has been developed by Mie,[1] Debye,[2] Jobst[3] and others in their work on the colors of colloidal solutions and the pressure of light. A general outline of the solution of the problem is given below but for a detailed exposition the reader is referred to the excellent papers of Mie and Debye.

Consider a sphere of a given material suspended in a medium of a second material. The field equations for this case are expressed in spherical coördinates so that the boundary conditions may be more readily introduced. In

[1] G. Mie, Ann. d. Physik **25,** 377 (1908).
[2] P. Debye, Diss. München, 1908, Ann. d. Physik **30,** 57 (1909).
[3] G. Jobst, Ann. d. Physik **76,** 863 (1925).

order that the fields may be represented by simple scalar potentials the total field is arbitrarily split into two partial fields which are so defined that the radial magnetic component of the first and the radial electric component of the second are zero. There are then four partial fields, two within the sphere and two outside each of which may be represented by a scalar potential. For each of these potentials a wave equation of the form

$$\Delta^2 p + m^2 p = 0 \qquad (1)$$

may be developed where p is one of the partial potentials. This differential equation is solved by replacing p with the product of three functions each dependent on a single variable and thereby obtaining three differential equations. The solutions of these equations are known and are, respectively, a Hankel function, a Legendre polynomial and a circular function and the solution of the original wave equation is then the product of these three functions. The boundary conditions now may be readily introduced by equating the tangential components of the inner and outer fields at the boundary of the two media.

Now consider a plane polarized incident wave travelling in the direction of the negative Z axis with its electric vector along the X axis. To be consistent with the above developments for the secondary fields of the sphere the field of this incident wave is represented by two scalar potentials expressed in spherical coordinates. The total field external to the sphere consists of the field due to the incident wave plus the field of the wave reflected from the sphere.

Up to this point this outline has very closely followed the development as given by Debye[4] and the reader is referred to this paper for details. Debye was interested in the pressure of light and the remainder of his derivation is not directly applicable to our problem. Mie,[5] however, was studying the colors exhibited by colloidal solutions and we may follow him from this point.

The energy loss due to the sphere is given by the surface integral taken over the sphere, of the time average of the Poynting or energy-flow vector of the total field. By collecting the terms involving only the incident wave, those containing only the reflected wave and lastly those terms containing a combination of the two, the integral may be separated into three components. The value of the integral including only the incident wave taken over the surface of the sphere is evidently equal to zero. The second integral represents the portion of the energy which is r radiated by the sphere. The third integral gives the total energy loss including both the absorbed and the reradiated portions. The absolute value of this integral is given by

$$|A| = \frac{\lambda^2}{2\pi N_a^2} Re \sum_{u=1}^{\infty} (-1)^u (2u+1)(C_u^1 + C_u^2) \qquad (2)$$

where

[4] P. Debye, reference 2.
[5] G. Mie, reference 1.

$$C_u^1 = (-1)^u \frac{N_a\psi_u(x)\psi_u'(y) - N_i\psi_u'(x)\psi_u(y)}{N_a\phi_u(x)\psi_u'(y) - N_i\phi_u'(x)\psi_u(y)}$$

$$C_u^2 = (-1)^u \frac{N_i\psi_u(x)\psi_u'(y) - N_a\psi_u'(x)\psi_u(y)}{N_i\phi_u(x)\psi_u'(y) - N_a\phi_u'(x)\psi_u(y)}$$

λ is the wave-length of the incident wave; a is the radius of the sphere; $x = 2\pi a N_a/\lambda$; $y = 2\pi a N_i/\lambda$; N_a = complex index of refraction of medium outside of sphere; N_i = complex index of refraction of the sphere; $\psi_u(x) = (\pi x/2)^{1/2} J_{u+1/2}(x)$; $\phi_u(x) = (\pi x/2)^{1/2} H^2_{u+1/2}(x)$ and Re = real part of. Primes denote first derivatives with respect to x or y.

It is assumed that the spheres are so far apart that the scattering is incoherent so that if the number of spheres per unit of volume is n we may write for k the coefficient of absorption or the energy loss per unit of volume

$$k = n|A| . \tag{3}$$

For values of x which are large compared to unity Jobst[6] has derived certain approximate expressions for $|A|$ with the aid of Debye's semi-convergent developments of Bessel and Hankel functions.[7] These expressions unfortunately do not apply to the region of principal importance in this investigation and it was necessary to obtain $|A|$ by direct summation of Eq. (2).

For the special case of fog it has been assumed that the fog droplets are dielectric spheres having an index of refraction of 1.33. Hence

$$N_a = 1 \quad N_i = 1.33$$

$$y = 1.33x.$$

Since fog droplets are formed around nuclei of hygroscopic salts, the conductivity is not zero but the inclusion of a finite conductivity would increase the complexity of the expression for $|A|$ to such an extent that numerical evaluation would be practically impossible.

For the purposes of the numerical summation of $|A|$ it is convenient to arrange C_u^1 and C_u^2 as follows

$$C_u^1 = (-1)^u \frac{\psi_u(x)\psi_u'(1.33x) - 1.33\psi_u'(x)\psi_u(1.33x)}{\phi_u(x)\psi_u'(1.33x) - 1.33\phi_u'(x)\psi_u(1.33x)}$$

$$\phi_u(x) = \psi_u(x) + i\chi_u(x)$$

$$\phi_u'(x) = \psi_u'(x) + i\chi_u'(x)$$

where

$$\chi_u(x) = (-1)^u \left(\frac{\pi x}{2}\right)^{1/2} J_{-u-1/2}(x)$$

[6] H. Jobst, reference 3.

[7] P. Debye, Math. Ann. **67**, 535 (1909).

whence

$$C_u^1 = (-1)^u \frac{B}{B + iD}$$

and

$$ReC_u^1 = (-1)^u \frac{B^2}{B^2 + D^2}$$

where

$$B = \psi_u(x)\psi_u'(1.33x) - 1.33\psi_u'(x)\psi_u(1.33x)$$

and

$$D = \psi_u'(1.33x)\chi_u(x) - 1.33\psi_u(1.33x)\chi_u'(x).$$

An entirely similar expression may be obtained for ReC_u^2. In the processes of summation it was found that available tables of half order Bessel functions were rather limited and it was necessary to compute a number of these functions.

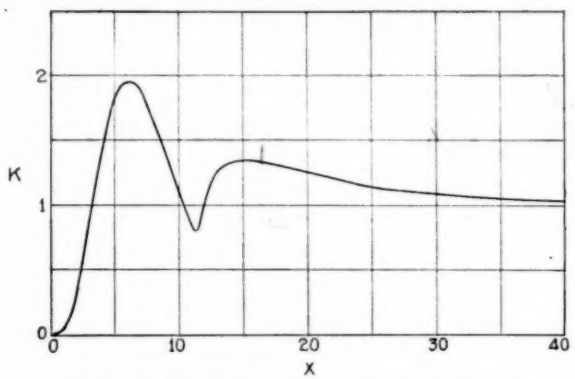

Fig. 1. Curve of K against x, where $x = 2\pi a/\lambda$.

The portion of $|A|$ under the summation sign is a numeric and is a function of x. Instead of multiplying this sum by $\lambda^2/2\pi$ to obtain $|A|$, thereby introducing a new variable, it is more convenient to multiply by $1/x^2$. The resultant expression is a function of x alone and is directly proportional to $|A|$. If this expression is designated by K we have

$$|A| = 2\pi a^2 K. \tag{4}$$

The curve for K as a function of x is given in Fig. 1. For values of x beyond the second maximum K has been computed from Jobst's approximate expressions referred to above. Care must be taken not to join these expressions just beyond the first maximum as this would eliminate the extremely important minimum.

An experimental curve for the transmission of light through an artificial fog is reproduced in Fig. 2. The methods employed in obtaining this curve are covered in detail in another paper.[8] The ordinates of the curve are ratios of the intensity of the light after passing through the fog to the initial inten-

[8] H. G. Houghton, "The Transmission of Visible Light Through Fog."

sity. This ratio will be hereafter called the transmission ratio or simply the transmission. For this case

$$E/E_0 = e^{-kZ} \tag{5}$$

where E is the final intensity, E_0 the initial intensity, Z the length of absorbing medium and k the coefficient of absorption. From Eqs. (3), (4) and (5)

$$E/E_0 = e^{-2\pi na^2ZK}. \tag{6}$$

The particles of the fog on which these measurements were made were found to range from about two to three microns in diameter but no values of n were determined. However, it is apparent from an inspection of Figs. 1 and 2, that

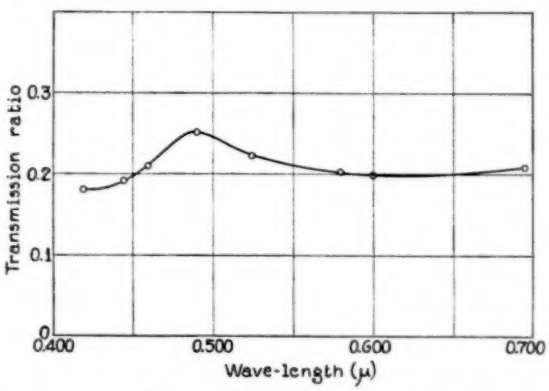

Fig. 2. Experimental curve for the transmission of light through a fog composed of particles, $2.5 \pm 0.5\mu$ in diameter.

the maximum of the experimental curve corresponds to the minimum of the K curve. From the curves

when $\lambda = 0.490\mu$ $E/E_0 = 0.245$

and when $x = 11.2$ $K = 0.825$

also since $x = \dfrac{2\pi a}{\lambda}$ $2a = \dfrac{11.2 \times 0.490}{\pi} = 1.75\mu$

This agrees as well as can be expected with the lower end of the observed range of particle diameters.

From Eq. (6)

$$2\pi na^2 = \frac{\log_e E_0/E}{K}$$

$$= \frac{\log_e (1/.245)}{0.825} = 1.705$$

so that $E_0/E = \log_e^{-1} (1.705K)$.

This expression is plotted in Fig. 3 but this curve is not directly comparable with Fig. 2 since the experimental points represent the transmission ratios for finite bands of radiation while the theoretical expression gives a true spectral curve. With the aid of the transmission curves of the filters used a

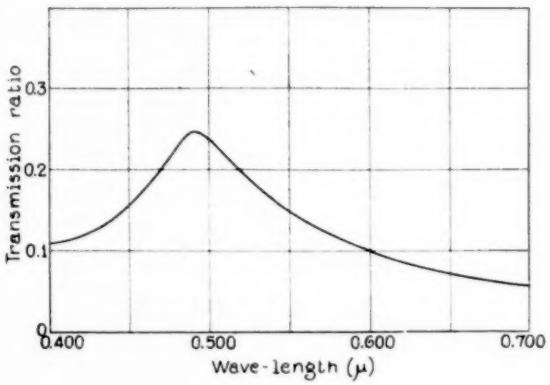

Fig. 3.

theoretical curve may be derived which can be compared directly with the experimental data. This curve is given in Fig. 4, together with the experimental data. The divergence of the two curves is due to the fact that the theoretical curve is for a single particle size while the experimental curve is

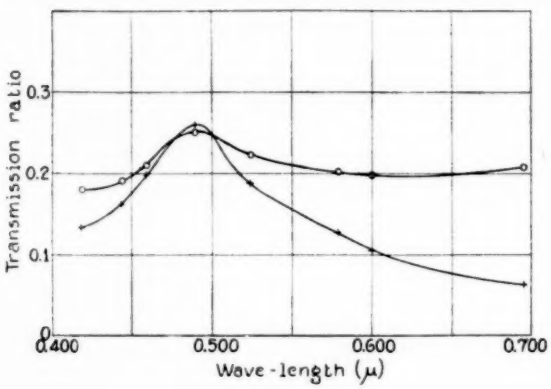

Fig. 4.

for a fog consisting of particles of various sizes within the range of two to three microns. Although a large number of the particles were evidently about 1.75μ in diameter, there were a sufficient number of other sizes present to keep the experimental curve above the theoretical curve. By a proper selection of as few as three particles sizes it was found possible to fit the experimental curve quite closely but in the absence of definite data on the size distribution of the particles such a curve is of doubtful value.

Although no very satisfactory methods of measuring fog particle sizes have been developed, it has generally been assumed that natural fog par-

ticles are from five to twenty microns in diameter. For the visible spectrum this corresponds to values of x greater than about twenty. By reference to Fig. 1 it will be seen that K is practically constant in this region and hence little change in transmission would be expected in the case of natural fog. In their measurements on natural fogs, Granath and Hulburt[9] found a very definite increase in transmission for the red end of the spectrum but observed no peaks. Anderson[10] obtained similar results in his work on artificial fogs. If the particle sizes of these fogs were as large as has been assumed, it is hardly possible to explain their results on the basis of this paper.

It has been assumed that the conductivity of the fog particles is negligible but it is possible that in the case of natural fogs the conductivity is sufficient to seriously modify the results. Although it does not appear feasible to obtain a K curve for a finite conductivity by direct summation it is probable that a curve for large values of x can be obtained by some of Jobst's approximate expressions. Work is now being undertaken to determine the probable conductivity of natural fog particles and further theoretical work will await the results of this investigation.

It is also possible that although the larger particles in natural fogs are five to twenty microns in diameter there are a sufficient number of smaller particles present to control the shape of the transmission curve. This can hardly be settled until data are available on the particle size distribution and work is now in progress to develop methods for making such measurements.

Several attempts have recently been made to use a formula given by King[11] as a theoretical expression for the transmission of light through fog. The King formula is essentially Rayleigh's inverse fourth power law for the scattering of light by particles which are small compared to the wave-length of the light. There is no theoretical justification for the application of this formula to the case of fog where the particles are larger than the wave-lengths of light but it may prove useful in some cases as an empirical expression.

The authors desire to take this opportunity to express their thanks to Mr. F. C. Breckenridge of the Bureau of Standards for his many helpful comments and his work in applying the results of this paper to the work of other investigators.

[9] L. P. Granath and E. O. Hulburt, Phys. Rev. **34,** 140 (1929).
[10] S. H. Anderson, Aviation **28,** No. 19, May 10 (1930).
[11] King, Proc. Royal Soc. **A88,** 83 (1913).

INTERFERENCE IN THIN METALLIC FILMS

By Hiram W. Edwards
University of California at Los Angeles

(Received February 2, 1931)

Abstract

The phenomenon of the colored appearance of thin metallic films sputtered upon glass or upon other metals, when viewed in white light, is explained as being caused by interference. Some qualitative observations of cyclic changes of color are given which support this viewpoint. Mathematical expressions are derived from Maxwell's electromagnetic equations to express the change of phase as the wave train is reflected from a metal surface in air, from metal in metal, for refraction as the wave enters the metal from air and from air into metal. Use of the values of the indices of refraction and absorption for massive metals indicates fair substantiation of experimental results. Fritze's values of the optical constants for thin metals do not seem to give agreement between theory and experiment. The thickness of the film of copper necessary to produce a yellow color (interference for $\lambda = 0.48\mu$) when calculated from the index of refraction (1.13) is found to be three and one-half times larger than the value found by weighing the total deposit. The balance of evidence seems to support the theory of interference.

Introduction

An occasional observation has been made of the fact that thin metallic films may appear to be variously colored when viewed in normal white light. Fritze[1] noticed that the color of a film of silver sputtered upon glass first appeared blue, then changed to violet and finally a clear red as the thickness increased. When red, the film thickness was from 2.4 to $2.9\mu\mu$. A chemically deposited silver film had likewise a red color when $4.7\mu\mu$ thick. Fritze offers no explanation other than that the color is a characteristic of pure silver in a film of such a thickness.

Other observers have thought that the color observed was due to some chemical compound. Recently Bockstahler and Overbeck[2] described "concentric rings of color similar in appearance to Newton's rings," when sputtering tin upon glass. They report a cyclic change of color as the thickness of the film increases. No explanation is offered.

The writer of this article reported[3] the color of nickel films sputtered upon platinum. The thinnest film to show a color appeared to be yellow. With increasing thickness the color changed to orange, purple, blue and then white.

The occasion for this paper is to offer an explanation for the observed phenomenon. It is thought that the production of colors under the indicated circumstances is due to interference between two beams of light in a manner which is very similar to that of the more familiar case of thin soap films or

[1] Fritze, Ann. d. Physik **47,** 763 (1915).
[2] Bockstahler and Overbeck, Bull. Phys. Rev. **5,** No. 7, Paper 39 (1930).
[3] Edwards, Phys. Rev. **33,** 463 (1929).

oil upon water. The distinguishing feature of the metallic case seems to be the more complicated manner in which difference of phase is produced.

The argument in favor of interference is based upon the following facts all of which have been observed by the writer and some of which have been reported by others:

(1). Colors are produced only when the film is transparent, obviously excluding those colors which are characteristic of massive metals such as the red of copper.

(2). The colors are more intense when a white metal such as silver, nickel, platinum, etc. (and therefore having a high reflection coefficient) lies under a thin film of some other metal.

(3). Several cycles of color may occur as the thickness of the thin film increases. In one case, i.e., that of copper upon silver, five distinct color cycles have been noticed. In this particular, the order was, first yellow then followed by gold, purple, blue and back to yellow. This indicated sequence of colors was also observed with copper upon nickel, and copper upon aluminum.

(4). The intensity of any one color increases up to a maximum in the series of cycles and then decreases. A single case will illustrate. The second appearance of blue when depositing copper upon "tin" foil was the most intense. In this particular case only three cycles were observed. At the first appearance of the blue the film was so thin that the reflecting power of the copper must have been small in comparison with that of the tin foil underneath. In the third appearance the transmission coefficient of the copper must have materially reduced the intensity of the transmitted beam.

(5). The color of the film varies with the angle of incidence which the white light makes with the film. This phenomenon required a change of incidence of 70°–80° in order for the color to make a pronounced change.

(6). In general the same cycle of colors is found to occur even though the pairs of metals used may be different. This is true so far as the writer's observations are concerned. A study of the theoretical considerations indicated that one should not expect the first color to appear to be the same in all cases.

(7). Different thicknesses of a particular metal sputtered upon other dissimilar metals are required to produce the first appearance of a particular color. This phenomenon was observed when sputtering copper upon contiguous strips of silver, nickel, and aluminum.

When considered collectively these facts seem to uphold the explanation of the color production as being one of interference. In addition to this qualitative evidence, a partial corroboration is to be found quantitatively. Equations are derived below which express the difference in phase of the two wave trains concerned in terms of the optical constants of the metals.

Theoretical Treatment

If we may assume that the color phenomenon under consideration is one of interference then we must determine the total difference in phase between the wave reflected from the surface of the metal in contact with air and the

wave emerging from that surface after reflection from the surface between the two metals. The total change in phase is due to five factors: (1) reflection at the surface between air and the first metal; (2) refraction at the same surface; (3) reflection at the surface between the two metals; (4) refraction as the ray which passes both ways through the first metal emerges into the air and (5) the optical length of the path traversed by the refracted ray.

In order to find expressions for the change of phase we may start with Maxwell's equation for the propagation of a wave in an absorbing medium

$$\frac{m\epsilon}{c^2}\left(\frac{\partial^2 E}{\partial t^2} + \sigma \frac{\partial E}{\partial t}\right) = \nabla^2 E \tag{1}$$

where m is the magnetic permeability, ϵ the dielectric constant, σ the specific conductivity of the medium, and E the electric field intensity. For the media under consideration we may put both m and ϵ equal to unity. If the wave front is plane and parallel to the Z axis then the equation becomes:

$$\frac{1}{c^2}\left(\frac{\partial^2 E}{\partial t^2} + \sigma \frac{\partial E}{\partial t}\right) = \frac{\partial^2 E}{\partial x^2} + \frac{\partial^2 E}{\partial y^2}. \tag{2}$$

Since the disturbance is periodic and may be put proportional to $pe^{-i\omega t}$ when p may be complex, we may write

$$-\frac{1}{c^2}(i\omega\sigma + \omega^2)E = \frac{\partial^2 E}{\partial x^2} + \frac{\partial^2 E}{\partial y^2}$$

or

$$\frac{\partial^2 E}{\partial y^2} + \frac{\partial^2 E}{\partial y^2} + A^2 E = 0 \tag{3}$$

in which A depends upon the constants. A is real only when $\sigma = 0$.

For a particular solution of (3) we have

$$E = E_0 e^{i(ax+by-\omega t)}. \tag{4}$$

Substituting this value of E in Eq. (3) gives:

$$a^2 + b^2 = A^2.$$

If there is no absorption a and b are both real. In the case of absorbing media a and b are both complex and may be expressed as follows

$$a = \frac{2\pi}{\lambda'}\cos\theta + ik_1 \quad b = \frac{2\pi}{\lambda'}\sin\theta + ik_2.$$

If we take the direction of propagation of the wave along x and use the following defining equations

$$k_1 = \frac{2\pi}{\lambda}\kappa\cos\alpha, \quad k_2 = \frac{2\pi}{\lambda}\kappa\sin\alpha, \quad \nu = \frac{\lambda}{\lambda'} = \frac{c}{v}$$

when λ is the wave-length in air and λ' the wave-length in the absorbing medium, then the equation for E becomes:

$$E = E_0 e^{-2\pi\kappa x/\lambda} \cos \frac{2\pi\nu}{\lambda}(x - vt)$$

and

$$a^2 + b^2 = \frac{4\pi^2}{\lambda^2}\left[\nu^2 - \kappa^2 + 2i\nu\kappa \cos(\theta - \alpha)\right] \tag{5}$$

$$= \frac{4\pi^2}{\lambda^2}(\nu + i\kappa)^2 \tag{6}$$

if the light is incident normally to the surface. In these expressions ν is the ordinary optical index of refraction and κ the absorption index.

In order to simplify the mathematical detail we shall determine the change of phase for the phenomenon of reflection at the boundary surface between any two media and for refraction as the ray passes from one medium into the other. We shall use the subscript 1 to designate the constants of the first medium and the subscript 2 for the second medium and assume that the wave is plane polarized with E perpendicular to the plane of incidence. We may then write expressions for E as follows:

In the incident wave $e^{i(a_1x+by-\omega t)}$
In the reflected wave $re^{i(-a_1x+by-\omega t)}$
In the refracted wave $se^{i(a_2x+by-\omega t)}$

By the use of the usual boundary conditions, it follows that

$$1 + r = s \text{ and } a_1(1 - r) = a_2 s$$

hence

$$r = \frac{a_1 - a_2}{a_1 + a_2} \quad \text{and} \quad s = \frac{2a_1}{a_1 + a_2}. \tag{7}$$

It may be shown that the wave velocities in the first medium and in the second medium, respectively, are:

$$v_1 = \frac{c}{(a_1^2 + b^2)^{1/2}} \qquad v_2 = \frac{c}{(a_2^2 + b^2)^{1/2}}.$$

The ratio of the velocities (v_1/v_2) in the two absorbing media may be defined as the complex index of refraction which we will designate by μ. Hence, using Eq. (6), we may write:

$$\mu = \frac{(a_2^2 + b^2)^{1/2}}{(a_1^2 + b^2)^{1/2}} = \frac{\nu_2 + i\kappa_2}{\nu_1 + i\kappa_1}. \tag{8}$$

In order to simplify this expression we may put $\mu = C + iD$ where

$$C = \frac{\nu_1\nu_2 + \kappa_1\kappa_2}{\nu_1^2 + \kappa_1^2} \qquad D = \frac{\nu_1\kappa_2 - \nu_2\kappa_1}{\nu_1^2 + \kappa_1^2}. \tag{9}$$

By assigning the direction of propagation of the disturbance parallel to the x axis it follows that $\mu = a_1/a_2$ and hence Eqs. (7) become:

$$r = \frac{\mu - 1}{\mu + 1} \quad s = \frac{2\mu}{\mu + 1}. \tag{10}$$

Since r is the amplitude of the reflected wave, assuming the amplitude of the incident wave is unity, the intensity J^2 and change of phase δ may be found in the usual manner by putting

$$r = Je^{i\delta} = \frac{C - 1 + iD}{C + 1 + iD}.$$

If the right hand member is designated by the symbol M and N is used for the conjugate of M, then the intensity of the reflected wave is

$$J^2 = MN = \frac{(C - 1)^2 + D^2}{(C + 1)^2 + D^2} \tag{11}$$

and the desired expression for the change in phase of the reflected wave is:

$$\tan \delta = \frac{M - N}{i(M + N)} = \frac{2D}{C^2 + D^2 - 1}. \tag{12}$$

The change in phase which the wave experiences on refraction is found in a similar manner using the expression for s, as given in Eq. (7), as a starting point. The result is

$$\tan \delta = \frac{D}{C^2 + D^2 + C}. \tag{13}$$

The two general expressions for the phase difference as given by Eqs. (12) and (13) may now be applied to the four particular cases in the present problem. For air $\nu = 1$ and $\kappa = 0$.

The phase difference (δ_1) on normal reflection of the incident wave at the first metal is

$$\tan \delta_1 = \frac{2\kappa_1}{\nu_1^2 + \kappa_1^2 - 1}. \tag{14}$$

As the wave enters the first metal from air the phase change (δ_2) is:

$$\tan \delta_2 = \frac{\kappa_1}{\nu_1^2 + \kappa_1^2 + \nu_1}. \tag{15}$$

When the transmitted wave is reflected back into the first metal from the boundary surface between the two metals the phase change (δ_3) is given by the expression:

$$\tan \delta_3 = \frac{2D}{C^2 + D^2 - 1}. \tag{16}$$

As the transmitted ray emerges from the first metal into air the phase change (δ_4) may be written:

$$\tan \delta_4 = \frac{-\kappa_1}{1 + \nu_1}. \tag{17}$$

The phase change (δ_5) due to length of the optical path traversed by the transmitted wave passing twice through the first metal of thickness d is:

$$\delta_5 = \frac{2d}{\lambda'} \times 2\pi. \tag{18}$$

The total phase difference δ may be then written:

$$\delta = \delta_2 + \delta_3 + \delta_4 + \delta_5 - \delta_1. \tag{19}$$

Experimental Results

The apparatus consisted of a sputtering chamber, a vacuum pump, synchronous rectifier and a one-half kilowatt 10 kv transformer. The sputtering chamber had a volume of about 2 liters. A small piece of glass ($\frac{1}{2} \times 2 \times 4$ cm) was placed in the chamber upon an inverted beaker with the receiving surface about 2 cm below the cathode. Usually a narrow strip of foil (silver, nickel or aluminum) was folded about the piece of glass, so that both glass and metal strip were sputtered at equal rates. Sometimes 2 or 3 strips of different metals were used simultaneously. Argon was used as a residual gas. The pressure in the chamber was kept constant at 0.04 mm which made the edge of the Crookes dark space tangent to the receiving surfaces. All metal parts (except the cathode) in the apparatus were made of aluminum. A piece of mica covered the receiving surface during a preliminary sputtering period. This was necessary in order to be able to adjust the pressure to the desired value and also to permit the cathode to warm up to a temperature at which the radiation losses equalled the heating effect of the discharge. This precaution is very necessary if one wishes to maintain a constant rate of sputtering. Preliminary measurements indicated that a 20 minute warming up period carried the temperature, of the particular cathode used, to 350°C at which thermal equilibrium was established. When steady conditions were obtained the mica was removed by an electromagnet device.

The time-record of the appearance of colors commenced at the instant of uncovering the receiving surfaces. It is impossible to assign a definite time of appearance for any particular color because the change of color is continuous and gradual. A record of the color was made at small intervals of time from which data one may select a "middle" value for the appearance of a particular color. The following table presents a partial typical record. In this case copper was sputtered upon glass and strips of nickel and aluminum simultaneously.

The rate of deposit of the copper was determined by weighing the glass before and after sputtering. Precautions were taken to reduce errors in weighing to a minimum. In the particular illustration the thickness of copper deposited per minute was found to be 3.8×10^{-7}cm.

In this record the glass also showed color changes. Yellow was first to appear and this occurred at 15 minutes. Following this it became purple at 20, blue at 25, and yellow again at 32 minutes.

Sputtering was continued for 2 hours and during this time color changes became weaker and uncertain due to the accumulation of copper upon the walls of the glass chamber.

In not all cases was the succession of colors as definite as that given in Table I. It is possible that the surface of the metal strips in such cases may not have been properly cleaned.

TABLE I. *Appearance of colors upon Ni and Al when sputtered by Cu.*

Time (min.)	Nickel	Aluminum	Time (min.)	Nickel	Aluminum
2.	Yellow	Yellow	18	Yellow	Yellow
3.25	Gold	Gold	20	Yellow	Bluish yellow
4.5	Purple	Dark gold	22	Light purple	Light purple
6.	Dark purple	Purple	25	Dark purple	Purple
8.	Blue	Pruple	30	Blue	Purplish blue
9.	Blue	Blue	33	Bluish green	Blue
11.	Lighter blue	Blue	37	Yellow	Blue
13.	Still bluish	Lighter blue	40	Yellowish purple	Bluish
16.	Yellowish	Yellowish blue	44	Purple	

One particularly interesting observation was that when the pressure in the sputtering chamber was lowered to 0.01 mm no colors, except perhaps a pale yellow, appeared. In this case the rate of sputtering was not determined but was more than 10 times as rapid as it was under a pressure of 0.04 mm. It is not clear why the color formation occurs at one pressure and not at another. The existence of the fact, however, indicates that there may be a critical pressure through which sputtering conditions change rapidly.

APPLICATION OF THEORETICAL CHANGE OF PHASE TO EXPERIMENTAL RESULTS

Change of phase for a copper film upon aluminum.

We assume, for the appearance of a yellow color when viewed in white light, that blue light (selected value $\lambda = 0.48\mu$) is eliminated by interference. The following numerical values of the optical constants for massive metals were taken from the International Critical Tables:

$$\text{Copper: } \nu_1 = 1.13,\ \kappa_1 = 1.96;\ \text{Aluminum: } \nu_2 = 0.93,\ \kappa_2 = 3.15$$

Substituting these values in Eqs. (14) to (17) gives:

$$\delta_1 = 43°30',\ \delta_2 = 17°23',\ \delta_3 = 30°35' \text{ and } \delta_4 = 137°20'.$$

Assuming that all of these changes of phase are in the same direction we find that $\delta_5 = 39°12'$, since δ must equal 180°. Reference to table 1 shows that a complete cycle of color change occurs in approximately 16 min. The time required to deposit sufficient metal to make $\delta_5 = 39°12'$ would be approximately 1/9 of 16 min. which is 1.8 minutes. The observed time for the first appearance of yellow is 2 minutes. This agreement is as good as could be expected.

Copper upon nickel.

Phase changes for a thin film of copper upon nickel were determined for appearance of a yellow color (interference produced in light for $\lambda = 0.46\mu$) by using the following constants for massive metals.

$$\text{Copper: } \nu_1 = 1.13,\ \kappa_1 = 1.92 \quad \text{Nickel: } \nu_2 = 1.46,\ \kappa_2 = 1.89$$

The calculated value of δ_5 was found to be $\pi + 110°$. Since $\tan(\pi + \alpha) = \tan\alpha$, we may assume that δ_1 was greater than that found by the formula by π. With this assumption $\delta_5 = 70°$ which would indicate that the yellow color should appear in 3.1 minutes. The observed time was 2 minutes.

These two illustrations may serve to indicate the character of confirmation obtained when using optical constants of massive metals. Fritze[4] has shown that the optical constants of metals vary also with the thickness of the sputtered film. When using his values of the constants for the thin metallic film, the calculated values of the change of phase did not agree with the experimental results.

Another test of the explanation given lies in an examination of the wave-lengths of light as determined by the thickness of the film. In the case of the deposition of a copper film upon aluminum or upon nickel the color cycles are of approximately the same length of time in each of the two cases. This fact substantiates interference.

We may also use the wave-length of a particular color to determine the thickness of the film. Using the index of refraction ($\nu_1 = 1.13$) of copper for $\lambda = 0.48\mu$ gives a value of 0.425μ for the wave-length in copper and for the thickness of the film a value of 0.212μ. Since a complete cycle of color change occurs in 16 min. (Table I) the thickness of the film is 0.0608μ. This latter value is approximately one-third of the former. The discrepancy is too large to be explained by possible errors in weighing the films, although it is possible that the rate of sputtering changes after the first few minutes of sputtering under the conditions of the experiment. The result given here is confirmed by a similar lack of agreement when sputtering other metals.

In conclusion it may be stated that the experimental evidence partially confirms the explanation of the colors of thin sputtered films as due to interference.

The writer wishes to express his appreciation of the services of Mr. Robert Wathen and Mr. Maxwell Kelch for their assistance in making experimental observations.

[4] Fritze, Ann. d. Physik **47,** 763 (1915).

THE MAGNETIC MOMENT OF THE DIATOMIC SULFUR MOLECULE

By E. J. Shaw and T. E. Phipps
Department of Chemistry, University of Illinois

(Received May 20, 1931)

Abstract

The magnetic properties of the diatomic sulfur molecule have been investigated by means of the Stern-Gerlach molecular-ray method. The diatomic sulfur was prepared by heating sulfur vapor at a pressure of 0.3 mm of mercury to temperatures of 300–450°C. At the higher temperature, the magnetic fields attainable were insufficient to break down the coupling between the rotational axis of the molecule and the spin axis of the electrons and only broadening of the image resulted. At 300°C the image was split into two lines, one at the position of the line obtained in the absence of a magnetic field and the other on the side of the stronger field. The results prove that the diatomic sulfur molecule possesses a magnetic moment due to electron spin; the indicated configuration is a $^3\Sigma$.

Introduction

SINCE the original application of the molecular-ray method for the determination of magnetic moments by Stern and Gerlach in 1922,[1] all applications of this method have been to atoms. However, a study of the magnetic properties of the molecules of paramagnetic gases would seem to be of interest. No satisfactory means of detecting a beam of oxygen or nitric oxide has been developed as yet. The diatomic sulfur molecule may be readily investigated by this method, detection consisting merely of condensation on a liquid air cooled surface until an image of sufficient depth to photograph is obtained.

Theoretical

The spectrum of the diatomic sulfur molecule has been investigated by Rosen[2] and by Henri and Teves[3] and has been found to be quite similar to that of oxygen which is known to have a $^3\Sigma$ ground state. Rompe[4] has analyzed the spectrum and drawn the conclusion that the ground state of S_2 is a $^1\Sigma$. There is some doubt concerning this analysis, since as Rompe points out, Rosen's results show a Q branch in what Rompe's conclusions indicate is a $^1\Sigma - {}^1\Sigma$ transition. More recently Naudé and Christy[5] have published a preliminary note on the analysis of the S_2 spectrum using much higher dispersion than Rompe did, and have found that the ground state is a $^3\Sigma$.

A $^1\Sigma$ state for the S_2 molecule is not in accord with its chemical behavior;

[1] W. Gerlach, and O. Stern, Zeits. f. Physik **8,** 110 (1922) ibid. **9,** 349 (1922).
[2] B. Rosen, Zeits. f. Physik **43,** 69 (1927); ibid. **48,** 545 (1928).
[3] Henri and Teves, Comptes Rendus **179,** 1156 (1924), Nature **114,** 894 (1924).
[4] R. Rompe, Zeits. f. Physik **65,** 404 (1930).
[5] Naudé and Christy, Phys. Rev. **36,** 1800 (1930).

the strong tendency which it shows to polymerize indicates an unsaturation such as might be expected from "unclosed shells," to use Mulliken's terminology. Also, its close relationship to O_2 would lead one to expect it to have a $^3\Sigma$ ground state. Unfortunately its magnetic susceptibility has not been determined.

The Stern-Gerlach experiment provides a convenient means of determining whether or not a molecule has a magnetic moment. A beam of $^1\Sigma$ molecules would be expected to pass undeflected thru an inhomogeneous magnetic field just as a beam of ^1S atoms would. Any other type of molecule would

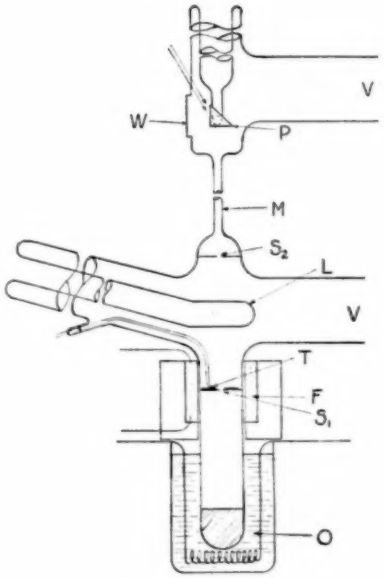

Fig. 1. Apparatus.

suffer deflection. A molecule with magnetic moment due to orbital electronic motion could not be expected to give a split image, since attainable magnetic fields would be far too low to uncouple the orbital axis from the molecular axis. In the case of Σ molecules, however, with a magnetic moment due to electron spin, it should be possible, at least in low rotational states, to uncouple the spin axis from the rotational axis of the molecule and obtain a split image. From this point of view, S_2 is not an ideal molecule to investigate, since sulfur vapor, even at the low pressure used in the Stern-Gerlach experiment, must be heated to about 300°C in order to give any considerable concentration of diatomic molecules; hence, low rotational states will not be favored. Splitting of the image is not necessary to show that a molecule is magnetic; broadening is sufficient to prove that.

The reader is referred to a preliminary note on this research for a further discussion of the theory.[6]

[6] E. J. Shaw, T. E. Phipps, and W. H. Rodebush, Phys. Rev. **35**, 1126 (1930).

Experimental

The apparatus is shown in Fig. 1. An electrically heated oil bath, O, stirred by means of a stream of air bubbles, maintains the sulfur at 155°C, at which temperature its vapor pressure is 0.3 mm.[7] The vapor passes up to the source slit, S_1, which is heated by means of an electric furnace, F, to a temperature of 300–450°C as measured by means of the platinum platinum-rhodium thermocouple, T. The thermocouple is welded to an annular sheet of platinum which serves to hold it in position and to make thermal contact with the glass. The thermocouple leads are brought out through separate small tubes sealed with deKhotinsky cement. The second slit, S_2, allows a beam of sulfur vapor to proceed through the tube, M, which passes between the pole-pieces of a large electromagnet, to the collecting surface on P, a liquid air cooled Pyrex prism. Between S_1 and S_2 is a liquid air cooled surface, L, which aids in removing the sulfur vapor which does not go through S_2 directly, and thereby prevents its undirected escape through S_2 and consequent fogging of the image. L also condenses any material which might volatilize from the deKhotinsky cement used to make the seals where the thermocouple leads leave the vacuum. The slits are 1.6 mm long and 0.03 mm wide, the distance between them being 70 mm. The distance from the second slit to the prism is about 85 mm. In front of the prism is an optical Pyrex window which makes possible the observation and photographing of the image at any time during the course of an experiment. The best visibility was obtained with light from the direction indicated by the parallel arrows.

The pole pieces used to produce the inhomogeneous magnetic field were the same as those used by Kurt and Phipps in their determination of the magnetic moment of the oxygen atom.[8]

Experimental procedure.

The vacuum pumps were started and the oil bath brought up to temperature. After pumping three or four hours, the furnace was brought to the desired temperature, liquid air was put in L, the current started through the magnet winding, and the prism cooled by means of liquid air. After two or three hours the line on the prism was visible. In order to develop side lines however, it is usually necessary to continue the experiment about five times as long as is required for the undeviated line. The experiment was usually terminated at the end of 14 hours.

At first it was believed that it would be desirable to have practically complete dissociation into S_2, so a temperature of 450°C was used at the bottom slit. Repeated attempts showed, however, that although in every case a widening of the central image was obtained, it was impossible to obtain the side lines that one would expect from a $^3\Sigma$ molecule. The temperature of the source slit was therefore lowered to 300°C so as to decrease the average rotational quantum number of the S_2 molecules. The concentration of the heavier

[7] O. Ruff, and H. Graf, Ber. D. Chem. Ges. **40,** 4199 (1907).
[8] O E. Kurt, and T. E. Phipps, Phys. Rev. **34,** 1357 (1929).

allotropic forms becomes rather high at this temperature, but this should serve only to make the undeviated line more pronounced. Under these conditions one side line was obtained and that on the side toward the higher field

Fig. 2. Images obtained. a, without field. b, field on, and source at 450°C. c, field on, and source at 300°C.

strength. This result indicates that the field strength at the normal position of the beam was just sufficient to uncouple the spin from the rotational axis in the case of the molecules in the lower rotational states. Those initially deflected in the direction of weaker field coupled again before passing through

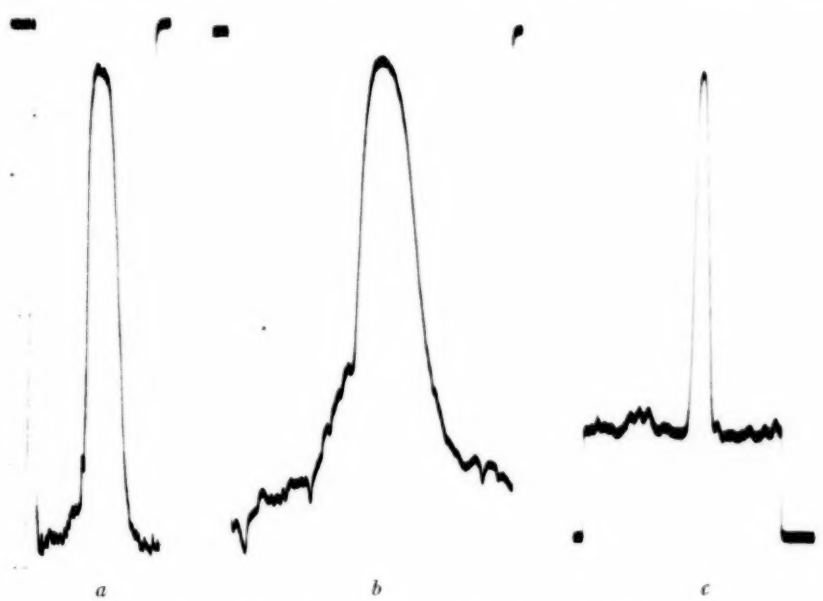

Fig. 3. Microphotometer records of images obtained.

the region of the field, and hence gave no line on that side. In order to show that the side line was caused by S_2, an experiment was made with the source slit at 200°C. The image obtained was indistinguishable from that obtained with no magnetic field.

Fig. 2 shows 10× magnifications of three characteristic results of experiments. *a* is the result obtained when no magnetic field was applied. *b* is an image obtained with the magnetic field and a source temperature of 450°C. *c* shows the split image obtained with the source at 300°C. Fig. 3 *a*, *b*, and *c* show microphotometer records of the corresponding photographs of images shown in Fig. 2.

It would seem desirable to determine the actual magnetic moment by comparing the deflection obtained with that obtained with a hydrogen atom. As the result of the form of the apparatus this could not be done with assurance that the beam would pass through the same part of the magnetic field as the sulfur beam did. A comparison of the deflection obtained with that obtained with hydrogen in a different apparatus with the same pole pieces indicates that the magnetic moment of S_2 is approximately 2 Bohr magnetons. This is the magneton value to be expected from a $^3\Sigma$ state.

Conclusion

The Stern-Gerlach experiment has been used to demonstrate that the ground state of the diatomic sulfur molecule is magnetic. The observation of a split image shows that it must be a Σ molecule, and since even multiplicities are excluded, the indicated conclusion is that the molecule is a $^3\Sigma$. This conclusion agrees with what would be predicted from the close relationship of S_2 to O_2, and with chemical and spectroscopic observations.

THERMOCOUPLES WHOSE ELEMENTS ARE LONGITUDINALLY AND TRANSVERSELY MAGNETIZED WIRES OF NICKEL AND OF IRON

By William H. Ross
Fayerweather Laboratory of Physics, Amherst, Massachusetts

(Received May 4, 1931)

Abstract

It has been shown that a thermal *emf* may be established between magnetized and unmagnetized elements of any ferromagnetic substance. In this paper the thermal emfs developed between longitudinally and transversely magnetized elements of the same ferromagnetic substance are quantitatively studied. Nickel and iron, both in the annealed and unannealed conditions, have been investigated.

IN 1856 Sir William Thomson[1] demonstrated, in a qualitative fashion, that if a continuous piece of an iron or a nickel wire were bent into a U-shaped form as shown in Fig. 1, it could be made to exhibit a thermal *emf* in a magnetic field. This thermocouple appears to be composed of elements which are longitudinally and transversely magnetized portions of the same piece of metal. Fig. 1 shows the arrangement of the wire and the magnetic field in

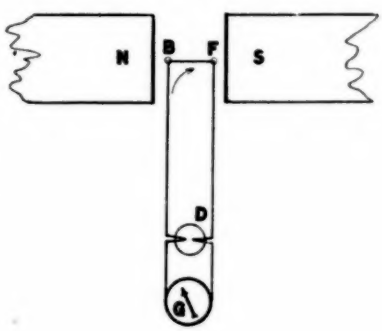

Fig. 1.

The direction of the current is from the transversely to the longitudinally magnetized portion through the hot junction.

which it was placed. The two bends, B and F, were kept at the temperature of steam and tap-water, respectively (100°C and 15°C). The latter was found by test to be remarkably constant. The field of the electromagnet NS is parallel to the section BF and transverse to the leads from B and F to the galvanometer.

Iron wire (Armco) was investigated first. It had the following chemical analysis:

[1] Thomson, Math. and Phys. Papers **2**, pp. 267–307.

Carbon	0.02 %	Sulphur	0.035%
Manganese	0.02 %	Silicon	Trace
Phosphorus	0.006%	Iron	99.9 %

The diameter of the iron wire was 0.690 mm and was studied both in the annealed and the unannealed state.

The bends, *B* and *F*, were 2.70 cm apart and the leads ran out normal to the field to a distance of about 100 cm where they were joined to copper leads connected to the galvanometer. These junctions, *D*, Fig. 1, were then placed in a thermos bottle to keep the two junctions at the same temperature.

The electromagnet had flat circular pole pieces of ferro-cobalt. These were 10.1 cm in diameter with a gap width of 4.25 cm. The field was determined both by a bismuth spiral and by a flip coil. The gap was topographically surveyed to find the most uniform section for the element *B-F*. At ten

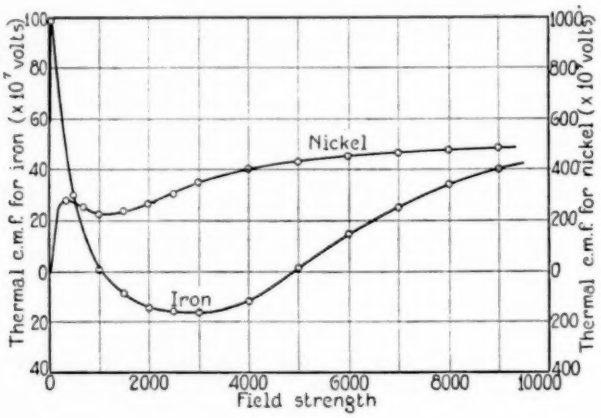

Fig. 2.

amperes this gap of 4.25 cm gave a field strength of 8500 gausses. Great care was taken to demagnetize the electromagnet before each new set of observations was taken.

In taking the observations, there were two ways which were followed: (1) The two junctions *B* and *F* were kept at steam and tap-water temperatures respectively, while the field was varied. Reversal of the field did not change the direction or the magnitude of the *emf*. (2) The steam and tap-water, by a system of reversing valves, were directed alternately to the two bends while the field was varied. Interchanging the temperatures of the two bends reversed the direction of the *emf*.

From these two methods various sets of observations were obtained and averaged. The shape and character of the curve showing the relation between the field strength and the *emf* developed, were reproduced time and again with great fidelity. Due to a slow change in temperature of the entire circuit, a slow creeping of the galvanometer constant always occurred but the average of deflections to right and to left rendered this error negligible. In Fig. 2 the curve is shown for annealed iron (Armco) wire.

In a similar fashion both annealed and unannealed nickel wires were studied. The chemical analysis of the nickel was:

Carbon	0.10 %	Silicon	0.06 %
Manganese	0.20 %	Copper	0.03 %
Iron	0.16 %	Nickel	99.42 %
Sulphur	0.005%		

The diameter of the nickel wire was 0.810 mm. The relation between the magnetic field applied and the *emf* produced in the annealed sample of nickel wire is shown in Fig. 2. It is to be noted that the thermal *emf* for nickel is very much larger than for iron. The curves for the unannealed wires are not shown as they are very similar in character to the annealed specimens. Both for iron and nickel, the values of the thermal *emf* are greater for the annealed samples in weak magnetic fields and less in the stronger. Both the magnitudes of the *emf*s and the characters of the curves indicate differences in the metals studied. The effect is not due merely to a special position in the magnetic field.

Other phases of this phenomenon are being investigated in this laboratory in the hope that it will throw more light on the general subject of thermo-electricity.

Thanks are due Professor S. R. Williams for suggesting the problem.

THE P-V-T RELATIONS OF NH_4Cl AND NH_4Br, AND IN PARTICULAR THE EFFECT OF PRESSURE ON THE VOLUME ANOMALIES

By P. W. Bridgman
Jefferson Physical Laboratory, Harvard University

(Received May 21, 1931)

Abstract

Measurements have been made of the volume as a function of pressure of NH_4Cl at 75°, 30°, and 0°C, and of NH_4Br at 75°, 0°, and −72°C. The pressure range was 12000 kg/cm², except at −72°, where it was 7500. There are discontinuities in the slope of the volume isotherm of NH_4Cl at 3370 kg at 0°, and at 9390 at 30°, and in the isotherm of NH_4Br at 1620 at −72°. The character of the discontinuity of NH_4Br is different from that of NH_4Cl, and is more like that of a polymorphic transition. These discontinuities correspond exactly to the discontinuities in the thermal expansion found by Simon and Ruhemann at atmospheric pressure. The displacement by pressure of the discontinuities to respectively higher and lower temperatures is that demanded by thermodynamics because of the opposite sign of the volume anomalies in the two cases. The thermodynamics of the effect of pressure and temperature on a discontinuity in a volume isotherm is discussed, and a generalized Clapeyron's equation shown to hold. By means of this equation the thermal effect accompanying the change can be calculated, and is found to be about 100 and 160 gm cal per mol for NH_4Cl and NH_4Br respectively. The thermal effect in NH_4Cl is approximately independent of pressure; the volume effect decreases rapidly with increasing pressure, being 0.0030 at 0° and 0.0015 at 30°. The volume effect in NH_4Br is approximately −0.017 at −72°. The explanation proposed by Pauling for the anomalies, namely passing from oscillational to rotational motion by the NH_4 radical, evidently must be supplemented by other considerations to account for the several marked differences between the behavior of the two substances. There are without doubt many other instances of such anomalies spread over a more or less localized range of pressure.

Introduction

In 1922 Simon[1] showed that NH_4Cl has anomalies in its specific heat, and in 1927 Simon, Simson, and Ruhemann[2] showed that NH_4Br has a similar anomaly, the maximum of both anomalies being at temperatures between −30° and −40° C. The anomaly consists of a very abnormally large specific heat distributed over a range of only a few degrees; both above and below this range the heat is of more normal magnitude. The phenomenon is not unlike that of a polymorphic transition spread over a temperature range by dissolved impurity, but x-ray analysis shows that the crystal structure is the same above and below the region of anomaly. In 1930 Simon and Bergmann[3] examined the volume-temperature relations of these substances, and found that the specific heat anomaly is accompanied by a volume anomaly, but this

[1] F. Simon, Ann. d. Physik **68,** 241 (1922).
[2] F. Simon, Cl. v. Simson, und M. Ruhemann, Zeits. f. physik. Chem. **129,** 339 (1927).
[3] F. Simon und R. Bergmann, Zeits. f. physik. Chem. **8,** 255 (1930).

has opposite signs in the two cases, the volume of NH_4Cl increasing and that of NH_4Br decreasing in the region of the specific heat anomaly. Thermodynamic principles at once suggest that it should be possible to displace the temperature of the anomalous region by the application of hydrostatic pressure, the temperature rising with pressure in the case of NH_4Cl because of the increase of volume, but falling with pressure for NH_4Br. These effects have in fact been found, and this paper contains a report of them. The primary purpose of the measurements was to establish the existence of the volume

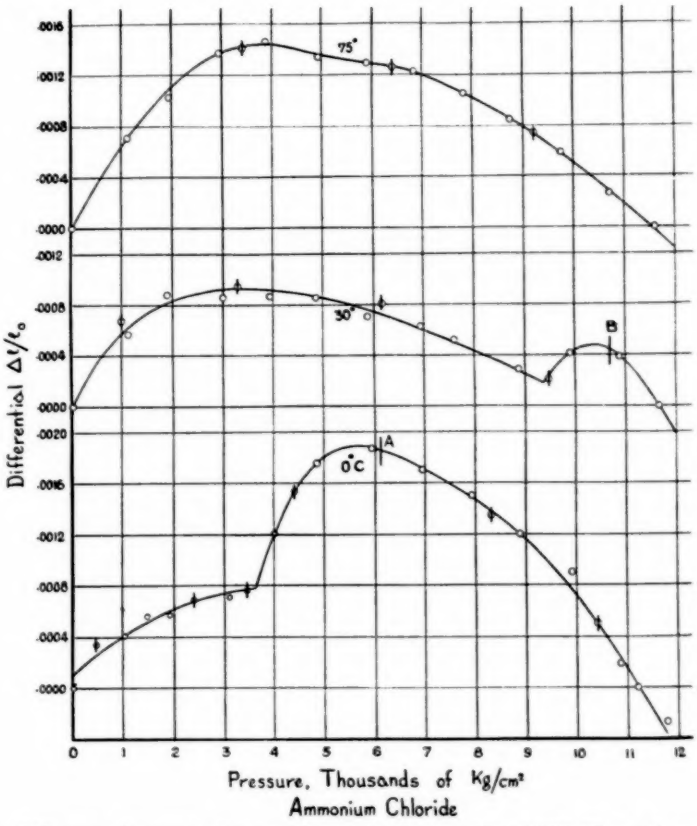

Fig. 1. Difference between the actual and the linear $\Delta l/l_0$ of NH_4Cl as a function of pressure at several temperatures. The open circles are data obtained with increasing pressure, the crossed circles with decreasing pressure.

anomalies at high pressure, but the method of measurement was such that it was possible to find the complete relation between temperature, pressure, and volume on both sides of the anomalous region.

The length, rather than the volume, of these substances was measured as a function of pressure, and from the changes of length the changes of volume were calculated. The materials were originally in the form of finely granulated powder; this was compressed dry at room temperature to a pressure between 20000 and 25000 kg/cm², forming a perfectly coherent mass. This was then turned in the lathe to the requisite dimensions, about 2 cm long and 6 mm in

diameter. The manner of formation should ensure that the volume changes take place equally in all directions, and thus justify the calculation of the change of volume from the change of length. There is particularly little danger in this procedure for these two substances, because they both crystallize in the cubic system and are equally compressible in all directions.

The source of the material was as follows: NH_4Cl, Kahlbaum's "K" grade, "for analysis"; NH_4Br, Kahlbaum's best listed grade, Ph. G. VI.

The length was measured at several different temperatures as a function of pressure in the "lever piezometer," with which the compressibility of many other materials has been measured,[4] so that no new description of the apparatus is necessary here.

The Data

NH_4Cl. Measurements were made on this at 30°, 75°, and 0°, in this order. At 30° and 75° nothing very striking displayed itself, but at 0° a very pronounced effect of the sort expected was found, and then reexamination of the 30° measurements showed the same sort of behavior near the end of the pressure range and of much smaller magnitude then at 0°, so that it might have been explained as an experimental irregularity if it had not been expected.

The calculations were made by the regular method. The potentiometer readings were converted into fractional changes of length, which were then plotted against pressure. A straight line was passed between the initial and final points, and the differences between the observed readings and this straight line plotted on a large scale, thus magnifying the effects. These differences, with reversed signs, are plotted in Fig. 1. It is particularly to be noticed that whatever the internal change is which is responsible for the breaks in the curves, it runs reversibly, the points obtained with increasing and decreasing pressure both lying on the curve within the limits of error. The large discontinuities at 0° and 30° are the ones which were looked for, and correspond to that found by Simon at atmospheric pressure, displaced by pressure to higher temperatures. In addition, there seems to be a new anomaly at 75° between 4000 and 6500 kg/cm², much less marked, but still almost certainly beyond experimental error.

The actual volumes of NH_4Cl at 0°, 30°, and 75° at intervals of 2000 kg, calculated from the changes of length, are shown in Table I. The volume at

Table I. *Volume of NH_4Cl as a function of pressure and temperature.*

Pressure kg/cm²	Relative volumes 0°	30°	75°
0	1.00000	1.00496	1.01398
2000	*.98870*	.99317	1.00159
4000	.97730	.98344	.99103
6000	.96586	.97420	.98209
8000	.95714	*.96562*	.97333
10000	.94914	.95599	.96535
12000		.94764	.95783

[4] P. W. Bridgman, Proc. Amer. Acad. **58**, 166 (1923).

atmospheric pressure as a function of temperature was taken from International Critical Tables. The horizontal lines in the 0° and the 30° columns indicate the range in which the discontinuity occurs. More accurate coordinates for the points of discontinuity, that is, the point at which the anomaly begins to appear on passing from the high temperature to the low temperature form, are shown in Table II.

TABLE II. *Coordinates of discontinuity of NH_4Cl.*

Pressure kg/cm²	Temperature
0	−30° C (Simon)
3370	0
9390	30

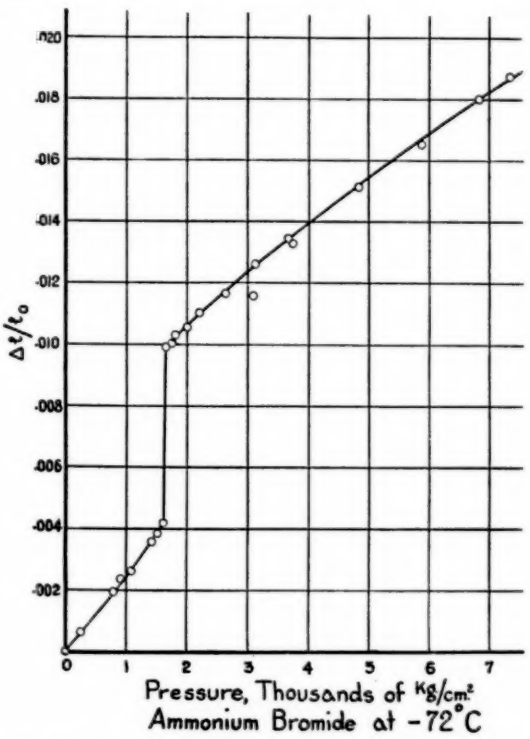

Fig. 2. $\Delta l/l_0$ of NH_4Br as a function of pressure at −72°C.

NH_4Br. Runs were first made at 0° and 75°. The curves of length against pressure at both these temperatures were perfectly smooth. A run was then made at −72°, the temperature of mixed solid CO_2 and ethyl alcohol. Fortunately it proved possible to make the run at this temperature with no essential modification in the regular pressure set-up. The regular temperature bath was used; about 4 gallons of alcohol and 50 pounds of solid CO_2 were sufficient to cool the pressure cylinder and fill the bath; the bath was maintained at temperature for something more than 24 hours, and for this a total of about 100 pounds of solid CO_2 was sufficient. This was purchased in

the form of "dry ice" from a commercial company. A more serious consideration than the refrigerant was the pressure transmitting liquid, most liquids freezing at the pressure expected at this temperature. It turned out that iso-pentane, the freezing point of which at atmospheric pressure is 28° lower than that of normal pentane, was capable of transmitting pressures up to more than 7000 kg/cm² without freezing, and this proved more than sufficient.

The effect with NH_4Br is much larger than with NH_4Cl, so that the phenomena can be sufficiently well displayed by plotting against pressure the total change of relative length, instead of the difference between the total and the linear change, as was done for NH_4Cl. The results are shown in Fig. 2. The experimental points include points obtained from five separate excursions, three with increasing and two with decreasing pressure; three of these excursions spanned the break in the curve. It is obvious from the points that the effect is essentially repeatable and reversible. The discontinuity is seen to be very abrupt, quite unlike that of NH_4Cl, and practically indistinguishable from an ordinary polymorphic transition.

In Table III are collected the numerical results for the relative changes of volume as fractional parts of the volume at atmospheric pressure at room temperature. The volume as a function of temperature at atmospheric pressure is not given in International Critical Tables, so that it was not possible

TABLE III. *Fractional volume changes of NH_4Br as a function of pressure on three isotherms.*

Pressure kg/cm²	$\Delta V/V_0$ −72°	0°	75°
0	0.00000	0.00000	0.00000
400	.00264		
800	.00558		
1200	.00876		
1600	*.01233*		
1800	.03021		
2000	.03144		
3000	.03666	.01803	.01932
4000	.04131		
5000	.04548		
6000	.04968	.03297	.03549
7000	.05358		
7500	.05547		
9000		.04617	.04998
12000		.05817	.06324

to give the actual volumes, as in the case of NH_4Cl. The horizontal line in the column at −72° indicates the pressure interval of the discontinuity. More accurately, the major part of the transition takes place between 1613 and 1646 kg/cm², the points at these two pressures lying on the lower and the upper branches of the curve, respectively.

DISCUSSION

It will be convenient first to examine the simple thermodynamics of a discontinuity in the volume-pressure isotherm. In Fig. 3 are represented two isotherms at τ and $\tau+\Delta\tau$, with a discontinuity, the discontinuity on the

$\tau+\Delta\tau$ isotherm occurring at a pressure dp higher than on the τ isotherm. Let (1) and (2) refer to the two parts of the isotherm on the two sides of the discontinuity. An examination of the purely geometrical relations, without the use of any thermodynamics, will yield the relation

$$\frac{d\tau}{dp} = -\left\{\left(\frac{\partial v_2}{\partial p}\right)_\tau - \left(\frac{\partial v_1}{\partial p}\right)_\tau\right\} \Big/ \left\{\left(\frac{\partial v_2}{\partial \tau}\right)_p - \left(\frac{\partial v_1}{\partial_\tau}\right)_p\right\}.$$

This may be written in the equivalent form, by means of the thermodynamic relation $(\partial Q/\partial p)_\tau = -\tau(\partial v/\partial \tau)_p$, where Q is heat absorbed

$$\frac{d\tau}{dp} = \tau\left\{\left(\frac{\partial v_2}{\partial p}\right)_\tau - \left(\frac{\partial v}{\partial p}\right)_\tau\right\} \Big/ \left\{\left(\frac{\partial Q_2}{\partial p}\right)_\tau - \left(\frac{\partial Q_1}{\partial p}\right)_\tau\right\}.$$

$(\partial v_2/\partial p)_\tau - (\partial v_1/\partial p)_\tau$, the difference of the rate of change of volume with pressure after and before the discontinuity, may be described as the rate of change

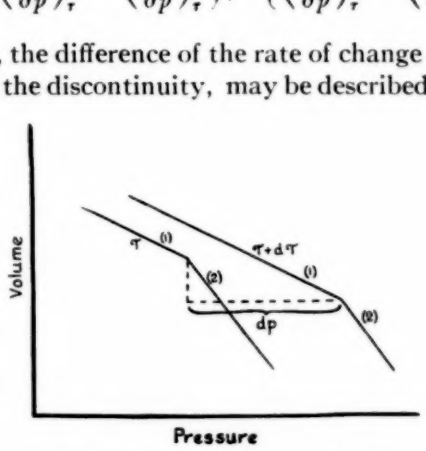

Fig. 3. Figure for computation of the displacement with pressure and temperature of a discontinuity in the volume isotherms.

with pressure of that part of the total volume which arises from whatever agency it is that is responsible for the discontinuity. Similarly, $(\partial Q_2/\partial p)_\tau - (\partial Q_1/\partial p)_\tau$ is the rate of change with pressure of that part of the total heat absorption due to the agency responsible for the discontinuity. The ratio, which may be written as dv/dQ, is merely the ratio of volume change to heat absorbed due to the internal change. The result may then be written

$$\frac{d\tau}{dp} = \tau\frac{dv}{dQ}.$$

This equation is the exact analogue of the ordinary Clapeyron's equation, and also of the more general equation controlling the relation between temperature and pressure in a system in which internal chemical reactions are taking place. In this latter case, $d\tau/dp$ is to be taken at constant composition, and dv/dQ, ordinarily written as $\Delta v/\Delta Q$, is the ratio of volume change to heat for one gram molecule's worth (or any other amount) of the reaction. The requirement that $d\tau/dp$ be taken at constant composition in the conventional analysis for reacting substances is replaced by the requirement, in our

case, that $d\tau/dp$ be taken at the initial point of discontinuity, obviously an entirely equivalent requirement. The analysis given above has the advantage for our present purpose that it demands somewhat less specialized assumptions about the nature of the internal changes in the system than the conventional analysis applicable to chemical reactions.

If whatever causes the discontinuity runs its course and is exhausted, so that there is a second discontinuity to mark the completion of the process, then obviously a similar formula applies for the $d\tau/dp$ of the relation between τ and p at the completion of the process. Or a similar formula holds, for example, for the half way completion of the process, dv/dQ now being the ratio of volume change to heat at the half way stage.

This formula may now be applied to NH_4Cl. We have in the first place three points on the P-T curve for the initial point of the discontinuity, as given in Table II, from which a curve may be drawn, and values found for $d\tau/dp$ with some accuracy. The values so found are 0.0067 at 0° and 0.0036 at 30°. The diagrams make it very probable that the internal change is entirely completed in a finite pressure range. The point of completion of the change is of course difficult to locate and indefinite, but it would seem that the points marked A and B at 0° and 30° give fair estimates of such points. This means that the internal change is spread through a pressure range of about 2500 kg at 0° and 1300 kg at 30°. This roughly justifies us in writing the formula as $d\tau/dp = \tau\Delta v/\Delta Q$, where Δv and ΔQ are the total changes of volume and heat accompanying the completed internal change, and $d\tau/dp$ refers to the initial discontinuity. The total Δv at 0° and 30° may also be found roughly by making a small extrapolation of the curves below the discontinuity, and I find in this way $\Delta v/v_0 = 0.0030$ and 0.0015 respectively. Substituted into the generalized Clapeyron's equation these give for the total heat of the change at 0° and 30° respectively 122 and 126 kg cm/cm³, or 99 and 102 gm cal per mol, or 100 gm cal per mol at both temperatures, within experimental error. The total heat of the change therefore appears to be approximately unaffected by increasing pressure, although the change of volume falls off rapidly.

The values for ΔQ just obtained do not check at all well with those found by Simon at atmospheric pressure. Simon gives for the total ΔQ 356 gm cal per mol, against 100 found above. Part of the discrepancy may be due to my assumption that the transition is completed in a pressure range corresponding to 17° at 0° (0.0067×2500) and 4.7° at 30° (0.0036×1300), whereas at atmospheric pressure Simon found the transition to begin perceptibly at 140° and to end abruptly at 243°K, a range of 103°. However, Simon found that 53 percent of the total thermal effect was concentrated in the 3° region between 240° and 243°, so that the major part of the difference cannot be explained by considerations of this sort. It seems to me that a very appreciable part of Simon's large heat may be due to the contribution made by the internal degrees of vibrational energy within the NH_4 radical, which is not supposed to be the effect concerned at the discontinuity. In any event, the very marked narrowing with increasing pressure and temperature of the temperature range within which the transition is perceptible is worthy of comment.

The drop in Δv with increasing pressure is entirely in line with the difference of compressibility. It is evident at once from Fig. 1 that NH_4Cl is very materially less compressible after the change has been completed than before. At 0° the linear compressibility at 6100 kg, where the transition has been completed, is 1.9×10^{-7} less than at 3600, just before the transition starts. Perhaps a third of this difference is to be ascribed to the natural decrease of compressibility with increasing pressure, leaving outstanding something of the order of 1.2×10^{-7} as the intrinsic difference of compressibility of the two states of NH_4Cl. At 30° the intrinsic difference of compressibility is not far from this same figure.

The discontinuity in $(\partial v/\partial p)_\tau$ at the beginning of the change is doubtless characteristic, and should be recorded; it seems to be very nearly the same at 0° and 30°. At 0°, where the more accurate estimate can be made, the discontinuity is about 18×10^{-7}. This abrupt discontinuity at the low pressure end of the range corresponds precisely to the abrupt discontinuity found by Simon at the *upper* end of the temperature range.

The anomaly of NH_4Br is evidently very different in character from that of NH_4Cl. There is in the first place the fact that the volume change is of the opposite sign. Furthermore, the shape of the discontinuity is different; the discontinuity of NH_4Br appears to end abruptly, when pressure has passed a critical value, but on the low pressure side there is an anomaly in that the curve of length against pressure is concave upward, as may be seen on inspection of Fig. 2. This means that in the low pressure range the compressibility increases with increasing pressure instead of decreasing, as is normal. This region of abnormally changing compressibility may well be a region of some sort of preparation for the approaching internal change. As already mentioned, by far the largest part of the change occurs in a very narrow range, with the abruptness characteristic of a polymorphic transition. The total abrupt fractional volume change is 0.017, almost six times as much arithmetically as the total change for NH_4Cl at 0°. It is a matter of general experience that the volume change usually becomes less as temperature increases, so that if the volume changes were compared at equal temperatures the arithmetical discrepancy between NH_4Cl and NH_4Br would not be quite so extreme.

It is not possible to obtain as accurate values for the heat of the change of NH_4Br as for NH_4Cl, because the change of NH_4Br has been studied at only two temperatures. We may, however, get a rough value by assuming $d\tau/dp$ constant between atmospheric pressure and $-72°$. Taking the temperature of the discontinuity as $-38°$ at atmospheric pressure and $-72°$ at 1600 kg/cm², $d\tau/dp$ is found to be -0.0210. This gives for the heat, $\Delta Q = 203\times.017\div.0210 = 160$ kg.cm/cm³, or 140 gm cal per mol, against 100 for NH_4Cl. The normal correction for the change of $d\tau/dp$ with temperature (or pressure) would raise the figure 140 somewhat, but in any event the heating effects in NH_4Cl and NH_4Br are not widely different, in spite of the difference of sign of the volume effects.

The generally accepted explanation of the anomalies at atmospheric

pressure is that of Pauling,[5] namely that the NH_4 radical passes from oscillational to complete rotational freedom as temperature rises, a process which is furthered by the weakening of the restoring forces due to the expansion of the crystal structure with rising temperature. The natural thermal expansion is in its turn increased as rotational freedom is acquired, so that the process is to a certain extent autocatalytic, thus accounting for the comparatively narrow temperature range. I think it very probable, however, in view of the facts detailed above, that this must be recognized to be an over-simplified picture. The small anomaly in NH_4Cl at 75°, not emphasized in the discussion above, suggests the same sort of thing. There can be little doubt that the large features of the phenomenon are the same in NH_4Cl and NH_4Br, as suggested by their chemical similarity and the approximate equality of the temperatures and heats of the transitions. But there must also be important differences, as shown by the difference of sign of the volume effects, and the marked differences in the abruptness and general character of the transitions.

It seems probable that small range anomalies may be of comparatively frequent occurrence in other substances. In many cases these need not involve as radical an internal change as passing from oscillational to rotational motion, but may be due to an intermediate type of change. For example, as the structure opens with thermal expansion, an oscillational motion, which at low temperatures was confined to a definite small amplitude range, may discontinuously acquire the possibility of oscillation through a greater amplitude, with accompanying change of natural frequency and thermal and volume effects. It seems to me highly probable that many of the small range anomalies which I found so characteristic of the P-V-T relations in liquids at high pressures[6] are of this character. There are doubtless many similar effects in solids. A possible example is the pressure transition of Ce[7]; this is like the change of NH_4Br in that below the transition pressure the compressibility increases abnormally with pressure. The sign of the volume change is different in the two cases, however. There are many interesting questions here for future experimental examination. For example, the persistently high compressibility of potassium[8] over a wide pressure range may be something of this nature.

In addition to the measurements described above, an exploration was made of $N(CH_3)_4Cl$, a compound very similar chemically to NH_4Cl, but not the slightest irregularity was found at either 0° or 75°. This is consistent with Pauling's picture, for the much greater moment of inertia of $N(CH_3)_4$ as compared with NH_4, should raise the temperature at which the transition might occur, if indeed the transition is not entirely suppressed. The details of the P-V-T relations for $N(CH_3)_4Cl$ will be published elsewhere.

Finally, a word of comment may be made on the absolute values of the compressibilities in the regions unaffected by the internal change. The initial

[5] L. Pauling, Phys. Rev. **36**, 430 (1930).
[6] P. W. Bridgman, Proc. Amer. Acad. **49**, 1 (1913).
[7] P. W. Bridgman, Proc. Amer. Acad. **62**, 207 (1927).
[8] P W. Bridgman, Proc. Amer. Acad. **58**, 204 (1923).

compressibility of NH_4Cl at 30° is about 5.9×10^{-6} and that of NH_4Br 6.1×10^{-6}. The corresponding compressibilities of NaCl and NaBr are 4.2 and 5.0×10^{-6}, and of KCl and KBr 5.5 and 6.6. The general order of the compressibilities of the NH_4 salts is therefore what might be expected. The difference between the compressibility of the chloride and the bromide is unusually small, however, and this again emphasizes the probability that complications obscure any simple picture.

This work is much indebted financially to the Rumford Fund of the American Academy of Arts and Sciences and to the Milton Fund of Harvard University. I am indebted to Mr. L. H. Abbot for the readings.

LETTERS TO THE EDITOR

Prompt publication of brief reports of important discoveries in physics may be secured by addressing them to this department. Closing dates for this department are, for the first issue of the month, the twenty-eighth of the preceding month; for the second issue, the thirteenth of the month. The Board of Editors does not hold itself responsible for the opinions expressed by the correspondents.

Transverse Barkhausen Effect in Iron

In observing the sudden small changes in magnetization discovered by Barkhausen, experimenters have generally confined themselves to determining the changes in magnetization taking place in the direction of the applied magnetic field, and have not considered the changes which may occur in the directions at right angles. It occurred to us that measurements of this transverse effect might give us more detailed knowledge of the nature of the reversal of the elementary regions. For example, if the magnetization is closely aligned with the field before and after the reversal (parallel and antiparallel), there will be little or no transverse effect. On the other hand, if the magnetization is inclined to the field at a considerable angle and the reversal is 180°, or if the reversal is less than 180°, the transverse effect will be relatively large.

The results, discussed more fully below, indicate that when the magnetization is small (at the coercive force) the reversals are practically all of the former kind, and when the average magnetization is large (over one half of saturation) reversals of the latter kind become of increasing importance.

The specimen used in the experiments was a drawn iron tube 60 cm long and 6 mm in diameter, and with a wall 0.5 mm thick. The longitudinal Barkhausen effect was determined in the way previously described[1] and the results expressed in terms of the average change in magnetic moment for a single discontinuity. To determine the transverse effect the tube was magnetized circularly by passing current through a copper wire placed along the tube axis, and the small sudden changes in transverse magnetization were picked up by the same search coils, used in the same position, as were used to detect the longitudinal effect. The magnetization cycle was in each case a hysteresis loop with a maximum field strength of 10 gauss.

The ratio of the change in moment perpendicular to the applied field, to the change parallel to the field, is plotted in the Fig. 1.

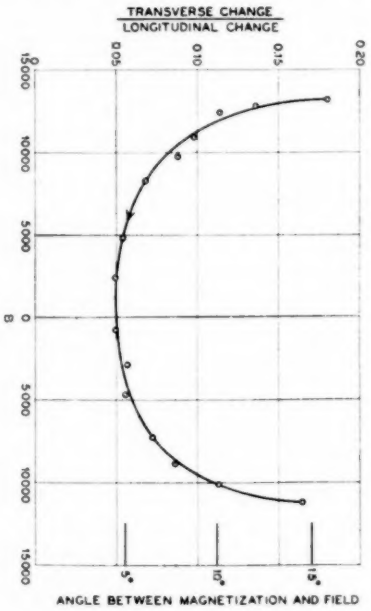

Fig. 1.

The minimum in the curve is for $B=0$, and corresponds to a reversal of 180°, with the average direction of magnetization inclined 5° to the direction of the field. This small inclination is probably best accounted for by the inhomogeneities in the material due to

[1] Bozorth and Dillinger, Phys. Rev. **35**, 733–52 (1930).

crystal boundaries and the local changes in the number of elementary regions magnetized in each direction. When the magnetization has larger values in either direction the ratio is larger, and when $B=13{,}000$ the ratio corresponds to the complete reversals of magnets having an average inclination of 15° to the field. It has been shown by several experimenters, and recently emphasized by the theoretical studies of Akulov,[2] that iron crystals are magnetically isotropic until the induction exceeds 10,000 gauss, and that in the neighborhood of 16,000 gauss the direction of magnetization coincides with the crystallographic direction (100) within a fraction of a degree. When the material is anisotropic and the reversal is 180° or less the transverse component will be relatively large.

Although the results show the nature of the reversals at low inductions, they have not been extended so far to the high inductions for which the anisotropy is greatest; they indicate, however, that the transverse component is comparable with the longitudinal in this region, as would be expected.

R. M. Bozorth
J. F. Dillinger
Bell Telephone Laboratories
New York, New York
June 10, 1931

[2] Akulov, Phys. Zeits. **32,** [2] 107–8 (1931).

On the Elastic Scattering of Electrons by Spherically Symmetrical Atoms

In several recently published papers[1] the elastic scattering of electrons by A and (in particular) Hg atoms has been observed in its dependence upon the angle of scattering and for different electron energies. The experiments show very clearly a series of intensity maxima and minima which in general move toward smaller angles with increase of the electron velocity.

Although, from well-known wave-optical analogies, this sort of behavior may not seem surprising, we are nevertheless not in a position to designate precisely the mechanism responsible. In the first place it may be a matter of the diffraction of the electron wave in the field of unchanged atoms; the polarization of the atoms may, on the other hand, play a determining rôle; and finally it may prove necessary, in order to obtain complete agreement with observation, to treat the problem not in three dimensional but in configuration space so that the electron exchange may be taken into account.

The following considerations will perhaps somewhat clarify this situation. If it is a matter of first order scattering in a centrally symmetrical field the eigenfunctions, in their dependence upon the scattering angle θ and the electron velocity v, will be of the form $\psi(v \sin(\theta/2))$. This displacement law may easily be tested on the minima given by Pearson and Arnquist, which should belong to the same value of the argument. Table I shows to what extent the law is obeyed.

Table I

θ	$\sin(\theta/2)$	v	$v \sin(\theta/2)$
65	0.537	10.0	5.37
57	.477	11.2	5.34
50	.423	12.2	5.18
44	.375	13.2	4.96
40	.342	14.1	4.84

The argument decreases by about 10 percent corresponding to an increase of the electron energy by the factor 2. These experiments can thus only approximately be explained by this simple scattering process.

It is the intention of the authors to return to this problem in a more detailed treatment.

F. W. Doermann
Otto Halpern
Department of Physics,
New York University,
June 4, 1931.

[1] E. C. Bullard and H. S. W. Massey, Proc. Roy. Soc. **A130,** 579 (1931); F. L. Arnot, *ibid.* **A130,** 655 (1931); J. M. Pearson and W. N. Arnquist, Phys. Rev. **37,** 970 (1931).

Excitation of High Optical Energy Levels

The one-way high tension condensed spark method used by Professor Siegbahn's students[1] in the photography of spark spectra, is capable of ionizing and exciting atoms to energy levels considerably higher than any reported hitherto in optical spectra.

Plates taken on the spectrograph described by Ekefors[1] with 400 sparks at $7 \cdot 10^4$ volts and $0.63 \cdot 10^{-6}$ farads between aluminum electrodes cored with rubidium halide salts, show the principal doublet of the copper-like spectrum of rubidium ($Z=37$):

Rb IX $4s^2S_{1/2}-4p^2P_{3/2}$ 583.37A 171417 cm^{-1}
$4s^2S_{1/2}-4p^2P_{1/2}$ 628.62A 159078 cm^{-1}

with about the same intensity as the strongest lines of the 833A group of oxygen. They are present in three orders. With a self inductance of $6 \cdot 10^{-6}$ henrys in series with the gap, the stronger (583A) is perceptible, but the weaker is entirely cut out, while neighboring lines of lower excitation energy are little affected. With only $8 \cdot 10^{-6}$ henrys in series, however, the intensity of the Rb IX lines is but slightly less than with none, whereas some still unidentified fairly intense lines are cut out, indicating that they require considerably more energy for excitation. A crude preliminary estimate gives for the energy required to remove eight electrons from rubidium:

Rb I $4s^24p^65s^2S$ – Rb IX $4s^2S = 5 \cdot 10^2$ electron volts.

The corresponding Br VII lines are among the most intense on the plates.

Complete details will be given later with a more general study of the ultraviolet spark spectra of the heavier halogens and alkali metals, in collaboration with Mr. J. C. Betz, to whom I am indebted for aid in the measurements and calculations.

J. E. Mack

Department of Physics,
University of Wisconsin,
Madison, June 6, 1931.

[1] B. Edlén and A. Ericson, Zeits. f. Physik **64**, 64 (1930); E. Ekefors, Phys. Zeits. **31**, 737 (1930). The circuit used here differs from that of these investigators in that the air gap in series with the vacuum spark gap is here omitted.

The Scattering of X-rays from Polyatomic Gases

P. Debye[1,2] has recently discussed the interference pattern of the x-rays scattered by gases such as CH_2Cl_2 and CCl_4. These gases can be considered approximately as diatomic and tetratomic gases respectively, because such a great proportion of the intensity of the scattered rays comes from the chlorine atoms. According to Debye, the intensity per electron of the x-rays scattered by a gas consisting of molecules made up of point atoms of the same kind is

$$S = \frac{Z}{n} \sum_{r=1}^{n} \sum_{s=1}^{n} \frac{\sin kl_{rs}}{kl_{rs}} \qquad (1)$$

where

$$k = 4\pi \sin(\phi/2)\lambda \qquad (2)$$

and Z is the number of electrons massed together into each point atom, n is the number of atoms in each molecule, and l_{rs} is the distance between the rth and sth atoms of a molecule.

More recently, Jauncey[3] has investigated the theory of the scattering of x-rays by a solid consisting of atoms of one kind. This theory can also be applied to a single molecule of gas, the atoms having size and the molecule a given orientation. The formula for this case is

$$S = 1 + (Z-1)f'^2/Z^2 + (f^2/nZ) \sum_{r=1}^{n}{}' \sum_{s=1}^{n}{}' \cos k(z_r - z_s) \qquad (3)$$

where the symbol $\sum'\sum'$ indicates that in the summation $r \neq s$, f is the atomic structure factor of an atom and f', which is nearly equal to but less than f, has been discussed by Jauncey.[4] Eq. (3) is valid for a particular orientation of the molecule. For random orientation, it can easily be shown that

$$S = 1 + (Z-1)f'^2/Z^2 + (f^2/nZ) \sum_{r=1}^{n}{}' \sum_{s=1}^{n}{}' \frac{\sin kl_{rs}}{kl_{rs}} \qquad (4)$$

For point atoms, $f'=f=Z$ and the right side of Eq. (4) becomes identical with Debye's Eq. (1). For diatomic atoms, Eq. (4) becomes

$$S = 1 + (Z-1)f'^2/Z^2 + (f^2/Z)\frac{\sin kl}{kl} \qquad (5)$$

where l is the separation of the centers of the two atoms. For a molecule consisting of atoms whose centers are at the corners of a regular tetrahedron, Eq. (4) becomes

$$S = 1 + (Z - 1)f'^2/Z^2 + (f^2/Z)\frac{3 \sin kl}{kl} \quad (6)$$

where l is the length of a side of the tetrahedron. Debye gives an experimental curve for CCl_4, whose humps are flatter than required by Eq. (1). According to Debye, this flatness is due partly to the size of the atoms of Cl. We see that the size can be taken account of by Eq. (6). However, when Wollan's[5] f' values for argon are put in Eq. (6), the humps are somewhat but not sufficiently flattened.

Eqs. (3) and (4) are based on the assumption of no thermal vibrations of the atoms within a molecule of the gas and Debye has suggested that part of the flatness of the experimental curve is due to thermal vibration of the atoms. If there is thermal vibration of the atoms, it is only the double summation of Eq. (4) which is affected. Let us find the average value of $(\sin kl)/kl$ as l varies. If we suppose that $l = l_0 + x$ where l_0 is the average separation and also that the fraction x/l_0 is small and that the probability of x being between x and $x+dx$ is $\exp(-x^2/\alpha^2)dx$, we find neglecting squares and higher powers of α/l_0, that

$$\text{Ave}\,\frac{\sin kl}{kl} = \frac{\sin kl_0}{kl_0}\exp(-k^2\alpha^2/4). \quad (7)$$

Hence to take care of the thermal vibration of the atoms we multiply the double summation term in Eq. (6) by $\exp(-k^2\alpha^2/4)$, where α is the most probable change in the separation of any pair of atoms from the value l_0. This has the effect of further reducing the humps at large angles as has been noted by Bewilogua.[6]

G. E. M. JAUNCEY

Washington University,
St. Louis, Missouri.
June 12, 1931.

[1] P. Debye, Phys. Zeits. **31,** 419 (1930).
[2] P. Debye, Proc. Phys. Soc. Lond. **42,** 340 (1930).
[3] G. E. M. Jauncey, Phys. Rev. **37,** 1193 (1931).
[4] G. E. M. Jauncey, Phys. Rev. July 1, (1931).
[5] E. O. Wollan, Phys. Rev. **37,** 862 (1931).
[6] L. Bewilogua, Phys. Zeits. **32,** 265 (1931).

The Effect of Internal Stress on Magnetic Susceptibility

Honda and Shimizu have found (Nature **126,** 990, 1930) that copper and silver when severely cold worked suffer a decrease of diamagnetic susceptibility. Subsequent annealing restores the susceptibility (and the density, which is decreased by cold working) to the original value. Copper may even be made paramagnetic, but when heated in a vacuum the original diamagnetism is completely restored at about 350°C.

These experiments seem to corroborate the previous work of Francis Bitter (Phys. Rev. **36,** 978, 1930) who found that stretching copper and silver wires beyond the elastic limit altered their susceptibilities. H. E. Banta, (Phys. Rev. **37,** 634, 1931) has repeated Bitter's work but failed to find any effect of stretching on the susceptibility. Since there was a possibility that Banta's wires were not given sufficiently large internal stresses to produce the desired effect some further measurements have been made of the density change caused by stretching annealed copper wires. These wires were cut from the same piece which had furnished samples for the susceptibility measurements and were stretched by practically the same amount as those samples. A density decrease was produced which was adequate to cause an easily measurable susceptibility change, assuming the curve given by Honda and Shimizu to hold. However, no susceptibility change was found. The negative result of Banta cannot, therefore, be due to insufficient strains.

In a private communication to one of the writers Francis Bitter has pointed out that the equation $dI/dp = de/dH$, expressing the reciprocal relationship between intensity of magnetization I, pressure p, strain e, and field H, does not necessarily imply a value of dI/dp too small to measure even though de/dH cannot be observed. In Banta's paper this equation and the absence of magnetostriction in copper was adduced as an argument against an effect of strain on susceptibility. Bitter, however, states that in a piece of copper stretched to the breaking point the pressures may be a good deal larger than 5000 kg/cm². This is a surprisingly large value, since the International Critical Tables give 2277 kg/cm² as the ultimate tensile strength of electrolytic copper. Using $dp > 5\times10^9$ dynes/cm² and $dI < 2\times10^{-2}$ as reasonable values for his own experiments, Bitter gets

$dI/dp < 4 \times 10^{-12}$. Hobbie (Phys. Rev. **19,** 456, 1922) appears to have shown that in brass $de/dH < 3 \times 10^{-12}$. However, such small values of magnetostriction are very difficult to measure and could well escape detection, whereas values of dI/dp as small as this could be measured quite easily if dp is as large as Bitter's estimate. Failure to measure magnetostriction in copper, therefore, does not constitute a serious objection to the existence of an effect of internal strain on susceptibility.

To explain the experiments of Honda and Shimizu, and of Bitter, two theories have recently been proposed. W. Gerlach (Nature **127,** 556, 1931) suggests that the high internal pressures partially destroy the crystal lattice of the copper so that parts of the metal become amorphous and show paramagnetic behavior. The amorphous parts disappear by recrystallization when the metal is heated and their paramagnetic contribution is thus removed. Kussmann and Seemann (Naturwissenschaften **14,** 309, 1931) on the other hand, suppose that cold working the copper causes iron impurities to crystallize out of the copper, thus making the susceptibility of the mixture less diamagnetic. Heating the strained metal allows the iron to go back into solution in the copper, so that its susceptibility returns to the initial value.

Since Banta's copper does not show any susceptibility change due to internal strain it is difficult to accept Gerlach's explanation. However if Banta's copper contained no iron his negative result is to be expected on the theory of Kussmann and Seemann. This latter theory is therefore probably the correct explanation of the phenomenon.

C. W. Heaps
H. E. Banta

Department of Physics,
Rice Institute,
June, 5, 1931.

The Entropies of Methane and Ammonia

In a recent number of the Journal of the American Chemical Society (**53,** 2006 (1931)) there has appeared a communication by D. S. Villars in which he gives values for the entropies of methane and ammonia gases calculated from spectroscopic data. These are shown to compare favorably with thermodynamic values. The author states that details of the calculations will probably appear in the Physical Review.

Since we have also made these calculations with considerably different results it seems worth while to present a brief statement at this time. A full account will appear in the Journal of the American Chemical Society following the completion of calorimetric investigations at low temperatures for the purpose of obtaining the entropies from the third law of thermodynamics.

For the calculation of entropy at ordinary temperatures little error is made in assuming rigid molecules and the Sakur-Tetrode equation (Sackur, Ann. d. Physik **36,** 968 (1911); Tetrode, ibid. **38,** 434 (1912)) properly modified to consider the molecule symmetry number (see Ehrenfest and Trkal, Proc. Akad. Sci. Amsterdam **23,** 162 (1920)). Assuming the tetrahedral model, the symmetry number of methane is 12 and the moment of inertia, obtained from Raman spectra, is 5.17×10^{-40} gr cm^2. (Dickinson, Dillon and Rasetti, Phys. Rev. **34,** 582 (1929)). The entropy at 298.1°K and atmospheric pressure is readily calculated as follows, neglecting vibration:

$$\begin{aligned} S_{CH_4} &= (3/2)R \ln 16.03 + 4R \ln 298.1 \\ &\quad + (3/2)R \ln 5.17 \times 10^{-40} \\ &\quad - R \ln 12 + 265.35 \\ &= 44.35 \text{ E.U.} \end{aligned}$$

Villars obtained 42.0 E.U. from the above data.

The value, 44.35 E.U., although it does not include the nuclear spin entropy ($R \ln 16$), is the value which should be used in conjunction with the entropy values in common use for other substances. This convenient practice is justified by the cancellation of nuclear spin in chemical reactions. (Gibson and Heitler, Zeits. f. Physik **49,** 465 (1928)).

For the sake of completeness we may also state the absolute entropy of methane as $44.35 + 5.51 = 49.86$ E.U.

The value, 44.35 E.U., compares favorably with the calorimetric value, 44.3 E.U., calculated from the low temperature data of Clusius (Zeits. f. physik. Chemie B, **3,** 41 (1929)) and the vapor pressure measurements of Stock, Henning and Kuss (Ber. **54,** 1119 (1921)) and of Keyes, Taylor and Smith (J. Math. Phys. Mass. Inst. Tech. **1,** 191 (1922)).

Although the close agreement of the value obtained from the third law is undoubtedly fortuitous it, nevertheless, proves that me-

thane is a regular tetrahedron. If, for example, methane were a symmetrical pyramid, the symmetry number would be 4, thus increasing the entropy calculated from spectroscopic data by $R \ln 12/4 = 2.18$ E.U., an amount that could hardly be compensated by any reasonable change in the product of the moments of inertia. If three of the C-H bonds were identical, and one different, the increase due to the corresponding symmetry number of 3 would be $R \ln 12/3 = 2.75$ E.U., which is also unreasonable. A more complete discussion of these points would lead us too far from the purpose of our present communication. We may add, however, that the method of attack has the great advantage that it leads to definite information about the methane molecule in its normal state and does not involve the usual and unproved assumptions as to what happens during chemical substitution reactions.

From the equilibrium measurements of Randall and Mohammad (Ind. Eng. Chem. **21,** 1048 (1929)) we obtain:

$S_{CH_4} = 45.7$ E.U. at 25°C, while a somewhat better calculation by Storch (J. Am. Chem. Soc. **53,** 1266 (1931)), combining thermal and equilibrium measurements, leads to 45.26 E.U. Villars obtained 42.5 E.U. from the data of Randall and Mohammad. Because of the long extrapolation required and other uncertainties the values obtained from the equilibrium measurements are, however, somewhat in doubt.

Combining $S_{C\ (graphite)} = 1.3$ E.U. with the spectroscopic entropies of methane and hydrogen and Rossini's (Bur. Standards J. Research **6,** 37 (1931)) calorimetric data, we obtain a very reliable value for the free energy of formation of methane, namely:

$$\Delta F_{298.1} = -12{,}440 \pm 100 \text{ cal./mole.}$$

This accuracy may be extended to high temperatures when sufficient information about the rotation-vibration levels of methane becomes available.

A convincing interpretation of the infrared spectrum of ammonia has been given by Barker (Phys. Rev. **33,** 684 (1929)). The most reliable moments of inertia are 5.47×10^{-40} and 2.792×10^{-40} gr cm², the latter value being that obtained from the Raman spectra of Dickinson, Dillon and Rasetti (loc. cit.) and from the pure rotation measurements of Badger and Cartwright (Phys. Rev. **33,** 692 (1929)). Barker gave 2.8×10^{-40} gr cm².

The symmetry number for ammonia being 3, the entropy of translation and rotation is obtained as follows:

$$\begin{aligned} S_{NH_3(T+R)} &= (3/2)R \ln 17.031 + 4R \ln 298.1 \\ &\quad + (R/2)\ln 2.792^2 \times 5.47 \times 10^{-120} \\ &\quad - R \ln 3 + 265.35 \\ &= 46.13 \text{ E.U. at } 298.1°\text{K.} \end{aligned}$$

The heat capacity data of Haber and Tamaru (see Thermodynamics, Lewis and Randall, p. 80) indicate, however, that the vibrational entropy is too large to be neglected, since the molecule is beginning to vibrate at room temperature. The entropy associated with vibration may be estimated as 0.3 E.U. Thus $S_{NH_3} = 46.4$ E.U. at 298.1°K. This value does not include the effect of nuclear spin, namely $R \ln 24 = 6.31$ E.U. The absolute entropy of ammonia is thus 52.7 E.U. The value 46.4 E.U., may be compared with the third law value which we calculate from the work of Eucken and Karwat (Zeits. f. physik. Chemie **112,** 467 (1924)) and the vapor pressure measurements of Henning and Stock (Zeits. f. Physik **4,** 226 (1921)), namely, 47.2. The agreement is not good but is within the limit of error of Eucken and Karwat's work as their other results deviate by similar amounts and sign.

From the free energy equation given by Lewis and Randall (Thermodynamics, page 557), combined with the entropies of nitrogen and hydrogen, we obtain $S_{NH_3} = 46.1$ E.U. at 298.1 in very satisfactory agreement with the spectroscopic value.

Villars' calculation of $S_{NH_3} = 43.5$ E.U. from the equation of Lewis and Randall is evidently in error. His value from spectroscopic data is $S_{NH_3} = 44.0$ E.U., compared with our value of 46.4 E.U. A small part of the difference is due to the use of a somewhat different and, we believe, incorrect moment of inertia around the symmetry axis.

In addition to the gases mentioned above, a low temperature calorimetric investigation is in progress on hydrogen sulfide, and it is expected that measurements on N_2O, CO_2, and a number of other polyatomic molecules will be carried out in the near future.

W. F. GIAUQUE
R. W. BLUE
ROY OVERSTREET

Chemical Laboratory of the
University of California,
Berkeley, California,
June 5, 1931.

Electronic Velocities In the Positive Column of High Frequency Discharges

In the April 15th number of the Physical Review, **37,** 978–982, a note under this title has been published by the author. This note contains calculations which prove that small mean values of the electric force in the positive column of high frequency discharges do not necessarily prohibit the production of electrons of sufficient velocity to excite or even ionize gas atoms. The calculations are based on the consideration of the effect of elastic impact occurring simultaneously with a change of direction of the electric field. It has been overlooked by the author that this effect of elastic impacts in high frequency discharges has first been pointed out by F. M. Penning in a paper in the Dutch journal "Physica" **7,** 80–87, 1927, on which otherwise the author would of course have based his calculations.

EGON HIEDEMANN
Physikalisches Institut,
Universität Köln,
June 2, 1931.

BOOK REVIEWS

Der Aufbau der hochpolymeren organischen Naturstoffe auf Grund molekular-morphologischer Betrachtungen. KURT H. MEYER AND H. MARK. Pp. 264+viii, figs. 89. Akademische Verlagsgesellschaft m.b.H., Leipzig, 1930. Price, RM 18.

This book provides a critical summary of the first application of a new method of treatment to the solution of a difficult problem in structural organic chemistry. The method consists of combining chemical information and x-ray diffraction data with empirical rules regarding the equilibrium distances between atoms. After introductory chapters on interatomic forces, crystal structure, and molecular models, and an excellent general discussion of highly polymerised substances (of which bakelite, a condensation product of phenol or cresol and formaldehyde, is an extreme example), a detailed discussion of all available information on cellulose is given, culminating in the formulation of a structure which satisfies the x-ray data and agrees with the chemical and physical properties of the substance. The physicist may be interested in the calculation (pp. 153–8) showing that the suggested structure can account for the observed tensile strength of cellulose fibers of over 100 kg/mm², which may be compared with the value 180 kg/mm² for the best hardened chromium-vanadium steel. A briefer discussion of the structure of mercerised cellulose, nitrocellulose, rubber, starch, pectin, albumin, silk, tendon substance, and other fibrous substances ends the book.

Despite the efforts of a number of well-qualified investigators, progress in the deduction of the structures of organic crystals from x-ray data alone has been rather slow. The work discussed by Meyer and Mark shows the importance of utilizing also chemical information and structural rules, and we may expect that with the acquisition of more detailed and definite information on interatomic forces many structural problems of biological importance will be solved.

LINUS PAULING

Intermediate Physics. R. A. HOUSTOUN. Pp. 638, figs. 588. Longmans, Green and Company, New York, 1930. Price $4.20.

Despite its title, this book is a quite elementary text using no mathematics more advanced than the simplest trigonometrical relations. It treats the subjects of Dynamics and Properties of Matter, Heat, Sound, Light, and Electricity and Magnetism, taken in the order named. Incidentally, each of the five sections, with the exception of that on Sound, is published also as a separate pamphlet. Illustrative problems are interspersed through the text, and numerous problems for the student to solve are placed at the end of each chapter. Twenty-four pages of examination questions are appended at the end of the book.

The subject matter is carefully and clearly presented, although altogether in the conventional manner. Mass is defined as "the quantity of matter" in a body and force is not defined at all. Little mention is made of the tremendous advances in physics of the last twenty-five years. The subject of electricity and magnetism is treated with too little use of the electron theory of matter. In the short chapter on electrical oscillations and waves more than a page is devoted to the crystal detector but there is no mention of the vacuum tube.

The author has a pleasant style and has taken care to avoid ambiguous or inaccurate statements. The book should prove useful in elementary college courses in physics or in high school courses.

LEIGH PAGE

The Dynamic Universe. JAMES MACKAYE. Pp. 308+x. Charles Scribner's Sons, New York, 1931. Price $3.50.

There are three states of sophistication in physics, and particularly in modern physics. In the first, one accepts, in a superficial way, everything at face value. In the second, he sees

that many of the verbal statements require qualification. Certain conclusions are limited in their validity. The significance of the statements are not quite what is implied by the words. The arguments presented are not a proof of something, but an analytic expression of a hypothesis, and so forth. State of sophistication No. 2 is destructive rather than constructive. There is a tendency to look not for the rose, but for the thorns. In state of sophistication No. 3, one admits many of the points raised in state No. 2, but realizes that the main essence of the theories under discussion lies in realms other than those in which one in state 2 is looking for them. In state 3 one sees the thought structure bound in places by bars of steel. The author has painted them with gold paint to call attention to them, or he has inadvertently spilled gold paint upon them. In state 2 one complains of the gold and says that gold would not serve for the structure. In state 3 one sees that the gold paint is irrelevant.

Words are mere imitative grunts designed for the purpose of setting minds into harmony with each other. They are catalysts of thought, but it always remains for the parties concerned to become adjusted in their thinking so that each gains a correct comprehension of what the other wishes to convey.

The author of "The Dynamic Universe" appears to be in state of sophistication No. 2. He starts out with a discussion of the relativistic concepts of space and time. He points out, what is, of course, admitted by all relativists, that the definition of simultaneity in the Einstein sense is different from what it is in the Newtonian sense; and he seems to see here some subtle confusion of ideas by which relativity becomes enthroned through the agency of these deceptive sentinels, Einsteinian space and time. Nobody wishes to contend that it may not be possible to build up a system of physical laws in terms of any arbitrary concepts of space and time—time could be defined as given by the watch of the richest man in the neighborhood—but the laws would, in general, be very complicated. The author fails to give weight to the fact that all sorts of schemes have been tried to correlate physical phenomena in terms of the older concepts of space and time. It was the people who invented the theories which lead finally to relativity that struggled hardest in this matter. Everybody has been conscious of those feelings of absolute distance and time so dear to the heart of the layman, and it was only when it came to be realized that those feelings were illusory that they were allowed to give place to something else.

The author quarrels with the statement that the Doppler effect is a relativity effect and goes to great pains to remark that it is a physical effect in that it occurs with sound—that it can be enhanced by multiple reflections from moving mirrors, and so forth, all of this being quoted as a rebuttal of the idea that the Doppler effect is a relativity effect. He seems to imply that the relativists believe if the things which are objectionable to the non-relativists were not there, there would be no Doppler effect. It is hard to believe that with his reasonably wide acquaintance with the literature the author can seriously believe that there is any conflict of principle involved in what is obviously implied in the statement that the Doppler effect is a relativity effect. If the author had acquainted himself less with the superficial aspects of statements and more with their inner content—if he had worked through the theories in detail, not only would he have avoided troubles of the foregoing kind, but he would have avoided drawing such erroneous conclusions as those cited at the bottom of page 75, when he implies that the usual relativistic argument concerning the "drag" of light in a moving medium provides for no continuity of behavior of a medium which gradually merges into a vacuum. He fails to observe that the relativistic argument does make the "drag" depend upon the refractive index of the medium and gives, in fact, the well-known "Fresnel coefficient." Then again, in another place, we find criticisms raised against relativistic arguments, as a result of the refractive index of metals for x-rays being less than unity. The superficial implication is that we have a propagation with velocity greater than normal light velocity. The elucidation of this apparent paradox is well known to every student of the subject. Another example of the use of terms in a sense other than that implied in relativity theory is found when it is stated that "when two cathode-ray streams having a velocity through their tubes more than half that of light pass one another, going in opposite directions, their relative velocity is greater than that of light."

One dislikes to use unkind expressions, but the violent language in which the author speaks of the arguments of relativity prompts the retort that he has formed a confused view of the content of relativity and has then proceeded to become confused in its application to nature.

It is naturally impossible to deal, in a short review, with all the matters upon which

comment might be made. Almost every page calls for some remark. On page 240 the author commences and proceeds for several pages to quarrel with the contention that the general theory of relativity "explains" gravitation. In the sense in which he uses the word "explain," nobody would contend that it did. Thus he is satisfied about the explanation of a man who slips on a piece of banana peel, because he can describe it all in terms of our knowledge of friction, bananas, human equilibrium, and so forth. If, however, he should go down to the ultimate origin of friction, he would, in going into what we may call the fundamental phenomena soon have to leave explanations in terms of large-scale phenomena. We might explain the slipperiness of bananas in terms of atoms and molecules, but we should not like to explain the properties of atoms and molecules in terms of slipperiness such as occurs in bananas. The word "explain" in its ultimate sense must imply a hypothesis, or a set of hypotheses which are the starting points, and things which are the logical consequences of these hypotheses may be said to be "explained" in terms of them. If one is sufficiently sophisticated, he may contend that nothing has any explanation, for the results are all contained in the hypotheses, and the statement of the results is simply another way of stating the hypotheses. Usually, when one of the consequences is sufficiently far removed from the hypothesis, so that we do not realize immediately that it is a consequence of the hypothesis but receive a pleasant mental jog on finding that it is, we say that the consequence is explained by the hypothesis.

In another place the author raises a more trivial objection in questioning the title "Solution of the Problem of Gravitation" given by Einstein in a section of his book. He seems to think that the word "solution" is intended in the sense of "explanation" as he would use it in connection with banana peels etc., whereas what is obviously intended is the application of the relativity postulates, etc., already formulated, to the case of gravitation.

One is disposed to have a good deal of sympathy with the author in his objection to such terms as "curved space," and so forth. The concepts which the layman has of a "curve" and of "space" are indefinite. In them is much which is irrelevant from a mathematical point of view; and before they can be used to provide much aid to the theory of relativity they must be so amended, cleaned up, and generalized that the layman would cease to recognize them, and they would then be a hindrance rather than an aid to his thinking. There are many things as to the significance and content of the restricted and general theories of relativity in which the writer of this review would find much to take exception to in the customary presentation. He feels, however, that such criticism should be in the first place sound; in the second place it should be made in a constructive spirit and with an effort to minimize trivialities.

Presumably the main purpose of Professor Mackaye's book is to present a theory which he calls the "Radiation Theory," a theory which is to account for gravitation and many other things. As is the case with most attempts of this kind, the theory contents itself with a qualitative application to a few phenomena. It is possible to invent innumerable theories, but only about one percent of the work has been done when the theory is stated in qualitative form. Before it can receive the serious attention of men of science, it must be worked out so as to give a quantitative answer to, at any rate, a few of the crucial phenomena, and the theory will be judged by its richness of content as drawn from as few hypotheses as possible. From what is given in Professor Mackaye's book, it does not seem that he has developed his theory to such a stage. Until he has done so, it would perhaps be unfair to say more than to wish him good fortune and hide one's pessimism as much as possible.

All in all, "The Dynamic Universe" provides interesting reading. To some in state of sophistication No. 1, it may be a firebrand. In state 2, in which it has been written with evidence of much thought, it will find much sympathy. In state 3, it will provide some entertainment, coupled with a sort of sadness that the limitations involved in the use of words have resulted in there having been conveyed to the author so little of the content of the theory of relativity in the form in which it is visualized by its creators.

W. F. G. SWANN

Chemische Thermodynamik. DR. HERMANN ULICH. xvi+363 pp. 30 figures. Steinkopff, Dresden and Leipzig, 1930.

This book offers to the reader a systematic exposition of the principles of thermodynamics and their application to physical and chemical problems. The first and second laws are taken as

based on experience. A comprehensive and detailed system of notation is developed which possesses many logical advantages when it has once been mastered but renders the text difficult to follow if the reader has forgotten the exact meaning of some of the numerous symbols. The treatment is exact and the applications include most of the topics which interest the modern scientist. Extensive entropy tables add to the value of this book.

F. H. MacDougall